

**“Study of Advanced Oxidation Processes (AOPs) based on
Hydrodynamic Cavitation for the Degradation of Bio-refractory
Pollutants”**

Submitted in

fulfillment of the requirements for the degree of

Doctor of Philosophy

by

Sunil Rajoriya

2013RCH9519

Under the supervision of

DR. VIRENDRA KUMAR SAHARAN

Assistant Professor



DEPARTMENT OF CHEMICAL ENGINEERING

MALAVIYA NATIONAL INSTITUTE OF TECHNOLOGY JAIPUR

JAIPUR-302017

July, 2018

DECLARATION

I hereby certify that the work which is presented in the thesis entitled “**Study of Advanced Oxidation Processes (AOPs) based on Hydrodynamic Cavitation for the Degradation of Bio-refractory Pollutants**” in partial fulfilment of the requirements for the award of Doctor of Philosophy, in the Department of Chemical Engineering, Malaviya National Institute of Technology, Jaipur, is an authentic record of my own work unless otherwise referenced or acknowledged. The thesis was completed under the supervision of Dr. Virendra Kumar Saharan, Assistant Professor, Department of Chemical Engineering, Malaviya National Institute of Technology, Jaipur. The results presented in this thesis have not been submitted in part or full, to any other University or Institute for award of any degree. The content of the thesis has been checked using online software “Turnitin”.

Date:

Sunil Rajoriya
2013RCH9519
Department of Chemical Engineering
MNIT, Jaipur



MALAVIYA NATIONAL INSTITUTE OF TECHNOLOGY

DEPARTMENT OF CHEMICAL ENGINEERING

JAIPUR – 302017 (RAJASTHAN) INDIA

CERTIFICATE

This is to certify that the work reported in this thesis entitled “**Study of Advanced Oxidation Processes (AOPs) based on Hydrodynamic Cavitation for the Degradation of Bio-refractory Pollutants**” has been carried out by Mr. Sunil Rajoriya and submitted to Malaviya National Institute of Technology, Jaipur for the award of Doctor of Philosophy. It is a bonafide record of research work carried out by him under my supervision. The thesis work has reached the requisite standard, fulfilling the requirements for the degree of Doctor of Philosophy. The thesis embodies the original work done by him and has not been carried out earlier to the best of my knowledge and belief.

Place:

Dr. Virendra Kumar Saharan

Date:

Assistant Professor

Department of Chemical Engineering

MNIT Jaipur

ACKNOWLEDGEMENT

First of all, I would like to thank the almighty for his blessings in this journey and for giving me all the grace that I need to pursue this study.

I would like to express my deep sense of gratitude to my supervisor **Dr. Virendra Kumar Saharan** for his guidance, encouragement, tremendous support and advice throughout my work. He is a very knowledgeable and responsible supervisor. I have gained a lot from his fundamental and thorough knowledge in the area of cavitation phenomena. He provided me good research opportunities. I thank him not just for providing valuable guidance throughout the course of research work but also having developed in me the attitude required to carry out high quality research. I would like to thank him for spending his precious time to discuss thoroughly on my research topic and make me what I am today. This thesis would not have been possible without his help. I wish his blessings are bestowed on me forever.

Besides my supervisor, I am also thankful to Dr. Kailash Singh, Head, Department of Chemical Engineering for providing infra-structure support and facilities. I would like to pay my gratitude towards my Departmental Research Evaluation Committee (DREC): Dr. Suja George, Dr. R. K. Vyas, and Dr. Prabhat Pandit for their continuous evaluation and suggestions throughout my Ph.D. work. I am particularly indebted to Dr. Suja George for helping and motivating me when I faced with difficulties during my Ph.D.

I also want to give special thanks to my colleagues Mr. Jitendra Carpenter, Mr. Swapnil Bargole for spending his valuable time patiently listening and clearing my doubts. I extend my appreciation to the technical assistants and office staffs of Chemical Engineering Department, for supporting me in this journey.

I would like to thank Ministry of Human Resource Development (MHRD), Government of India for the financial support.

I would also acknowledge to Material Research center (MRC), MNIT Jaipur for providing the characterization facilities during my Ph.D. work.

I cannot complete this acknowledgment without mentioning my beloved family members. I would like to acknowledge with gratitude to my beloved family members for their support and encourage me throughout my life. I extend my gratefulness to my brothers, who have been the motivation behind my hard work, patience and character. I express my heartfelt

thanks to my loving son (Aditya) and daughter (Saumya) for their prayers. A special thanks to my loving wife, Garima, for her co-operation and support.

Sunil Rajoriya

July, 2018

ABSTRACT

In recent years, water pollution has become a major problem for the environment and human health due to the industrial effluents discharged into the water bodies. Day by day, new molecules such as pesticides, dyes, and pharmaceutical drugs are being detected in the water bodies, which are bio-refractory to microorganisms. In the last two decades, researchers have tried different AOPs such as Fenton, photocatalytic, hydrodynamic, acoustic cavitation processes, etc. to mineralize such complex molecules. Among these processes, HC has emerged as a new energy-efficient technology for the treatment of various bio-refractory pollutants in wastewater either operated alone or in combination with other advanced oxidative reagents and/or processes. Most of the studies have been reported on the laboratory scale and few studies report on the treatment of real industrial effluent and more studies are necessary to validate the efficiency of treatment process. This research work mainly focused on the implementation of HC based hybrid methods for the treatment of three different bio-refractory pollutants present in wastewater. Three organic molecules such as Rhodamine 6G (Rh6G), Reactive blue 13 (RB13) and 4-Acetamidophenol (4-AMP) were selected as model pollutants and the treatment studies were carried out in three parts. Thereafter, real textile dyeing industry effluent from nearby industry was also treated using HC based hybrid methods in order to check the efficiency of this process on an industrial scale.

Hybrid processes provide better degradation efficiency as compared to the individual process due to the enhanced generation of $\cdot\text{OH}$ radicals in the presence of process intensifying agents. The efficiency of hybrid processes also depends on the type of organic molecules, formation of hydroxyl radicals and its effective interaction with organic pollutants. Moreover, the different configurations of the cavitating device in HC reactor affect the extent of degradation of organic pollutants. Therefore, the study on various cavitating devices with different throat shape and size was carried out in order to enhance the cavitation activity which in turn increased the formation of highly reactive $\cdot\text{OH}$ radicals due to the dissociation of H_2O molecules.

In the first part, decolorization and mineralization of a cationic dye, Rh6G has been investigated using HC. Two cavitating devices such as slit and circular venturi were used to generate cavitation in HC reactor. The process parameters such as initial dye concentration (10-50 ppm), solution pH (2-12), operating inlet pressure (over a range 3-11 bar) were investigated in detail to evaluate their effects on the decolorization efficiency of Rh6G.

Decolorization of Rh6G was marginally higher in the case of slit venturi as compared to circular venturi. The kinetic study showed that decolorization and mineralization of the dye fitted first-order kinetics. Maximum decolorization of Rh6G using HC alone was found to be 32.06% at 10.0 pH and pressure of 5 bar. In the intensification studies using H₂O₂ and ozone, different molar ratios of concentration of Rh6G to H₂O₂ over a range of 1:10 to 1:50 were used to study the combined effect whereas ozone loading was optimized over a range of 1 to 7 g/h. Nearly 54% decolorization of Rh6G was obtained using a combination of HC and H₂O₂ at a dye to H₂O₂ molar ratio of 1:30. The combination of HC with ozone resulted in 100% decolorization in almost 5 to 10 min of processing time depending upon the initial dye concentration. To quantify the extent of mineralization, TOC analysis was also performed and almost 84% TOC removal was obtained using HC coupled with 3 g/h of ozone. The degradation by-products formed during the complete degradation process were qualitatively identified by LC-MS and a detailed degradation pathway has been proposed for mineralisation of Rh6G.

In the second part, decolorization of RB13, a sulphonated azo dye, was investigated using HC. The aim of this study was to check the influence of HC geometrical parameters such as total flow area, the ratio of throat perimeter to its cross-sectional area, throat shape, size, etc. and configuration of the cavitating devices on decolorization of RB13 in aqueous solution. For this purpose, eight cavitating devices i.e. Circular and slit venturi, and six orifice plates having different flow area and perimeter were used in the present work. Initially, the effects of various operating parameters such as solution pH (over a range 2-8), initial dye concentration (30-60 ppm) and operating inlet pressure (over a range of 0.3 -1.2 MPa) on the decolorization of RB13 have been investigated, and the optimum operating conditions were found. Almost 47% decolorization of RB13 was achieved using HC alone with slit venturi as the cavitating device at an optimum inlet pressure of 0.4 MPa and pH of the solution as 2.0. Kinetic analysis revealed that the decolorization and mineralization of RB13 using HC followed first order reaction kinetics. It has been found that in case of orifice plates, higher decolorization rate of $4 \times 10^{-3} \text{ min}^{-1}$ was achieved using OP2 which had higher flow area and perimeter ($\alpha = 2.28$). The effect of process intensifying agents such as H₂O₂ (RB13 to H₂O₂ molar ratios ranging from 1:1 to 1:40) and ferrous sulphate (H₂O₂: FeSO₄.7H₂O molar ratios ranging from 1:2 to 1:10) and different gaseous additives like oxygen (1–4 L.min⁻¹) and ozone (1–4 g.h⁻¹) on the extent of decolorization of RB13 were also examined. Almost 66% decolorization of RB13 was achieved using HC combined with 2 L.min⁻¹ of oxygen and in

combination with ferrous sulphate (1:3). Nearly 91% decolorization was achieved using HC combined with H₂O₂ at an optimum molar ratio (dye:H₂O₂) of 1:20 while almost complete decolorization was observed in 15 min using a combination of HC and ozone at 3 g.h⁻¹ ozone feed rate. Maximum 72% TOC was removed using HC coupled with 3 g.h⁻¹ ozone feed rate.

The third part dealt with the synthesis of TiO₂ photocatalysts doped with samarium (Sm) and nitrogen (N) using Conventional sol-gel process (CSP) and Ultrasound assisted sol-gel process (USP). The prepared TiO₂, Sm and N doped TiO₂ photocatalysts were characterized by XRD, FTIR, FESEM, and EDX analysis. Photocatalytic activity of the catalysts has also been evaluated for the degradation of 4-AMP using different combinations of UV irradiation, HC and US. All the experiments have been carried out using a 50 ppm solution of 4-AMP excluding initial concentration study. Initially, the effects of operating parameters i.e. catalyst dosage (0.5 to 3 g/L), solution pH (acidic pH=2.0, natural pH=6.8 and basic pH=10.0), and 4-AMP initial concentration (50 to 200 ppm) on the extent of degradation have been investigated. It was observed that degradation of 4-AMP followed first order reaction kinetics and almost 50% degradation with a degradation rate constant of 4.4×10^{-3} (min⁻¹) was achieved using only photocatalytic oxidation at an optimum TiO₂ catalyst loading of 2 g/L and natural pH (6.8). Nearly 60% and 63% degradation was obtained using Sm and N doped TiO₂ at the optimized molar ratio of Sm to TiO₂ (1.5:1) and N to TiO₂ (1:1) respectively. It was also established that combination of photocatalytic oxidation with US and HC yielded synergistic results with extent of degradation as 87% and 91% respectively under optimized conditions in 180 min treatment. The degradation by-products formed during the combined treatment of HC and photocatalytic oxidation were identified by LC-MS. HC in combination with photocatalytic oxidation was found to be most energy efficient process. Overall the current work has established that a novel combination of HC (slit venturi used as a cavitating device), UV and photocatalysts can be effectively applied for the treatment of wastewater containing persistent organic pollutants at large scale operation.

The fourth part reports the potential of HC for real industrial effluent showing its suitability and efficiency against a wide variety of pollutants. In this study, treatment of TDI effluent was investigated using HC and in combination with advanced oxidation reagents such as air, oxygen, ozone and Fenton's reagent. Slit venturi was used as the cavitating device in HC reactor. Initially, the effects of process parameters such as inlet pressure (3 to 10 bar) and dilution of the effluent on the extent of reduction of TOC and COD was studied. It was observed that almost 17% TOC, 12% COD, and 25% color removal was obtained using HC

alone at inlet pressure of 5 bar and pH of 6.8. The rate of reduction of TOC and COD decreased with dilution of the samples. Intensification studies have been carried out using different intensifying agents like Fenton's reagent ($\text{FeSO}_4 \cdot 7\text{H}_2\text{O}:\text{H}_2\text{O}_2$ ratios as 1:1, 1:2, 1:5 and 1:10), oxygen feed rates (1 to 4 L/min) and ozone feed rate (1 to 5 g/h). The use of intensifying agents resulted in the enhancement of the extent of reduction of TOC, COD and color of TDI effluent. Efficiency of the hybrid treatment processes were evaluated on the basis of their synergetic coefficient. HC in combination with Fenton's reagent ($\text{FeSO}_4 \cdot 7\text{H}_2\text{O}:\text{H}_2\text{O}_2$ as 1:5) was most effective with reduction of 48 % TOC and 38% COD in 15 min and 120 min respectively with almost complete decolorization (98%) of the TDI effluent. Whereas HC in combination with oxygen (2 L/min) and ozone (3 g/h) produced reduction of 48% TOC, 33% COD, 62% decolorization and 48% TOC, 23% COD, 88%, decolorization of TDI effluent respectively.

Overall, the obtained results revealed that HC based hybrid processes can be a better option for the treatment of bio-refractory pollutants as well as real industrial wastewater. Process intensification studies have indicated that HC in combination with other advanced oxidation processes gave higher degradation efficiency than the individual processes and found to be more energy efficient. However, process parameters such as solution pH, initial concentration of pollutants, dosages of different oxidizing agents, inlet pressure, cavitation number etc. and the geometrical parameters of the cavitating devices which are specific to the chosen hybrid technique needs to be optimized in order to obtain the maximum degradation efficiency of organic pollutants. HC based hybrid techniques are found to be a promising advanced technique for treatment of industrial wastewaters.

LIST OF PUBLICATIONS

The following papers on the research work presented in this thesis have been published.

- **S. Rajoriya**, J. Carpenter, V. K. Saharan, A. B. Pandit, Hydrodynamic cavitation: An advanced oxidation process for the degradation of bio-refractory pollutants, *Reviews in Chemical Engineering*, 32 (4) (2016) 379–411.
- **S. Rajoriya**, S. Bargole, V. K. Saharan, Degradation of a cationic dye (Rhodamine 6G) using hydrodynamic cavitation coupled with other oxidative agents: reaction mechanism and pathway, *Ultrasonics Sonochemistry*, 34 (2017) 183–194.
- **S. Rajoriya**, S. Bargole, V.K. Saharan, Degradation of reactive blue 13 using hydrodynamic cavitation: Effect of geometrical parameters and different oxidizing additives, *Ultrasonics Sonochemistry*, 37 (2017) 192–202.
- **S. Rajoriya**, S. Bargole, Suja George, Virendra Kumar Saharan, Treatment of textile dyeing industry effluent using hydrodynamic cavitation in combination with advanced oxidation reagents, *Journal of Hazardous Materials*, 344 (2017) 1109–1115.
- J. Carpenter, M. Badve, **S. Rajoriya**, S. George, V. K. Saharan, A. B. Pandit, Hydrodynamic cavitation: An emerging technology for the intensification of various chemical and physical processes in a chemical process industry, *Reviews in Chemical Engineering*, 33 (2016), 433–468.
- Shivendu Saxena, **Sunil Rajoriya**, Virendra Kumar Saharan, Suja George, An advanced pretreatment strategy involving hydrodynamic and acoustic cavitation along with alum coagulation for the mineralization and biodegradability enhancement of tannery waste effluent, *Ultrasonics Sonochemistry* 44 (2018) 299–309.
- **Sunil Rajoriya**, Swapnil Bargole, Suja George, Virendra Kumar Saharan, Parag R. Gogate, Aniruddha B. Pandit, Synthesis and characterization of Samarium and Nitrogen doped TiO₂ photocatalysts for photo-degradation of 4-Acetamidophenol in combination with hydrodynamic and acoustic cavitation, *Separation and Purification Technology*, 2018 (published).

Dedicated

To

My Supervisor & Family members

TABLE OF CONTENTS

<i>Declaration</i>	<i>i</i>
<i>Certificate</i>	<i>ii</i>
<i>Acknowledgement</i>	<i>iii</i>
<i>Abstract</i>	<i>v</i>
<i>List of publications</i>	<i>ix</i>
<i>List of Tables</i>	<i>xv</i>
<i>List of Figures</i>	<i>xvii</i>
<i>List of abbreviations and nomenclature</i>	<i>xxi</i>
Chapter 1: Introduction and Literature Review	1
1.1 Introduction.....	1
1.1.1 Objectives of Research.....	2
1.1.2 Organization of the thesis	3
1.2 Literature Review.....	5
1.2.1 Acoustic Cavitation.....	5
1.2.2 Hydrodynamic Cavitation.....	6
1.2.3 Mechanism of degradation of organic pollutants in HC.....	7
1.2.4 Summary of HC process in the area of wastewater treatment	8
1.2.5 HC reactors	25
1.2.6 The effect of various geometrical and operating parameters on the degradation efficiency of HC reactor	34
1.2.6.1 Geometrical aspects of cavitating device.....	34
1.2.6.1.1 Geometrical parameters of orifice	34
1.2.6.1.2 Geometrical parameters of venturi.....	35
1.2.7 Effect of various operating parameters on the cavitation process	38
1.2.7.1 Effect of inlet pressure and cavitation number	38
1.2.7.2 Effect of solution pH.....	39
1.2.7.3 Effect of temperature	41
1.2.7.4 Effect of initial concentration	42

1.2.8 Efficiency enhancement of HC process by combining with various other AOPs (hybrid methods)	44
1.2.8.1 HC combined with Fenton process	45
1.2.8.2 HC combined with hydrogen peroxide	48
1.2.8.3 HC combined with ozone.....	50
1.2.8.4 HC combined with photocatalysis	53
1.3 Summary of the Chapter.....	56
References.....	57

Chapter 2: Degradation of a cationic dye (Rhodamine 6G) using Hydrodynamic

Cavitation coupled with other oxidative agents	64
2.1 Introduction.....	64
2.2 Experimental details.....	66
2.2.1 Reagents.....	66
2.2.2 Hydrodynamic cavitation reactor setup	66
2.2.3 Experimental Procedure.....	69
2.2.4 Analytical procedure.....	69
2.3 Results and discussion	70
2.3.1 Effect of initial Rh6G concentration.....	70
2.3.2 Quantification of chemical effects (dosimetry study).....	72
2.3.3 Effect of solution pH.....	74
2.3.4 Effect of inlet pressure, cavitation number and geometrical parameters.....	75
2.3.5 Combination of hydrodynamic cavitation and H ₂ O ₂	78
2.3.6 Combination of Hydrodynamic cavitation and ozone	81
2.3.7 Mineralization study	83
2.3.8 Degradation products and degradation pathway.....	86
2.4 Novelty of the work.....	90
2.5 Summary of the chapter	90
References.....	91

Chapter 3: Degradation of Reactive Blue 13 using Hydrodynamic Cavitation: Effect of geometrical parameters and different oxidizing additives

3.1 Introduction.....	97
3.2 Materials and methods	98
3.2.1 Materials	98

3.2.2 Experimental and analytical procedure.....	100
3.3 Results and discussion	101
3.3.1 Hydraulic Characteristics.....	101
3.3.2 Optimization of solution pH	102
3.3.3 Effect of initial RB13 concentration	104
3.3.4 Optimization of different cavitating devices.....	106
3.3.5 Effect of geometrical parameters	108
3.3.5.1 Effect of α (throat perimeter/throat cross-sectional area)	108
3.3.5.2 Effect of β (throat area/pipe cross-sectional area)	109
3.3.5.3 Effect of geometrical configurations (Comparison of venturies and orifice plates)	110
3.3.6 HC combined with H ₂ O ₂	111
3.3.7 HC combined with oxygen	114
3.3.8 Effect of addition of ferrous sulphate	116
3.3.9 HC combined with ozone.....	118
3.3.10 Mineralization study	121
3.4 Novelty of the work.....	122
3.5 Summary of the chapter	123
References.....	123
Chapter 4: Synthesis and characterization of Samarium and Nitrogen doped TiO₂ photocatalysts for photo-degradation of 4-Acetamidophenol in combination with hydrodynamic and acoustic cavitation	
	128
4.1 Introduction.....	128
4.2 Materials and methods	131
4.2.1 Materials	131
4.2.2 Synthesis of pure TiO ₂ and doped TiO ₂ photocatalysts.....	131
4.2.2.1 Conventional sol-gel process (CSP)	131
4.2.2.2 Ultrasound assisted sol-gel process (USP)	132
4.2.3 Characterization Techniques.....	133
4.2.4 Degradation of 4-AMP	134
4.2.4.1 Photocatalytic oxidation.....	134
4.2.4.2 Combination of ultrasound (US) and photocatalysis	135
4.2.4.3 Combination of HC and photocatalysis	136
4.2.5 Analytical Methods.....	136

4.3 Results and discussion	137
4.3.1 Characterization of photocatalysts	137
4.3.1.1 XRD patterns	137
4.3.1.2 FT-IR spectroscopy analysis	139
4.3.1.3 FESEM with EDX analysis	140
4.3.1.4 Photoluminescence (PL) analysis	142
4.3.1.5 Diffuse reflectance spectra (DRS) analysis	142
4.3.1.6 X-ray photoelectron spectroscopy (XPS) analysis	144
4.3.2 Degradation of 4-AMP using photocatalytic oxidation	146
4.3.2.1 Effect of pure TiO ₂ loading on the extent of degradation	146
4.3.2.2 Effect of Solution pH on the extent of degradation	147
4.3.2.3 Effect of 4-AMP initial concentration	150
4.3.2.4 Effect of dopants	151
4.3.2.5 Comparison of photocatalytic activity for UV and visible light irradiations	153
4.3.2.6 Degradation of 4-AMP using ultrasound coupled with photolytic and photocatalytic oxidation	154
4.3.2.7 Degradation of 4-AMP using hydrodynamic cavitation coupled with photolytic and photocatalytic oxidation	156
4.3.2.8 Analysis of by-products formed during photo-degradation	158
4.4 Energy efficiency evaluation	160
4.5 Novelty of the work	162
4.6 Summary of the chapter	162
Appendix	164
References	165
Chapter 5: Treatment of textile dyeing industry effluent using hydrodynamic cavitation in combination with advanced oxidation reagents	172
5.1 Introduction	172
5.2 Material and methods	174
5.2.1 Textile dyeing industry (TDI) effluent	174
5.2.2 Chemicals	175
5.2.3 Experimental set-up and procedure	175
5.2.4 Analytical procedure	176
5.3 Results and discussion	176

5.3.1 Effect of operating inlet pressure	176
5.3.2 Effect of dilution on TOC and COD reduction.....	178
5.3.3 Treatment of TDI effluent using HC coupled with oxygen	179
5.3.4 Treatment of TDI effluent using HC coupled with ozone	181
5.3.5 Treatment of TDI effluent using HC coupled with Fenton’s reagent.....	184
5.3.6 Characteristics of treated TDI effluent obtained from different processes.....	186
5.4 Novelty of the work.....	187
5.5 Summary of the chapter	187
References.....	188
Chapter 6: Conclusions and Recommendations for Future Work	192
6.1 Conclusions.....	192
6.2 Recommendations for Future Work.....	193

LIST OF TABLES

Table No.	Table Caption	Page No.
1.1	Overview of work done in the area of HC process to wastewater treatment in recent years	14
2.1	Molecular structure, maximum absorption, and molecular weight of Rh6G	66
2.2	Dimension of the cavitating devices (circular and slit venturi)	68
2.3	Kinetic rate constants at different initial concentration of Rh6G	72
2.4	Kinetic rate constants at various solution pH	75
2.5	Kinetic rate constants at different operating pressures	77
2.6	Effect of H ₂ O ₂ addition on the extent of decolorization	80
2.7	Effect of ozone addition on the decolorization and mineralization of Rh6G	83
2.8	The values of mineralization rate constant and reduction in TOC (%) using various processes	85
3.1	Flow geometry of the cavitating devices	99
3.2	Effect of solution pH on extent of decolorization	104
3.3	Effect of initial concentration on extent of decolorization	105
3.4	Effect of geometrical parameters (α , β) on decolorization rate of RB13	107
3.5	Effect of H ₂ O ₂ addition on extent of decolorization	113
3.6	Effect of oxygen dosages on extent of decolorization and first order rate constant	116
3.7	Effect of addition of ferrous sulphate on decolorization of RB13	118
3.8	Effect of ozone addition on the decolorization and mineralization of RB13	121
3.9	Reduction in TOC, and mineralization rate constant using various processes	122
4.1	The crystallite sizes of photocatalysts synthesized using USP and CSP	139
4.2	Photocatalytic activity of different photocatalyst prepared using USP under UV and visible light irradiation	154

4.3	Identified degradation intermediates formed during photocatalytic degradation of 4-AMP in the presence of HC	159
4.4	Energy Efficiency Evaluation of different processes under optimized conditions	161
5.1	Characteristics of TDI effluent	175
5.2	Effect of inlet pressure on TOC and COD reduction of TDI effluent	178
5.3	Hydrodynamic characteristics and cavitation number of the experimental setup	178
5.4	Effect of dilution on TOC and COD reduction of TDI effluent	179
5.5	Effect of addition of oxygen on the TOC, COD and color reduction of TDI effluent	181
5.6	Effect of ozone addition on the TOC, COD and color reduction of TDI effluent	184
5.7	Effect of addition of Fenton's reagent on the TOC, COD and color reduction of TDI effluent	185
5.8	Comparison of the characteristics of TDI effluent for all processes at the optimized conditions	187

LIST OF FIGURES

Figure No.	Figure Caption	Page No.
1.1	Pressure variation & flow conditions in hydrodynamic cavitating device	6
1.2	Schematic diagram of the orifice and venturi based HC Reactor	27
1.3	Schematic representation of the experimental set-up showing liquid whistle reactor in combination with advanced Fenton process	28
1.4	Schematic representation of the hydrodynamic acoustic cavitation Reactor	29
1.5	Schematic diagram of the Ozonix reactor	31
1.6	Schematic diagram of the high speed rotor	32
1.7	Schematic diagram of the swirling jet reactor	33
2.1	Schematic diagram of HC reactor set-up	67
2.2	Schematic view of circular and slit venturi	68
2.3	Effect of initial Rh6G concentration on the decolorization rate of Rh6G (Experimental Conditions: inlet pressure, 5 bar; solution pH, 10.0; volume of solution, 6 L)	72
2.4	The formation of H ₂ O ₂ concentration during degradation in HC reactor	73
2.5	Effect of solution pH on the decolorization rate of Rh6G (Experimental Conditions: Initial concentration, 10 ppm; pressure, 5 bar; volume of solution, 6 L)	75
2.6	Effect of H ₂ O ₂ addition on decolorization rate of Rh6G (Experimental Conditions: initial concentration, 10 ppm; solution pH, 10.0; volume of solution, 6 L; pressure, 5 bar)	80
2.7	Kinetics of mineralization process of Rh6G (Experimental conditions: slit venturi; solution pH, 10.0; volume of solution, 6 L; initial concentration, 50 ppm)	85
2.8	LC-MS of (a) Rh6G solution before treatment (b) degradation by-products of Rh6G after 30 min of treatment	88
2.9	Proposed degradation pathway for the degradation of Rh6G	89

3.1	Molecular structure of Reactive Blue 13 dye	98
3.2	Hydraulic characteristics of the various cavitating devices	102
3.3	Effect of solution pH on decolorization rate of RB13. (Experimental conditions: inlet pressure, 0.4 MPa; volume of solution, 6 L; concentration, 30 ppm; slit venturi)	103
3.4	First order kinetic fitting into RB13 decolorization at different initial concentrations. (Experimental conditions: inlet pressure, 0.4 MPa; volume of solution, 6 L; solution pH, 2; slit venturi)	105
3.5	Effect of cavitation number on decolorization rate of RB13. (Experimental conditions: initial concentration, 30 ppm; pH of the solution, 2.0; volume of solution, 6 L)	107
3.6	Effect of H ₂ O ₂ addition on decolorization rate of RB13. (Experimental conditions: initial concentration, 30 ppm; solution pH, 2.0; volume of solution, 6 L; pressure, 0.4 MPa, slit venturi)	113
3.7	Effect of oxygen dosages on decolorization rate of RB13. (Experimental conditions: inlet pressure, 0.4 MPa; volume of solution, 6 L; solution pH, 2; slit venturi)	116
3.8	Effect of ozone addition on mineralization rate of RB13. (Experimental conditions: initial concentration, 150 ppm; volume of solution, 6 L; solution pH, 2; inlet pressure, 0.4 MPa)	120
4.1	Schematic representation of the ultrasound assisted sol-gel synthesis process	133
4.2	Schematic representation of experimental set-ups: (a) photocatalytic reactor, (b) photocatalytic reactor combined with US, and (c) HC reactor coupled with photocatalysis	135
4.3	XRD patterns: (a) pure TiO ₂ , (b) N-doped TiO ₂ , and (c) Sm-doped TiO ₂	138
4.4	FTIR spectra of synthesized photocatalysts: (a) Pure TiO ₂ , (b) N-TiO ₂ , and (c) Sm-TiO ₂	140
4.5	FESEM images with EDX of synthesized photocatalysts: (a) pure TiO ₂ , (b) N-TiO ₂ , and (c) Sm-TiO ₂	141

4.6	PL spectra of (a) pure TiO ₂ (b) Sm-TiO ₂ , and (c) N-TiO ₂	142
4.7	UV-Vis diffuse reflectance spectra (b): Kubelka-Munk plots and band gap energy estimation of (a) pure TiO ₂ (b) Sm-TiO ₂ , and (c) N-TiO ₂	143
4.8	Survey XPS spectrum of (a) pure TiO ₂ (b) N-TiO ₂ , and (c) Sm-TiO ₂	145
4.9	High resolution XPS spectrum of (a) Ti 2p (b) O 1s (c) N 1s (d) Sm 3d core levels	146
4.10	Effect of catalyst loading on degradation rate of 4-AMP (Conditions: solution volume: 400 mL, initial concentration: 50 ppm, natural pH: 6.8, treatment time: 180 min)	147
4.11	Zeta potential of TiO ₂ , N-TiO ₂ and Sm-TiO ₂ at different pH	149
4.12	Effect of solution pH on degradation rate of 4-AMP (Conditions: solution volume: 400 mL, initial concentration: 50 ppm, TiO ₂ loading: 2 g/L, treatment time: 180 min)	149
4.13	First order kinetic fitting for 4-AMP degradation at different initial concentrations (Conditions: solution volume: 400 mL, TiO ₂ loading: 2 g/L, solution pH: 6.8 treatment time: 180 min)	151
4.14	Photocatalytic degradation of 4-AMP over different (a) N-doped TiO ₂ and (b) Sm-doped TiO ₂ (Conditions: solution volume: 400 mL, catalyst loading: 2 g/L, solution pH: 6.8 treatment time: 180 min)	153
4.15	Effect of combination of AC and photocatalytic process on degradation rate of 4-AMP (Conditions: solution volume: 400 mL, catalyst loading: 2 g/L, solution pH: 6.8 treatment time: 180 min)	156
4.16	Effect of combination of HC and photocatalytic process on degradation rate of 4-AMP (Conditions: solution volume: 3 L, catalyst loading: 2 g/L, solution pH: 6.8 treatment time: 180 min)	158
5.1	Effect of inlet pressure on TOC and COD reduction of TDI effluent using HC alone (Conditions: solution volume, 6 L; pH,	177

	6.8; treatment time, 120 min)	
5.2	Effect of addition of oxygen on the TOC, COD and color reduction of TDI effluent (Conditions: solution volume, 6 L; pH, 6.8; pressure, 5 bar; treatment time, 120 min)	181
5.3	Effect of addition of ozone on the TOC, COD and color reduction of TDI effluent (Conditions: solution volume, 6 L; pH, 6.8; pressure, 5 bar; treatment time, 120 min)	183
5.4	Physical appearance of TDI effluent (a) before and (b) after 60 min treatment using HC combined with Fenton's reagent	186

LIST OF ABBREVIATIONS AND NOMENCLATURE

Abbreviations

HC	Hydrodynamic Cavitation
AC	Acoustic Cavitation
AOPs	Advanced Oxidation Processes
HAC	Hydrodynamic Acoustic Cavitation
VFD	Variable Frequency Distribution
TOC	Total Organic Carbon, mg/L
COD	Chemical Oxygen Demand, mg/L
BOD	Bio-chemical Oxygen Demand, mg/L
BI	Bio-degradability Index
UV	Ultraviolet
CFD	Computational Fluid Dynamics
Rh6G	Rhodamine 6G
[Rh6G] ₀	Initial Concentration of Rh6G, ppm
[Rh6G]	Concentration of Rh6G at time t, ppm
RB13	Reactive blue 13
4-AMP	4-Acetamidophenol
LC-MS	Liquid Chromatography-Mass Spectrometry
SV	Slit Venturi
CV	Circular Venturi
OP1	Orifice Plate 1
OP2	Orifice Plate 2
OP3	Orifice Plate 3
OP4	Orifice Plate 4
OP5	Orifice Plate 5
OP6	Orifice Plate 6
US	Ultrasound
USP	Ultrasound assisted sol-gel Process
CSP	Conventional sol-gel Process
XRD	X-ray Diffraction
FTIR	Fourier Transform Infrared Spectroscopy
FESEM	Field Emission Scanning Electron Microscopy
EDX	Energy-dispersive X-ray Analysis
ZPC	Zero Point Charge

EE	Energy Efficiency
TDI	Textile Dyeing Industry
TS	Total Solids, mg/L
TDS	Total Dissolved solids, mg/L
TSS	Total suspended solids, mg/L
EE	Energy Efficiency

Nomenclature:

C_v	Cavitation Number
C_{vi}	Cavitation Inception Number
P_2	Fully Recovered Downstream Pressure, N/m^2
P_v	Vapor Pressure of the Liquid, N/m^2
v_o	Velocity at the Throat, m/s
ρ	Density of Liquid, kg/m^3
α	The Ratio of the Perimeter of Throat to its Cross Section Area, mm^{-1}
B	The Ratio of Throat Area to Pipe Cross Section Area
f_T	Frequency of Turbulence, kHz
C_o	Initial Concentration of Pollutants, ppm
C	Concentration of Pollutants at time t, ppm
k	Degradation/decolorization Rate Constant, min^{-1}
t	Degradation/decolorization Time, min
D	Average Crystallite Size, nm
λ	Wavelength of the X-ray Radiation
K	Scherrer's equation Constant (used in equation 4.3 (Chapter 4; Section 4.3.1.1), value = 0.89)
β	Full Width at Half Maximum Intensity
θ	Half Diffraction Angle

CHAPTER 1

Introduction and Literature Review

1.1 Introduction

The treatment of wastewater containing bio-refractory pollutants (which have the tendency to resist the conventional biological treatment) from various industries has been a major environmental problem. Water is being polluted by industrial and commercial actions, agricultural practices, and day to day human activities. Water pollution has many sources; the most polluting of them are the city sewage and industrial waste discharged into the rivers. Apart from that, excessive use of fertilizers and insecticides in the farm lands causes seepage of these pollutants into the water bodies. Downward infiltration of these chemicals into surface and groundwater may be facilitated by flood irrigation and storm water leading to groundwater contamination. Human health is affected by water pollution typically due to the contamination of drinking water from waste streams. Several industries such as pesticides, dyes, textiles and many other industries are continuously polluting water as they contain large quantity of organic pollutants. These organic molecules are bio-refractory or very toxic to the microorganisms. Hence, conventional biological methods are not capable of completely degrading such complex compounds due to high toxicity and carcinogenicity [1-2]. In the past years, many researchers have developed various methods for the degradation of organic pollutants such as carbon bed adsorption, biological methods, oxidation using chlorination and ozonation, electrochemical methods, membrane processes and many other advanced oxidation processes (AOPs) [3-8]. Most of the AOPs such as Fenton, photocatalytic, hydrodynamic and acoustic cavitation have been established in the research laboratories effectively but several challenges are faced by many industries to scale them up. In general, AOPs are a set of processes that involve the generation and utilization of free radicals such as highly reactive and non-selective hydroxyl radicals ($\cdot\text{OH}$) which has high oxidation potential (2.80 eV), $\text{HO}_2\cdot$ (hydroperoxy), $\text{O}\cdot$ and $\text{O}_2\cdot^-$ (oxygen). These radicals are capable of oxidizing toxic organic/inorganic compounds and non-biodegradable pollutants [9-12]. Among all the AOPs, HC process is found to improve the treatment ability to a greater extent and gives better energy efficiency for the removal/degradation of bio-refractory pollutants on an industrial scale [13-15].

Cavitation is a phenomenon that involves the formation, growth, and subsequent collapse of the micro-bubbles or cavities within a liquid (resulting in very high energy densities of the order of 1 to 10^{18} kW/m³, [16]) occurring in an extremely small interval of time (milliseconds), releasing large magnitudes of energy [17].

Various types of cavitation can be classified based on the method of production of cavities as optical, particle, hydrodynamic and acoustic cavitation [18]. Out of these techniques, hydrodynamic and acoustic cavitation is proved to be effective in bringing about the desired chemical and physical transformation.

1.1.1 Objectives of Research

In view of the advantages of HC process, the present research work is aimed at studying the effect of HC for the treatment of bio-refractory pollutants present in wastewater and its applicability towards the treatment of real industrial effluent on an industrial scale. The model organic pollutants that have been selected for the studies are common pollutants looking in wastewater discharge of textile and pharmaceutical industries. These model organic compounds includes cationic and reactive dyes (Rhodamine 6G and Reactive blue 13) and a pharmaceutical drug named as 4-Acetamidophenol. In the area of wastewater treatment, the desired transformation depends on the potentiality of HC in generating the highly oxidizing free radicals that are responsible for the effective degradation of water pollutants.

Conventional treatment processes such as adsorption, coagulation, membrane separation, and biological process are not capable in decolorization and complete mineralization of dye wastewater. Also, these processes provide a poor performance in breaking larger complex molecules and take longer time for completion of treatment. On the other side, these processes can only transfer organic load from one phase to other phases rather than eliminating the organic load from discharge waste.

Hence, alternative treatment process is required for the effective treatment of bio-refractory pollutants and one such process which has been received a greater attention in recent years is the hydrodynamic cavitation process. HC process does not produce any secondary load during the treatment process due to the high oxidative capability.

Following are the major objectives of this research work:

- The main source for the surface and ground water contamination in Rajasthan is due to direct disposal of treated and untreated wastewater from textile and dyeing industries. In order to develop an energy efficient technology for the treatment of textile and dyeing industry effluent, two synthetic textile dyes were identified to optimize the various operating parameters using batch study. Therefore, the first

objective is to investigate the degradation of two model organic pollutants such as Rhodamine 6G (Rh6G) and Reactive blue 13 (RB13) using HC reactor.

- Optimization of various operating parameters such as solution pH, initial pollutant concentration, inlet pressure, cavitation number and dosages of different advanced oxidative reagents etc.
- Optimization of the geometrical parameters of the different cavitating devices to achieve the maximum efficiency of HC reactor.
- Process intensification studies in the presence of hydrogen peroxide, ferrous sulphate, oxygen, air and ozone.
- Synthesis of pure and doped TiO₂ photocatalysts using conventional sol-gel process and ultrasound assisted sol-gel process and studies on its photocatalytic activity for the degradation of 4-Acetamidophenol in combination with HC.
- Devolvement of hybrid approaches based on HC reactor in combination with other AOPs such as Fenton's oxidation, ozonation and Photocatalytic oxidation for obtaining maximum degradation efficiency.
- Studies on the performance of HC based hybrid processes for treating the real textile dyeing industry effluent.

1.1.2 Organization of the thesis

The present doctoral thesis is divided into six chapters. The highlights of each chapter have been presented as follows:

Chapter 1 provides an introduction of the problem statement, objectives of the present research work, organization of the thesis and an extensive literature review on the work done in the area of HC and its hybrid processes in waste water treatment.

Chapter 2 describes the ability of HC to mineralize and decolorize the Rhodamine6G (Rh6G) in aqueous solution and to intensify the mineralization of Rh6G by combining HC with other oxidizing agents. The effects of operating parameters like solution pH, initial concentration of dye, inlet pressure, and cavitation number on the decolorization efficiency of Rh6G were investigated. The degradation by-products were identified using LC-MS study and subsequently a possible degradation pathway of Rh6G has been proposed. The dosimetry studies were carried out to investigate the scavenging action on $\cdot\text{OH}$ radicals generated through HC. The chapter presents the suitable hybrid technique identified for the maximum degradation efficiency of Rh6G which was HC in combination with ozone.

Chapter 1: Introduction and Literature Review

Chapter 3 describes the ability of HC in combination with H₂O₂, Fenton's reagent, oxygen, air and ozone as well as the effect of geometrical parameters of various cavitating devices for the degradation of reactive blue 13 (RB13) as a model pollutant. In this chapter, two venturies (slit and circular) and six orifice plates with different geometries are discussed. The chapter presents the novelty of the work carried out especially in the effect of geometrical parameters of the cavitating devices, the effect of advanced oxidation reagents and implementation of hybrid methods in order to achieve maximum degradation efficiency.

Chapter 4 presents the synthesis and characterization of Samarium (Sm) and Nitrogen (N) doped TiO₂ photocatalysts for photo-degradation of 4-Acetamidophenol (4-AMP) in combination with hydrodynamic and acoustic cavitation. Sm and N doped TiO₂ photocatalysts which were synthesized using conventional sol-gel process (CSP) and ultrasound assisted sol-gel process (USP) were studied for the degradation efficiency using HC+photocatalytic process. The chapter presents the novelty of the work especially in the photocatalytic activity of the doped catalysts in the degradation of 4-AMP using different combinations of HC with UV radiations and US and its extension in to the visible light range. The energy consumption analysis for all the approaches have also been presented based on the amount of pollutant degraded per unit energy supplied.

Chapter 5 presents the performance of hydrodynamic cavitation system in order to treat the real textile dyeing industry (TDI) effluent from a nearby industry. The process parameters studied in order to obtain the optimized conditions for maximum reduction in TOC, COD and color in the TDI effluent are also presented. This chapter presents the various hybrid approaches such as HC+O₂, HC+O₃, and HC+Fenton studied in order to identify the best technique for maximum degradation with respect to TOC, COD and color and for its suitability for industrial applications on a large scale.

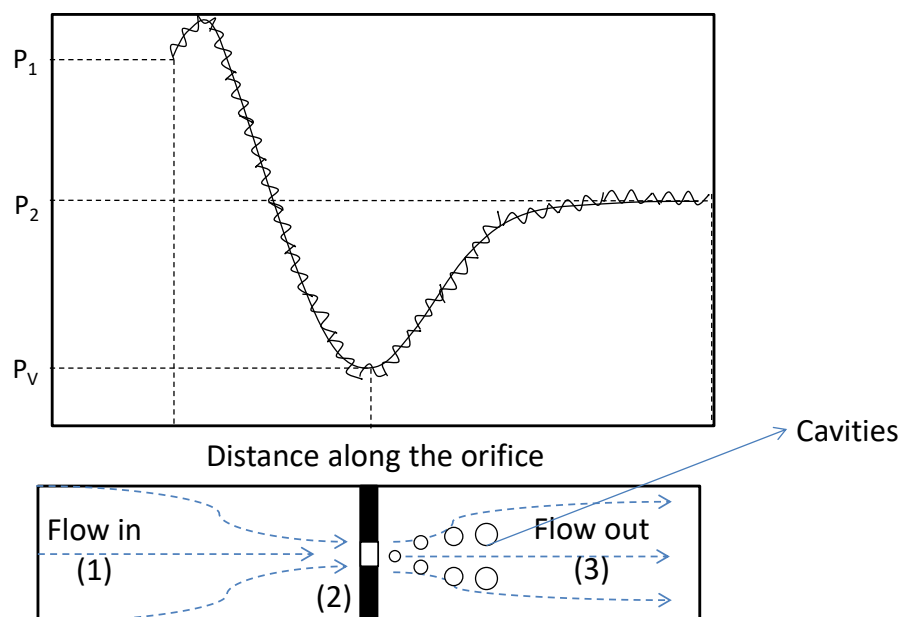
Chapter 6 presents the major conclusions drawn from the present study and the recommendations for future work.

1.2 Literature Review

A comprehensive literature review on HC process in the area of wastewater treatment has been described in detail. The accountability and effect of other operating and geometrical parameters on the performance of the cavitating devices is being discussed. The recent findings on synergetic effects of HC in coupling with other AOPs to improve the efficiency of individual AOPs have been discussed.

1.2.1 Acoustic Cavitation: Cavities are created by passing the sound waves through the liquid medium. The range of sonic spectrum is 20 kHz to 10 MHz, which may be subdivided into three main sections as Low frequency and high power ultrasound (20 -100 kHz), High frequency and medium power ultrasound (100kHz-1MHz), and High frequency and low power ultrasound (1-10 MHz). The ultrasound range for chemical and biological applications can be 20 kHz to 1 MHz while the range of spectrum from 1-10 MHz must be used for the medical and diagnostic purposes. Ultrasonic waves consist of a rarefaction (expansion) and compression cycles, when these waves are transmitted through a liquid, bubble/cavity are formed followed by a rapid growth and finally the collapse of these generated cavities. The average distance between the liquid molecules is larger in rarefaction cycle, however smaller in the compression cycle. Cavitation occurs in rarefaction cycles where negative acoustic pressure is sufficiently large to pull apart the liquid molecules from each other and the distance between the adjacent molecules can exceed the critical molecular distance. At that moment, the voidage is created in the liquid which causes the formation of cavities. Subsequently, in the compression cycle of the sound wave, acoustic pressure is positive which pushes the molecules together. The cavities will compress (decrease in size) during the compression cycle of ultrasonic wave, and few of them may collapse in a very small time interval. The final collapse phase is adiabatic in nature, thus producing high local temperatures and pressures. Acoustic cavitation has also been employed to degrade bio-refractory pollutants in aqueous solution [19-23]. However, it was found that the design of acoustic devices and its large scale of operation have a major problem because of higher cost of operation and low energy efficiencies [24-25]. In recent years, HC process is found to be a good alternative to the acoustic cavitation for the degradation of complex molecules from wastewater. Also, it has been proved energy efficient in destroying of bio-refractory pollutants, better prospects for scale up, cost-effective, and higher cavitation activity [3, 15-16, 26-27].

1.2.2 Hydrodynamic Cavitation: Hydrodynamic cavitation can be produced by the passage of liquid through the constriction such as venturi. When the liquid is allowed to pass through the geometries, the kinetic energy/velocity of the liquid increases at the expense of the pressure. The pressure at the throat or vena-contracta of the constriction drops below or equals the vapor pressure of the liquid, the liquid gets vaporized and thus creating number of vaporous cavities and these cavities are further collapsed when the pressure recovers downstream of the mechanical constriction. The cavity collapse causes the creation of hot spots, releasing highly reactive free radicals due to thermal breakdown of molecules and intensification in mass transfer rates. The collapse of bubbles/cavities generates confined “hot spots” where the temperatures can reach up to 5,000 K and pressures of about 1000 atm [28-33]. Figure 1.1 shows a typical pressure profile of an orifice plate. In the downstream section, boundary layer separation occurs, and some amount of energy is lost in the form of permanent pressure drop due to local turbulence. The magnitude of the pressure drop greatly influences the intensity of cavitation and turbulence in the downstream section [34]. The intensity of turbulence has a significant impact on cavitation intensity.



(1 – upstream of the orifice; 2 - vena contracta; Point 3 - downstream of the orifice)

Figure 1.1: Pressure variation & flow conditions in hydrodynamic cavitating device

In HC, a dimensionless parameter known as cavitation number (C_v) is used to characterize the condition of cavitation inside a cavitating device [1]. It is defined as the ratio

of the pressure drop between the throat and extreme downstream section of the cavitating device to the kinetic head at the throat. Cavitation number is given by the following equation:

$$C_v = \left(\frac{P_2 - P_v}{\frac{1}{2} \rho v_o^2} \right) \quad (1.1)$$

The C_v is known as cavitation inception number (C_{vi}) at which the formation of cavity is initiated. Ideally speaking, cavitation inception take place at C_{vi} equal to one, and there are significant cavitation effects at the values of C_v less than 1. But in many cases cavities can get generated at $C_v > 1$ due to the existence of small quantity of dissolved gases and suspended particles [35]. For a better cavitation yield, the cavitating device should be operated at lower cavitation number. A very low value of cavitation number may also results in the condition of choked and super cavitation which has no practical utility [17]. Thus, cavitating device should always be operated at an optimum value (depends on the application) to prevent such condition [36].

1.2.3 Mechanism of degradation of organic pollutants in HC:

HC is capable of generating hot spots, and thus any molecules which are trapped inside the cavities or locating itself near the cavity-liquid interface gets thermally breakdown into smaller molecules and highly reactive free radicals. In case of wastewater solution subjected to the HC, the water molecules will get dissociated into hydroxyl radicals ($\cdot\text{OH}$) under extreme temperature and pressure conditions. These hydroxyl radicals having high oxidation potential can oxidize any organic molecules present in waste water solution and thereby mineralizing such compounds. There are two main mechanisms involved in the destruction of organic pollutants by cavitation i.e. first, the thermal decomposition/pyrolysis of the volatile pollutant molecule entrapped inside the collapsing cavity and secondly, the reaction of $\cdot\text{OH}$ radicals with the pollutants. Both mechanisms can take place in the core of cavity, at the interface of cavity and in bulk liquid medium. Sometimes the mechanical effects are also significant in destruction of such pollutants. In some cases the high intensity of shockwaves (which is generated by the collapsing cavity) can break molecular bonds especially the complex large molecular weight compounds. The broken down intermediates are more vulnerable to $\cdot\text{OH}$ attack as well as biological oxidation and thus it is feasible to increase the rate of mineralization/oxidation of such compounds using HC as a pretreatment method. The

following reactions may occur during oxidation of organic pollutant molecules using HC in equations (1.2) – (1.5) [10, 17].



1.2.4 Summary of HC process in the area of wastewater treatment

HC can be produced using the constrictions mainly the orifice and venturi with their different geometry in the flowing liquid. The cavitating conditions generated in HC are identical to AC where it can induce the chemical as well as mechanical effects. In case of wastewater treatment, mainly the chemical effects contribute where the highly reactive free radicals are generated leading to the degradation or decomposition of pollutants present in water. The generated radicals and other induced effects can effectively oxidize the organic compounds and simultaneously break the large molecules into smaller intermediates which are more amenable for further treatment with subsequent biological methods. Thus, HC can be used as a pretreatment technique and can couple with conventional methods for improving the degradation efficiency. HC has been successfully employed in degradation of toxic dyes, pesticides, pharmaceutical discharge and other complex organic compounds and also most of the studies have recommend this technique for its scale up on industrial scale for the removal of such kind of pollutants from water [37]. Additionally, HC has shown its capability in coupling with other AOPs and this synergetic effect can effectively produce the desirable results in this area of application. The individual AOPs such as H_2O_2 , O_3 , Fenton process and photocatalysis etc. may not produce desirable outputs, but in combination with HC, the combined effect can overcome the drawbacks of individual techniques and consequently reduce the load of such pollutants from water significantly. In last few years, several investigators [1-2, 38-51] have studied the applicability of HC process for the degradation of complex bio-refractory pollutants from waste streams.

In this context, Sivakumar and Pandit [28] have first reported the degradation of colored pollutant present in water using HC. They have used various configurations of orifice plates for the degradation of Rhodamine B dye as a model pollutant. The maximum degradation rate constant of $5.33 \times 10^{-5} \text{ (s}^{-1}\text{)}$ was obtained at 30 psig using the optimized geometry of orifice plate. They have also concluded that the orifice based devices can degrade such kinds of

Chapter 1: Introduction and Literature Review

pollutants as orifice can generate the higher number of transient cavities with high collapse intensity for producing the desirable changes. Saharan et al. [2] have also examined the degradation of orange-G dye using orifice, slit and circular venturi as a cavitating device. They have reported that HC alone can efficiently degrade almost 92% of dye using slit venturi at an optimum pressure of 3 bar and cavitation number of 0.29. This study has shown the higher throughput using venturi than orifice for the degradation of orange-G dye. The cavitation formed in a venturi is stable but produces more number of cavities than orifice plate. In venturi, the pressure recovers smoothly which leads to the maximum growth of cavities and thus result into large magnitude of cavity collapse pressure. In the another study by Saharan et al. [1], they have studied the degradation of Reactive Red 120 dye using circular venturi and also analyzed the different cavitating conditions with respect to the operating pressure using photographic study. They have observed the formation of cavity cloud due to the generation of a large number of cavities, when operated at a higher pressure than optimum operating pressure (5 bar). At a very high inlet pressure or velocity at the throat, the cavities start to coalesce with each other and results into a condition of choked cavitation which ultimately results into the decreased rate of degradation. A maximum 60% decolorisation and 28% mineralization was obtained using venturi at an optimum operating pressure of 5 bar and 0.15 cavitation number. In a similar way HC has also been well established for the degradation of other toxic substances such as pharmaceutical and agricultural pesticides molecules. In this area, Gogate and Patil [52] have investigated the treatment of Triazophos (an insecticide) using HC and observed that almost 49.7% degradation and 29% reduction in TOC was achieved in 2 h of operation at an optimum conditions. It was observed that the lower pH favors the degradation as higher degradation was achieved at pH 3. It was concluded that the number of hydroxyl radicals being generated is more under the acidic conditions which in turn increases the degradation capacity. Bagal and Gogate [53] have also investigated the applicability of HC reactor for the degradation of pharmaceutical drug (diclofenac sodium) and found that, the maximum extent of degradation of diclofenac sodium was achieved as 26.85% at an optimized inlet pressure of 3 bar and solution pH of 4.

On the other side, HC is found as a better option in the treatment of real industrial effluent and for subsequent reduction in toxicity of the pollutants as well as it increases the biodegradability of effluents. Padoley et al. [48] have investigated the applicability of HC reactor as a pretreatment tool for the complex recalcitrant biomethanated distillery

wastewater (B-DWW). The objective of this study was to increase the biodegradability of B-DWW which was examined by estimating the bio-degradability index (BI) which is the ratio of BOD_5/COD . If BI is more than 0.3, the aqueous effluent has a better biodegradability while the aqueous effluent is difficult to biodegrade at the BI less than 0.3. They have found that at optimized operating pressure of 13 bar, BI increases from 0.14 to 0.32 with 32.24% reduction in COD and 31.43% reduction in TOC during the HC treatment which indicates that the complex molecules can get broken down into the smaller intermediates using HC which are more amenable to further treatment with conventional processes. Chakinala et al. [39] have first reported on the processing of real industrial effluents using the combination of HC and advanced Fenton process. They have developed Liquid whistle reactor (LWR) which comprises an orifice plate with multiple holes followed by a blade for the purpose of increasing the extent of cavitation and the treatment of effluent which contains high loading of organics, COD and phenolic compounds. They have observed around 65% TOC removal and 80% COD reduction of waste effluents in 150 min of treatment under optimized conditions. Similarly in another study by Chakinala et al. [14], an investigation was carried out for the treatment of real effluent stream using HC combined with heterogeneous Fenton process based on the use of zero-valent iron as a catalyst. They have observed almost 60% and 40% reduction in TOC using HC in the presence of iron pieces and copper windings on iron pieces respectively, in 150 min of treatment time. The presence of copper and iron pieces ultimately increase the extent of the generation of hydroxyl radicals which significantly enhance the degradation rate of the pollutants.

In recent years, in order to increase the degree of cavitation activity and intensity and number of cavities being generated for producing high magnitude of collapse pressure, many researchers have studied the HC in combination with AC to yield large extent of hydroxyl radicals which can sufficiently increase the decomposition rate of water pollutants. Many studies have been reported on the combination of HC with AC to increase the efficiency of the combined processes in terms of cavitation yield. In this context, Franke et al. [54] have illustrated the use of combination of orifice based HC reactor and AC for the degradation of chloroform and observed a significant improvement in the degradation efficiency achieved in the combined process rather than that obtained in individual operations. This synergetic effect shows that the hybrid methods are 73% more efficient than the sum of individual operation in the degradation of chloroform. Gogate et al. [55] have also developed the hybrid technique for wastewater treatment, in which HC was combined with AC and with other methods such

Chapter 1: Introduction and Literature Review

as electrochemical oxidation and ozonation and develop a reactor which called as Ozonix reactor. It was observed that this synergetic effect significantly enhances the degradation efficiency, decolorisation rate as well as the disinfection capacity of the real effluent.

From the above discussion, the HC have a potential in degrading the organic pollutants effectively to a certain level which depends on the pollutants to be treated and other operating conditions. The efficiency of the process in degrading various pollutants depends on the number of hydroxyl radicals that are being generated and their effective utilization. Hence, in this regards, various researcher have studied the combined process of HC with other AOPs such as H_2O_2 , O_3 , Fenton's reagent, Photocatalysis, etc. in order to improve the efficiency of combined process with an aim of maximizing the generation of $\cdot OH$ radicals and their effective distribution. This combination effect can better exploit in the area of wastewater treatment than individual operation. In this regard, Mishra and Gogate [40] have examined the degradation of Rhodamine B by coupling venturi based HC reactor with H_2O_2 . At optimum operating conditions, on increasing the concentration of H_2O_2 from 0–200 mg/L, the degradation of Rhodamine B was increased from 59.3% to 99.9% and also 55% removal in TOC was achieved in 120 min of treatment time.

Gore et al. [41] studied the degradation of reactive orange 4 dye by combining HC with other AOPs such as ozone and H_2O_2 . They have reported that about 37% decolorisation was achieved using HC only at an operating pressure of 5 bar and pH of 2.0 while the decolorisation has reached to 99% extent and TOC reduced to 50.73% on the addition of H_2O_2 at the optimum molar ratio of 1:30 (reactive orange 4 to H_2O_2). Almost 76 % reduction in TOC was achieved in 60 min of treatment time when combining HC with ozone at an optimum ozone feed rate of 3 g/h. The synergetic coefficient of 3.87 indicates that the combination effect of HC and H_2O_2 was more dominant to achieve the higher decolorization efficiency due to the generation of more number of free radicals as compared to the individual techniques.

Patil and Gogate [42] investigated the degradation of methyl parathion using the combination of HC (used orifice as a cavitating device) and Fenton's reagent. They have observed that on increasing the ratio of $H_2O_2:FeSO_4$ from 1:0.5 to 1:4, at fixed hydrogen peroxide concentration as 100 mg/L, the extent of degradation increases from 78.5% to 93.8% and also achieved the maximum 76.6% of mineralization at an optimum conditions as compared to only 44.4% degradation achieved using HC alone. Bagal and Gogate [53]

Chapter 1: Introduction and Literature Review

considered the degradation of diclofenac sodium by hybrid processes based on HC and heterogeneous photocatalysis. In case of HC only, 26.85% of degradation was achieved at an optimized inlet pressure of 3 bar and solution pH of 4. The degradation efficiency was increased to 95% and achieved 76% reduction in TOC when HC is combined with Ultra-violet/Titanium dioxide/hydrogen peroxide.

Raut-Jadhav et al. [56] have also studied the degradation of imidacloprid in water using a combination of HC with various AOPs such as Fenton, photo-Fenton, photolytic and photocatalytic processes. The venturi was used as a cavitating device in this study. In HC with fenton process, complete degradation was obtained at lower molar ratio of fenton to H_2O_2 i.e. 1:20 in 15 min of treatment time with a synergetic index of 3.636 which indicates that the combination effect of HC and Fenton can effectively generates higher radicals as compared to the individual processes. In HC with photo-Fenton process, again the combination effect produces higher degradation of 99 % in 15 min than obtained in individual processes with a synergetic effect of 2.912. In HC with photolytic process, only up to 45% degradation was achieved and they observed that the degradation efficiency may increase if UV source is placed at cavitation zone rather than to put it outside the cavitator. Thus the synergetic effect of this combination was found to be lower than obtained in previous two combinations. In HC with photocatalytic process, the synergetic effect obtained was low as compared to other combinations because the cavitation effects were insufficient to increase the catalytic activity of Nb_2O_5 . Thus, the combination of HC with Fenton process was found to be more energy efficient for complete degradation of imidacloprid as compared to other techniques as the synergetic effect was higher in HC with Fenton than the other combinations.

HC has proven its capability in generating an intense cavitation condition identical to AC and on the other hand it can process higher volume as compared to AC. It is evident from the above studies that HC has a potential in the reducing the adverse effect of various other water pollutants as its induced effects are effectively capable of degrading them. Also, various other AOPs can be combined with HC in order to increase its performance and efficiency. The technique can be established as a pretreatment in reducing the high load of complex organics and also for increasing the biodegradability of real industrial effluent as is evident from the previous reports and thus it has a great scope to be used as a treatment and/or pre-treatment technique prior to conventional biological treatment so that the efficiency of conventional

Chapter 1: Introduction and Literature Review

processes may be enhanced many fold. It can be concluded that the bio-refractory pollutants from waste streams can be degraded successfully using HC and it is feasible to scale up HC on an industrial scale of operation as it is found to be more energy efficient technique. The overview of work done in the area of HC process to wastewater treatment in recent years is shown in Table 1.1.

Chapter 1: Introduction and Literature Review

Table 1.1: Overview of work done in the area of HC process to wastewater treatment in recent years

Types of pollutants/ chemicals present in wastewater	Cavitating Device	Type of equipment and experimental details	Optimized parameters	Important Findings	Ref.
I. Dyes					
Acid Red 88	Venturi	HC reactor: 15 L tank capacity, control valves, power of pump 1.1 kW, cooling jacket to maintain the temperature, volume of solution 4 L	Inlet pressure = 5 bar; pH of solution = 2.0; Cavitation number = 0.3; Concentration of dye = 100 μ M; concentration of H ₂ O ₂ : 4000 μ M; molar ratio of dye to H ₂ O ₂ = 1:40	HC only: About 92% decolorization and 35% reduction in TOC; HC/H ₂ O ₂ : 100% decolorization, 72% TOC reduction; Cavitational yield in HC was 13 times higher than acoustic cavitation, Process time = 120 min Cavitational yield for HC = 8.97×10^{-10} gmol/J	Saharan et al. [26]
Reactive Red 120	Venturi	HC reactor: 15 L volume of tank capacity, two types of venturi (first made from acrylic for photographic study second made from brass metal), control valves, power of pump 1.1 kW, cooling jacket	Inlet fluid pressure = 5 bar; Cavitation number = 0.15; Solution pH = 2.0; Optimum concentration of H ₂ O ₂ = 2040 μ M	HC only: Almost 60% decolorization and 28% TOC removal; HC/H ₂ O ₂ : 100% decolorization and 60% reduction in TOC; Photographic study, Choked cavitation occurs higher operating pressure (more than the 5 bar); Treatment time = 180 min	Saharan et al. [1]

Chapter 1: Introduction and Literature Review

Orange-G	Circular Venturi Slit Venturi and Orifice Plate	HC reactor: 15 L tank size, control valves, power of pump 1.1 kW, cooling jacket pump power of 1.1 kW, circular venturi (hole of 2 mm diameter), slit venturi (width 6.0 mm; height 1.9 mm; length 1.9 mm), orifice plate (1 mm thickness) with 2 mm hole at the center,	Inlet pressure for slit venturi = 3 bar; circular venturi and orifice plate = 5 bar; pH of solution = 2.0; Cavitation number = 0.29 for slit venturi, 0.15 for circular venturi and 0.24 for orifice plate; Orange-G initial concentration = 50 μ M	HC only: Around 92% decolorization rate in case of slit venturi while 76% and 45% decolorization rate for circular venturi and orifice plate respectively; Almost 37% reduction in TOC for slit venturi while 28% and 14% reduction in TOC for circular and orifice plate; Process time = 120 min Cavitational yield = 3.78×10^{-6} mg/J	Saharan et al. [2]
Reactive Orange 4	Venturi	HC reactor: 15 L tank capacity, control valves, pump power of 1.1 kW, cooling jacket, variable frequency drive(VFD) provided to control the motor rpm,	Inlet pressure to the system = 5 bar; pH of solution = 2.0; Initial concentration of dye = 40 ppm; Molar ratio of dye to H ₂ O ₂ = 1:30 Feed rate of ozone = 3g/h	HC only: 37.23% decolorisation, 22.22% reduction in TOC; HC/H ₂ O ₂ : Nearby 99.56% decolorization and 50.73% reduction in TOC, Synergetic coefficient of 3.87; HC/ozonation: around 76.25% TOC removal in 60 min time of treatment, Synergetic coefficient of 3.03; Cavitational yield = 12.36×10^{-6} mg/J, processing time = 120 min	Gore et al. [41]

Chapter 1: Introduction and Literature Review

C.I. Reactive Red 2	Venturi	Water jet cavitation: reactor capacity 5 L, an electric power of 0.75 kW and speed of 2900 rpm, pressure gauges, inside diameter of line 15 mm, venturi made from organic glass	TiO ₂ loading = 100 mg/L; pH of solution = 6.7; Initial concentration of dye = 20 mg/L	HC only: 76.6% decolorization; HC/TiO ₂ : Around 98.8% degradation; Treatment time = 90 min,	Wang et al. [13]
Rhodamine B	Venturi and orifice	HC reactor: tank capacity of 15 L, reciprocating pump power of 1.1 kW, orifice plate thickness 25 mm with a single hole of 2 mm diameter, pressure gauges, control valves	Inlet pressure = 4.84 atm; Temperature = 35°C; Initial concentration of pollutants = 10 ppm; Solution pH = 2.5; Concentration of H ₂ O ₂ = 200 mg/L; FeSO ₄ :H ₂ O ₂ = 1:5 Amount of CCl ₄ = 1 g/L	HC only: 59.3% degradation, 30% reduction in TOC; HC/H ₂ O ₂ : 99.9 % extent of degradation and 55% TOC reduction; HC/Fenton: 100% degradation and 57% reduction in TOC; HC/CCl ₄ : about 82% degradation, 34% TOC reduction; Treatment time = 120 min;	Mishra and Gogate [40]
Reactive brilliant red K-2BP	Venturi	Swirling jet cavitation reactor: tank of 40 L	Initial concentration of dye = 20 mg/L; Fluid	HC only: around 14% removal of dye HC/H ₂ O ₂ : maximum degradation of 98%	Wang et al. [50]

Chapter 1: Introduction and Literature Review

		volume, centrifugal pump power 3.5 kW with 3000rpm, swirling chamber length of 100 mm and diameter of 10 mm, flow rate of water fixed about 3.6 m ³ /h	pressure = 0.6MPa; pH of aqueous medium =5.5; Temperature of aqueous medium = 323 K; H ₂ O ₂ concentration = 300 mg/L	Process time = 120 min	
Orange acid-II and Brilliant green	Orifice	HC reactor: reciprocating pump with power rating of 1.1 kW, orifice plate with diameter 25 mm and a hole inside of 2 mm, Control valves and pressure gauges are provided to control the flow rate	Temperature = 20°C; initial dye concentration = 20mg/L; inlet pressure = 5kg/cm ² ; solution pH= 3; Amount of H ₂ O ₂ = 571.2 mg/L for orange acid II and 244.8 mg/L for brilliant green	HC only: 34.2% extent of decolorization and 27.3% TOC removal for orange acid II HC/H ₂ O ₂ : the extent of degradation 96% in case of orange acid II while the extent of decolorization 86% for the brilliant green; Treatment time =120 min Cavitation yield = 5.67 x 10 ⁻⁶ mg/J	Gogate and Bhosale [44]
II. Insecticides					
Imidacloprid (a systemic chloronicotinoid insecticide)	Venturi	HC reactor: 15 L tank capacity, control valves, positive displacement pump power 1.1 kW,	Inlet pressure to the system = 15 bar ; Initial concentration of imidacloprid = 25 ppm;	HC only: 26.24% degradation of imidacloprid after 15 min of treatment and 10% TOC removal after 3 h; HC/Fenton: 100% degradation and	Raut-Jadhav et al. [56]

Chapter 1: Introduction and Literature Review

		variable frequency drive (VFD) provided to control the motor rpm	pH of solution = 2.0; imidacloprid:H ₂ O ₂ = 1:40; FeSO ₄ .7H ₂ O:H ₂ O ₂ = 1:20	<p>maximum TOC removal of 49%, synergetic index of 3.636;</p> <p>HC/Photo-fenton: around 99% removal of imidacloprid and synergetic index of 2.912;</p> <p>HC/Photolytic: 46% degradation in 120 min of operation;</p> <p>HC/Photo-catalytic: 55% degradation after 2h of treatment;</p> <p>Cavitation yield was higher in case of HC with Fenton process as compared to other combination</p> <p>Cavitation yield for HC = 1.179×10^{-10} mol/J, Cavitation yield for HC/Fenton = 1.41×10^{-9} mol/J</p>	
Imidacloprid (neonicotinoid class of insecticide)	Venturi	HC reactor: 15 L tank capacity, control valves, positive displacement pump power 1.1 kW, cooling jacket to control the liquid flow, pressure	Inlet pressure to the system = 15 bar; pH of solution = 2.0; Cavitation number = 0.067; Imidacloprid Initial concentration of dye =	<p>HC only: 26.5% Extent of degradation;</p> <p>HC/H₂O₂: Around 100% degradation of imidacloprid and 9.65% reduction in TOC in 45 min; Synergetic coefficient was 22.79;</p> <p>Treatment time = 180 min,</p> <p>Cavitation yield for HC = 1.179×10^{-10}</p>	Raut-Jadhav et al. [57]

Chapter 1: Introduction and Literature Review

		gauges	25mg/L; Ratio of imidacloprid to H ₂ O ₂ = 1:40	mol/J, cavitation yield for HC/H ₂ O ₂ = Cavitation yield for HC = 1.044 x 10 ⁻⁹ mol/J	
Alachlor	Cylindrical Swirling chamber	Swirling jet cavitation reactor: holding tank of 40 L volume, centrifugal pump (3000 rpm, 2.5 kW), chamber length of 100 mm and diameter of 10 mm, flow rate of water 3.6 m ³ /h,	Inlet pressure to the system = 0.6 MPa; pH of solution = 12; Initial concentration of dye = 50 mg/L; Temperature = 40°C,	HC only: The degradation rate constant was found to be 4.90×10 ⁻² min ⁻¹ ; degradation rate increased with an increasing the temperature of medium and the pressure; degradation pathway was also described using gas chromatography-mass spectrophotometer (GC-MS),	Wang and Zhang [9]
2,4-dichlorophenoxy acetic acid	Orifice	Hydrodynamic cavitation reactor: tank capacity 25 L, maximum discharge pressure of 4500 psi, orifice area about 7 x 10 ⁻⁷ m ² , heat exchanger, catalyst bed,	Iron pieces = 150 gm; pH of solution = 2.5; Temperature=20°C	HC/Fenton: The residual TOC was reduced to 30%; Process time = 90 min	Bremner et al. [51]
Dichlorvos	Orifice	HC reactor: reciprocating	Inlet pressure = 5 bar;	HC/Fenton: Maximum extent of	Joshi and

Chapter 1: Introduction and Literature Review

		pump of power rating 1.1 kW, control valves, orifice plate with diameter of 2 mm, flowmeter,	Temperature = 31°C; Solution pH = 3; Dichlorvos initial concentration = 20 ppm; Ratio of Dichlorvos: H ₂ O ₂ = 1:0.8; Ratio of FeSO ₄ :H ₂ O ₂ = 3:1	degradation around 91.5%; energy consumption achieved about 0.074 g/(kJ/m ³); Treatment time = 60 min	Gogate [27]
Methyl parathion	Orifice	HC reactor: reciprocating pump of power rating 1.1 kW, orifice plate of diameter 25 mm with a 2 mm hole inside, control valves, pressure gauges,	Inlet pressure to system = 4 bar; Solution pH = 3.0; Initial concentration = 20 ppm; concentration of H ₂ O ₂ = 200 mg/L; Amount of CCl ₄ = 6 g/L Ratio of H ₂ O ₂ :FeSO ₄ = 1:3	HC only: the extent of removal 45% HC/H ₂ O ₂ : 100% degradation and 56.4% TOC reduction; HC/CCl ₄ : Around 83% extent of degradation HC/Fenton: Maximum extent of degradation 93.4%; treatment time = 60 min Cavitation yield for HC = 4.44 x 10 ⁻⁶ mg/J	Patil and Gogate [42]
Triazophos	Orifice	HC reactor: reciprocating pump of power rating 1.1 kW, orifice plate of diameter 25 mm with a 2 mm hole inside, control	Inlet pressure = 5 bar; pH of solution = 3; initial concentration of Triazophos = 20 mg/L; ratio of	HC only: Around 50% degradation and 30% removal in TOC; HC/Fenton: Almost 83% degradation and 56% TOC removal, synergetic index of 3.34;	Gogate and Patil [52]

Chapter 1: Introduction and Literature Review

		valves, pressure gauges,	triazophos:FeSO ₄ :H ₂ O ₂ = 1:4:4; Feed rate of ozone=1.95 g/h	HC/ozonation: 100% degradation in 90 min of reaction time and 96% reduction in TOC	
III. Pharmaceutical drugs					
Carbamazepine	Orifice	Hydrodynamic –Acoustic-Cavitation (HAC) reactor: inner pipe diameter of 10 mm, frequency about 24 kHz and power of 200 W, diameter of orifice plate 12 mm and thickness of 2 mm	Temperature = 25°C, concentration of pollutants = 48.8 µg/L,	HC only: 27 % conversion of carbamazepine; AC only: 33% conversion; HAC: Maximum conversion of more than 96% for 15 min,	Braeutigam et al. [58]
Diclofenac sodium	Venturi	HC reactor: pump of power rating 1.1 kW, control valves, pressure gauges,	Inlet Pressure = 3 bar; initial concentration of diclofenac = 20 mg/L; Temperature = 35°C; solution pH = 4; loading of TiO ₂ = 0.2 g/L; H ₂ O ₂ = 0.2 g/L	HC only: 26.85% extent of degradation; HC/UV: 66% extent of degradation; HC/TiO ₂ : 30.37% removal; HC/UV/TiO ₂ : around 80% degradation and synergetic effect of 1.43; HC/UV/TiO ₂ /H ₂ O ₂ : About 95% extent of degradation,76%TOC removal with synergetic effect of 2.5;	Bagal and Gogate [53]

Chapter 1: Introduction and Literature Review

				LC-MS analysis to identify the byproducts formation during degradation of diclofenac sodium	
levofloxacin hydrochloride	Nozzle	HC mixer: three feed lines for supercritical as CO ₂ , solution and hot N ₂ , three vessels like mixer, precipitator and condenser,	Concentration of levofloxacin hydrochloride = 7.5 mg/ml; temperature = 60°C; pressure = 8 MPa	HC mixer only: A HC mixer was found to be more suitable to intensify the mass transfer between the solution and CO ₂ ; Micronization of the levofloxacin hydrochloride amorphous micro-particles were achieved with diameters lesser than 2.1 μm	Cai et al. [59]
Ibuprofen, naproxen, ketoprofen, Clofibric acid, carbamazepine and diclofenac	Venturi	HC reactor: 3-way valve, two 2 L reservoirs and a Venturi pipe with a constriction of 1 mm height and 5 mm width, The valve is electrically controlled	Pressure = 6 bar; addition of 30% H ₂ O ₂ = 20 ml	HC/H ₂ O ₂ : 23, 19, 99.9, 29, 89, and 99.9 % degradation was achieved for Clofibric acid, Ibuprofen, naproxen, carbamazepine and diclofenac respectively; Treatment time = 60 min	Zupanc et al. [60]
IV. Chemicals					
p-Nitrophenol	Venturi and orifice	HC reactor; Holding tank of capacity 15 L, a centrifugal pump of power	Initial concentration of pollutant = 5 g/L; Inlet pressure = 42.6 psi;	HC only: about 53.4% degradation in case of venturi and 51% removal for orifice; HC/H ₂ O ₂ : 60% extent of removal;	Pradhan and Gogate [22]

Chapter 1: Introduction and Literature Review

		rating 370 W with 2900 rpm, cavitating device made from acrylic,	Solution pH = 3.75; ratio of FeSO ₄ :H ₂ O ₂ = 1:5; H ₂ O ₂ concentration = 10g/L	HC/Fenton: 63.2% degradation using orifice plate; process time = 90	
Chloroform	Orifice	Hydrodynamic –Acoustic-Cavitation reactor: centrifugal pump with power of 1.1 kW, pipe with inner and external diameter of 10 and 12 mm, frequency of 850 kHz,	Orifice plate diameter = 2.8 mm; power = 40 W; Temperature = 25°C	HC only: Total conversions was 7%; HAC: 90% conversion of chloroform and 0.5% conversion per pass; Process time = 30 min	Franke et al. [54]
Alkylarenes	Orifice	HC reactor: tank with 10 L capacity, pump power of 1.5 kW,	Temperature = 35°C; diameter of each hole = 2 mm; flow area = 113.1 mm ² ; Total perimeter of holes = 150.796 mm	HC only: Cavitation yield of terephthalic acid achieved about 60% for the time of 5 h; The cavitation yields in HC for all substrates were found to be more than the acoustic cavitation For p-xylene, cavitation yield for HC = 1.10×10^{-5} mol/kJ	Ambulgekar et al. [61]

Chapter 1: Introduction and Literature Review

Chitosan	Vortex	Swirling cavitation: holding tank with volume of 10 L, control valves and pressure gauges, Jackett used to maintain the temperature	Concentration of chitosan = 5 g/L; temperature = 70°C; treatment time = 3 h; Inlet pressure = 0.3 MPa	HC only: around 89% intrinsic viscosity reduction rate of chitosan; Fourier-Transform infrared spectra analysis confirmed that the monomer structure before degradation of chitosan existed in the subsequent after the degradation of chitosan	Wu et al. [62]
Dimethyl hydrazine	Orifice	HC reactor: holding tank with capacity of 200 L, centrifugal pump of 3.0 kW and 2850 rpm, catalyst chamber, Turbine type flowmeter, flow control valves,	Solution pH = 2.0; initial concentration = 2 mg/L; inlet pressure to the system = 7.8 bar	HC only: The extent of degradation of Unsymmetrical dimethyl hydrazine was found about 98.6%; Treatment time = 120 min; Formic and acetic acid were recognized as oxidation by-products using GC-MS analysis	Angaji and Ghiaee [45]
2,4-dinitrophenol	Orifice	HC reactor: volume of tank with capacity of 15 L, a centrifugal pump of power rating 370 W with 2900 rpm, cavitating device made from acrylic	Inlet pressure = 4bar; temperature = 35°C; pH of solution = 4.0; ratio of 2,4-dinitrophenol: H ₂ O ₂ = 1:5; H ₂ O ₂ :FeSO ₄ ratio = 1:6	HC only: Around 12.4% extent of degradation; HC/H ₂ O ₂ : 21.3% extent of degradation; HC/Fenton: 100% degradation; The formation of intermediate compounds during the degradation of 2,4-dinitrophenol was identified by High Pressure Liquid Chromatography Cavitation yield = 1.25 x 10 ⁻⁶ mg/J	Bagal et al. [63]

1.2.5 HC reactors

As discussed, HC was found a suitable and efficient technique in the degradation of bio-refractory pollutants from water in order to treat the waste discharges. It is the generation of intense cavitating condition in terms of high magnitude collapse in cavitating devices which effectively produced a large amount of hydroxyl radicals that are responsible in decomposition of such toxic water pollutants. The desirable physical and chemical changes that are induced during the degradation of pollutants greatly depend on the constructional and designing aspect of the cavitating devices. The throttling can be created using various devices such as venturi, orifice, high speed rotor and homogenizer etc. Also, the operating parameters such as pressure, cavitation number, and flow rates are also important in achieving the higher extent of degradation. Although these conditions vary with different throttling devices but the phenomena is same where the sufficient throttling transform the liquid in fine vaporous or vapour-gas cavities and leads to the generation of hot spot condition on collapse which in turn produces the highly reactive radicals. Many studies have reported these devices and have analyzed their effect on the pollution degradation efficiency.

Orifice and venturi based HC reactors are found as most efficient in creating an intense cavitation condition. The cavitation occurs in orifice is transient in nature and generate high intensity cavity collapse due to the presence of larger fraction of transient cavities. On switching the configuration of orifice from single hole to multiple holes, the cavitation intensity can be increased as shear area developed around the orifice edges will be more in the case of multiple holes. However, multiple hole orifice plate causes an increase in the pressure drop which resulted into high pumping cost. Similarly, in venturi, the geometry and its shape provides a substantial variation in flow in the convergent and divergent section instead of sudden contraction and expansion as expected in orifice. For a venturi, the pressure recovery is nearly linear. However, in orifice flow the pressure recovery profile is slightly fluctuating causing rapid oscillation and thereby producing transient cavitation. Due to the smooth recovery of pressure in the downstream section, the cavities get enough time to remain in low pressure region to grow up to their maximum size before their collapse and therefore, the intensity of collapse of cavitation bubbles in venturi is lesser than that in an orifice. Thus the cavitation occurring in venturi is stable in nature and beneficial for the application like in wastewater treatment where the pollutant molecules need higher exposure time in cavitating condition for their complete mineralization. The HC can also be generated using devices such as high speed homogenizer by adjusting the rotation speed and its

geometry where sufficient throttling reduces the local pressure below or equals the vapor pressure of the flowing liquid. But this device is unable to produce an intense cavitation condition for generating the spectacular impact of the induced effects. Also, the flexibility of controlling the cavitation intensity is much less than that of the venturi and orifice [64]. Although some kind of high speeds rotors are well applicable in the wastewater treatment and provide better efficiency towards the reduction of organics load from water [65]. Some other devices such as high pressure homogenizer can also create the cavitation condition but as compared to the orifice and venturi based devices, these devices are not found suitable in generating high intensity of cavitation as required by the pollutant molecules present in aqueous effluent which needs cavitation exposure for a longer duration.

Many studies have been reported the use of various types of devices and have proposed the different kinds of HC set up that can be used on industrial scale for the treatment of wastewater. These HC setups can be an alternative to the conventional treatment methods which are not much efficient in terms of degradation efficiency and energy consumption. Moreover, HC reactor has higher potential in processing the large volume of waste in a continuous mode. In venturi and orifice based HC devices, Saharan et al. [2] have developed an HC reactor set up for the degradation of Orange-G dye as shown in Figure 1.2. The proposed set up mainly consist a feed tank with 15 L capacity, pump of power 1.1 kW, and the suction side of pump is attached to the bottom of the tank. The single hole orifice, slit and circular venturi was used as cavitating device in the set up to study the degradation of dye. The pump discharges the effluent into two lines, (i) main line that consists of a flange to accommodate the cavitating device (ii) bypass line to control the liquid flow. The inlet pressure (P_1) and fully recovered downstream pressure (P_2) are measured by providing pressure gauges. In their study, they have found that slit venturi was found as an optimized geometry for degrading the large quantum of dye molecules. Using slit venturi having a flow area of 11.4 mm^2 , at optimum pressure of 3 bar, more than 90% of decolorisation was achieved which was found higher than using circular venturi and orifice (flow area 3.14 mm^2 each) where the decolorisation was 76% and 45% respectively at optimum pressure of 5 bar. The cavitation number obtained using slit venturi was 0.29, using circular venturi was 0.15 and using orifice was 0.24. The maximum degradation obtained in case of slit venturi was attributed to the fact that the slit venturi has higher shear area than circular hole and thus produces higher cavitation yield and degradation rate. They have further suggested that the induced chemical effects for the degradation of such colored pollutants can be controlled by

manipulating the operating conditions as well as geometrical configuration. Some other studies have also employed similar configuration of the HC set up with different cavitating device for the degradation of various other organic pollutants from water [41, 56-57].

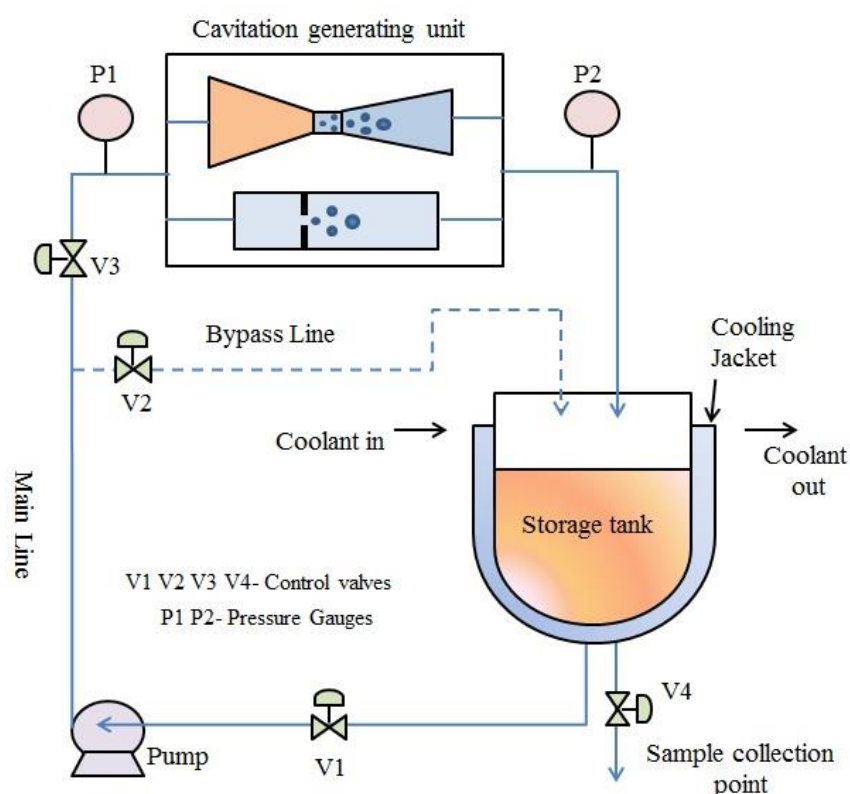


Figure 1.2: Schematic diagram of the orifice and venturi based HC Reactor.

Chakinala et al. [39] have proposed a new kind of a reactor which was named as LWR (liquid whistle reactor) which includes an orifice unit followed by a horizontal blade which helps in increasing the extent of cavitation thereby to enhancing the degradation rate of the pollutants. The orifice having a flow area of 0.774 mm^2 whereas the blade (length: 26.8 mm; width: 22.2 mm and thickness: 1.5 mm) is placed at some adjustable distance downstream of the orifice. The effect induced by the blade was supposed to be equivalent to the use of two orifices in sequence which thereby increases the extent of cavitation. The flow process also consist a feed tank of capacity 5 L and pump of power 3.6 kW (speed of 1750 rpm) with pressure and flow measuring devices as shown in Figure 1.3. In order to combine HC with fenton, a reaction chamber consists of iron pieces are placed just after the cavitation chamber. The proposed set up was used to treat the real industrial effluent. The effluent (effluent

characteristics were not mentioned) was processed through cavitation chamber at fixed flow rate of $8.67 \times 10^{-5} \text{ m}^3/\text{s}$ under the high pressure range of 700-1500 psi at pH 2.5. The higher pressure was favoring the system as is evident from the maximum reduction in TOC and COD obtained at higher discharge pressure. The TOC reduction was increased from 39% to 51% on increasing the pressure from 700 psi to 1500 psi and similarly, the maximum reduction in COD was obtained as 65% at 1500 psi. In the presence of other oxidants such as H_2O_2 , there was a marginal reduction in TOC with corresponding 85% of COD reduction. On processing another effluent 2 (effluent characteristics were not mentioned) at the optimum conditions, maximum 60% of TOC was removed in 100 minute of operation whereas the COD was reduced by 80% . At a loading of H_2O_2 at 1900 mg/L, the TOC and COD were removed to 70% and 85% respectively and simultaneously 100% decolorisation was achieved. The study show that the efficiency of the reactor system greatly depends not only on the operating conditions but it significantly depends on the physio-chemical characteristics of effluent also. Thus, the combination of such reactor with advance Fenton process was found to be more effective in the treatment of industrial wastewater.

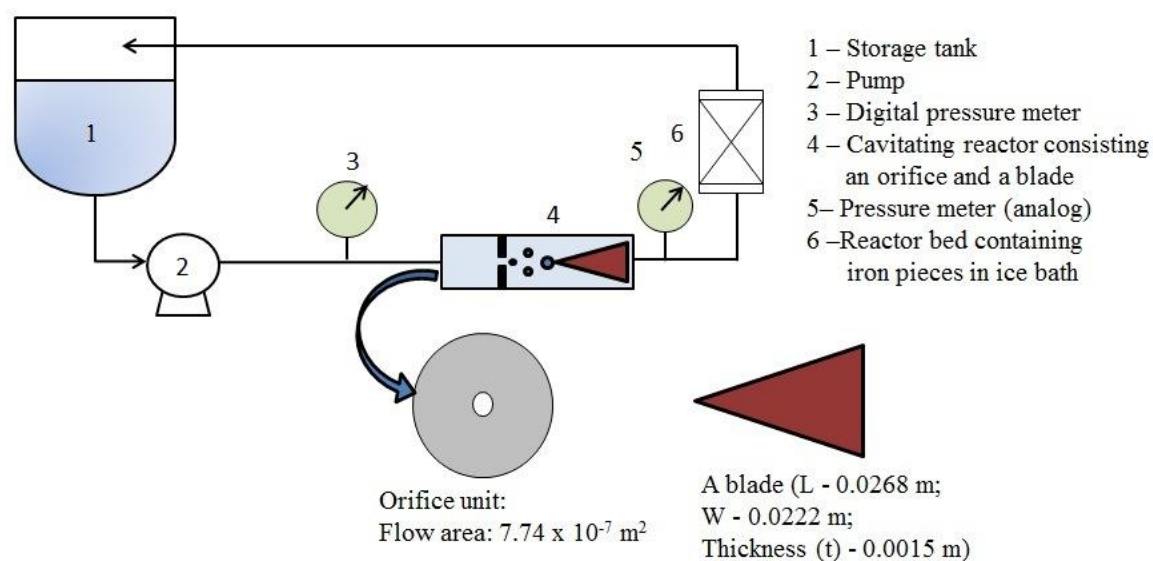


Figure 1.3: Schematic representation of the experimental set-up showing liquid whistle reactor in combination with advanced Fenton process.

To increase the extent of cavitation, an experimental setup comprising a HC and an ultrasonic unit was proposed by Franke et al. [54]. In their proposed setup an orifice unit was combined with an ultrasonic horn to measure its effectiveness based on the degradation of

Chapter 1: Introduction and Literature Review

chloroform from water as shown in Figure 1.4. In the experimental set up, a pump of capacity 1.1 kW was used to transport the liquid in lines. The orifice plate with different flow areas as shown in Figure 1.4 and an ultrasonic transducer unit having the electrical power of 120 W, 850 kHz frequency and acoustic power of 40 W was used to generate cavitating condition for producing the desired transformation. The different orifice configurations produced large number of transient cavities and in the acoustic field. These nuclei undergo more violent collapse in the acoustic pressure field. This combination could produce higher cavitation yield which eventually increases the degradation capacity of chloroform as a pollutant. Also, due to its continuous mode of operation, this hybrid technique (HAC) can be used on an industrial scale for wastewater treatment. In hybrid method, at the higher flow area of orifice, the conversion of chloroform was less. The optimum flow area was found as 6.16 mm^2 which induces a sufficient fluid velocity and consequently results into more than 90% conversion in 30 minute of operation. The individual techniques were not efficiently giving desirable outputs especially, the orifice device which reaches up to only 7% extent of conversion and ultrasonic treatment reaches up to 70% conversion in 30 minute if used alone whereas the hybrid method was 73% better than the sum of the individual methods per pass.

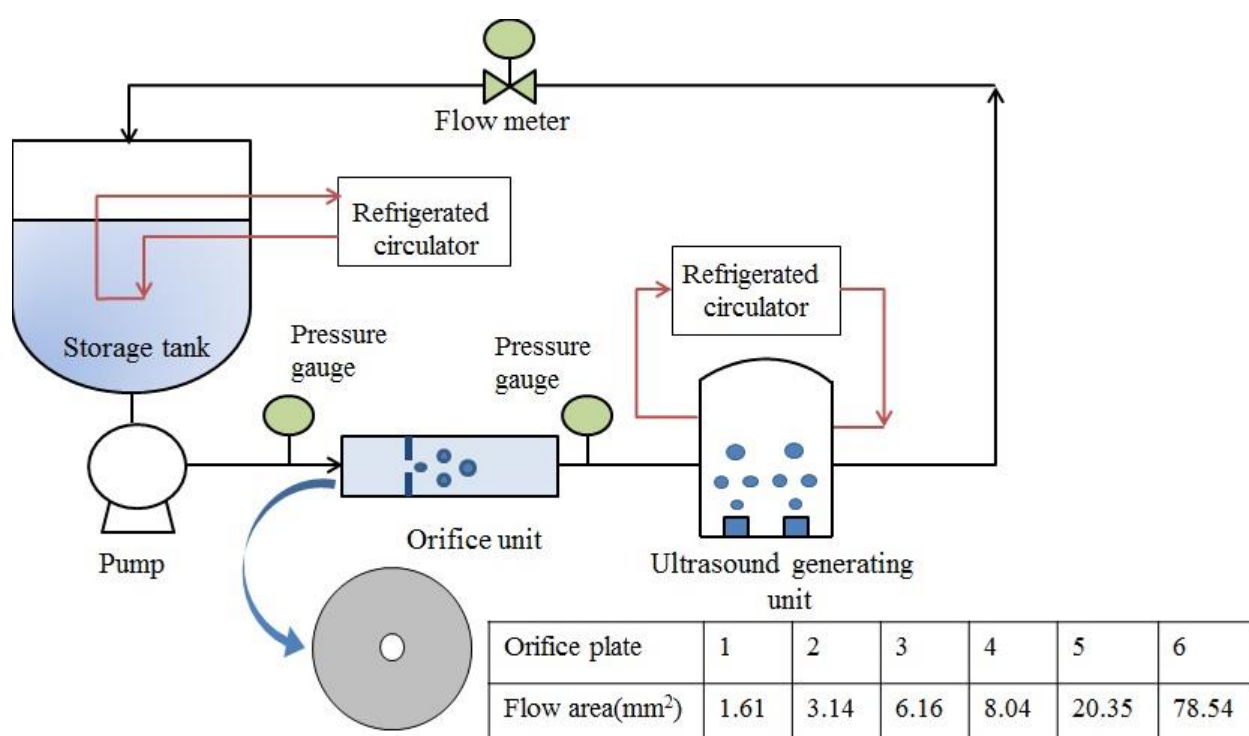


Figure 1.4: Schematic representation of the hydrodynamic acoustic cavitation Reactor.

Gogate et al. [55] have used a patented technology known as Ozonix reactor that utilizes the synergetic effect of ozone, HC, AC and electrochemical oxidation in the treatment of various types of effluent. The purpose of establishing such a technique was to increase the generation rate and amount of hydroxyl radicals and reduce the mass transfer resistances due to the turbulence generated under cavitating condition. The reactor mainly consists three sections as shown in Figure 1.5. The water effluent first flows through the static reactor where cavitation occurs using multiple orifices that are placed in series. The effluent is then passes through the main ozonix reactor where multiple transducers are fixed in the line to create an intense cavitating condition in the AC zone and simultaneously ozone is also injected in this zone to increase the extent of oxidation rate and finally it passes through the electrochemical reactor for further treatment. In the initial stage, HC initiates the oxidation process by generating the large quantum of hydroxyl radicals due to multiple orifices in series thereby breaking large pollutant molecules into the smaller intermediate molecules. Later in the second stage a very high intense cavitation condition is created due to multiple transducers are connected in the flow line as well as ozone gets dissociated into more reactive hydroxyl radicals [17] under intense cavitation condition which causes complete mineralization of generated intermediates into end products. In the final stage electrochemical method is applied to remove the ionic impurities. In the acoustic zone, the level of high turbulence is also created using multiple transducers attached on the reactor wall which can significantly enhance diffusion of ozone gas bubbles. The main reaction (oxidation) occurs in the AC region where the pollutant molecules get degraded and vanishes under the effect of extraneously generated radicals which are produced due to the combined effect of cavitation and ozone. This suggested technique is well applied in the treatment of saline wastewater, disinfection of water in food industries, ballast water, sludge control in biological processes etc. This hybrid technique was found superior in complete decolorisation, reducing the load of organic pollutants, bio-refractory pollutants and eventually its treated effluent meets the required norms for the water quality. It is 98% efficient in the disinfection of water. Overall this technique was able to improve the water quality of discharge from industries as well as from other sources and thus it has attracted the focus of many researchers to implement it as a future technique for the wastewater treatment.

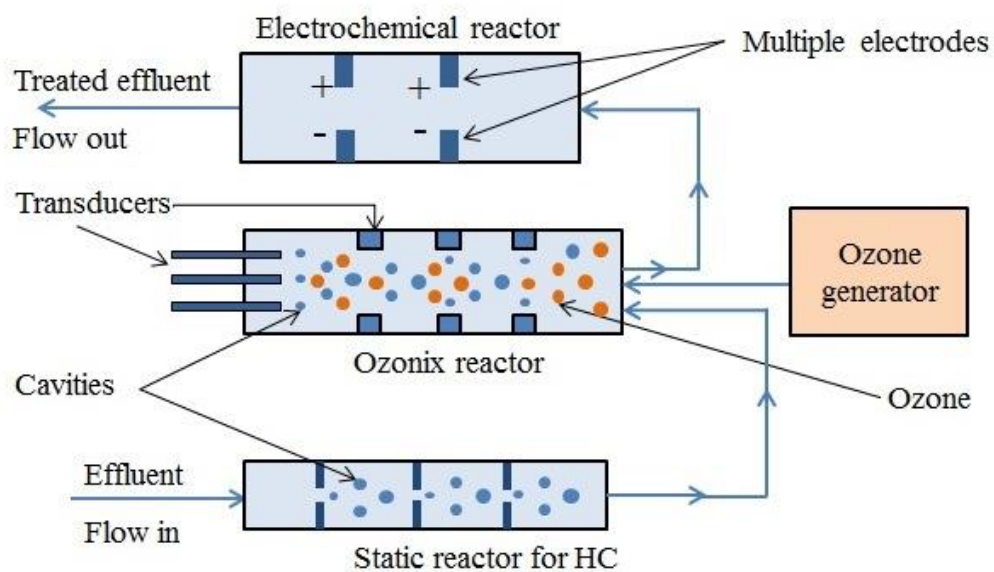


Figure 1.5: Schematic diagram of the Ozonix reactor.

Badve et al. [65] have established a new type of HC device comprising of a stator and a rotor assembly for creating a cavitation condition similar to the device such as high speed homogenizer. The liquid flows in the annular region (between stator and rotor) and passed through the indentations provided on the rotor surface as shown in Figure 1.6. Due to high speed of rotation, a high surface velocity is created at the rotor surface and the liquid discharge from indentations in the form of cavities where the vacuum is created near the upper surface of indentations and results into cavitation. This high speed rotation leads to develop a better cavitation condition and enhances the generation of hydroxyl radicals due to the generation and participation of large number of cavities in the process. The magnitude of the cavity collapse was increased by providing hundreds of indentations which results into an active cavitation. When this device was applied in the treatment of wastewater generated from wood finishing industry, it successfully reduces the load of organics and other volatile compounds from the wastewater to a maximum extent. The parameter such as high speed of rotation, residence time, and presence of oxidants (H_2O_2) was found to greatly affect the extent of degradation. The reactor favors high speed of rotation where at an optimum speed of 2200 rpm, the cavitation number was found as 0.4 which is the indication of the occurrence of intense cavitation and thus the COD was reduced to 49%. This optimum speed gave enough time for the molecule to get attacked by the hydroxyl radicals in order to get oxidized. On increasing the number of passes, the degradation rate was found to increase. The maximum reduction in COD was found as 56% after 195 passes (half open valve) which

was higher than obtained after 270 passes (fully open valve) and 160 passes (1/3rd open valve). In half open valve condition the molecules get enough exposure or residence time to interact with hydroxyl radicals and oxidized. In the fully open condition, there was a possibility of the occurrence of choked cavitation which reduces the intensity of collapse and consequently reduces the extent of degradation. The efficiency of the reactor was also tested based on its combination with oxidants such as H₂O₂ and they observed that at an optimum loading of 5 g/L of H₂O₂, the COD reduction enhances to 80% in 20 minute of treatment time and the cavitation yield found 1.5 times higher than obtained in the absence of H₂O₂. Thus, as evident from this study, the devices other than venturi and orifice, can also deliver the desirable effects in order to minimize the capacity and toxicity of such organics and other toxic substances from water.

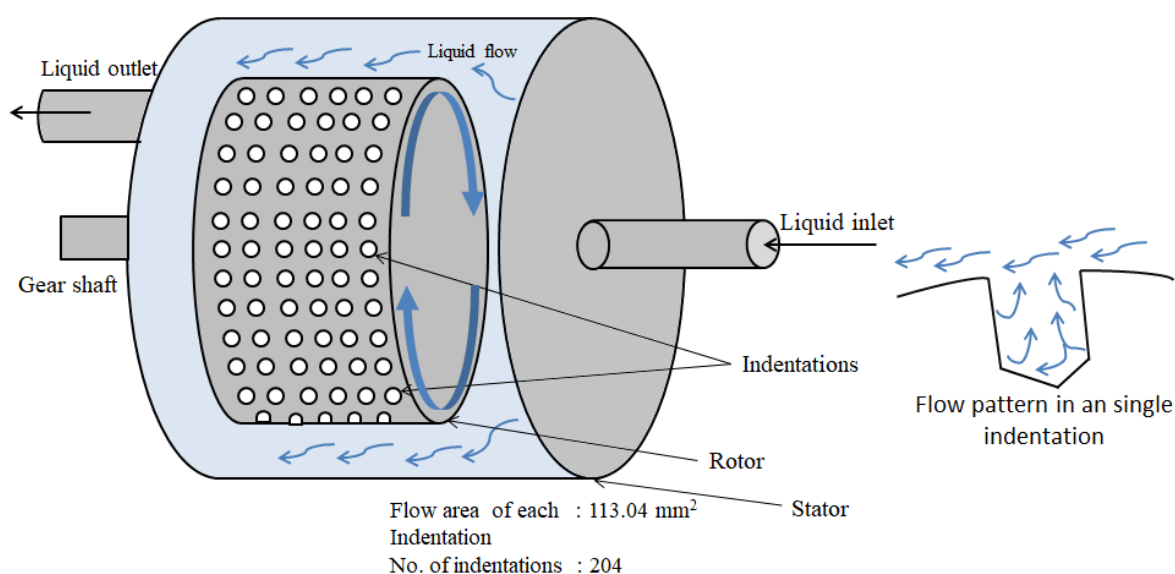


Figure 1.6: Schematic diagram of the high speed rotor.

HC can also generated by using swirling jet phenomena as proved by Wang et al. [50] in their study. They have proposed a swirling jet cavitation chamber for the degradation of reactive brilliant red K-2BP dye and analyzed its applicability on an industrial scale. The reactor as shown in Figure 1.7 mainly consist a cylindrical swirling chamber that was placed concentrically in a combined chamber. The water pumped into the combined chamber and then gets injected into swirling chamber through tangential injection port and a vortex is formed in the swirling chamber. Due to the formation of vortex, a swirling jet is formed which reduces the local pressure below the vapor pressure of water and produces cavitation.

On ejection of swirling jet from the cavitation chamber, the pressure rapidly increases which leads to a condition of adiabatic collapse. During the experimentation, the high pressure, high temperature and low pH conditions were favoring for the degradation of K-2BP dye where 97.2% of degradation was achieved at higher inlet pressure of 0.6 MPa, temperature of 323 K and pH at 2.0.

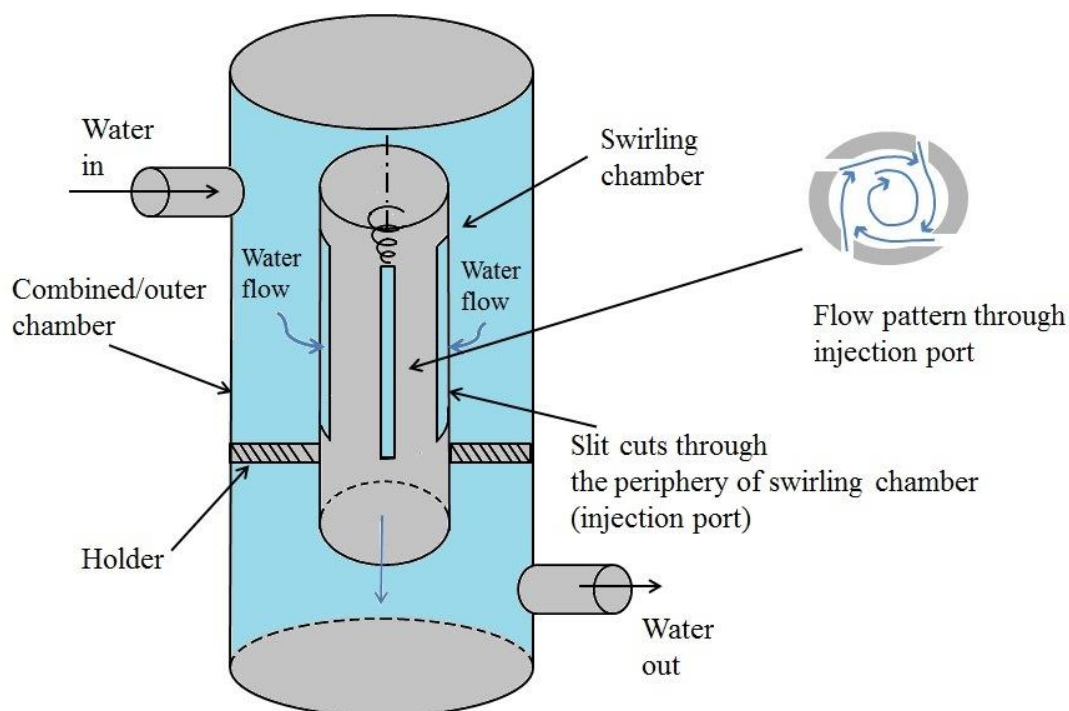


Figure 1.7: Schematic diagram of the swirling jet reactor.

As evident from these reported studies, the cavitation can not only be generated by the orifice and venturi based devices but also the devices based on high speed rotation, swirling jet reactor etc. are capable of generating the cavitation condition that can induce the desirable effects, gives higher exposure time for the pollutant molecules in the cavity collapse region for their complete mineralization. All these HC reactors are very efficient in terms of better degradation efficiency, energy consumption, less maintenance, easy to couple with other AOPs to produce the desired outputs in the area of wastewater treatment. The effects of geometrical and operating parameters are important in improving the performance and the efficiency of these reactors. The better design based on optimization of various geometrical and operating parameters can give better efficiency towards the desirable results in the wastewater applications. These geometrical and operating parameters are being discussed in further section.

1.2.6 The effect of various geometrical and operating parameters on the degradation efficiency of HC reactor

1.2.6.1 Geometrical aspects of cavitating device

As discussed in the previous sections, various HC reactors have been investigated by many researchers for their applicability on wastewater treatment and also suggested their implementation on industrial scale to degrade the pollutants from water. Thus, it is very important to account for the geometrical aspect for designing of such reactors. Most of the studies have reported and discussed the effect of geometrical parameters of venturi and orifice based devices and only few studies have reported the use of high speed rotor. Therefore, in this section we have only discussed the effect of geometrical parameters of venturi and orifice based devices on the wastewater treatment applications. The geometrical parameters play an important role when the focus is on achieving the higher cavitation yield for producing the desirable transformation. For an optimum cavitation yield, the parameters such as number of cavitation events, cavitation intensity, the residence time of the cavities in a low pressure region and the pressure recovery rate in the downstream section are very important [68]. These parameters are significantly depend on the geometry of the cavitating device. In case of venturi, it may be a rectangular, elliptical, and circular in shape whereas in case of orifice it could be a single orifice and multiple orifices with throat of different shape. These conditions act as a controlling factor for creating an intense cavitation and thus it becomes important to study the effect of these parameters and to measure their dependency on the cavitation activity.

1.2.6.1.1 Geometrical parameters of orifice

As discussed earlier, due to the generation of transient cavities and high intensity collapse, orifice was found to be as a suitable and capable device that can mineralize the pollutant present in water as evident from many previous studies. The possible variation in geometry of orifice such as varying number of holes, size and shape of orifice can be a better approach towards achieving higher cavitation yield. The orifice becomes a better option to use it as a cavitating device not only in the application of wastewater but in other application also, such as biodiesel synthesis, emulsification, disinfection etc [69-71]. Sometimes multiple holes in an orifice plate can deliver high intensity collapse than single hole orifice for the same flow area since more shear area is developed in the case of orifice having large number of holes which result into the generation of large number of cavities. The other parameters

such as ratio of the perimeter of throat to its cross section area (α) and ratio of throat area to pipe cross section area (β) have also shown their dependency on the generation of active cavitation and high magnitude of collapse pressure. These parameters are prominently affecting the cavitation activity inside the cavitation chamber i.e. the number of cavities being generated and their final collapse pressure. Many studies [28, 69-70, 72] emphasize on maximizing the value of α in the different area of applications. But in wastewater applications, only few studies have been reported on the effect of these parameters. Sivakumar and Pandit [28] have found that on increasing the α from 0.8 to 4 mm⁻¹, the rate constant increased by 100% which shows that the degradation of Rhodamine B was favoring at higher value of α and they also observed that the extent of degradation increases with decreasing the value of β and found the maximum degradation rate with plate having lower value of β (0.023).

The optimization of the geometry and the flow conditions was done based on the frequency of turbulence (f_T). For a given cross section area, the f_T was higher for the larger perimeter of holes i.e. the large number of holes in small size. This configuration provides more shear layer area generating larger number of cavities and it also increases the intensity of turbulence. Thus, the increasing trend of f_T leads to the more efficient cavity collapse and reaches highest peak of cavitation yield. Ultimately these parameters are dependent on the operating cavitation number and therefore on the velocity of flowing liquid at the throat.

Thus, in order to design a suitable device for the required application, it is necessary to optimize the cavitation number along with these geometrical parameters (α and β). The throat area should be decided based on throat velocity and volumetric flow rate which can give the required cavitation number. The higher α value should be used to get better cavitation yield for a required cross sectional area.

1.2.6.1.2 Geometrical parameters of venturi

The capability and suitability of venturi as a cavitating device is being explored in the last few years as it efficiently generate stable cavitating conditions which are beneficial for the wastewater applications requiring cavitation exposures for a longer duration. Also venturies are known to generate more number of cavities than orifice plate. In venturi, the size and shape of the throat and convergent section mainly affects the number of cavities being generated and its dynamic behaviour. Further, the maximum size reached by the cavities and their life depends on the shape of the divergent section. The shape of the

divergent section prevents early cavity collapse which results into higher growth of cavities to its maximum size before their more violent collapse. Due to the smooth convergent section before the throat, the venturies are proved to be better than the orifice plate in terms of generating the higher cavitation events at the throat as well as the use of lower amount of energy.

A computational study conducted by Mahulkar and Pandit [73] have proved that in case of an orifice plate the cavities are grown only at the edge of the orifice (perimeter), whereas in venturi the entire throat is filled with the cavities which signifies the advantage of venturi over an orifice. Further, higher cavitation yield can be achieved by varying the shape and size of the throat and the divergent sections of venturi. Saharan et al. [2] in their study have proved that the venturies are more efficient than orifice in degrading the orange-G dye. The slit and circular venturi gives higher degradation than orifice at optimum operating conditions. This was attributed to the fact that in case of venturies, the cavitation number was lower than the orifice for the same pressure drop across the cavitating device. Also, in both the venturies, the energy dissipated in the form of cavitation per unit energy supplied to the pump was higher than in the orifice and hence venturies generates more number of cavities than the orifice plates which ultimately results into higher degradation rates. They have further concluded that the slit venturi was more efficient than the circular venturi due to higher value of α (perimeter to cross sectional area ratio) than the circular venturi. Also, the geometrical parameters such as the throat shape, ratio of throat height/diameter to its length and convergent and divergent angles are important and become necessary to account them during the designing of a venturi.

(a) Throat area

As the throat is an important parameter, its cross section and perimeter ratio may greatly affect the generation rate of cavities. For a given cross sectional area, higher perimeter generates more cavities and therefore rectangular and elliptical shapes of the throats are desirable rather than a circular throat. It is reported that the net pressure drop for a given flow rate is higher in circular cross-section as against elliptical and rectangular cross-section for the same cross-sectional area [2]. Saharan et al. [2] have studied the degradation of orange G using three cavitating devices such as slit venturi, circular venturi and circular orifice plate. They have reported that the decolorization rate and the % decolorization per pass are higher in the case of slit venturi as compared to the other two cavitating devices. They have reported that in the case of slit venturi, a higher volumetric flow rate was obtained for a given pressure

drop as compared to orifice plate and circular venturi. The higher dissipated power ($\Delta P \times Q$) in the case of slit venturi enhances the number of cavitation events occurring inside the cavitating device which ultimately resulted in higher cavitation yield. Further, the internal area of the throat is also dependent on the generation and growth rate of cavities. In this instance, it is necessary to optimize the ratio of throat height/diameter to its length. Bashir et al. [68] carried out the CFD analysis of venturi for different slit height to its length ratios such as 1:0.5, 1:1, 1:2 and 1:3. The optimum ratio was found to be 1:1 based on the length of the cavitation zone and the velocity achieved at the throat. A large throat length i.e. beyond a certain limit (1:1) may result into the formation of inactive cavities or simply vapors which will further dissolve into the surrounding liquid without collapsing. A similar observation was also made by Kuldeep et al. [66] and Jain et al. [74]. Chavan et al. [75] have also numerically optimized the convergent/divergent angles and the curvature radii to propose further optimization showing 18 % higher yields over the optimized straight (linear) venturi designs. Thus, as evident from these studies, it is advisable to use the venturi of higher perimeter for a given cross section for getting maximum cavities and the rectangular or elliptical shape of the throat should be preferred over circular throat and also throat length (convergent/divergent angles) should not be higher than the diameter/height of the throat. An optimum value of throat height/diameter to length ratio as 1:1 or there about can be used.

(b) Divergent angle

Another parameter i.e. the divergent angle which can greatly affect the life of cavity and the generated collapse pressure. Bashir et al. [68] have studied the different half divergent angle in range of 5.5° to 8.5° and have optimized the factor based on the obtained cavitation number and density profile in the divergent section. It was observed that on increasing the angle from 5.5° to 8.5° the optimum cavitation number was increased from 0.23 to 0.28. At the lower half, divergent angle, the pressure recovers very smoothly and thus the cavities grow to their maximum size but at the higher angle the venturi tends to behave as an orifice and hence the pressure recovers immediately and results into a rapid collapse. They have found 5.5° as an optimum half divergent angle where the cavities grow to their maximum size before their collapse and give higher length of the cavitation zone. In another study by Jain et al. [74] they have also found 5.5° as an optimum angle for slit venturi and 6.5° for the circular venturi. Some experimental studies (Saharan et al. [2], Saharan et al. [26], Gore et al. [41], Padoley et al. [48]) have also used the same configuration of venturi having half divergent angle of 5.5° for slit and 6.5° for circular venturi to produce desirable

physicochemical changes in wastewater treatment application. Therefore, for a better cavitation yield, it is recommended to use optimum divergent angle in range of $11^{\circ} - 13^{\circ}$ as estimated in the CFD studies [68, 74] and validated through various experimental studies [2, 26]. Chavan et al. [75] defined a cavitation efficacy parameter defined as “Maximum collapse pressure/permanent pressure drop” and maximized the same using numerical studies of venturi CFD and cavity dynamics and have proposed an optimum configurations.

1.2.7 Effect of various operating parameters on the cavitation process

1.2.7.1 Effect of inlet pressure and cavitation number

The inlet pressure and cavitation number are the most important parameters to observe the cavitation intensity inside the cavitating device. These parameters are intercorrelated with each other. The desirable pressure applied to the liquid induces some velocity through the cavitating device. As the operating pressure increases, the velocity increases through the cross section of throat and consequently the cavitation number decreases as per the equation (1.1) which indicates the generation of more number of cavities. The lower cavitation number as a result of high pressure input generates more cavities which would ultimately results into large quantum of hydroxyl radicals. Higher number of $\cdot\text{OH}$ radicals thus generated at lower cavitation number increases the extent of oxidation or degradation of the pollutants but a very low cavitation number i.e. below the optimum value leads to the condition of choked cavitation which has no practical significance. The optimum cavitation number is greatly influenced by the physicochemical properties, chemical structure of the pollutants and geometry of the cavitating device. The variation of these parameters may significantly alter the cavitation number. Thus, it is very important to take account of these parameters to optimize the required cavitation number.

Most of the studies have found different value of cavitation number for different type of pollutant medium. Saharan et al. [1], [26] in their studies have examined the higher degradation efficiency at optimum pressure of 5 bar for the degradation of different dyes with corresponding optimum cavitation number as 0.15 using circular venturi and 3 bar optimum operating inlet pressure with cavitation number as 0.29 using a slit venturi. They have found that on further increasing the pressure i.e. beyond the optimum value, there is a drop in the rate of degradation due to the onset of super (choked) cavitation. The optimum cavitation number found in their studies ranges from 0.14 – 0.29 with operating inlet pressure in the range of 3 – 5 bar depending on the type of cavitating device. Contrary to their studies, Raut-Jadhav et al. [57] have found that the degradation rate of imidacloprid increased with

increasing the pressure up to 15 bar where the cavitation number was 0.067 and no significant increment in the degradation rate was observed at pressure above 15 bar. Such a high optimum value of pressure found in their study may be due to the complexity of the chemical structure and the nature of the pollutant compound which required the exposure to high magnitude of cavitating effects that are induced under high pressure condition. In another study by Padoley et al. [48], during the treatment of methanated distillery wastewater using HC, they have observed maximum reduction in COD and TOC at high pressure of 13 bar. The difference in the percent reduction of COD and TOC achieved at 5 bar and 13 bar were not too high but the BI index increases significantly at higher operating pressure of 13 bar. This was attributed to the fact that high operating pressure is more capable in breaking down the large molecules into smaller molecules which ultimately improves the BOD/COD ratio and thus improves the final methane generation in subsequent anaerobic digestion unit.

Some other studies (Capocellia et al. [38], Li et al. [76]) have also found the cavitation number in the range 0.25-0.5 depending on the type of liquid processed and geometry of the devices. Thus, it can be said that the optimum cavitation number or the condition of super cavitation greatly depends on physicochemical properties of the liquid and also on the geometry of the devices. As evident from these studies, the lower the cavitation number i.e. $C_v < 1$ better it is for treatment of bio-refractory pollutants from water but a care must be taken to avoid choked cavitation condition and a cavitation number between 0.15 – 0.29 is found to be the most favorable condition.

1.2.7.2 Effect of solution pH

The solution pH is an effective parameter that is necessary to optimize the efficient degradation of pollutants using HC. The operating solution pH greatly depends on the nature and state of the substrate (pollutant) molecule i.e. ionic or molecular form. The pH can alter the state of the molecules and depends on the functional group attached to it. In its molecular state it is hydrophobic in nature, the molecules locate themselves at the cavity-water interface and thus are more readily attacked by $\cdot\text{OH}$ radicals since the concentration of $\cdot\text{OH}$ radicals is higher in the core of the cavity and at the cavity water interface. Whereas, if the molecule is in ionic form it becomes hydrophilic in nature and thus it would remain in the bulk solution and can only react with the residual unreacted $\cdot\text{OH}$ radicals in the bulk liquid where the concentration of $\cdot\text{OH}$ radicals are limited. Therefore, it is very important to identify the molecular structure and functional groups present in the pollutant molecules. In this regard,

Chapter 1: Introduction and Literature Review

Saharan et al. [26] have studied the effect of solution pH on the degradation of Acid Red 88 dye. They have observed higher degradation under acidic condition because AR88 gets protonated under acidic medium due to hydrogen ion attached to sulphonic group SO_3^- present at the aromatic ring. Due to protonation, AR88 molecules become hydrophobic in nature and thus locate itself at the cavity water interface and become more vulnerable to $\cdot\text{OH}$ radicals attack. Thus the maximum decolorisation was achieved at low pH of 2.

Apart from the effect of solution pH on the state and nature of the pollutant molecules, few authors have reported that the reactivity and generation of $\cdot\text{OH}$ radicals can also be affected by changing the solution pH. Wang et al. [77] have studied the effect of pH on the degradation of Rhodamine B at an optimized pressure of 0.6 MPa and temperature of 50°C . Almost 99% degradation was achieved at an optimum solution pH of 3.0 in 3 h of treatment using HC. They have stated that the acidic condition gives higher degradation of Rhodamine B because of higher oxidation potential of $\cdot\text{OH}$ radicals at low pH. On the other hand under basic conditions CO_3^{2-} and HCO_3^- forms which are responsible to scavenge the free radicals and thus basic condition causes a decrease in degradation rate. Similarly, Patil et al. [78] have investigated the degradation of imidacloprid using HC at various pH. It was observed that acidic conditions are more relevant for the degradation of such pollutants due to their higher oxidation potential and higher generation rate of hydroxyl radicals in acidic medium. Therefore, maximum degradation of 23.85% was achieved at a low pH of 3.0. In a similar study by Joshi and Gogate [27], the maximum degradation of dichlorvos was achieved in acidic medium and acidic conditions was reported to be favorable condition since it inhibits the recombination of $\cdot\text{OH}$ radicals and increases the oxidation potential of $\cdot\text{OH}$ radicals. On the contrary a study by Wang et al. [9] has reported that basic pH is more favorable for the degradation of alachlor. The degradation rate increases with increasing the pH from 2.0 to 12 due to the presence of more hydroxide radicals in the solution under basic pH condition which induces more of $\cdot\text{OH}$ radicals under cavitation conditions. On the other hand, the recombination reaction between protons and the hydroxyl radicals could occur as the pH decreases which decreases the concentration of $\cdot\text{OH}$ radicals available for pollutant degradation and hence the degradation rate reduces under acidic condition.

Thus it can be concluded from the above studies that the state of the molecule and molecular structure and its functional groups are very important as they affects the state in which the pollutant molecules present itself in the solution i.e. whether hydrophobic or hydrophilic. Similarly, the reactivity of $\cdot\text{OH}$ radicals may also get affected by the solution

pH. It is necessary to get maximum utilization of generated $\cdot\text{OH}$ radicals by reacting them with the pollutant molecules as soon as they are generated in the collapsing cavity and simultaneously reducing the recombination of these $\cdot\text{OH}$ radicals into H_2O_2 as the later has a much lower oxidation potential. In all, it is important to optimize the solution pH independently for the waste water application in which cavitation is used for mineralization.

1.2.7.3 Effect of temperature

The effect of temperature on the degradation rate is another crucial factor which affects the cavitation yield and thereby the degradation efficiency. The optimum operating temperature is much dependent on the boiling point and the vapour pressure of the pollutant and media. At high operating temperature, the number of cavities formed may be large due to the higher rate of transformation of liquid into vaporous cavities as threshold lower pressure required to vaporize liquid is lower, but these cavities (vaporous bubbles) are not much useful for creating sonochemical effect. Moreover, at a very higher temperature, cavitation bubbles will get filled up through medium vapor with the lowering of viscosity, surface tension and density of the liquid. This reduces the extremes of temperature and pressure conditions generated when the cavities collapse and thereby decrease the degradation efficacy of bio-refractory pollutants [77]. Thus, high temperature conditions can only favor in case of less volatile liquid mixture such as in the degradation of high viscous liquids, slurry mixtures, polymers etc. Wang et al. [77] have investigated the effect of temperature over a range of 30°C to 60°C on the degradation of Rhodamine B using HC and observed higher degradation extent at high temperature due to the formation of large number of cavities which is affected by vapor pressure of liquid. The maximum extent of degradation was found at 50°C but further increase in the temperature leads to the formation of more water vapors which causes choked cavitation condition and thereby reducing cavitation effects. Thus, the temperature was optimized at 50°C for the degradation of such substance. In another study by Wu et al. [62], the maximum extent of degradation of high molecular substance i.e. chitosan was found at high temperature. It was observed that on increasing the temperature from 30°C to 70°C , the degradation was increased from 54% to 89%. This study proves that the high temperature condition depends on the liquid vapor pressure. For liquid having high boiling temperature, a high temperature condition is required in order to reduce the required threshold lower pressure or velocity at the throat to form more number of cavities. A similar trend was also reported by Mishra et al. [40] which favor moderately high temperature condition for the

degradation of Rhodamine B. The degradation extent was increased from almost 58% to 65% on increasing the temperature from 30°C to 40°C. It can be seen that an increase in temperature beyond 30°C has only a marginal effect on % degradation and therefore it would not be an economical option to increase the temperature beyond 30°C for merely a 7% increment in degradation. Some other studies have found the favoring of low temperature conditions for the degradation of water pollutants. Joshi and Gogate [27] have observed a maximum degradation of 13.5% at a temperature of 31°C but on increasing the temperature to 39°C, the extent of degradation was reduced only to 4%. Brautegam et al. [58] have also observed 90% degradation of carbamazepine in water solution at 25°C rather than high temperature conditions but the trend was same i.e. the degradation rate initially increases up to 25°C and then decreased with further increasing in the temperature. This may be due to the fact that initially, at very low temperature i.e. lower than 25°C, the vacuum required at the throat to form vaporous cavities is very high and therefore a very high liquid velocity at the throat is required in order to get a threshold low pressure at a lower operating temperature. Therefore, the inlet pressure needs to be high but with increase in temperature the vapor pressure also increases and thus the cavities can form at lower operating pressure as well at higher temperature.

All in all, it can be stated that a moderate operating temperature in the range of 25 to 45°C should be kept for the treatment of diluted wastewater whereas high temperature may be required for highly viscous wastewater and for the effluent involving less volatile pollutants. Since very high temperature may reduce the final cavity collapse pressure due to the formation of choked cavitating condition. Similarly, on the other hand, to achieve higher temperature more thermal energy needs to be provided and that will add to the operating cost. On the other hand, high temperature will reduce pumping cost as lower operating pressure will be required to create the same cavitation as generated under high inlet pressure and low temperature conditions. Therefore, it is very important to find the optimum condition of temperature and operating pressure considering the heating and pumping cost together and simultaneously choked cavitation conditions should be avoided.

1.2.7.4 Effect of initial concentration

The initial concentration of pollutant molecules is other important parameters which affects the degradation rate of the organic pollutants. It was reported by many studies that the degradation efficiency in terms of % reduction in pollutant concentration is reduced at the

higher initial concentration of the substrate. However, at higher loading of the substrate, if the actual number of moles of the pollutant degraded remains constant for identical operating conditions, then the decolorization follows zeroth order reaction kinetics. Even though, high initial concentrations may increase the probability of pollutant-radical interaction, the overall degradation rate will depend upon the rate of generation of $\cdot\text{OH}$ radicals which is the rate limiting step. Different authors have seen the effect of concentration with different perspective as some author have studied the effect of initial concentration on the degradation rate of pollutant, whereas others have studied the effect of concentration on only % reduction of pollutant level in aqueous effluent. Although, at high concentration of pollutant, the consumption rate of $\cdot\text{OH}$ radicals would be high as compared to the lower loading of pollutant molecule and hence the rate of degradation of pollutants would be high but the % reduction may be lower due to higher loading of pollutants. In this context, Saharan et al. [26] have investigated the effect of initial concentration of AR 88 dye using HC at an operating pressure of 5 bar and pH of 2.0 and found that the rate of degradation increases with an increase in initial concentration of dye from 50 to 150 μM under the first order reaction kinetics. The similar observation was also made in their other study (Saharan et al. [2]) at the concentration range of 30 – 150 μM of orange-G dye. Thus, the degradation rate needs to be reported in terms of moles degraded rather than only percentage degradation.

In this regard, Wang et al. [77] have illustrated the degradation of Rhodamine B at different initial concentration of Rhodamine B using swirling jet reactor and found that % degradation decreased from 98.9% to 63.4% on increasing the initial concentration of Rhodamine B from 10 to 50 mg/L. The similar observation was also made in their study [50] for the degradation of K-2BP using HC. It was observed that on increasing the concentration from 10 to 50 mg/L, the % degradation decreases from 94.2% to 24.7%. In above mentioned studies, if the total quantum of pollutant molecules which gets degraded is calculated, it is seen that though the % reduction gets reduced with an increase in the initial concentration, the actual number of moles of pollutant degraded per unit time per unit volume are higher. Therefore, it is important to observe and report the rate of degradation rather than reporting only the % reduction because the true rate-constant would ultimately decide the size of the reactor and residence time of the pollutant molecule within the cavitation reactor. The reduction in the extent of degradation was due to the fact that the number of hydroxyl free radicals being generated was constant under uniform cavitating conditions irrespective of pollutant concentration. Patil et al. [78] have also observed the similar result where the extent

of degradation of imidacloprid was reduced on increasing the initial concentration from 20 to 60mg/L after 120 min for the degradation of imidacloprid. This was observed to be due to the reduction in the efficiency of generation of $\cdot\text{OH}$ radicals at higher loading of the pollutant.

In all it may be concluded that the concentration should also be decided based on the process requirement of other processes in a treatment facility because higher loading of the pollutant may reduce the efficiency of conventional biological treatment units and advanced treatment processes such as membrane separation, reverse osmosis, ion exchange, etc. and hence the dilution of waste effluent may be required prior to such units. Though, the concentration of pollutant in the case of diluted sample causes the least effect on the efficiency of HC it may be worthwhile to dilute the highly concentrated effluent sample in order to enhance the cavity generation process by varying the physio-chemical properties of the treated samples.

1.2.8 Efficiency enhancement of HC process by combining with various other AOPs (hybrid methods)

HC is an emerging technology and capable to generate highly reactive hydroxyl radicals which has the highest oxidation potential (2.80 eV) for the degradation of bio-refractory pollutants from wastewaters. On combining with other AOPs, HC gives better degradation efficiency as compared to the individual processes. The efficiency of AOPs is strongly dependent on the rate of generation of hydroxyl radicals. The purpose of these hybrid techniques is to increase the generation rate of hydroxyl radicals and thereby the oxidation rate of pollutants. For example, as H_2O_2 cannot easily dissociate into $\cdot\text{OH}$ radicals, but in combination with HC, the rate of generation of $\cdot\text{OH}$ radicals is increased because H_2O_2 may get dissociated at the bubbles interface, due to the higher temperature at the interface (~700-800 K). The combination with HC also increases the mixing and the dispersion of the generated $\cdot\text{OH}$ radicals thereby reducing the recombination reaction rate. Likewise, the cavitation effects eliminate the mass transfer limitations and fouling of the solid catalyst particles during photocatalytic oxidation when combined with HC [17]. Similarly, HC in combination with Fenton's reagent, ozone and other AOPs lead to the complete degradation of bio-refractory pollutants present in the water improving the efficiency of the combined techniques. Different AOPs combined with HC reactor for the treatment of wastewater are further discussed in detail below.

1.2.8.1 HC combined with Fenton process

Fenton's oxidation is a very effective process to treat many industrial pollutants as it involves the application of iron salts and H_2O_2 to produce hydroxyl radicals. Fenton reagent is a combination of ferrous ions, Fe (II) and hydrogen peroxide (H_2O_2) which produces large quantity of hydroxyl radicals ($\cdot OH$) by dissociating H_2O_2 to oxidize the bio-refractory pollutants under low pH conditions [63, 79]. The free hydroxyl radicals are generated through following reaction under the Fenton chemistry [80].



In equation (1.6), a ferrous ion reacts with hydrogen peroxide and forms the hydroxyl radicals. These free radicals are further react with other ferrous ions (Fe^{2+}) to form ferric ions due to the scavenging effect according to equation (1.7).



The subsequent Fe^{3+} ions react with hydrogen peroxide which gives the intermediate complex ($Fe-OOH^{2+}$) as shown in equation (1.8) which further converts into Fe^{2+} and $HO_2\cdot$ as per equation (1.9) under cavitating conditions [81].



Additionally, hydrogen peroxide can directly decomposes into the hydroxyl radicals under HC as shown in equation (1.10):



From the above reactions it can be seen that in the Fenton reaction mechanism $\cdot OH$ radicals are generated via equation (1.6) which further react with pollutant molecules (equation (1.11)) as well as few of them also reacts with Fe^{2+} to give Fe^{3+} (equation (1.7)) which mainly causes the reduction in $\cdot OH$ concentration and therefore reduces the degradation rate beyond a certain concentration of Fe^{2+} . These ferric ions then further react with H_2O_2 to give a complex ion of $Fe-OOH^{2+}$ which is an unwanted intermediates in this reaction. Under the cavitation effect these intermediates are broken into Fe^{2+} and $HOO\cdot$ radicals which further enhances the generation of $\cdot OH$ radicals. In addition to this HC effects also generate more $\cdot OH$ radicals by dissociating H_2O_2 via equation (1.10). Therefore HC coupled with Fenton process gives higher efficiency than the individual process because of

more $\cdot\text{OH}$ radicals are generated under combined effects, though the optimum concentration of FeSO_4 and H_2O_2 in Fenton and Fenton-HC combination may be different.

Many studies have been reported on the applicability and potentiality of Fenton process for the oxidation of different organic pollutants as it is capable in generating higher concentration of oxidizing radicals. The mechanism responsible for its successful applicability on laboratory scale is still facing the challenge for their large scale operations. Because of unpredictable toxicity of wastewater pollutants, it is very difficult to control the operating parameters in large scale operations. Thus, it becomes necessary to design such reactor which can not only control the operating conditions but also increases its efficiency towards the treatment of complex pollutants in aqueous streams. In recent years, HC have found as an emerging and suitable technique to intensify such process and give a direction to its large scale operations. The HC with Fenton reagent has been applied successfully for the degradation of a wide range of pollutants, mainly persistent bio-refractory pollutants and has shown better degradation efficiency [22, 27, 40, 51, 52, 63, 78]. The combined effect increases the density of hydroxyl radicals and also increases the oxidation rate of the pollutant molecules inside the reactor. To achieve such high (nearing 100 %) efficiency in Fenton process driven oxidation combined with HC, it is necessary to optimize the operating conditions such as the operating pH, ratio of H_2O_2 to ferrous ion concentration and the initial concentration of pollutants. The operating pH is an important factor as discussed earlier in section 1.4.2.2. As evident from many studies, the acidic condition favors the degradation of the pollutant using this combined effect. Generally pH below 4 is found as a suitable pH to carry out the fenton process in combination with HC. Under the acidic conditions, generation of hydroxyl radicals is favored and also the oxidation potential of $\cdot\text{OH}$ radicals is higher [22, 27, 52]. But it is also necessary to optimize the pH as at low pH (< 2.5), the quantum of utilizable hydroxyl radicals is less because of the formation of $(\text{Fe}(\text{II}) (\text{H}_2\text{O}))^{2+}$ which react slowly with H_2O_2 . At higher pH (>4), the degradation rate reduces again because of the formation of Fe (II) complexes which reduces the free iron species in the solution and inhibit the formation of free radicals. Some authors have found the pH in the range 3 – 3.75 under the combination of HC with Fenton reagent for the efficient degradation of different aqueous pollutants [22, 27, 52]. Thus, it can be said that a lower pH, in the range of 3–4 is most suitable for HC+ Fenton process. Similarly, it is desirable to optimize the dosage of H_2O_2 and Fe^{2+} to improve the overall efficacy of the degradation process. Generally, the extent of degradation increases on increasing the amount of H_2O_2 up to an optimum value because of

Chapter 1: Introduction and Literature Review

the generation of higher number of hydroxyl radicals. The excess of unreacted H_2O_2 can add to COD and also it acts as scavenger for the hydroxyl radicals at higher concentration level. If it is present in large quantum, it can also be harmful to the microorganism during the subsequent biological treatment after Fenton process. Thus, the loading of H_2O_2 should be optimized for its complete utilization during the treatment using hybrid processes.

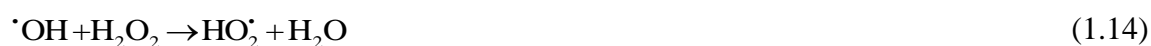
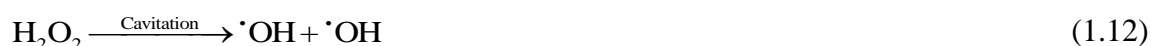
Many studies have found the effect of the operating conditions during the treatment of wastewater using this combined process. Pradhan et al. [22] have found maximum removal of p-nitrophenol at 5 g/L loading of H_2O_2 . At this loading, the quantum of free radicals was high and thus, the % degradation increased from 54 % to 63.2% when HC was combined with Fenton process at an optimum molar ratio of 1:5 (ferrous ion to H_2O_2) and pH of 3.75. A similar observation was also made by Raut-Jadhav et al. [56] where they have observed a complete degradation of imidacloprid at an optimum molar ratio of ferrous sulphate to H_2O_2 as 1:20 and pH of 2.7 which was more efficient than obtained in HC alone i.e. 6.15 % after 15 minute of operation. Additionally, the synergetic index was found as 3.63 which signify that this combined effect is more advantageous over the individual use of both processes. This was owing to the effect of the generated extraneous radicals due to the synergetic effect of HC and Fenton reagent because $\cdot OH$ radicals are simultaneously generated by two mechanisms, one by Fenton chemistry and other by cavitation mechanism which significantly improves the oxidation of pollutant molecules. On the other hand sometimes higher molar ratio of Fenton to H_2O_2 leads to a generation of excess radicals by reacting Fe^{2+} with most of the H_2O_2 available and therefore reduces the scavenging of $\cdot OH$ radicals by H_2O_2 due to less availability of un-dissociated H_2O_2 . In this regard, Joshi and Gogate [27] have studied the degradation of dichlorvos using combined HC and Fenton process. They have reported that additional free radicals were generated at higher concentration of ferrous ions which increases the degradation rate of dichlorvos at low pH of 3. Using the combination process, the % degradation has increased to 7 times than obtained in HC alone. The maximum degradation of 91.5% was achieved at an optimum ratio of 3:1 (ferrous sulphate to H_2O_2) which shows that the fenton effectively generates the additional free radicals and also increases their generation rate which significantly increases the oxidation rate of the pollutant molecule. In contrast to above studies, it has also been reported that an equal amount of ferrous ion and H_2O_2 can also lead to higher degradation rate. Gogate and Patil [52] have studied the degradation of Triazophos using HC+Fenton and reported that a synergetic coefficient of 3.34 was obtained using the combination of HC with fenton process at an

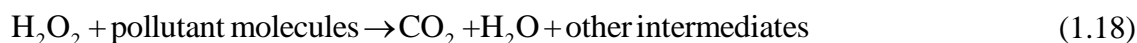
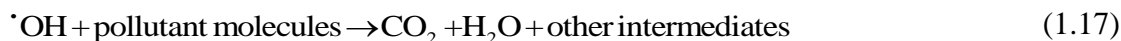
optimum molar ratio of 1:4:4 (Triazophos:FeSO₄:H₂O₂) and pH of 3, where maximum of 83% degradation was achieved.

In overall it can be concluded that a lower pH is more favorable for the degradation of pollutants using HC+Fenton and a pH in the range of 3-4 is more suitable. The molar ratio of Fe²⁺ to H₂O₂ is reported to be in the range of 1:1 to 1:20 but a very high concentration of H₂O₂ and Fe²⁺ (1:50) should be avoided because unreacted H₂O₂ will kill the microorganism in the subsequent biological processes and also adds to the treated effluent COD thereby reducing the overall efficiency of the whole treatment facility. Similarly, high Fe²⁺ concentration will increase the turbidity and TDS (total dissolved solids) load and will cause coagulation which will further reduce the efficiency of the advanced tertiary processes such as reverse osmosis and ion-exchange resulting into increased treatment cost in order to remove excess ferrous ion.

1.2.8.2 HC combined with hydrogen peroxide

As evident from many studies, hydrogen peroxide becomes more proficient to improve the efficiency of HC for reducing the organic pollutant load from aqueous effluent. Under the cavitation effect, the H₂O₂ gets dissociated into [•]OH radical and hence additional [•]OH radicals enhance the rate of degradation of pollutants. The efficiency of H₂O₂ for the degradation of pollutants greatly depends on the generation of [•]OH radicals and their subsequent utilization by the pollutant molecules. The individual use of H₂O₂ may result into a poor dissociation of H₂O₂ into the [•]OH radicals but under the HC effect, due to the generation of extreme conditions of temperature, pressure and increased energy dissipation, the rate of generation of [•]OH radicals is enhanced as well as the [•]OH radicals get properly dispersed in liquid in order to increase the overall oxidation rate. The dissociation energy for O–H bond in H₂O and O–O bond in H₂O₂ was found to be ~418 kJ/mol and ~213 kJ/mol respectively [81] and therefore under cavitation H₂O₂ can easily break into [•]OH radicals and thus increases [•]OH concentration. Following reactions (equations (1.12)–(1.18)) may occur during this combination effect as described below [17].





The HC reactor combined with hydrogen peroxide addition has more potential to degrade the bio-refractory pollutants and also shows better efficiency in case of combined processes as compared to a single process. In order to achieve better synergistic effect of this combined process, the loading of H_2O_2 should be optimized so that the entire amount of added H_2O_2 gets utilized by pollutant molecules and prevents scavenging of $\cdot\text{OH}$ radicals. Since beyond the optimum concentration, the rate of reaction between $\cdot\text{OH}$ radicals and pollutant molecules surpassed by the rate at which $\cdot\text{OH}$ radicals gets scavenged by H_2O_2 itself and therefore concentration of H_2O_2 need to be optimized to avoid excess scavenging of $\cdot\text{OH}$ by H_2O_2 itself.

Many authors have studied the effect of combination of HC and H_2O_2 with different concentration to achieve maximum degradation of pollutants [1, 22, 26, 40, 41, 44, 50, 53]. Saharan et al. [1] have studied the effect of H_2O_2 on the degradation of reactive red 120 dye (RR120) using HC and H_2O_2 addition. The extent of degradation was increased with an increase in H_2O_2 concentration and hence a complete decolorization and 60% reduction in TOC was obtained at an optimum ratio of 1:60 (RR120: H_2O_2). There was no further enhancement in degradation rate and the extent of TOC reduction at higher concentration of H_2O_2 due to the scavenging effect of this excess H_2O_2 . Thus, this combination effect significantly increases the degradation efficiency of the process. Gore et al. [41] have also observed almost complete decolorization of reactive orange 4 at an optimum loading of H_2O_2 at 1:30 molar ratio of Orange-G to H_2O_2 and no further increment in the degradation rate was observed at higher ratio because of the scavenging effect of H_2O_2 itself at its higher concentration. It was concluded that this combination method (HC+ H_2O_2) was 2.5 times more efficient than the HC process. Saharan et al. [26] have also reported a similar result for the degradation of Acid red 88 dye (AR88) and observed almost 72% reduction in TOC using HC+ H_2O_2 at an optimum ratio of 1:40 (AR88: H_2O_2) which was higher than 35% TOC reduction obtained using HC alone and concluded that in presence of H_2O_2 , HC process generates more number of $\cdot\text{OH}$ radicals and enhances the degradation rate at optimum concentration of H_2O_2 (4000 μM). Raut-Jadhav et al. [56] have also investigated the effect of

different loading of H_2O_2 on the degradation of imidacloprid using HC and observed a maximum degradation at an optimum molar ratio of 1:40 (imidacloprid to H_2O_2). Jawale et al. [82] have studied the degradation of cyanide using HC in combination with H_2O_2 at different molar ratio of $\text{K}_4\text{Fe}(\text{CN})_6:\text{H}_2\text{O}_2$ in the range of 1:1 to 1:30 and achieved a maximum 51.29 % degradation of cyanide at an optimum molar ratio of 1:5. It was observed that the extent of degradation was increased by 16.5 % with this combination as compared to only HC in 120 minute of operation.

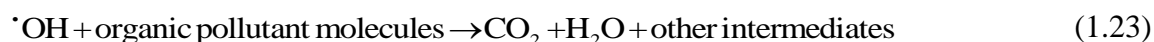
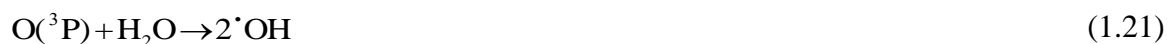
Overall it can be concluded that the presence of H_2O_2 during the HC treatment indicates the presence of extraneous $\cdot\text{OH}$ radicals and under the cavitation effects these radicals get perfectly dispersed in the bulk solution and thereby increase the rate of the oxidation reaction between radicals and the pollutant molecules. In order to take the benefits of such oxidants in combination with HC, it is desired to optimize its concentration as its excessive amount can reduce the degradation efficiency and may also affect its economic feasibility. The molar ratio of substrate to H_2O_2 is to be optimized based on the nature of the pollutant molecule. It can be concluded that for the larger molecules having large molecular weight such as dyes and pesticides higher molar ratio of substrate to H_2O_2 would be preferred as higher $\cdot\text{OH}$ radicals are required to simultaneously oxidize the intermediates formed due to the degradation of the parent pollutant molecule. It has also been observed from the previous studies that molar ratio of substrate to H_2O_2 in range of 1:30 to 1:60 gives higher degradation efficiency for most of complex pollutants. However, few of the studies suggested that for low molecular weight compounds, lower molar ratio is preferred as they can instantly decompose under the attack of $\cdot\text{OH}$ radicals and also less intermediates are formed requiring lower quantity of $\cdot\text{OH}$ radicals as against required for large chain complex molecule. Thus, the optimum molar ratio reported in the literature is found to be in the range of 1:5 to 1:20 for the degradation of such low molecular weight compounds. Furthermore, its excess presence in the effluent stream can be harmful and can effectively introduce secondary contamination of the effluent. Thus, it is necessary to optimize the concentration of H_2O_2 with the other operating parameters such as operating pH, state, nature and the loading of the pollutant molecules for getting the higher degradation efficiency and better synergistic effect of this combined process.

1.2.8.3 HC combined with ozone

Ozone (O_3) is a simple compound comprised of three oxygen atoms (O_2) and has a high oxidation potential than H_2O_2 towards the degradation of organic pollutants as compared to

Chapter 1: Introduction and Literature Review

the other oxidants such as H_2O_2 , Fenton reagent etc. [83-84]. Because of its greater tendency to generate the highly reactive free radicals, O_3 can be easily combined with other AOPs for the efficient removal of pollutants from water. Likewise, HC can be used with ozone for improving the degradation efficiency as HC is capable of generating the extreme conditions of temperature and pressure. Under the cavitation effect, O_3 get easily decomposed and yields into molecular O_2 and atomic oxygen $\text{O} (^3\text{P})$ [17], which can form $\cdot\text{OH}$ radicals on reacting with water molecules. There are several advantages of using the combination of HC with O_3 , as O_3 get easily decomposed into radicals under the extreme conditions of hot spot created during cavity collapse, O_3 molecules get easily dispersed into a bulk solution under the high interfacial turbulence created, which thereby increases the mass transfer rate between the gas molecules and bulk liquid solution [84-85] and also the contact time between ozone and pollutant molecule is more due to the micro-level mixing of ozone in the aqueous solution which thus leads to the degradation of pollutant to a higher extent. Moreover, the dissolved oxygen as well as oxygen generated due to ozone decomposition give rise to conversion of O^\cdot and $\cdot\text{OH}$ radicals (equations 3.12 and 3.13) and helps in enhancing the interaction probability of $\cdot\text{OH}$ radicals with pollutant molecules under HC. Hence, it can be said that both chemical and mechanical (mixing and dispersion) effect of cavitation equally contributes in order to improve the efficiency of such combination process. The chemical effects effectively increase the generation rate and the number density of free hydroxyl radicals, whereas mechanical effects significantly increase the mass transfer rate between the gas phase to the bulk liquid molecules. The following reactions (equations (1.19)–(1.24)) are known to occur during the HC process combined with ozone [17].



In past years, the use of ozone combined with HC process has been increased in the area of wastewater treatment to obtain a maximum removal efficiency of water pollutants. This combined process can enhance the generation of hydroxyl radicals and thus has established

itself as the most effective with greater degradation efficacy as compared to the individual processes [41, 52]. Only few studies have been reported on the use of such combination technique for the degradation of various water pollutants. Gore et al. [41] have studied the effect of combination of HC with ozone for the mineralization of Reactive orange 4 dye containing solution at various feed rate of ozone from 1 to 8 g/h. The maximum reduction of 76.25 % in TOC was observed at optimum feed rate of 3 g/h whereas only 14.67 % was achieved using HC alone in 60 minute of operation which shows that the combination effect was 5 times better than individual HC for the mineralization of the reactive orange 4 dye containing solution. Gogate and Patil [52] have also studied the effect of HC with ozonation at two different loading of ozone as 0.576 g/h and 1.95 g/h for the degradation of Triazophos. In their experimental study the ozone was injected at two different locations in two separate experiments i.e. one at the vena-contracta of orifice and in another experiment the ozone was injected in the holdup tank. It was a marginal increment (almost 8%) in the % degradation on increasing the feed rate from 0.576 g/h to 1.95 g/h in both cases of injection. It was also observed that the almost 90 % degradation was achieved when ozone was injected at feed tank whereas 82% of degradation was obtained on injecting ozone at orifice throat at the ozone feed rate of 1.95 g/h. This combination effect was found to be 2.5 times more efficient than the HC alone and 1.2 times more efficient than ozone alone for the degradation of Triazophos.

From these reported studies, it can be seen that for the better use and to take the benefits of this combined technique, it is necessary to optimize the parameters such as O₃ dosage, type of pollutant molecules and its initial concentration. As it can be seen from these two studies, O₃ dosage needs to be optimized because, beyond an optimum dose of O₃, some unreacted O₃ could be released from the system and also special care needs to be taken before selecting its dose in order to minimize the energy consumption and environmental hazard due to unreacted O₃ in the exhaust gas. Thus, by keeping these conditions in mind, it is advised to inject the ozone at the throat or vena contracta of the cavitating device for getting the maximum exposure of ozone to the pollutant molecules under the cavitating conditions. Injection at throat improves the mixing and gas bubble breakage which ensures complete utilization of ozone. Since the dosage of ozone will depend on the type of pollutant molecules, the wastewater characteristics is necessary to optimize the loading of ozone before scale up on an industrial scale on case to case basis.

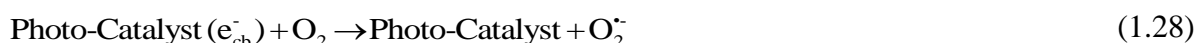
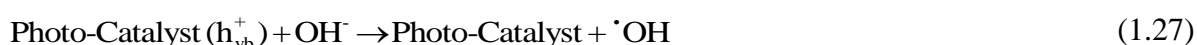
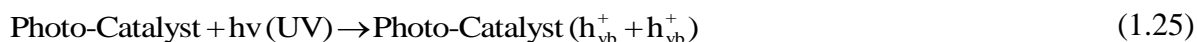
1.2.8.4 HC combined with photocatalysis

The photocatalysis process involves incident of photons on the surface of the catalyst such as titanium dioxide (TiO_2), niobium pentoxide (Nb_2O_5) etc. and thus creates electron hole pair which initiate the electron transfer mechanism and creates $\cdot\text{OH}$ radicals by dissociating water molecule. The efficiency of photocatalytic process depends very much on the characteristics of the irradiating surface, irradiating surface area, concentration of the reactants, and the mass of the photo-catalyst. Now days, Photocatalytic process coupled with HC has become a proficient technique in the area of wastewater treatment because of its several advantages. The HC induced effect overcomes the limitations of photocatalytic oxidation such as adsorption of contaminants at surface which blocks the UV activated sites and eventually reduces the efficiency and also mass transfer limitations that may occurs in different catalytic reactors. Under the influence of extreme conditions of temperature and pressure during cavity collapse, due to the generation of liquid micro-jet, the photocatalyst gets activated in terms of high porosity and surface cleaning and also due to the shock wave propagation, the mass transfer of the reactant and product species increases on the surface of the catalyst and in the bulk solution. The surface area of the catalyst increases due the fragmentation and deagglomeration of catalyst particles into fine solids thereby increasing adsorption rate of pollutant molecules as more active sites are made available. In addition to that, the chemical effects are also imparted which significantly increases the concentration of $\cdot\text{OH}$ radicals under the combination with photocatalytic process which enhances the degradation rate of the pollutant. With this combined technique, the process development in terms of activation of the photocatalyst and higher oxidation rate due to the availability of more $\cdot\text{OH}$ radicals in continuous mode of operation can have a much scope for its implementation on an industrial scale. The photo-activated chemical reactions can be understood by the mechanism of free radical attack on the pollutant molecules which are initiated by the interaction of photon with pollutant molecules present in the solution with or without the presence of catalyst [17].

When the catalyst suspension is irradiated through UV radiation larger than its band gap energy, then the valance band holes (h_{vb}^+) and conduction band electrons (e_{cb}^-) are generated as proposed in equation (1.25). The photo-generated holes can react with H_2O and/or hydroxyl ions (OH^-) (equations (1.26-1.27)) to produce more number of free hydroxyl radicals under cavitating conditions. While the photo-generated electrons can react with O_2 which is adsorbed on the catalyst surface to produce superoxide radical anion ($\text{O}_2^{\bullet-}$) as shown

Chapter 1: Introduction and Literature Review

in equation (1.28) and it further react with H^+ to form HO_2^{\bullet} via equation (1.29). The resulting free hydroxyl radicals can oxidize the pollutant molecules (equation (1.30)). The oxidation and reduction of pollutants (equations (1.31–1.32)) may not proceed simultaneously which may be because of an electron accumulation in the conduction band and thereby causing a recombination of positive electron holes and electrons. Hence, effective consumption of electrons is required to encourage the photocatalytic oxidation process under cavitation effects.



The combination technique of HC with photocatalysis is found to be more superior and gives desirable outputs in the area of wastewater treatment as the basic mechanism of both the processes is greatly dependent on the generation of free radicals that are capable of oxidizing the pollutant molecules. The degradation efficiency of photocatalytic oxidation under cavitation effect can be improved through activating the photocatalyst by increasing its surface area and also through its proper dispersion in the solution so that the pollutant molecules have more exposure time to get catalyzed.

Some researchers have used the combination of HC with photocatalysis for the decolorisation and mineralization of waste streams [13, 53, 56]. Wang et al. [13] have studied the degradation of reactive red 2 using a combination of HC and photocatalysis using TiO_2 as photo-catalyst over a catalyst loading range from 25 to 500 mg/L. It was observed that the extent of degradation rate was increased on increasing the TiO_2 loading from 25 to 100 mg/L but on further increase in the amount of TiO_2 , the degradation efficiency was reduced because the zone of influence of UV irradiation becomes low due to the optical blockage created by the additional amount of TiO_2 particles. The degradation of 76 % was obtained using HC alone which was enhanced up to 98 % when HC is combined with Photocatalysis at an optimum loading of TiO_2 (100 mg/L). Hence the extent of degradation was increased at

low concentration of catalyst and improved degradation efficiency of photocatalyst under HC process signifies the advantage of the combined process. Raut–Jadhav et al. [56] have reported the degradation efficiency of imidacloprid by applying the combination of HC and photocatalysis. The Niobium Pentoxide (Nb_2O_5) was used as a photo-catalyst which is having a wide band gap of 3.4 eV and is capable of getting photo-activated using broad wavelength spectrum of irradiation. It was observed that the synergetic effect of HC+photocatalyst was 2 times more efficient than the individual technique in terms of degradation efficiency at an optimum loading of 200 mg/L of the catalyst. Bagal and Gogate [53] have also reported the degradation of diclofenac sodium from water using HC+ photocatalyst. The amount of TiO_2 was varied from 50-300 mg/L in this study and observed that the extent of degradation was increased from 67.68% to 79.23% with an increase in the amount of TiO_2 from 50-200 mg/L and beyond which there was no significant enhancement in the degradation of diclofenac sodium was found. Also, this combination effect was found to be 3 times more efficient than HC alone.

It thus can be concluded from above studies that the HC coupled with photocatalysis process has a potential for degrading the complex bio-refractory pollutants from wastewater because of the increase in irradiating surface area and the regeneration of the photocatalyst particles. In HC combined with the photocatalysis process, the stability of photocatalyst plays an important role in monitoring the overall degradation efficiency. From above studies, lower loading of photocatalyst in the range of 100–200 mg/L is found to be more suitable to achieve the higher degradation efficiency of the pollutant molecules when combined with HC. Higher amount of photocatalyst in suspension may decrease the degradation efficiency of the organic pollutants because of insufficient dispersion of UV radiation due to higher turbidity under cavitation conditions and also due to the obstruction in the irradiating light path. Hence, it is necessary to optimize the amount of photocatalyst and operating conditions to achieve a better efficiency of degradation of the pollutant molecules which can provide a great prospect on large scales of operation. Moreover, the size of the photocatalyst particles also plays a crucial role in deciding the performance and operation of hybrid HC + Photocatalytic process. The catalyst particles may clog the hydrodynamic cavitating devices as well as particles may also settle in the tank and therefore, agitation will have to be provided to keep them suspended. In case of HC + Photocatalytic process, slurry pump is required with a screen in the suction line so that the catalyst particles do not enter into the main line.

1.3 Summary of the Chapter

HC technique has been found as a suitable technology for wastewater treatment as proven by its capability in processing large volumes of waste effluent, being more efficient in terms of cavitation yield, and also has a potential to treat the water containing most complex organic pollutants on a large scale. In the area of wastewater treatment, the desired transformation depends on the potentiality of HC in generating the highly oxidizing free radicals that are responsible for the effective degradation of water pollutants. Further, these generations of radicals depend on the geometrical configuration of cavitating device as well as operating parameters such as inlet pressure, cavitation number, and physicochemical properties of liquid medium to be treated. The geometrical and operating parameters can be altered to obtain the controlled cavitation conditions during the cavitation process to get the desired yield. The optimization of these parameters is very necessary, and as evident from the previous studies these parameters need to be optimized separately for the different bio-refractory pollutants.

The different shapes and respective size of the cavitating device can significantly dominate the number of cavities that are being generated in these devices. Therefore, it is required to optimize the cavitating device with different shape and size for wastewater treatment. The energy efficiencies of venturi based cavitating devices have been reported two times higher than orifice plates. In the case of operating pressure and cavitation number, it is better to use high pressure and low cavitation number, but care must be taken to avoid the choked cavitation condition, and hence the cavitating device should always be operated at higher cavitation number than choked cavitation number. Apart from these geometrical and operating parameters, it has been proved that physicochemical properties of the treated effluent are very much important for, e.g. density, viscosity, and impurities present in the form of suspended solids and dissolved gases that can significantly alter the inception of cavitation and final collapse pressure generated, and therefore a laboratory-scale trial must be done before the scaleup of HC. Furthermore, the HC reactors can easily be coupled with other AOPs, and these hybrid methods are proved to be more energy efficient. Therefore, HC combined with other AOPs can be a better option for the treatment of industrial wastewater.

The next chapter provides the degradation of Rh6G using HC coupled with other oxidative agents. An attempt has been made to identify the degradation by-products using LC-MS

study and subsequently a possible degradation pathway of Rh6G has been proposed. Furthermore the mechanism of degradation of Rh6G using HC was also verified.

References

- [1] V.K. Saharan, M.P. Badve, A.B. Pandit, Degradation of Reactive Red 120 dye using hydrodynamic cavitation, *Chem. Eng. J.* 178 (2011) 100–107.
- [2] V.K. Saharan, M.A. Rizwani, A.A. Malani, A.B. Pandit, Effect of geometry of hydrodynamically cavitating device on degradation of orange-G, *Ultrason. Sonochem.* 20 (2013) 345–353.
- [3] P.R. Gogate, A.B. Pandit, A review and assessment of hydrodynamic cavitation as a technology for the future, *Ultrason. Sonochem.* 12 (2005) 21–27.
- [4] S. Rajoriya, B. Kaur, Adsorptive Removal of Zinc from Waste Water by Natural Biosorbents, *Int. J. Eng. Sci. Inv.* 3 (2014) 60–80.
- [5] M. Mrowetz, C. Pirola, E. Selli, Degradation of organic water pollutants through sonophotocatalysis in the presence of TiO₂, *Ultrason. Sonochem.* 10 (2003) 247–254.
- [6] M.F.N. Secondes, V. Naddeo, V. Belgiorno, F. Ballesteros, Removal of emerging contaminants by simultaneous application of membrane ultrafiltration, activated carbon adsorption, and ultrasound irradiation, *J. Hazard. Mater.* 264 (2014) 342–349.
- [7] Q. Dai, L. Chen, W. Chen, J. Chen, Degradation and kinetics of phenoxyacetic acid in aqueous solution by ozonation, *Sep. Purif. Technol.* 142 (2015) 287–292.
- [8] M.M.B. Martin, J.A.S. Perez, J.L.G. Sanchez, L.M. de Oca, J.L.C. Lopez, I. Oller, S.M. Rodriguez, Degradation of alachlor and pyrimethanil by combined photo-Fenton and biological oxidation, *J. Hazard. Mater.* 155 (2008) 342–349.
- [9] X. Wang, Y. Zhang, Degradation of alachlor in aqueous solution by using hydrodynamic cavitation, *J. Hazard. Mater.* 161 (2009) 202–207.
- [10] M.A. Behnajady, N. Modirshahla, M. Shokri, B. Vahid, Effect of operational parameters on degradation of Malachite Green by ultrasonic irradiation, *Ultrason. Sonochem.* 15 (2008) 1009–1014.
- [11] M.V. Bagal, P.R. Gogate, Sonochemical degradation of alachlor in the presence of process intensifying additives, *Sep. Purif. Technol.* 90 (2012) 92–100.
- [12] F. Mendez-Arriaga, R.A. Torres-Palma, C. Petrier, S. Esplugas, J. Gimenez, C. Pulgarin, Mineralization enhancement of a recalcitrant pharmaceutical pollutant in water by advanced oxidation hybrid processes, *Water res.* 43 (2009) 3984–3991.

- [13] X. Wang, J. Jia, Y. Wang, Degradation of C.I. Reactive Red 2 through photocatalysis coupled with water jet cavitation, *J. Hazard. Mater.* 185 (2011) 315–321.
- [14] A.G. Chakinala, P.R. Gogate, A.E. Burgess, D.H. Bremner, Industrial wastewater treatment using hydrodynamic cavitation and heterogeneous advanced Fenton processing, *Chem. Eng. J.* 152 (2009) 498–502.
- [15] P.R. Gogate, A.B. Pandit, A review of imperative technologies for wastewater treatment I: oxidation technologies at ambient conditions, *Adv. Environ. Res.* 8 (2004) 501–551.
- [16] P.R. Gogate, R.K. Tayal, A.B. Pandit, Cavitation: A technology on the horizon, *Curr. Sci.* 91 (2006) 35–46.
- [17] V.K. Saharan, D.V. Pinjari, P.R. Gogate, A.B. Pandit, Advanced oxidation technologies for wastewater treatment: an overview, in: V.V. Ranade, V.M. Bhandari (Eds.), *Industrial Wastewater Treatment, Recycling and Reuse*, Elsevier, Butterworth, Heinemann, UK, (2014) 141–191.
- [18] F.R. Young, *Cavitation*, McGraw Hill Book Co., New York, 1989.
- [19] N. Golash, P.R. Gogate, Degradation of dichlorvos containing wastewaters using sonochemical reactors, *Ultrason. Sonochem.* 19 (2012) 1051–1060.
- [20] M. Siddique, R. Farooq, G.J. Price, Synergistic effects of combining ultrasound with the Fenton process in the degradation of Reactive Blue 19, *Ultrason. Sonochem.* 21 (2014) 1206–1212.
- [21] M.V. Bagal, B.J. Lele, P.R. Gogate, Removal of 2,4-dinitrophenol using hybrid methods based on ultrasound at an operating capacity of 7 L, *Ultrason. Sonochem.* 20 (2013) 1217–1225.
- [22] A.A. Pradhan, P.R. Gogate, Removal of p-nitrophenol using hydrodynamic cavitation and Fenton chemistry at pilot scale operation, *Chem. Eng. J.* 156 (2010) 77–82.
- [23] M.A. Behnajady, N. Modirshahla, S.B. Tabrizi, S. Molanee, Ultrasonic degradation of rhodamine B in aqueous solution: influence of operational parameters, *J. Hazard. Mater.* 152 (2008) 381–386.
- [24] P.R. Gogate, A.B. Pandit, Sonochemical reactors: scale up aspects, *Ultrason. Sonochem.* 11 (2004) 105–117.
- [25] P.R. Gogate, P.A. Tatake, P.M. Kanthale, A.B. Pandit, Mapping of Sonochemical reactors: review, analysis, and experimental verification, *AIChE J.* 48 (2002) 1542–1560.

- [26] V.K. Saharan, A.B. Pandit, P.S. SatishKumar, S. Anandan, Hydrodynamic cavitation as an advanced oxidation technique for the degradation of Acid Red 88 dye, *Ind. Eng. Chem. Res.* 51 (2012) 1981–1989.
- [27] R.K. Joshi, P.R. Gogate, Degradation of dichlorvos using hydrodynamic cavitation based treatment strategies, *Ultrason. Sonochem.* 19 (2012) 532–539.
- [28] M. Sivakumar, A.B. Pandit, Wastewater treatment: a novel energy efficient hydrodynamic cavitation technique, *Ultrason. Sonochem.* 9 (2002) 123–131.
- [29] V. S. Moholkar, A. B. Pandit, Modeling of hydrodynamic cavitation reactors: a unified approach, *Chem. Eng. Sci.* 56 (2001) 6295–6302.
- [30] J.S. Krishnan, P. Dwivedi, V.S. Moholkar, Numerical Investigation into the Chemistry Induced by Hydrodynamic Cavitation, *Ind. Eng. Chem. Res.* 45 (2006) 1493–1504.
- [31] P. Kumar, S. Khanna, V.S. Moholkar, Flow regime maps and optimization thereof of hydrodynamic cavitation reactors, *AIChE J.* 58 (2012) 3858–3866.
- [32] K.S. Kumar, V.S. Moholkar, Conceptual design of a novel hydrodynamic cavitation reactor, *Chem. Eng. Sci.* 62 (2007) 2698–2711.
- [33] Y.T. Didenko, W.B. McNamara, K.S. Suslick, Hot spot conditions during cavitation in water, *J. Am. Chem. Soc.* 121 (1999) 5817–5818.
- [34] V.S. Moholkar, A.B. Pandit, Bubble behavior in hydrodynamic cavitation: effect of turbulence, *AIChE J.* 43 (1997) 1641–1648.
- [35] Y.T. Shah, A.B. Pandit, V.S. Moholkar, *Cavitation Reaction Engineering*, Plenum Publishers, USA, (1999).
- [36] Y. Yan, R.B. Thorpe, Flow regime transitions due to cavitation in the flow through an orifice, *Int. J. Multiphase Flow* 16 (1990) 1023–1045.
- [37] P.R. Gogate, Cavitation reactors for process intensification of chemical processing applications: A critical review, *Chem. Eng. Process.* 47 (2008) 515–527.
- [38] M. Capocellia, M. Prisciandaro, A. Lancia, D. Musmarra, Hydrodynamic cavitation of p-nitrophenol: A theoretical and experimental insight, *Chem. Eng. J.* 254 (2014) 1–8.
- [39] A.G. Chakinala, P.R. Gogate, A.E. Burgess, D.H. Bremner, Treatment of industrial wastewater effluents using hydrodynamic cavitation and the advanced Fenton process, *Ultrason. Sonochem.* 15 (2008) 49–54.

- [40] K.P. Mishra, P.R. Gogate, Intensification of degradation of Rhodamine B using hydrodynamic cavitation in the presence of additives, *Sep. Purif. Technol.* 75 (2010) 385–391.
- [41] M.M. Gore, V.K. Saharan, D.V. Pinjari, P.V. Chavan, A.B. Pandit, Degradation of reactive orange 4 dye using hydrodynamic cavitation based hybrid techniques, *Ultrason. Sonochem.* 21 (2014) 1075–1082.
- [42] P.N. Patil, P.R. Gogate, Degradation of methyl parathion using hydrodynamic cavitation: Effect of operating parameters and intensification using additives, *Sep. Purif. Technol.* 95 (2012) 172–179.
- [43] M. Petkovseka, M. Zupanc, M. Dular, T. Kosjek, E. Heath, B. Kompare, B. Sirok, Rotation generator of hydrodynamic cavitation for water treatment, *Sep. Purif. Technol.* 118 (2013) 415–423.
- [44] P.R. Gogate, G.S. Bhosale, Comparison of effectiveness of acoustic and hydrodynamic cavitation in combined treatment schemes for degradation of dye wastewaters, *Chem. Eng. Process.* 71 (2013) 59–69.
- [45] M.T. Angaji, R. Ghiaee, Decontamination of unsymmetrical dimethylhydrazine waste water by hydrodynamic cavitation-induced advanced Fenton process, *Ultrason. Sonochem.* 23 (2015) 257–265.
- [46] S.L. Gayatri, V.M. Bhandari, V.V. Ranade, Industrial wastewater treatment - removal of acid from wastewater, *J. Environ. Res. Develop.* 8 (2014) 697–704.
- [47] Huang Y, Wu Y, Huang W, Yang F, Ren EX. Degradation of chitosan by hydrodynamic cavitation. *Polym Degrad Stab* 2013; 98: 37–43.
- [48] K.V. Padoley, V.K. Saharan, S.N. Mudliar, R.A. Pandey, A.B. Pandit, Cavitationally induced biodegradability enhancement of a distillery wastewater, *J. Hazard. Mater.* 219 (2012) 69–74.
- [49] S. Rajoriya, V.K. Saharan, Degradation of Diclofenac Sodium Salt Using Hydrodynamic Cavitation, *Energy Technology & Ecological concerns: A Contemporary Approach*, (2014) 82–86.
- [50] J. Wang J, X. Wang, P. Guo, J. Yu, Degradation of reactive brilliant red K-2BP in aqueous solution using swirling jet-induced cavitation combined with H₂O₂, *Ultrason. Sonochem.* 18 (2011) 494–500.

- [51] D.H. Bremner, S.D. Carlo, A.G. Chakinala, G. Cravotto, mineralisation of 2,4-dichlorophenoxyacetic acid by acoustic or hydrodynamic cavitation in conjunction with the advanced Fenton process, *Ultrason. Sonochem.* 15 (2008) 416–419.
- [52] P.R. Gogate, P.N. Patil, Combined treatment technology based on synergism between hydrodynamic cavitation and advanced oxidation processes, *Ultrason. Sonochem.* 25 (2015) 60–69.
- [53] M.V. Bagal, P.R. Gogate, Degradation of diclofenac sodium using combined processes based on hydrodynamic cavitation and heterogeneous photocatalysis, *Ultrason. Sonochem.* 21 (2014) 1035–1043.
- [54] M. Franke, P. Braeutigam, Z.L. Wu, Y. Ren, B. Ondruschka, Enhancement of chloroform degradation by the combination of hydrodynamic and acoustic cavitation, *Ultrason. Sonochem.* 18 (2011) 888–894.
- [55] P.R. Gogate, S. Mededovic-Thagard, D. McGuire, G. Chapas, J. Blackmon, R. Cathey, Hybrid reactor based on combined cavitation and ozonation: from concept to practical reality, *Ultrason. Sonochem.* 21 (2014) 590–598.
- [56] S. Raut-Jadhav, V.K. Saharan, D. Pinjari, S. Sonawane, D. Saini, A. Pandit, Intensification of degradation of imidacloprid in aqueous solutions by combination of hydrodynamic cavitation with various advanced oxidation processes (AOPs). *J. Env. Chem. Eng.* 1 (2013) 850–857.
- [57] S. Raut-Jadhav, V.K. Saharan, D.V. Pinjari, S. Sonawane, D. Saini, A. Pandit, Synergetic effect of combination of AOP's (hydrodynamic cavitation and H₂O₂) on the degradation of neonicotinoid class of insecticide, *J. Hazard. Mater.* 261 (2013) 139–147.
- [58] P. Braeutigam, M. Franke, R.J. Schneider, A. Lehmann, A. Stolle, B. Ondruschka, Degradation of carbamazepine in environmentally relevant concentrations in water by Hydrodynamic-Acoustic Cavitation (HAC), *Water res.* 46 (2012) 2469–2477.
- [59] M.Q. Cai, Y.X. Guan, S.J. Yao, Z.Q. Zhu, supercritical fluid assisted atomization introduced by hydrodynamic cavitation mixer (SAA-HCM) for micronization of levofloxacin hydrochloride, *J. Supercrit. Fluids* 43 (2008) 524–534.
- [60] M. Zupanc, T. Kosjek, M. Petkovseka, M. Dular, B. Kompare, B. Sirok, Z. Blazeka, E. Heath, Removal of pharmaceuticals from wastewater by biological processes, hydrodynamic cavitation and UV treatment, *Ultrason. Sonochem.* 20 (2013) 1104–1112.

- [61] G. V. Ambulgekar, S. D. Samant, A. B. Pandit, Oxidation of alkylarenes using aqueous potassium permanganate under cavitation: comparison of acoustic and hydrodynamic techniques, *Ultrason. Sonochem.* 12 (2005) 85-90.
- [62] Y. Wu, Y. Huang, Y. Zhou, X. Ren, F. Yang, Degradation of chitosan by swirling cavitation, *Innov. Food Sci. Emerg. Technol.* 23 (2014) 188–193.
- [63] M.V. Bagal, P.R. Gogate, Degradation of 2, 4-dinitrophenol using a combination of hydrodynamic cavitation, chemical and advanced oxidation processes, *Ultrason. Sonochem.* 20 (2013) 1226–1235.
- [64] P. Gogate, Application of cavitational reactors for water disinfection: current status and path forward, *J. Environ. Manage.* 85 (2007) 801–815.
- [65] M. Badve, P. Gogate, A. Pandit, L. Csoka, Hydrodynamic cavitation as a novel approach for wastewater treatment in wood finishing industry, *Sep. Purif. Technol.* 106 (2013) 15–21.
- [66] Kuldeep, J. Carpenter, V.K. Saharan, Study of cavity dynamics in a hydrodynamic cavitation reactor, *Energy Technology & Ecological concerns: A Contemporary Approach*, (2014) 37–43.
- [67] P. Senthil Kumar, M. Siva Kumar, A.B. Pandit, Experimental quantification of chemical effects of hydrodynamic cavitation, *Chem. Eng. Sci.* 55 (2000) 1633–1639.
- [68] A. Bashir A, A.G. Soni, A.V. Mahulkar, A.B. Pandit, The CFD driven optimization of a modified venturi for cavitation activity, *Can. J. Chem. Eng.* 89 (2011) 1366–1375.
- [69] D. Ghayal, A.B. Pandit, V.K. Rathod, Optimization of biodiesel production in a hydrodynamic cavitation reactor using used frying oil, *Ultrason. Sonochem.* 20 (2013) 322–328.
- [70] Y. Wang, A. Jia, Y. Wu, C. Wu, L. Chen, Disinfection of bore well water with chlorine dioxide/sodium hypochlorite and hydrodynamic cavitation, *Environ. Technol.* 36 (2015) 479–486.
- [71] S. Parthasarathy, T.S. Ying, S. Manickam, Generation and Optimization of Palm Oil-Based Oil-in-Water (O/W) Submicron-Emulsions and Encapsulation of Curcumin Using a Liquid Whistle Hydrodynamic Cavitation Reactor (LWHCR), *Ind. Eng. Chem. Res.* 52 (2013) 11829–11837.
- [72] B. Balasundaram, S.T.L. Harrison, Optimizing orifice geometry for selective release of periplasmic products during cell disruption by hydrodynamic cavitation, *Biochem. Eng. J.* 54 (2011) 207–209.

- [73] A. Mahulkar, A. Pandit, Analysis of Hydrodynamic and Acoustic Cavitation Reactors. VDM publishing, 2010.
- [74] T. Jain T, J. Carpenter, V.K. Saharan, CFD Analysis and Optimization of Circular and Slit Venturi for Cavitation Activity, J. Mater. Sci. Mechan. Eng. 1 (2014) 28–33.
- [75] K. Chavan, B. Bhingole, J. Raut, A.B. Pandit, Numerical Optimization and Experimental Validation of converging diverging cavitating nozzles, 9th International Symposium on Cavitation CAV (2016) Switzerland.
- [76] P. Li, Y. Song, S. Wang, Z. Tao, S. Yu, Y. Liu, Enhanced decolorisation of methyl orange using zero-valent copper nanoparticles under assistance of hydrodynamic cavitation, Ultrason. Sonochem. 22 (2015) 132–138.
- [77] X. Wang, J. Wang, P. Guo, W. Guo, C. Wang, Degradation of Rhodamine B in aqueous solution by using swirling jet-induced cavitation combined with H₂O₂, J. Hazard. Mater. 169 (2009) 486–491.
- [78] P.N. Patil, S.D. Bote, P.R. Gogate, Degradation of imidacloprid using combined advanced oxidation processes based on hydrodynamic cavitation, Ultrason. Sonochem. 21 (2014) 1770–1777.
- [79] H. Tekin, O. Bilkay, S.S. Ataberk, H.T. Balta, H.I. Ceribasi, F.D. Sanin, B.F. Dilek, U. Yetis, Use of Fenton oxidation to improve the biodegradability of a pharmaceutical wastewater, J. Hazard. Mater. 136 (2006) 258–265.
- [80] E. Chamarro, A. Marco, S. Esplugas, Use of Fenton reagent to improve organic chemical biodegradability, Water Res. 35 (2001) 1047–1051.
- [81] Y.L. Pang, A.Z. Abdullah, S. Bhatia, Review on Sonochemical methods in the presence of catalysts and chemical additives for treatment of organic pollutants in wastewater, Desalination 277 (2011) 1–14.
- [82] R.H. Jawale, P.R. Gogate, A.B. Pandit, Treatment of cyanide containing wastewater using cavitation based approach, Ultrason. Sonochem. 21 (2014) 1392–1399.
- [83] P.S. Bailey, The reactions of ozone with organic compounds, Chem. Rev. 58 (2014) 925–1010.
- [84] D. Ridgway, R.N. Sharma, T.R. Eanlay, Determination of mass transfer coefficients in agitated gas liquid reactors by instantaneous reactions, Chem. Eng. Sci. 44 (1989) 2935–2942.
- [85] F.J. Beltran, V. Gomez-Serrano, A. Duran, Degradation kinetics of p-nitrophenol ozonation in water, Water Res. 26 (1992) 9–17.

CHAPTER 2

Degradation of a cationic dye (Rhodamine 6G) using Hydrodynamic Cavitation coupled with other oxidative agents

2.1 Introduction

In recent years, the discharge of wastewater coming from various textile industries is becoming a major environmental problem due to loading of the enormous quantity of different toxic dyes. It is estimated that nearly 18-20% of the total production of dyes is discharged into the environment during dyeing process [1-4]. Among most of the toxic dyes, Rhodamine 6G dye is mostly used as a colorant in the textile industries. It is a non-volatile compound, highly water soluble, and dark reddish purple in color. It has some other applications in the biochemistry research laboratories where this dye is used as a diagnostic tool to detect the antigen in a liquid sample. Rh6G is also utilized for fluorescence microscopy and fluorescence correlation spectroscopy in the area of biotechnology [5]. Water containing Rhodamine dyes causes irritation of the skin, eyes and respiratory system of human beings. It has also medically verified that drinking water contaminated with Rhodamine dyes is highly carcinogenic and poisonous to living organisms [6-7]. Hence, these toxic pollutants must be treated before releasing them into the environment. These pollutants contain larger complex molecules (i.e. aromatic compounds) which cannot be treated efficiently by biological methods and other conventional methods such as adsorption, coagulation by chemical agents and membrane filtration. These methods are very costly and cannot mineralize these pollutants and rather separate them physically from the wastewater which causes secondary load on the environment. But over the past years, advanced oxidation processes (AOPs) such as Fenton, Photo-Fenton, photocatalytic process, and cavitation have been employed successfully by many authors [8-15] for the treatment of such pollutant molecules. In last decade, cavitation has also emerged as an effective oxidative process to degrade the organic pollutants present in wastewater.

The phenomena of cavitation may be described in three sections as 1) nucleation: formation of cavities within the liquid; 2) growth of bubbles/cavities under the fluctuating surrounding pressure field; 3) subsequent collapse of cavities: violent implosion of vapor/gas filled cavities. In recent years, most of the researchers have focused on the use of acoustic cavitation in the area of wastewater treatment. However, it was observed that utilization of acoustic cavitation on an industrial scale creates the difficulties due to the higher maintenance costs and low energy efficiency. In recent years, hydrodynamic cavitation (HC) is found to be an alternative to replace acoustic cavitation as an efficient technology for the mineralization of various organic pollutants from wastewater due to its ease of operation on an industrial

Chapter 2: Degradation of a cationic dye (Rhodamine 6G) using hydrodynamic cavitation coupled with other oxidative agents

level. In HC, cavitation can be produced by pressure variation in a flowing liquid through cavitating devices. The cavities are formed at the throat of a venturi or orifice where pressure of the liquid falls below the vapor pressure of the liquid. In the downstream side of the cavitating device, when pressure recovers these cavities implode violently resulting high temperatures of 5000 K and pressures of 1000 atm [16-20]. Under such extreme conditions, water molecules are thermally dissociated into $\cdot\text{H}$ and $\cdot\text{OH}$ radicals [14]. These generated $\cdot\text{OH}$ radicals (non-selective reactive species) inside the cavitating devices are capable of oxidizing the organic substances and thus mineralize these compounds [17-19, 21].

There have been many studies reported in literature for the treatment of Rh6G using different approaches mainly using photo-catalysis [5, 22-25]. In this regard, Bokhale et al. [22] studied sono-catalytic and sono-photocatalytic degradation of Rh6G and reported that the maximum degradation as 63.3% was achieved using sono-photocatalytic (US/UV) in the presence of TiO_2 (4 g/L). Lusic et al. [26] have investigated the photocatalytic degradation of Rh6G and reported that the maximum removal of 94% was achieved using photoactive ZnO after 90 min of treatment. Asiri et al. [27] have studied the photo-degradation of Rh6G using nano-sized TiO_2 in the presence of irradiation sources. It was observed that nanoparticles of TiO_2 with smaller size were found to be more efficient in the photo-degradation of Rh6G due to their large surface area. Though, the degradation of Rh6G was investigated in details using various processes at a laboratory scale but still these technologies do not find any application on an industrial scale due to their lower efficiency and higher cost for the treatment of real industrial effluent [25]. Moreover these studies have reported the degradation of Rh6G only which was evaluated by observing a reduction in color intensity of the dye and complete mineralization was not studied using these methods. The mineralization of Rh6G using HC has not been reported yet in the literature. Hence, the objectives of this study were to evaluate the ability of HC to mineralize the Rh6G in aqueous solution and to intensify the mineralization of Rh6G by combining HC with other oxidizing agents to establish HC on an industrial scale for the treatment of real effluent. The effects of operating parameters like solution pH, initial concentration of dye, inlet pressure, and cavitation number on the decolorization of Rh6G were investigated. The effect of oxidation additives such as hydrogen peroxide (H_2O_2) and ozone has also been studied since these two oxidizing agents are mostly used for the treatment of an industrial effluent. An attempt has been made to identify the degradation by-products using LC-MS study and subsequently a possible degradation

Chapter 2: Degradation of a cationic dye (Rhodamine 6G) using hydrodynamic cavitation coupled with other oxidative agents

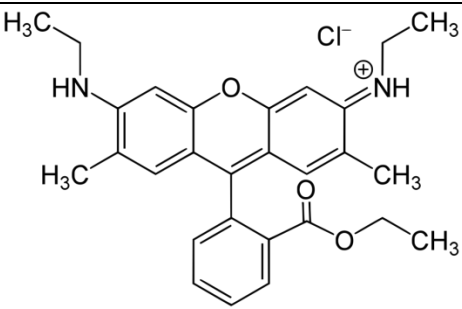
pathway of Rh6G has been proposed. Furthermore the mechanism of degradation of Rh6G using HC was also verified by observing the amount of H₂O₂ produced during HC.

2.2 Experimental details

2.2.1 Reagents

Rhodamine 6G dye (molecular weight: 479.02 g/mol; chemical formula: C₂₈H₃₁N₂O₃Cl) was procured from Central Drug House Pvt. Ltd (India). The chemical structure of Rh6G is shown in Table 2.1. Double distilled water (prepared freshly in the laboratory via distillation unit) was used to make the solution of Rh6G. Hydrogen Peroxide (30%, w/v) of AR grade was purchased from Lobachemie (India). Solution pH was adjusted using NaOH and H₂SO₄. All reagents as received from suppliers were used for the experiments without any further purification.

Table 2.1: Molecular structure, maximum absorption, and molecular weight of Rh6G

Name	Molecular structure	λ_{\max} (nm)	Appearance	Molecular weight (g/mol)
Rhodamine 6 G (cationic dye)		540	Dark reddish purple	479.02

2.2.2 Hydrodynamic cavitation reactor setup

Hydrodynamic cavitation reactor set-up used in the present work is shown in Figure 2.1. HC reactor set-up consists: (1) a storage tank with 20 L capacity, (2) a high pressure piston pump driven by a motor (power rating 2.2 kW) with a maximum discharge pressure of 30, (3) flow control valves (V₁–V₄), and pressure gauges (P₁, P₂), (4) a flow meter, (5) cavitating device (slit or circular venturi) accommodated with flanges. Pipes used in HC reactor have an internal diameter of 19 mm. The suction side of a pump is connected to the bottom of a

Chapter 2: Degradation of a cationic dye (Rhodamine 6G) using hydrodynamic cavitation coupled with other oxidative agents

storage tank. The discharge from the pump branches into main line and bypass line. The main line consists of a cavitating device and flow rate of water in the main line was controlled by regulating rpm of motor through variable frequency drive (VFD) and additionally a bypass line is also provided to control the flow in main line. Pressure gauges (P_1 and P_2) are provided in main line to check the fluid pressure. The dimensions of circular and slit venturi used in this work are given in Table 2.2. Schematic view of circular and slit venturi is shown in Figure 2.2. In this work, dimensions of the cavitating device selected were recommended by Bashir et al. [28], and Kuldeep and Saharan [29]. They have studied the effect of different geometrical parameters on the cavitation behavior inside a cavitating devices using CFD (Computational Fluid Dynamic) study and offered the optimized parameters of a cavitating device to achieve best cavitation activity.

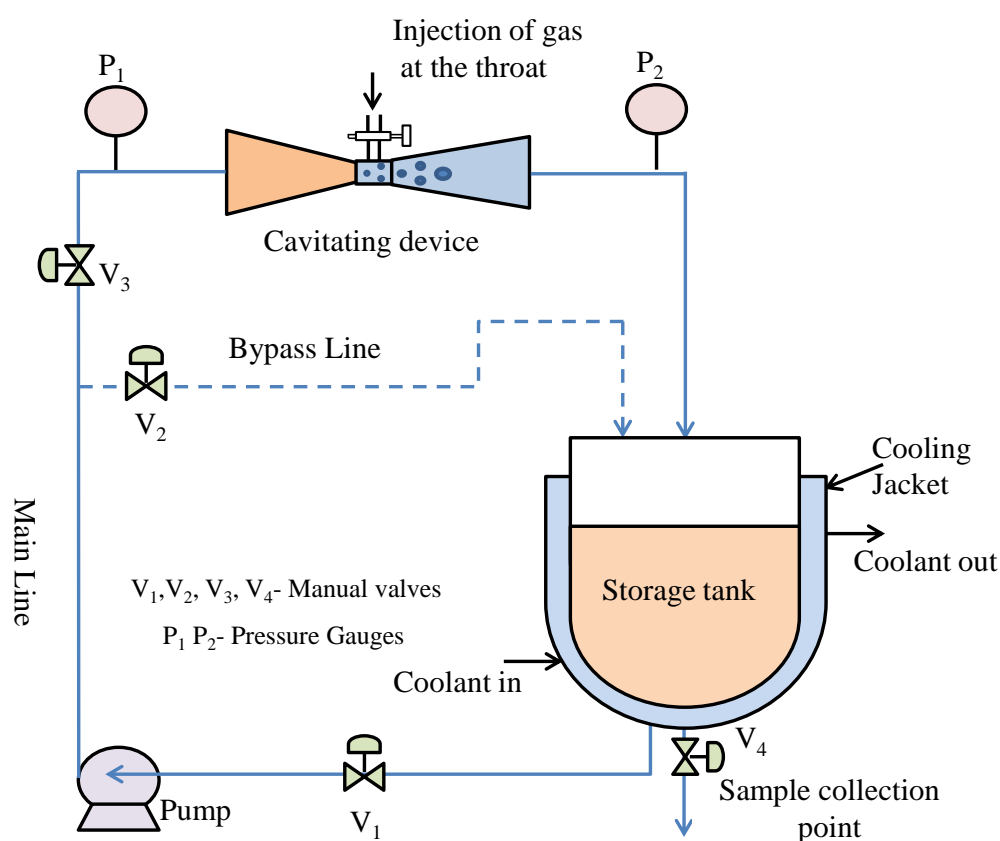
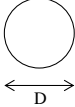
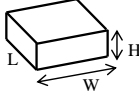


Figure 2.1: Schematic diagram of HC reactor set-up

Chapter 2: Degradation of a cationic dye (Rhodamine 6G) using hydrodynamic cavitation coupled with other oxidative agents

Table 2.2: Dimension of the cavitating devices (circular and slit venturi)

Hydrodynamic cavitating device	Dimension of throat	Venturi length	Length of convergent section	Length of divergent section	Half angle of convergent section	Half angle of divergent section	Ratio of perimeter to its cross-sectional area (α)
Circular venturi	 Circular hole of 2 mm diameter	96.14 mm	19.54 mm	74.60 mm	23.5°	6.5°	2.00
Slit venturi	 W=3.14 mm, H=1 mm, L=1 mm	100.6 mm	20.6 mm	79 mm	23.5°	6.5°	2.63

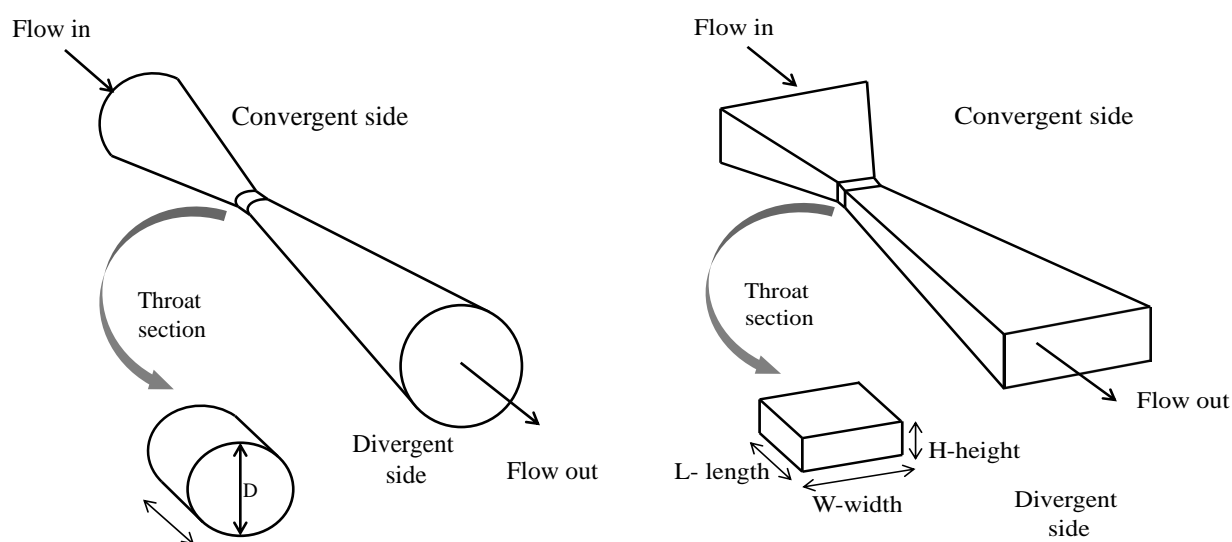


Figure 2.2: Schematic view of circular and slit venturi

2.2.3 Experimental Procedure

Decolorization of Rh6G has been carried out using HC at various conditions with a fixed aqueous Rh6G solution volume of 6 L. All the experiments were performed for 120 min and samples were taken from the storage tank at a fixed interval of time for further analysis. During all the experiments, temperature of the solution ($30 \pm 2^\circ\text{C}$) was kept constant and was maintained by circulating cooling water through the cooling jacket. Initially, effect of initial concentration of dye on the decolorization rate was studied in the range of 10-50 ppm using slit venturi. Then, experiments were conducted over the solution pH range of 2.0 to 12.0 to optimize solution pH. To optimize the cavitating devices, the effect of inlet pressure and cavitation number on the decolorization rate of Rh6G has been studied at an inlet pressure from 3 to 11 bar using slit and circular venturi. Two additional experiments were carried out to validate the degradation mechanism of Rh6G using HC. In the first experiment, effect of radical scavenger was studied by adding tert-butanol (1 g/L) in the system to investigate the scavenging action on $\cdot\text{OH}$ radicals. In the second experiment, doubled distilled water was circulated through HC at an optimized inlet pressure to determine the concentration of H_2O_2 produced in the system. During this experiment, samples were taken at a regular time of interval (15 min) and then concentration of H_2O_2 was measured. In order to enhance the decolorization of Rh6G, effect of process intensifying additives (H_2O_2 and ozone) in combination with HC were also investigated. Five different molar ratios of concentration of Rh6G to H_2O_2 as 1:10, 1:20, 1:30, 1:40 and 1:50 were selected to study the combined effect. Effect of H_2O_2 on the decolorization rate of Rh6G was also investigated individually i.e. without HC in the present work. The experiments were conducted using a combination of HC and ozone at various feed rate of ozone from 1 to 7 g/h. Ozone was directly injected at the throat of a venturi thereby exposing ozone directly to the cavitation effect. Ozone was generated by an ozone generator (maximum feed rate of ozone: 10 g/h, make: Eltech Engineers, India). Initially, Ozonator was calibrated in terms of feed rate of oxygen to acquire the desired mass flow rate of ozone.

2.2.4 Analytical procedure

Concentration of Rh6G was measured by UV/Vis-Spectrophotometer (Shimadzu-1800) at the maximum wavelength (λ_{max}) of 540 nm. Firstly, calibration chart was prepared for the known concentrations of Rh6G in the range of 2-12 ppm to calculate the concentration of unknown sample during experiments. A pH meter (Hanna Instruments, USA) was used to determine

Chapter 2: Degradation of a cationic dye (Rhodamine 6G) using hydrodynamic cavitation coupled with other oxidative agents

the pH of solution throughout the experiment. The degradation by-products of Rh6G during HC process were confirmed by liquid chromatography–mass spectroscopy (LC-MS) (make: Xevo G2-S Q-ToF, Waters, USA) using C18 column (4.6 mm x 250 mm). A mixture of Acetonitrile and phosphate buffer (45:55) was used as a mobile phase at a flow rate of 0.2 mL/min for 10 min. Total organic carbon (TOC) content of dye solution was measured using TOC analyzer (make: GE InnovOx). The amount of H₂O₂ produced during HC was measured by titrating sample against potassium permanganate (0.001M KMnO₄). Double distilled water was circulated through HC reactor and 100 mL of water sample was collected at a regular interval of 15 min. 4 mL of 4M sulfuric acid was added in the collected samples and titrated against 0.001M KMnO₄ until the purple color appeared. The end point of titration is colorless to purple. In the present work, all experiments were repeated at least twice to evaluate the repeatability of the observed data and the experimental errors were found to be within ±3% of the reported average values.

2.3 Results and discussion

2.3.1 Effect of initial Rh6G concentration

The effect of initial Rh6G concentration on the decolorization rate was investigated using HC. The degradation of dye molecules using HC involve mainly two mechanisms i.e. first, the oxidation of dye molecules by hydroxyl free radicals ([•]OH) and second, thermal decomposition of dye molecules which are located at the interfacial region of the collapsing cavities [2, 30]. Both mechanisms can occur at the multiple locations such as at the interface of cavity, in the bulk liquid medium, and in the core of cavity. Experiments were conducted with various concentrations of dye (10, 20, 30, 40, 50 ppm), at an inlet pressure of 5bar and solution pH of 10. The observed results are shown in Figure 2.3 and Table 2.3. Under the effect of HC, Rh6G gets dissociated into the intermediates which further react with [•]OH radicals and ultimately degrade into final products (CO₂, H₂O etc.). The following reaction takes place in HC:



$$-\frac{d[\text{Rh6G}]}{dt} = k[\text{Rh6G}][\text{}^{\bullet}\text{OH}] \quad (2.2)$$

A pseudo first order kinetic was used as a means to evaluate and correlate the observed data.

The concentration of [•]OH radicals is found to be constant during the decolorization process

Chapter 2: Degradation of a cationic dye (Rhodamine 6G) using hydrodynamic cavitation coupled with other oxidative agents

under the cavitation effect and also it is highly reactive and non-selective and therefore its concentration effect can be neglected [31]. The degradation kinetics can be represented by equation (2.3).

$$\ln \frac{[\text{Rh6G}]_o}{[\text{Rh6G}]} = k \times t \quad (2.3)$$

It can be seen from Figure 2.3a that percent decolorization of Rh6G decreases from 32.06% to 8.37% with an increase in initial concentration from 10 to 50 ppm. The kinetic analysis shows that degradation of Rh6G using HC fitted proposed pseudo-first order kinetics (shown in Figure 2.3b). It is observed that pseudo first order rate constant decreases from $2.9 \times 10^{-3} \text{ min}^{-1}$ to $0.7 \times 10^{-3} \text{ min}^{-1}$ for an increase in the concentration from 10 ppm to 50 ppm as shown in Table 2.3. The obtained lower decolorization rate at initial concentration of Rh6G higher than 10 ppm can be attributed to the insufficient generation of $\cdot\text{OH}$ radicals to degrade the dye, which shows that the relevant proportion of total amount of $\cdot\text{OH}$ radicals is a significant factor [10]. It can be seen from Table 2.3 that the rate of degradation ($k \times C_{A0}$) remained almost constant in the process, indicating that the rate of generation of $\cdot\text{OH}$ radicals is the rate controlling step whereas the concentration of the pollutant molecule does not have any effect on the overall degradation rate. Since, decolorization rate constant was found to be maximum at 10 ppm; therefore all the remaining experiments were carried out at 10 ppm concentration of Rh6G. In this study, the observed results can be validated with some other similar literature reports [2, 15, 32-34]. Saharan et al. [2] have investigated the degradation of reactive red 120 dye (RR120) using HC and reported that degradation kinetics of RR120 using HC follows first order reaction kinetic. Patil et al. [32] have studied the effects of initial concentration on the degradation of imidacloprid using HC and reported a decrease in the degradation rate with an increase in the initial concentration. Wang et al. [33] have investigated the degradation of reactive brilliant red K-2BP using HC. They have observed that, % degradation decreased from 94.2% to 24.7% with an increase in the concentration from 10 to 50 mg/L.

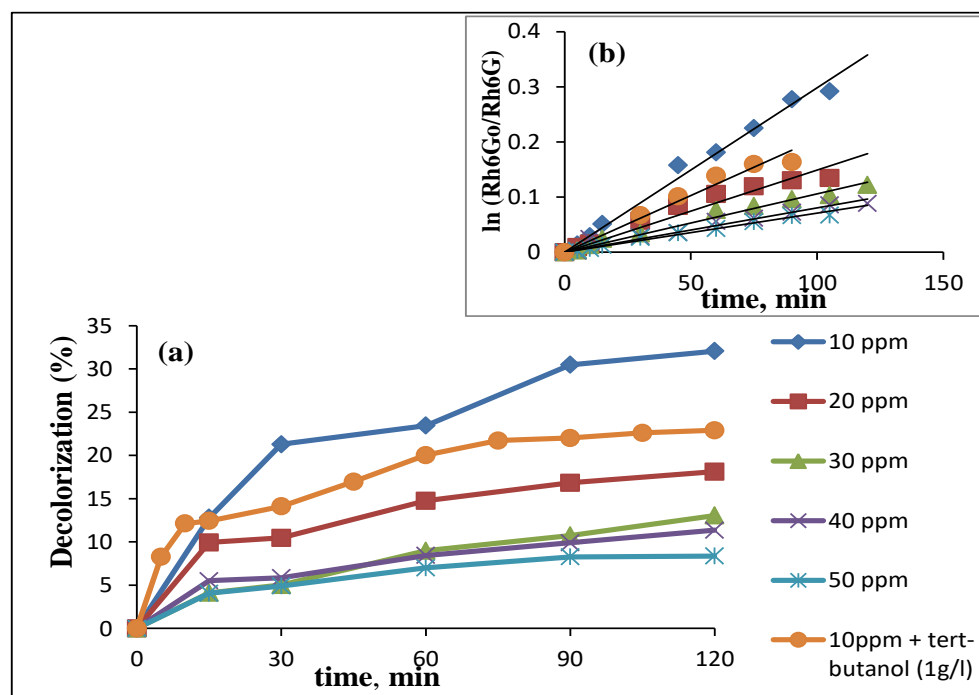


Figure 2.3: Effect of initial Rh6G concentration on the decolorization rate of Rh6G (Experimental Conditions: inlet pressure, 5 bar; solution pH, 10.0; volume of solution, 6L)

Table 2.3: Kinetic rate constants at different initial concentration of Rh6G

Concentration (ppm)	First order rate constant, $k \times 10^3 \text{ (min}^{-1}\text{)}$	Extent of decolorization (%)
10	3.0	32.06
20	1.4	18.13
30	1.1	13.05
40	0.8	11.36
50	0.7	8.37

2.3.2 Quantification of chemical effects (dosimetry study)

In order to validate the degradation mechanism which is driven by the attack of $\cdot\text{OH}$ radicals on the pollutant molecules, an experiment was carried out using HC with the addition of tert-butanol (a type of $\cdot\text{OH}$ scavenger). Tert-butanol is capable of neutralizing $\cdot\text{OH}$ radicals and it reacts with $\cdot\text{OH}$ and $\cdot\text{H}$ radicals and gives less reactive tert-butanol radical. It can be seen from Figure 2.3 that decolorization rate of Rh6G decreased from 3.0×10^{-3} to $2.1 \times 10^{-3} \text{ min}^{-1}$

Chapter 2: Degradation of a cationic dye (Rhodamine 6G) using hydrodynamic cavitation coupled with other oxidative agents

with the addition of tert-butanol and 22% decolorization was obtained after 120 min of treatment as against 32% obtained without tert-butanol at the same experimental condition using HC. The obtained result shows that $\cdot\text{OH}$ radicals were mainly responsible for the decolorization efficiency. Tert-butanol produces tert-butanol radicals on reacting with $\cdot\text{OH}$ radicals (in equation 2.4) which is less reactive species as compared to $\cdot\text{OH}$ radicals and therefore it reduces the degradation rate.



Tert-butanol can also react with $\cdot\text{H}$ radicals and it gives tert-butyl radical as shown in equation (2.5)



Similar results have also been reported in literature by Yao et al. [35] for the degradation of parathion using ultrasonic irradiation. They have observed that free radical reactions are predominant reactions occurs during the degradation of parathion using ultrasonication. Additionally, one more experiment was performed to check the occurrence of $\cdot\text{OH}$ radicals during HC by measuring the quantity of H_2O_2 produced at 5bar inlet pressure. It can be seen from Figure 2.4 that the amount of H_2O_2 formed with respect to time increases due to the recombination of $\cdot\text{OH}$ radicals which are generated under cavitating conditions. This study further proves that $\cdot\text{OH}$ radicals are formed during HC process.

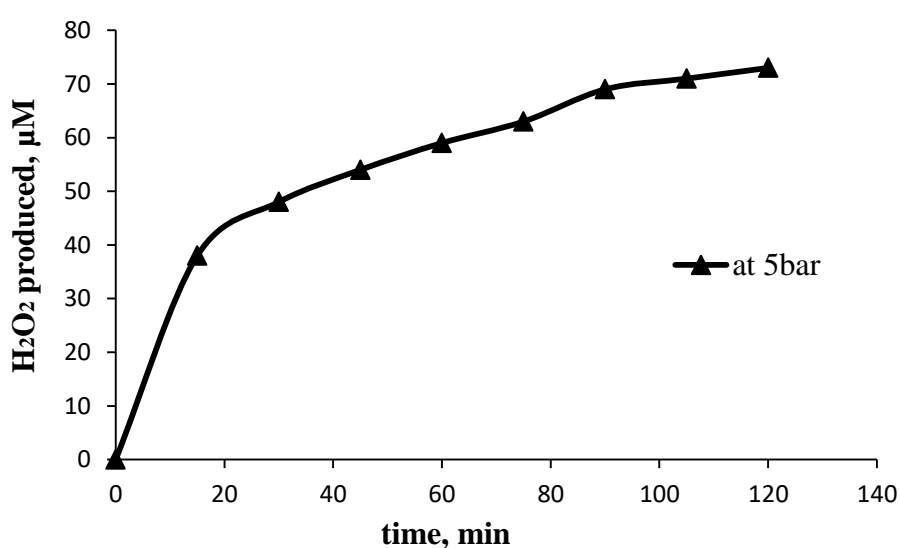


Figure 2.4: The formation of H_2O_2 concentration during degradation in HC reactor

2.3.3 Effect of solution pH

The solution pH is an important parameter for the decolorization rate of Rh6G using HC. The effect of solution pH was studied by varying solution pH over the range of 2.0-12.0. Experiments were carried out at an inlet pressure of 5 bar for 120 min of treatment time. The observed results are shown in Figure 2.5 and Table 2.4. It can be seen that extent of decolorization and first order rate constant increases with an increase in the solution pH from 2.0 up to an optimum value of 10.0. The decolorization rate decreases after pH 10. These results clearly show that decolorization rate was higher at basic medium than that obtained under acidic conditions. It has been reported that Rh6G molecule becomes hydrophobic under basic condition (i.e. at higher pH than its pKa value of 6.13) as the free electron pair on the amine nitrogen (primary amine group) transfer charges from amine nitrogen to aromatic rings. Under such condition Rh6G exists in its molecular state and therefore Rh6G locate itself at the cavity-water interface due to its hydrophobic nature. The concentration of $\cdot\text{OH}$ radicals is maximum at the cavity-water interface and therefore higher decolorization rate was obtained under basic condition. On the other hand, Rh6G molecule becomes hydrophilic in nature under acidic pH due to the protonation of nitrogen in the secondary amine group of the xanthene ring. Due to its hydrophilic nature, it remains in bulk of the solution where concentration of $\cdot\text{OH}$ radicals is minimum. Therefore, a lower decolorization rate was achieved under acidic conditions. In addition, the reduction in the decolorization beyond pH of 10 may be due to the enhanced viscosity and reduced surface tension due to the addition of NaOH which decreases the cavity collapse intensity and thereby reducing the generation rate of hydroxyl radicals. Therefore, the decolorization rate was decreased beyond solution pH of 10. The pH of solution was kept 10.0 for all the remaining sets of experiments. A few related results can be obtained in the literature where basic conditions are found to be superior for the degradation of pollutant molecules using cavitation. Eslami and Eslami [23] have investigated the degradation of Rh6G at different values of pH in the range 3.0-9.0 using ultrasonic cavitation in presence of H_2O_2 and zinc oxide and reported that higher degradation rate constant ($2.8 \times 10^{-2} \text{ min}^{-1}$) was achieved at high pH of 9.0. Wang et al. [36] have studied the degradation of alachlor over the range of pH from 2 to 12 using HC and reported that the rate constant increases from 4.45×10^{-2} to $5.77 \times 10^{-2} \text{ min}^{-1}$ with an increase in pH value from 2.0 to 12.0.

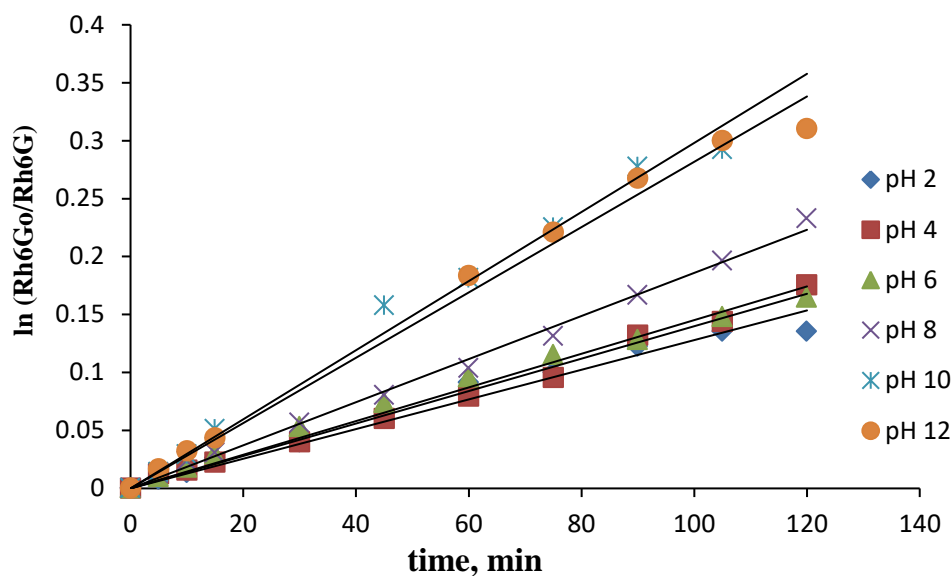


Figure 2.5: Effect of solution pH on the decolorization rate of Rh6G (Experimental Conditions: Initial concentration, 10 ppm; pressure, 5 bar; volume of solution, 6 L)

Table 2.4: Kinetic rate constants at various solution pH

Solution pH	First order rate constant, $k \times 10^3$ (min^{-1})	Extent of decolorization (%)
2	1.3	16.33
4	1.4	17.32
6	1.5	18.95
8	1.9	22.87
10	3.0	32.06
12	2.8	31.50

2.3.4 Effect of inlet pressure, cavitation number and geometrical parameters

In HC reactor, cavitation number is a dimensionless parameter used to characterize the cavitation intensity inside the cavitating device. It is defined as the ratio of pressure drop between the throat and extreme downstream section of the cavitating device to the kinetic head at the throat. It is given by the following equation (2.6):

$$C_v = \left(\frac{P_2 - P_v}{\frac{1}{2} \rho v_o^2} \right) \quad (2.6)$$

As the inlet pressure increases, velocity at the throat increases which in turn reduces the cavitation number. More number of cavities are generated under ideal condition ($C_v \leq 1$), but in many cases cavities can get generate at $C_v > 1$ due to the existence of little-dissolved gases and suspended particles [37]. It has been reported that the cavitation number in the range of 0.1 to 0.2 gives better degradation efficiency [2, 15, 31].

In order to examine the effects of inlet pressure and cavitation number on the decolorization rate of Rh6G, experiments were performed by varying inlet pressure in the range 3-11 at an optimum solution pH of 10.0 using circular and slit venturi. The obtained results are shown in Table 2.5. It has been observed that the decolorization rate increases with an increase in the inlet pressure up to an optimum value of 5 bar for both the venturies and then it decreases beyond an optimum. An increase in decolorization rate with an increase in inlet pressure or decrease in cavitation number may be attributed to the enhanced cavitation intensity due to more number of cavities are formed at higher inlet pressure leading to the generation of more $\cdot\text{OH}$ radicals. At higher inlet pressure beyond an optimum, it is estimated that choked cavitation takes place reducing the cavitation intensity due to partial collapse of cavities leading to lower degradation rate [38-41]. Also, inactive (unstable) cavities are formed in the cavitating devices at higher inlet pressure above an optimum value which reduce the degradation rate of pollutant molecules. An optimum inlet pressure for circular and slit venturi was found to be 5 bar with respective cavitation number as 0.11 and 0.07. Almost 32% decolorization with first order rate constant of $3.0 \times 10^{-3} \text{ min}^{-1}$ was observed in the case of slit venturi while about 29% decolorization with first order rate constant of $2.5 \times 10^{-3} \text{ min}^{-1}$ was found using circular venturi in 120 min at an optimum inlet pressure and cavitation number. The possible reason behind the higher decolorization using slit venturi can be attributed to the fact that velocity of liquid in case of slit venturi is higher as compared to circular venturi at the same operating inlet pressure. Therefore, number of passes through slit venturi would be higher as compared to circular venturi. Because of higher number of passes through the cavitating device, pollutant molecules experience longer exposure of the cavitating conditions resulting into higher decolorization rate of pollutant molecules [38]. In

Chapter 2: Degradation of a cationic dye (Rhodamine 6G) using hydrodynamic cavitation coupled with other oxidative agents

addition to this, there is another parameter, known as α (throat perimeter to its cross-sectional area ratio) which also affects the cavitation activity. A higher value of α provides better cavitation intensity. In the present work, slit venturi has a higher value of α (2.63) as compared to circular venturi (2.00) and therefore gives better degradation efficiency than circular venturi. It has been reported that higher ratio of throat perimeter to throat cross sectional area maximizes the frequency of turbulence which causes rapid oscillation of a cavity and thereby resulting into higher cavity collapse pressure [16, 42-43]. Hence, optimized slit venturi has been used for all the remaining sets of experiments. The cavitation number, velocity, and flow rate through the system with respect to operating pressure are given in Table 2.5. Similar results have been reported by Saharan et al. [15]. They have investigated degradation of Orange-G dye using three cavitating devices such as circular, slit and orifice and reported that degradation of Orange-G was higher in the case of slit venturi as compared to circular venturi and orifice.

Table 2.5: Kinetic rate constants at different operating pressures

Cavitating device	Pressure (bar)	Flow rate (LPH)	Velocity (m/s)	Cavitation number (C_v)	First order rate constant, $k \times 10^3$ (min^{-1})	Extent of decolorization (%)
Slit venturi	3	518	45.86	0.092	1.6	18.90
	5	592	52.55	0.070	3.0	32.06
	7	631	55.74	0.062	2.5	28.90
	9	678	59.88	0.054	2.3	26.14
	11	719	63.38	0.048	2.1	22.86
Circular venturi	3	412	36.30	0.147	2.3	24.38
	5	472	41.72	0.111	2.5	29.65
	7	507	44.90	0.096	2.4	28.59
	9	553	49.04	0.086	2.3	26.03
	11	585	51.60	0.073	2.0	25.19

(Experimental conditions: volume of solution, 6L; initial concentration, 10 ppm; pH of solution, 10.0)

2.3.5 Combination of hydrodynamic cavitation and H₂O₂

The main aim of this study is to generate the additional amount of $\cdot\text{OH}$ radicals by adding H₂O₂ in HC reactor. Hydrogen peroxide due to its high oxidation capacity (1.78 eV) can be used as an oxidizing agent to enhance the decolorization efficiency of dye and also it can easily be dissociated into more reactive $\cdot\text{OH}$ radicals under the effect of HC. The $\cdot\text{OH}$ radicals are highly reactive and therefore in addition to reaction with organic pollutant, radicals may react with other scavengers present in the liquid (including water itself) and with the intermediates formed during the degradation reactions. Since only a fraction of generated radicals will be used for degrading the pollutant, a higher pollutant to H₂O₂ ratios is needed. The effect of different molar ratios of dye to H₂O₂ concentration (1:10, 1:20, 1:30, 1:40, and 1:50) on the decolorization rate of Rh6G has been investigated using slit venturi at 5 bar inlet pressure and pH 10.0. The obtained results are depicted in Figure 2.6 and Table 2.6. It has been observed that decolorization rate constant of Rh6G was increased from $3.0 \times 10^{-3} \text{ min}^{-1}$ using HC alone to $21.6 \times 10^{-3} \text{ min}^{-1}$ when HC is combined with H₂O₂ at an optimum molar ratio of dye to H₂O₂ (1:30). There was no further increase in the decolorization rate of dye beyond the molar ratio of 1:30 (dye concentration: H₂O₂). Hence, molar ratio of 1:30 has been selected as an optimum loading at which 53.72% decolorization was achieved. The obtained higher decolorization rate is due to the continuous dissociation of H₂O₂ into $\cdot\text{OH}$ radicals under HC effect. Beyond an optimal molar ratio of dye to H₂O₂, reduction in the degradation rate is due to the recombination of $\cdot\text{OH}$ radicals and the scavenging of $\cdot\text{OH}$ radicals by H₂O₂ itself [32-33, 38, 44-46]. The following reactions (equations (2.7)-(2.14)) can occur during the degradation of pollutant molecules using the combined HC and H₂O₂ process [39].



Chapter 2: Degradation of a cationic dye (Rhodamine 6G) using hydrodynamic cavitation coupled with other oxidative agents



It can be concluded that H_2O_2 should be added at an optimal molar ratio to obtain best degradation efficiency of pollutant molecules. Similar trends were reported in the literature for the degradation of different organic pollutants [2, 21, 47-49]. Saharan et al. [2] have studied the degradation of reactive red 120 using hydrodynamic cavitation in the presence of H_2O_2 . They have observed that nearly 60% decolorization was obtained using HC alone at a solution pH of 2.0 and an operating inlet pressure of 5 bar. Whereas, decolorization has risen to about 100% by adding hydrogen peroxide at an optimum molar ratio of reactive red 120 to H_2O_2 as 1:60. Gore et al. [47] have observed almost complete decolorization of reactive orange 4 at 1:30 molar ratio of Orange-G to H_2O_2 and no further enhancement in the degradation rate was achieved at higher ratio because of the scavenging effect of H_2O_2 .

The study of H_2O_2 alone was also conducted in a stirred tank mixer at an optimum molar ratio of dye to H_2O_2 (1:30) for 2 h of operation time. A 10 ppm solution of Rh6G was taken in a stirred tank and solution pH was kept constant at 10.0. Normal stirring has been used to ensure complete mixing of H_2O_2 . It has been observed that almost 17% decolorization with a rate constant of $2.10 \times 10^{-3} \text{ min}^{-1}$ was obtained after 2 h of treatment time and thus it can be concluded that normal stirring is incapable to dissociate the H_2O_2 into $\cdot\text{OH}$ radicals and thereby reducing degradation efficiency.

To compute the efficiency of hybrid technique (HC + H_2O_2) as compared to the individual methods, synergetic coefficient has been determined. First order rate constant increased significantly from $2.10 \times 10^{-3} \text{ min}^{-1}$ in the case of only H_2O_2 to $21.6 \times 10^{-3} \text{ min}^{-1}$ for the combination of HC and H_2O_2 . The synergetic coefficient based on decolorization rate constant can be calculated for the hybrid technique by the following equation (2.15):

$$\begin{aligned} \text{Synergetic coefficient} &= \frac{k_{(\text{HC} + \text{H}_2\text{O}_2)}}{k_{\text{HC}} + k_{\text{H}_2\text{O}_2}} \quad (2.15) \\ &= 21.6 \times 10^{-3} / (3.0 \times 10^{-3} + 2.1 \times 10^{-3}) \\ &= 4.24 \end{aligned}$$

Chapter 2: Degradation of a cationic dye (Rhodamine 6G) using hydrodynamic cavitation coupled with other oxidative agents

The obtained synergetic coefficient as 4.24 demonstrates that the synergetic effect of combined method is better than the individual methods. This is due to enhanced generation of $\cdot\text{OH}$ radicals by the dissociation of H_2O_2 in presence of HC leading to the higher decolorization efficiency of Rh6G as compared to that obtained using only H_2O_2 .

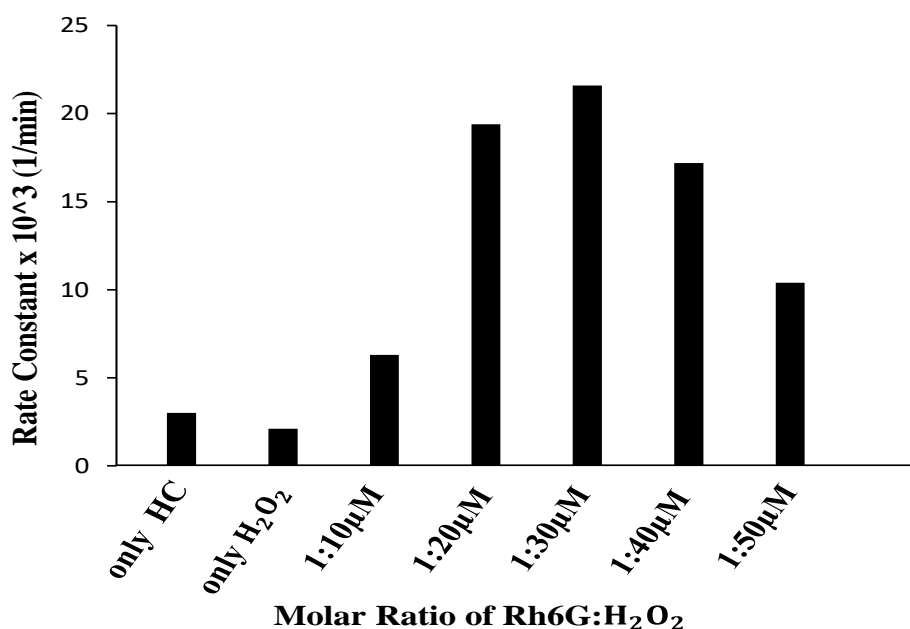


Figure 2.6: Effect of H_2O_2 addition on decolorization rate of Rh6G (Experimental Conditions: initial concentration, 10 ppm; solution pH, 10.0; volume of solution, 6 L; pressure, 5 bar)

Table 2.6: Effect of H_2O_2 addition on the extent of decolorization

Process	Molar ratio of Rh6G: H_2O_2	First order rate constant, $k \times 10^3 \text{ (min}^{-1}\text{)}$	Extent of decolorization (%)
HC alone	–	3.0	32.09
H_2O_2 alone	1:30	2.1	17.22
HC + H_2O_2	1:10	6.3	41.17
	1:20	19.4	49.08
	1:30	21.6	53.72
	1:40	17.2	49.82
	1:50	10.4	37.98

2.3.6 Combination of Hydrodynamic cavitation and ozone

Ozone (O₃) is a strong oxidizing agent which is capable in degrading the organic pollutants due to its high oxidation capacity (2.08 eV). The combination of HC and ozone can be used to intensify the degradation efficiency due to enhanced mass transfer of ozone molecules from gas phase to the bulk solution to react with organic pollutants under the cavitating conditions. Moreover, under the cavitation effect, ozone is easily decomposed yielding molecular O₂ and atomic oxygen which reacts with water molecules to form $\cdot\text{OH}$ radicals. The oxygen molecules can further decompose to O \cdot radicals which subsequently react with water molecule under cavitating conditions to form two $\cdot\text{OH}$ radicals per molecule of oxygen. The following reactions (equations (2.16)-(2.21)) can occur during the process of HC coupled with ozone [39, 47].



In order to study the effect of combination of HC with ozonation on the decolorization rate of Rh6G, experiments were performed at various loadings of ozone (1 to 7 g/h). A higher concentration of Rh6G (50 ppm) was taken to study the decolorization as well as mineralization rate using HC combined with ozone, since at lower concentration i.e. 10 ppm decolorization rate was very fast and also, the corresponding initial TOC was only 5ppm. Hence, there may be chances of higher experimental error. In order to avoid the experimental error and to observe the distinguishable reduction in TOC using TOC analyzer, a higher concentration of Rh6G was selected to analyze TOC with respect to time. The value of rate constant for mineralization and decolorization of Rh6G are shown in Table 2.7. It can be observed that the decolorization of Rh6G is 32.06% using HC alone after 120 min and further it is possible to achieve 100% decolorization in just 10 min by combining HC with ozone. As

Chapter 2: Degradation of a cationic dye (Rhodamine 6G) using hydrodynamic cavitation coupled with other oxidative agents

shown in Table 2.7, decolorization rate constant of Rh6G increases with an increase in the feed rate of ozone. When ozone feed rate increases, more $\cdot\text{OH}$ radicals may exist for the degradation of organic pollutants due to the dissociation of ozone under cavitating conditions. But mineralization study shows that reduction in TOC was found to be maximum at the ozone feed rate of 3 g/h. The mineralization rate constant increases with an increase in ozone feed rate till 3 g/h and further decreases. Maximum 73.19% reduction in TOC with rate constant of $10.9 \times 10^{-3} \text{ min}^{-1}$ was obtained in 120 min of operation at ozone feed rate of 3 g/h. Almost 10% reduction in TOC was obtained using only HC for the same treatment time. Hence, it can be concluded that optimum loading of ozone flow rate is 3 g/h for the degradation of Rh6G using hybrid method (HC + Ozone).

At this optimum flow rate of ozone, an experiment was conducted using only ozonation to evaluate the synergetic effect of combined process. During experimentation using only ozone, desired volume of Rh6G solution (6 L) was filled in the storage tank and ozone was directly injected into the Rh6G solution. Then, samples were withdrawn at regular time of interval by sampling valve which was connected at bottom of the storage tank. It can be seen from Table 2.7 that around 41% TOC reduction was achieved at the ozone flow rate of 3 g/h in 120 min of operation.

From Table 2.7, it can also be observed that mineralization rate constant ($10.9 \times 10^{-3} \text{ min}^{-1}$) for the HC combined with ozone was higher as compared to that obtained for the case of only ozone ($5.3 \times 10^{-3} \text{ min}^{-1}$) and only HC ($1.6 \times 10^{-3} \text{ min}^{-1}$). Synergetic coefficient based on the mineralization rate constant can be calculated for the combined method (HC + ozone) to examine the efficiency of this method using following equation (2.22):

$$\begin{aligned} \text{Synergetic coefficient} &= \frac{k_{(\text{HC}+\text{O}_3)}}{k_{\text{HC}} + k_{\text{O}_3}} & (2.22) \\ &= 10.9 \times 10^{-3} / (1.6 \times 10^{-3} + 5.3 \times 10^{-3}) \\ &= 1.58 \end{aligned}$$

The combination of HC and ozone indicates synergetic effect over individual method and observed value of the synergetic coefficient was 1.58. Similar results related to the effect of ozonation coupled with HC on the degradation rate of organic pollutants such as reactive orange 4 [47] and Triazophos [50] are reported in literature. Gore et al. [47] have investigated the effect of HC coupled with ozone for the mineralization of reactive orange 4 dye solution at various feed rate of ozone from 1 to 8 g/h. They have observed that about 76.25 %

Chapter 2: Degradation of a cationic dye (Rhodamine 6G) using hydrodynamic cavitation coupled with other oxidative agents

reduction in TOC obtained at optimal ozone feed rate of 3 g/h while only 14.67 % was obtained using HC alone in 60 min of treatment time. They have also reported synergetic effect for the combined process (HC + ozone).

Table 2.7: Effect of ozone addition on the decolorization and mineralization of Rh6G

Process	Flow rate of ozone (g/h)	Reduction in TOC (%) in 120min	Mineralization rate constant, $k \times 10^3(\text{min}^{-1})$	Decolorization (%)	Decolorization rate constant, $k \times 10^3(\text{min}^{-1})$
HC alone	–	10.32	1.6	8.37	0.7
Ozone alone	3	41.01	5.3	96.14	199.9
HC + Ozone	1	54.23	6.2	96.72	271.2
	2	62.12	7.1	97.85	312.5
	3	73.19	10.9	100	482.6
	5	69.68	10.3	100	571.3
	7	48.01	6.3	100	660.1

(Experimental conditions: initial concentration, 50ppm; pH of solution, 10.0; inlet pressure, 5bar)

2.3.7 Mineralization study

Total organic carbon (TOC) test is mostly used as an effective procedure to quantify the organic strength of wastewater. It is well known that degradation by-products generate throughout the oxidation of cationic dyes, and some of them could be more toxic and carcinogenic than their parent molecules. The dye decolorization is essentially due to the breaking of the chromophores of the dye molecules both due to the attack of $\cdot\text{OH}$ radicals as well as due to the shear generated during the cavity collapse. It is well known that various degradation by-products are generated throughout the oxidation of cationic dyes, and some of them could be more toxic and carcinogenic than their parent molecules. Decolorization results into the formation of various intermediates products and therefore cannot be used as a measure of the complete mineralization of the dye molecule. In order to quantify the mineralization of dye molecules into the end products such as CO_2 and H_2O , the Total organic carbon (TOC) test / or TOC content is normally measured which is an effective

Chapter 2: Degradation of a cationic dye (Rhodamine 6G) using hydrodynamic cavitation coupled with other oxidative agents

procedure to quantify the organic strength of wastewater. Hence, it is necessary to investigate the extent of mineralization of Rh6G by applying various processes such as HC alone, HC+H₂O₂, and HC+Ozone. Rh6G solution of 50 ppm (corresponding TOC as 22 ppm) was taken to study the effect of various processes on mineralization. The kinetics of mineralization of Rh6G is depicted in Figure 2.7. This figure clearly shows that mineralization of dye fitted first order kinetic data for all the above mentioned processes. The obtained results using various processes reveal that the combination of HC and ozone was more efficient as compared to other processes. The rate constants of mineralization process and reduction in TOC (%) using various processes are summarized in Table 2.8. First experiment was conducted using only HC to mineralize the dye at an optimum inlet pressure of 5 bar and pH of 10 using slit venturi. It has been observed that reduction in TOC was mostly occurred in the initial 60 min and overall 10% reduction in TOC was obtained. After that, slower mineralization rate was observed which indicates that the primary by-products were not mineralized easily into CO₂ and H₂O. After that mineralization study of Rh6G was performed using HC+H₂O₂ at an optimum molar ratio of dye to H₂O₂ (1:30 μM). Almost 16% TOC was reduced after 120 min of operation. In another experiment, same amount of H₂O₂ was added after every 15 min in order to check the effect of higher dosage of H₂O₂ on the extent of mineralization. It was observed that there was no significant change in TOC at the higher loading of H₂O₂ due to the scavenging action of [•]OH radicals by the excess amount of H₂O₂. The obtained results indicate that degradation by-products are hardly degraded using these two processes. Further experiments were carried out using combined HC and ozone at the optimized feed rate of ozone (3 g/h). It has been observed that TOC reduction was significantly increased to 73.19% within 120 min of treatment as compared to that obtained in HC and HC+H₂O₂. A high mineralization rate constant of $10.9 \times 10^{-3} \text{ min}^{-1}$ was obtained using HC+Ozone. Thereafter, further increase in the flow rate of ozone (5 g/h) decreases rate of mineralization ($10.3 \times 10^{-3} \text{ min}^{-1}$). At higher feed rate of ozone, scavenging action of undissociated ozone molecules under cavitating conditions may decrease mineralization rate of organic pollutants. Hence, optimum feed rate of ozone can be considered as 3 g/h.

In order to check the extent of mineralization at higher inlet pressure (10, 15, and 20 bar), experiments were also carried out at higher pressure using HC, HC + H₂O₂, and HC + Ozone. It was observed that in case of HC and HC + H₂O₂, there was no significant change in rate of mineralization at higher pressure. But in the case of HC combined with ozone, mineralization

Chapter 2: Degradation of a cationic dye (Rhodamine 6G) using hydrodynamic cavitation coupled with other oxidative agents

rate constant of Rh6G increased from $10.9 \times 10^{-3} \text{ min}^{-1}$ at an inlet pressure of 5bar to $22.3 \times 10^{-3} \text{ min}^{-1}$ at 20 bar (shown in Figure 2.7). It may be due to the enhancement of mass transfer rate between ozone molecules and bulk liquid solution due to high turbulent and shear created at higher operating inlet pressure. It may also possible that ozone molecules get easily dissociated into $\cdot\text{OH}$ radicals at higher operating inlet pressure of HC.

From obtained results, it is clear that the combination of HC with ozone contributes more in mineralization as well as enhances degradation efficiency of Rh6G.

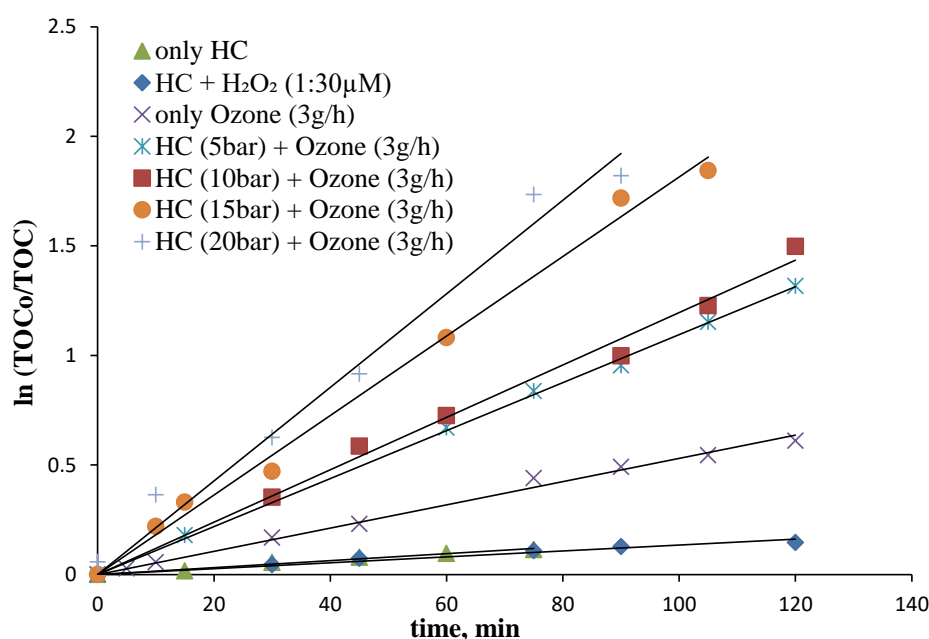


Figure 2.7: Kinetics of mineralization process of Rh6G (Experimental conditions: slit venturi; solution pH, 10.0; volume of solution, 6 L; initial concentration, 50 ppm)

Table 2.8: The values of mineralization rate constant and reduction in TOC (%) using various processes

Process	Reduction in TOC (%)	Mineralization rate constant,
HC alone	10.32	1.6
HC + H ₂ O ₂ (1:30 μM)	15.86	1.5
Ozone alone (3 g/h)	41.01	5.3
HC (5 bar)+ Ozone (3 g/h)	73.19	10.9
HC (10 bar)+ Ozone (3 g/h)	76.54	12.0
HC (15 bar)+ Ozone (3 g/h)	81.39	18.1
HC (20 bar)+ Ozone (3 g/h)	84.17	22.3

2.3.8 Degradation products and degradation pathway

In order to identify possible degradation by-products of Rh6G, liquid chromatography-mass spectrometry (LC-MS) analysis was performed on the samples collected during the combined process of HC and ozone at an optimum feed rate of 3 g/h. Since, degradation mechanism of Rh6G is the oxidation of Rh6G by the generated $\cdot\text{OH}$ radicals in all the three methods i.e. HC, HC+H₂O₂, and HC+ Ozone and therefore samples treated through HC+Ozone were taken for the LC-MS analysis. Moreover, similar mass spectra were observed for the samples treated using these three different methods. Samples were taken at fixed time interval (after every 15 min) and then analyzed by LC-MS immediately. This is a method to understand the reaction mechanism of Rh6G during HC. Rh6G was detected merely at $m/z = 443$ as shown in Figure 2.8a. The degradation by-products after 30 min of treatment using HC+Ozone were detected at $m/z = 415, 387, 359, 345, 312, 298, 286, 284, 272,$ and 258 as shown in Figure 2.8b. Based on the m/z value of by-products observed during the course of treatment, a possible degradation pathway of Rh6G has been proposed in Figure 2.9. It was found that the degradation of Rh6G follows oxidation mechanism which is initiated by the attack of $\cdot\text{OH}$ radicals on the Rh6G and then subsequent reaction with the intermediates under cavitating conditions. LC-MS analysis shows the formation of many aromatic by-products. It should be noticed that in the N-de-ethylation process, the hypsochromic shift of the absorption band is a characteristic phenomenon [50, 51]. In path 1 (Figure 2.9), the esterification reaction takes place to convert the ester group into carboxylic acid giving a possible by-product ($m/z = 415$). In HC, the generated $\cdot\text{OH}$ radicals may prefer to attack the central carbon atom with a high negative density charge to destruct the molecule structure of Rh6G and further degraded by N-de-ethylation process. The two major by-products with m/z as 415 and 387 obtained from mass spectra can be known as N-ethyl, N'-ethyl Rhodamine, and N-ethyl Rhodamine respectively. N-de-ethylated by-products such as N-ethyl Rhodamine ($m/z = 387$) was degraded into a possible by-products which has a m/z value of 359 and then it can be break into some other by-products with m/z values of 345 and 286. These formed by-products were further degraded into the m/z values of 272 and 258. In path 2, N-de-ethylation process as well as carboxylation process occurs which gives possible degradation by-product corresponding to the m/z value of 312. After carboxylation process, formed by-products further degraded into the other possible degradation by-products with m/z values of 298 and 284 by the dealkylation reactions. The obtained by-products were further oxidized into 3,4-

Chapter 2: Degradation of a cationic dye (Rhodamine 6G) using hydrodynamic cavitation coupled with other oxidative agents

dihydroxybenzoic acid ($m/z = 155$), adipic acid ($m/z = 146$), glutaric acid ($m/z = 132$), benzoic acid ($m/z = 122$), butane-1,3-diol ($m/z = 90$) and ethane 1,2-dioic acid ($m/z = 90$). Similar byproducts were also observed by other authors [51, 52] for the photocatalytic degradation of Rhodamine B. The similarity between the observed and reported data shows that degradation mechanism using HC is also initiated and propagated by the attack of $\cdot\text{OH}$ radicals on the pollutant molecules.

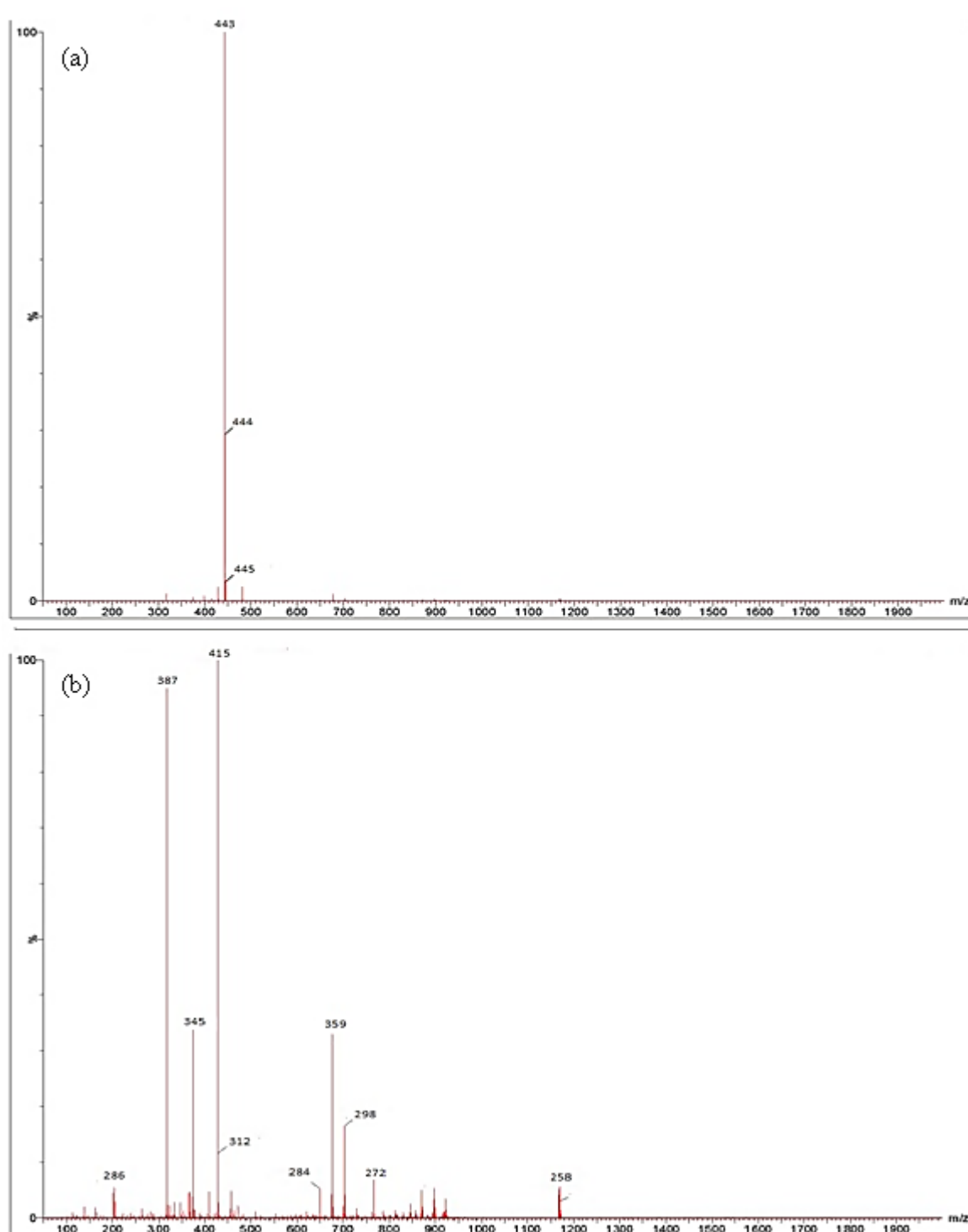


Figure 2.8: LC-MS of (a) Rh6G solution before treatment (b) degradation by-products of Rh6G after 30min of treatment

Chapter 2: Degradation of a cationic dye (Rhodamine 6G) using hydrodynamic cavitation coupled with other oxidative agents

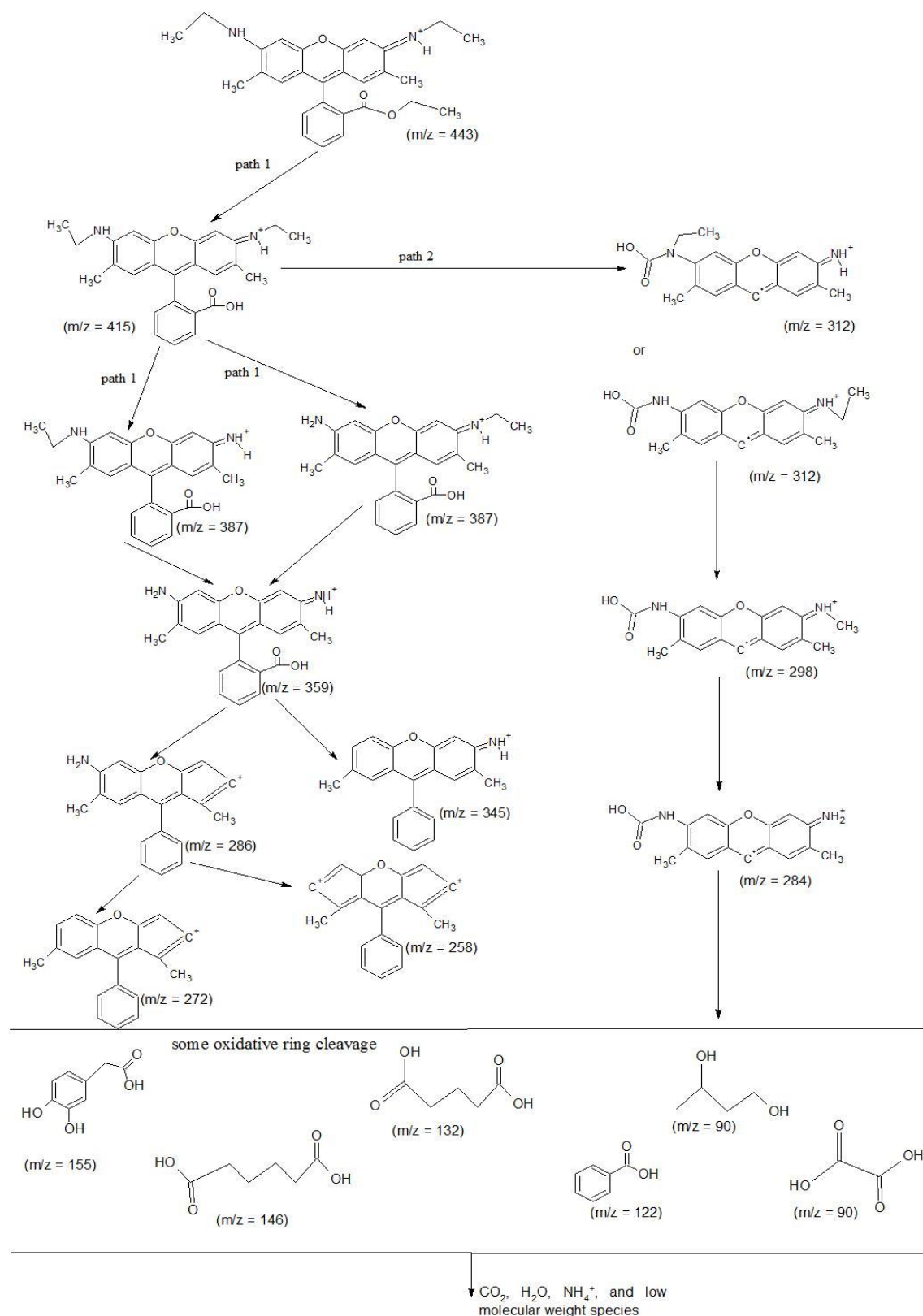


Figure 2.9: Proposed degradation pathway for the degradation of Rh6G

2.4 Novelty of the work

- The current work reports a novel approach based on HC for the treatment of Rhodamine 6G (Rh6G) dye which has not yet been reported.
- This study provides the optimized set of operating parameters of HC for achieving the maximum degradation efficiency of Rh6G dye solution.
- Two different cavitating devices such as slit and circular venturi were used in the present work and their comparison in terms of degradation efficiency is shown.
- In the present work, hybrid methods of HC in combination with H₂O₂ and ozone were established to achieve the maximum decolorization rate of Rh6G.
- The intensification of HC+Ozone has been established where the effect of higher inlet pressure (20 bar) on the mineralization process is reported for the first time.
- The degradation pathway of Rh6G has been proposed for better understanding of the degradation mechanism of Rh6G using HC. Additionally, the amount of H₂O₂ produced during HC was also evaluated to verify the production of [•]OH radicals during HC.

2.5 Summary of the chapter

The present study has shown the efficiency of HC for the decolorization and mineralization rate of Rh6G. Hybrid methods were found to be more efficient as compared to an individual process. At optimum parameters i.e. solution pH, inlet pressure and cavitation number, decolorization efficiency of Rh6G can be intensified in the presence of different oxidizing agent. The main conclusions drawn from present study can be summarized as follows:

1. The decolorization rate of Rh6G was influenced by the initial concentration of dye, solution pH, inlet pressure, and cavitation number using HC. The decolorization of Rh6G using HC process follows a first-order kinetic.
2. The concentration of H₂O₂ produced in the system confirms that the [•]OH radicals are formed during cavitation. The addition of radical scavenger such as tert-butanol decreases decolorization rate and thus indicating that decolorization of Rh6G using HC is dominated by the attack of [•]OH radicals.
3. The obtained results revealed that decolorization rate of Rh6G increased with an increase in inlet pressure till 5 bar for both the circular and slit venturi.

Chapter 2: Degradation of a cationic dye (Rhodamine 6G) using hydrodynamic cavitation coupled with other oxidative agents

4. Between the circular and slit venturi (used as cavitating devices in HC), slit venturi gives higher decolorization rate due to higher perimeter.
5. The decolorization rate of dye was also found to be strongly dependent on the solution pH. The maximum decolorization of Rh6G using HC alone was found to be 32.06% at 10.0 pH and pressure of 5 bar.
6. It was observed that HC coupled with H₂O₂ enhances the decolorization efficiency of Rh6G giving 53.72% decolorization at an optimum molar ratio of dye to H₂O₂ (1:30 μ M) as compared 32.06% obtained using HC alone.
7. The combination of ozone with HC gives the complete decolorization of Rh6G in 10 min of treatment time at 5 bar inlet pressure. Almost 84% TOC was removed at higher inlet pressure (20 bar) using HC coupled with ozone (3 g/h) in 120 min.
8. LC-MS was employed for identification of the degradation intermediates. It was observed that the degradation of Rh6G into the smaller intermediates and end products occurred through carboxylation and dealkylation process and initiated by the attack of \cdot OH radicals. A possible degradation pathway and reaction mechanism of Rh6G was proposed.

Overall, the obtained results revealed that the combination of HC with ozone can be a better technique to completely mineralize Rh6G and other similar dye effluents at large scale of operation.

The next chapter presents the study on a different dye reactive blue 13 using HC in combination with oxidative reagents such as H₂O₂, Fenton's reagent, oxygen and ozone as well as the optimization of the geometrical parameters of additional cavitating devices to get the maximum efficiency of HC reactor.

References

1. J. Wang, Y. Jiang, Z. Zhang, X. Zhang, T. Ma, G. Zhang, G. Zhao, P. Zhang, Y. Li, Investigation on the sonocatalytic degradation of acid red B in the presence of nanometer TiO₂ catalysts and comparison of catalytic activities of anatase and rutile TiO₂ powders, *Ultrason. Sonochem.* 14 (2007) 545-551.
2. V.K. Saharan, M.P. Badve, A.B. Pandit, Degradation of Reactive Red 120 dye using hydrodynamic cavitation, *Chem. Eng. J.* 178 (2011) 100-107.

3. M. Mrowetz, C. Pirola, E. Selli, Degradation of Organic Water Pollutants through Sonophotocatalysis in the presence of TiO₂, *Ultrason. Sonochem.* 10 (2003) 247-254.
4. U.G. Akpan, B.H. Hameed, Parameters affecting the photocatalytic degradation of dyes using TiO₂-based photocatalysts: a review, *J. Hazard. Mater.* 170 (2009) 520-529.
5. M. N. Ghazzala, H. Kebaili, M. Joseph, Photocatalytic degradation of Rhodamine 6G on mesoporous titania films: combined effect of texture and dye aggregation forms, *Applied Catalysis B: Env.* 115-116 (2012) 276–284.
6. R. Jain, M. Mathur, S. Sikarwar, A. Mittal, Removal of the hazardous dye rhodamine B through photocatalytic and adsorption treatments, *J. Environ. Manage.* 85 (2007) 956–964.
7. T.F. Robinson, G. McMullan, R. Marchant, P. Nigam, Remediation of dyes in textile effluent: a critical review on current treatment technologies with a proposed alternative, *Bioresour. Technol.* 77 (2001) 247-255.
8. M. Tamimi, S. Qourzal, N. Barka, A. Assabbane, Y. Ait-Ichou, Methomyl degradation in aqueous solutions by Fenton's reagent and the photo-Fenton system, *Sep. Purif. Technol.* 61 (2008) 103–108.
9. J. Madhavan, F. Grieser, M. Ashokkumar, Combined Advanced Oxidation Processes for the Synergistic Degradation of Ibuprofen in Aqueous Environments, *J. Hazard. Mater.* 178(2010) 202–208.
10. M. S. Lucas, J. A. Peres, Decolorization of the azo dye Reactive Black 5 by Fenton and photo-Fenton oxidation, *Dyes and Pig.* 71 (2006) 236-244.
11. F.M. Arriaga, S. Esplugas, J. Gimenez, Degradation of the emerging contaminant ibuprofen in water by photo-Fenton, *water res.* 44 (2010) 589-595.
12. E.E. Chang, H. Hsing, P. Chiang, M. Chen, J. Shyng, The chemical and biological characteristics of coke-oven wastewater by ozonation, *J. Hazard. Mater.* 156 (2008) 560–567.
13. Q. Dai, L. Chen, W. Chen, J. Chen, Degradation and kinetics of phenoxyacetic acid in aqueous solution by ozonation, *Sep. Purif. Technol.* 142 (2015) 287-292.
14. N. Golash, P.R. Gogate, Degradation of dichlorvos containing wastewaters using sonochemical reactors, *Ultrason. Sonochem.* 19 (2012) 1051-1060.

15. V.K. Saharan, M.A. Rizwani, A.A. Malani, A.B. Pandit, Effect of geometry of hydrodynamically cavitating device on degradation of orange-G, *Ultrason. Sonochem.* 20 (2013) 345–353.
16. V.S. Moholkar, A. B. Pandit, Modeling of hydrodynamic cavitation reactors: a unified approach, *Chem. Eng. Sci.* 56 (2001) 6295–6302.
17. J.S. Krishnan , P. Dwivedi , V.S. Moholkar, Numerical Investigation into the Chemistry Induced by Hydrodynamic Cavitation, *Ind. Eng. Chem. Res.* 45 (2006) 1493–1504.
18. P. Kumar, S. Khanna, V.S. Moholkar, Flow regime maps and optimization thereby of hydrodynamic cavitation reactors, *AIChE J.* 58 (2012) 3858–66.
19. K.S. Kumar, V.S. Moholkar, Conceptual design of a novel hydrodynamic cavitation reactor, *Chem. Eng. Sci.* 62 (2007) 2698 –2711.
20. Y.T. Didenko, W.B. McNamara, K.S. Suclick, Hot spot conditions during cavitation in water, *J. Am. Chem. Soc.* 121 (1999) 5817–5818.
21. V.K. Saharan, A.B. Pandit, P.S. SatishKumar, S. Anandan, Hydrodynamic cavitation as an advanced oxidation technique for the degradation of Acid Red 88 dye, *Ind. Eng. Chem. Res.* 51 (2012) 1981–1989.
22. N.B. Bokhale, S.D. Bomble, R.R. Dalbhanjan, D.D. Mahale, S.P. Hinge, B.S. Banerjee, A.V. Mohod, P.R. Gogate, Sonocatalytic and sonophotocatalytic degradation of Rhodamine 6G containing wastewaters, *Ultrason. Sonochem.* 21 (2014) 1797-1804.
23. K. Eslami, H. Eslami, Ultrasonic degradation of Rhodamine 6G in the presence of hydrogen peroxide and Zinc Oxide, *Int. J. Curr. Res. Aca. Rev.* 3 (2015) 187-195.
24. B.S. Banerjee, A.V. Khode, A.P. Patil, A.V. Mohod, P.R. Gogate, Sonochemical decolorization of wastewaters containing rhodamine 6G using ultrasonic bath at an operating capacity of 2L, *Desalin. Water Treat.* 52 (2013) 1378–1387.
25. N. Demir, G. Gunduz, M. Dukkanci, Degradation of a textile dye, Rhodamine 6G (Rh6G), by heterogeneous sonophotoFenton process in the presence of Fe-containing TiO₂ catalysts, *Environ. Sci. Pollut. Res.* 22 (2015) 3193–3201.
26. D. Lutic, C.G. Pastravanu, I. Cretescu, I. Poulivos, C.D. Stan, Photocatalytic treatment of Rhodamine 6G in wastewater using photoactive ZnO, *Int. J. of Photoenergy*, 2012 (2012) 1-8.

Chapter 2: Degradation of a cationic dye (Rhodamine 6G) using hydrodynamic cavitation coupled with other oxidative agents

27. A.M. Asiri, M.S. Al-Amoudi, T.A. Al-Talhi, A.D. Al-Talhi, Photodegradation of Rhodamine 6G and phenol red by nanosized TiO₂ under solar irradiation, *J. of Saudi Chem. Soc.* 15 (2011) 121–128.
28. A. Bashir, A.G. Soni, A.V. Mahulkar, A.B. Pandit, The CFD driven optimization of a modified venturi for cavitation activity, *Can. J. Chem. Eng.* 89 (2011) 1366-1375.
29. Kuldeep, V. K. Saharan, Computational study of different venturi and orifice type hydrodynamic cavitating devices, *J. Hydrodynamics* 28 (2016) 293–305.
30. M.A. Behnajady, N. Modirshahla, M. Shokri, B. Vahid, Effect of operational parameters on degradation of Malachite Green by ultrasonic irradiation, *Ultrason. Sonochem.* 15 (2008) 1009–1014.
31. S. Rajoriya, J. Carpenter, V. K. Saharan, A.B. Pandit, Hydrodynamic cavitation: an advanced oxidation process for the degradation of bio-refractory pollutants, *Rev. Chem. Eng.* In press, doi: 10.1515/revce-2015-0075.
32. P.N. Patil, S.D. Bote, P.R. Gogate, Degradation of imidacloprid using combined advanced oxidation processes based on hydrodynamic cavitation, *Ultrason. Sonochem.* 21 (2014) 1770–1777.
33. J. Wang, X. Wang, P. Guo, J. Yu, Degradation of reactive brilliant red K-2BP in aqueous solution using swirling jet-induced cavitation combined with H₂O₂, *Ultrason. Sonochem.* 18 (2011) 494–500.
34. X. Wang, J. Wang, P. Guo, W. Guo, C. Wang, Degradation of Rhodamine B in aqueous solution by using swirling jet-induced cavitation combined with H₂O₂, *J. Hazard. Mater.* 169 (2009) 486–491.
35. J. Yao, N. Gao, C. Li, L. Li, B. Xu, Mechanism and kinetics of parathion degradation under ultrasonic irradiation, *J. Hazard. Mater.* 175 (2010) 138–145.
36. X. Wang, Y. Zhang, Degradation of alachlor in aqueous solution by using hydrodynamic cavitation, *J. Hazard. Mater.* 161 (2009) 202-207.
37. Y.T. Shah, A.B. Pandit, V.S. Moholkar, *Cavitation Reaction Engineering*, Springer Science & Business Media, 2012.
38. K.P. Mishra, P.R. Gogate, Intensification of degradation of Rhodamine B using hydrodynamic cavitation in the presence of additives, *Sep. Purif. Technol.* 75 (2010) 385–391.
39. V.K. Saharan, D.V. Pinjari, P.R. Gogate, A.B. Pandit, *Advanced Oxidation Technologies for Wastewater Treatment: An Overview*, In *Industrial Wastewater*

Chapter 2: Degradation of a cationic dye (Rhodamine 6G) using hydrodynamic cavitation coupled with other oxidative agents

- Treatment, Recycling and Reuse, V.V. Ranade and V.M. Bhandari, eds, Elsevier, Butterworth, Heinemann, UK, (2014) 141-191.
40. M.V. Bagal, P.R. Gogate, Degradation of diclofenac sodium using combined processes based on hydrodynamic cavitation and heterogeneous photocatalysis, *Ultrason. Sonochem.* 21 (2014) 1035-1043.
 41. M.T. Angaji, R. Ghiaee, Decontamination of unsymmetrical dimethylhydrazine waste water by hydrodynamic cavitation-induced advanced Fenton process, *Ultrason. Sonochem.* 23 (2015) 257–265.
 42. V.S. Moholkar, A.B. Pandit, Bubble behavior in hydrodynamic cavitation: effect of turbulence, *AIChE J.* 43 (1997) 1641–1648.
 43. P.R. Gogate, A.B. Pandit, A review and assessment of hydrodynamic cavitation as a technology for the future, *Ultrason. Sonochem.* 12 (2005) 21–27.
 44. J.B. Bhasarkar, S. Chakma, V.S. Moholkar, Mechanistic features of oxidative desulfurization using sono-Fenton–peracetic acid (ultrasound/ Fe^{2+} – CH_3COOH – H_2O_2) system, *Ind. Eng. Chem. Res.* 52 (2013) 9038–9047.
 45. S. Chakma, V.S. Moholkar, Physical mechanism of sono-Fenton process, *AIChE J.* 59 (2013) 4303–4313.
 46. S. Chakma, V. S. Moholkar, Mechanistic analysis of hybrid sono-photo-ferrioxalate system for decolorization of azo dye, *J. Tai. Inst. Chem. Eng.* 60 (2016) 469–478.
 47. M.M. Gore, V.K. Saharan, D.V. Pinjari, P.V. Chavan, A.B. Pandit, Degradation of reactive orange 4 dye using hydrodynamic cavitation based hybrid techniques, *Ultrason. Sonochem.* 21 (2014) 1075–1082.
 48. S. Raut-Jadhav, V.K. Saharan, D.V. Pinjari, S. Sonawane, D. Saini, A. Pandit, Synergetic effect of combination of AOP's (hydrodynamic cavitation and H_2O_2) on the degradation of neonicotinoid class of insecticide, *J. Hazard. Mater.* 261 (2013) 139–147.
 49. R.H. Jawale, P.R. Gogate, A.B. Pandit, Treatment of cyanide containing wastewater using cavitation based approach, *Ultrason. Sonochem.* 21 (2014) 1392–1399.
 50. P.R. Gogate, P.N. Patil, Combined treatment technology based on synergism between hydrodynamic cavitation and advanced oxidation processes, *Ultrason. Sonochem.* 25 (2015) 60–69.

Chapter 2: Degradation of a cationic dye (Rhodamine 6G) using hydrodynamic cavitation coupled with other oxidative agents

51. T.S. Natarajan, M. Thomas, K. Natarajan, H.C. Bajaj, R.J. Tayade, Study on UV-LED/TiO₂ process for degradation of Rhodamine B dye, Chem. Eng. J. 169 (2011) 126–134.
52. Z. He, C. Sun, S. Yang, Y. Ding, H. He, Z. Wang, Photocatalytic degradation of rhodamine B by Bi₂WO₆ with electron accepting agent under microwave irradiation: mechanism and pathway, J. Hazard. Mater. 162 (2009) 1477–1486.

CHAPTER 3

Degradation of Reactive Blue 13 using Hydrodynamic Cavitation: Effect of geometrical parameters and different oxidizing additives

3.1 Introduction

In past years, many researchers have shown the utilization of hydrodynamic cavitation as an energy efficient process for treatment of bio-refractory pollutants [1-14]. The chemical effects that are induced during the degradation of organic pollutants using HC can be controlled by manipulating the operating (inlet pressure and cavitation number) and geometrical parameters (shape and size of the cavitating device). The effect of these parameters plays an important role in enhancing the efficiency and performance of HC reactors. Therefore, it is necessary to account for the geometrical parameters of a cavitating device to enhance the cavitation yield of a HC reactor.

The efficiency of HC reactor depends on the geometry of the cavitating devices which in turn depends on the residence time of a cavity in a low pressure region, pressure recovery rate at the downstream section, and number of cavitation events taking place inside the cavitating devices, i.e. the number of cavities being generated [15-16]. These parameters directly influence the cavity dynamic and thus the rate of generation of $\cdot\text{OH}$ radicals. Several numerical studies have been reported giving an insight about cavity dynamics combined with the chemical reactions and the mechanistic features of cavitation in various fields [17-20]. Also, CFD (computational fluid dynamics) analysis of the cavitating devices have been reported in literature providing information about the optimum geometries of venturies and orifices for the better cavitation yield [15-16]. The overall cavitation yield very much depends on the several parameters such as α (ratio of throat perimeter to its cross-sectional area), β (ratio of throat area to pipe cross-sectional area), and the ratio of the throat length to its height (in the case of a slit venturi) and divergence angle. These parameters can be altered to get the required cavitation yield in HC. In addition to the geometrical alteration, the efficiency of HC based degradation process can be enhanced by combining HC with other oxidizing additives such as ozone, H_2O_2 , Fenton reagent, CCl_4 , and sodium persulfate [3, 5-6, 8-13]. All these studies have reported that the efficiency of HC process can be increased by many folds if used in combination with oxidizing agents. Gore et al. [8] and Gogate and Patil [3] have reported that HC in combination with ozone is almost 3-5 times efficient than HC alone. Pradhan and Gogate [12] and Patil and Gogate [5] reported that addition of fenton reagent enhances the rate of degradation of organic pollutants using HC. These oxidizing agents produce more $\cdot\text{OH}$ radicals in presence of HC resulting into higher degradation efficiency of combined process as compared to individual process.

Chapter 3: Degradation of reactive blue 13 using hydrodynamic cavitation: Effect of geometrical parameters and different oxidizing additives

Some studies have been reported in the literature in which the geometry of cavitating devices such as orifice with a single and multiple holes, circular and slit venturi has been applied for wastewater treatment [21-24]. In the present study, two venturies (slit and circular) and six orifice plates with different geometries have been investigated to evaluate the effect of different geometrical parameters on the decolorization of RB13. As per our literature survey, there is no such study conducted which compares these cavitating devices with different geometrical parameters in the area of wastewater treatment. An attempt has also been made to enhance the decolorization efficiency of RB13 using the different intensifying agent (H_2O_2 and ferrous sulphate) and gaseous additives (oxygen and ozone). This study shows the optimization of the geometrical parameters of the different cavitating devices to get the maximum efficiency of HC reactor.

3.2 Materials and methods

3.2.1 Materials

Reactive Blue 13 dye (molecular weight-866.06 g/mol; molecular formula- $C_{29}H_{16}ClN_7Na_4O_{14}S_4$) was purchased from Alpha Aesar, Britain. The molecular structure of RB13 is shown in Figure 3.1. Double distilled water (prepared freshly in the laboratory via distillation unit) was used to prepare the solution of RB13. Hydrogen Peroxide (30%, w/v) of AR grade and ferrous sulphate heptahydrate ($FeSO_4 \cdot 7H_2O$) were obtained from Lobachemie (India). Solution pH was adjusted using NaOH and H_2SO_4 . All chemicals as received from suppliers were used for the experiments without any further purification.

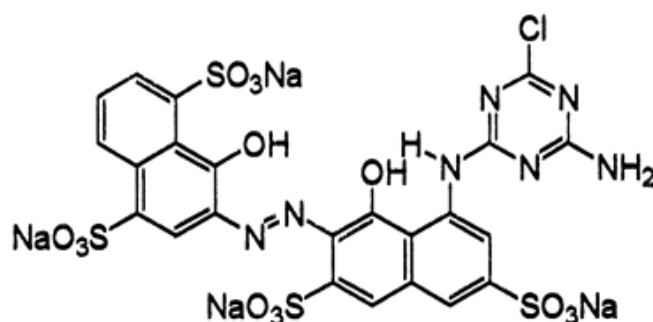
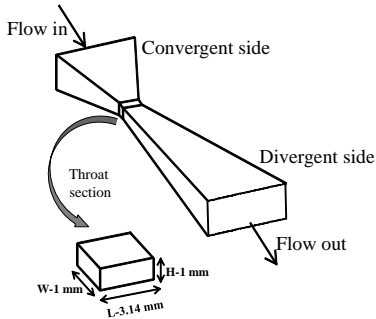
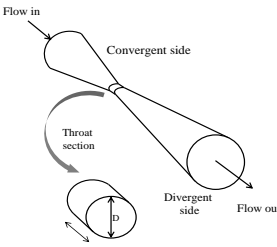
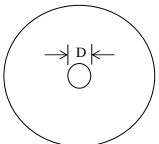
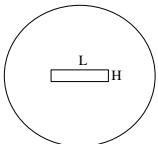
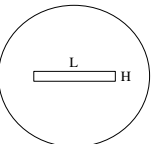
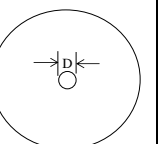
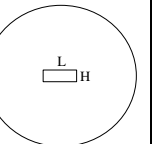
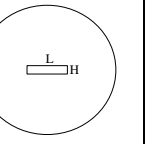


Figure 3.1: Molecular structure of Reactive Blue 13 dye

Table 3.1: Flow geometry of the cavitating devices

Cavitating devices/ Geometrical parameters	Slit venturi (SV) 	Circular venturi (CV) D = 2 mm 	 Orifice plate 1 (OP1) Diameter of hole (D): 3 mm	 Orifice plate 2(OP2) L – 7.065 mm, H – 1 mm	 Orifice plate 3(OP3) Length (L) – 14.14 mm, Height (H) – 0.5 mm	 Orifice plate 4(OP4) Diameter of hole (D): 2 mm	 Orifice plate 5(OP5) L – 3.14 mm, H – 1 mm	 Orifice plate 6(OP6) L – 6.28 mm, H – 0.5 mm
Total flow area, mm ²	3.14	3.14	7.065	7.065	7.065	3.14	3.14	3.14
Total perimeter, mm	8.28	6.28	9.42	16.13	29.28	6.28	8.28	13.56
α , mm ⁻¹	2.64	2.00	1.33	2.28	4.14	2.00	2.64	4.31
β	0.011	0.011	0.025	0.025	0.025	0.011	0.011	0.011

3.2.2 Experimental and analytical procedure

The detailed description and schematic of hydrodynamic cavitation reactor setup has been explained in chapter 2 (Section 2.2.2; Figure 2.1). The details of the cavitating devices used in the present work are given in Table 3.1.

Decolorization of RB13 has been carried out using HC at various conditions with a fixed aqueous RB13 solution of 6 L volume. All the experiments were performed for 120 min and samples were taken from the storage tank at a fixed interval of time for further analysis. During all the experiments, temperature of the solution ($30 \pm 2^\circ\text{C}$) was kept constant and was maintained by circulating cooling water through the cooling jacket. Initially, to optimize the cavitating devices, the effect of inlet pressure and cavitation number on the decolorization rate of RB13 has been studied at an inlet pressure from 0.3 to 1.2 MPa using all the cavitating devices. To study the effect of solution pH on the decolorization rate, experiments were conducted by varying the solution pH in range of 2.0–8.0. The effect of initial concentration of dye (in the range of 30–60 ppm) on the decolorization rate was studied using slit venturi. In order to enhance the decolorization of RB13, effect of process intensifying agent (H_2O_2 and ferrous sulphate) and gaseous additives (O_2 and O_3) in combination with HC were also investigated. Nine different molar ratios of concentration of RB13 to H_2O_2 as 1:1, 1:2, 1:3, 1:4, 1:5, 1:10, 1:20, 1:30, and 1:40 were selected to study the combined effect. Effect of H_2O_2 , oxygen, and ozone on the decolorization rate of RB13 were also investigated individually i.e. without HC in the present work. Additionally, one experiment was also performed using HC in the presence of air (flow rate: $1.5 \text{ L}\cdot\text{min}^{-1}$) for the same time of treatment at optimized conditions. Oxygen feed rate was varied from 1 to $4 \text{ L}\cdot\text{min}^{-1}$ to observe the optimum concentration of oxygen for getting the maximum decolorization effect. Pure oxygen was generated using an oxygen concentrator (maximum flow rate: $5 \text{ L}\cdot\text{min}^{-1}$, Eltech Engineers, India). The experiments were conducted using a combination of HC and ozone at a various feed rate of ozone from 1 to $4 \text{ g}\cdot\text{h}^{-1}$. Gases (Air, oxygen, and ozone) were injected at the throat of a cavitating device (slit venturi) through a nozzle thereby exposing gases directly to the cavitation effect. The Ozone was generated by an ozone generator (maximum feed rate of ozone: $10 \text{ g}\cdot\text{h}^{-1}$, Eltech Engineers, India).

Concentration of RB13 was measured by UV/Vis-Spectrophotometer (Shimadzu-1800) at the wavelength (λ_{max}) of 565 nm. Firstly, calibration chart was prepared for the known

concentrations of RB13 in the range of 10-50 ppm to calculate the concentration of unknown sample during experiments. A pH meter (Hanna Instruments, USA) was used to determine the pH of the solution throughout the experiments. Total organic carbon (TOC) content of dye solution was measured using TOC analyzer (GE InnovOx). In the present work, all experiments were repeated three times to evaluate the repeatability of the observed data, and the experimental errors were found to be within $\pm 3\%$ of the reported average values.

3.3 Results and discussion

3.3.1 Hydraulic Characteristics

In HC, a dimensionless parameter known as cavitation number (C_v) is used to characterize the condition of hydrodynamic cavitation inside a cavitating device. It is defined as the ratio of the pressure drop between the throat and extreme downstream section of the cavitating device to the kinetic head at the throat. Cavitation number is given by the following equation (3.1):

$$C_v = \left(\frac{P_2 - P_v}{\frac{1}{2} \rho v_o^2} \right) \quad (3.1)$$

The variation of cavitation number with operating inlet pressure for different cavitating devices is shown in Figure 3.2. This figure reveals that the cavitation number decreases with an increase in operating inlet pressure for all the cavitating devices. As the inlet pressure increases, volumetric flow rate through mainline and velocity at the throat increases which in turn reduces the cavitation number. A simulation study on HC conducted by Senthilkumar and Pandit [25] has also shown that the cavitation number decreases with an increase in the operating inlet pressure. More number of cavities are generated under ideal condition ($C_v \leq 1$), but in many cases, cavities can generate at $C_v > 1$ due to the existence of little-dissolved gases and suspended particles [26]. Hence, the overall cavitation number is affected by the inlet pressure and volumetric flow rate which also affects the number of cavitation events [22]. The cavitation number is known as cavitation inception number C_{vi} at which the first cavity occurs. Yan and Thorpe [27] have investigated the effect of geometry of orifice plates on the cavitation inception number. They have indicated that C_{vi} depends on the flow

geometry and increases with an increase in the orifice size and dimension. The effect of cavitation number on the decolorization rate of RB13 in detail has been discussed later.

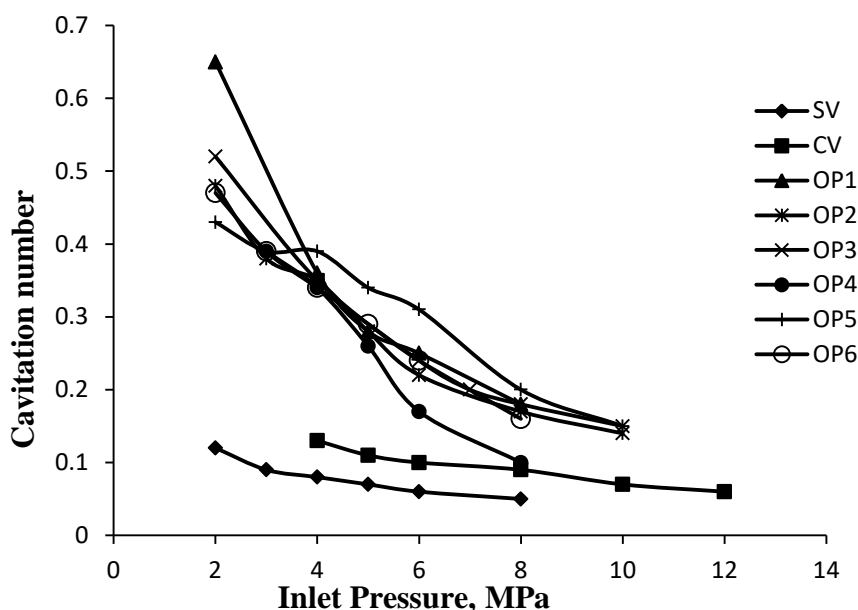


Figure 3.2 Hydraulic characteristics of the various cavitating devices

3.3.2 Optimization of solution pH

The solution pH plays a crucial role in determining the effective decolorization efficiency of pollutants using HC. The experiments related to optimization of solution pH were conducted at different solution pH ranging from 2 to 8 at an operating inlet pressure of 0.4 MPa and dye initial concentration of 30ppm. In this case, slit venturi was used to generate the hydrodynamic cavitation. The obtained results are shown in Figure 3.3 and Table 3.2. The results depict that the extent of decolorization increases with a decrease in solution pH. The maximum decolorization of 47% was obtained at a solution pH of 2. Kinetic study shows that first order rate constant decreased from 5.2×10^{-3} to $2.1 \times 10^{-3} \text{ min}^{-1}$ with an increase in the solution pH from 2 to 8 (shown in Figure 3.3). Based on these experimental results, all remaining experiments were performed at solution pH of 2.

The results clearly show that the extent of decolorization at acidic condition was higher as compared to that obtained at basic condition. Higher decolorization rate at acidic condition can be attributed to the fact that the production of $\cdot\text{OH}$ radicals in HC system are more favorable under acidic condition since it prevents the recombination of $\cdot\text{OH}$ radicals and

Chapter 3: Degradation of reactive blue 13 using hydrodynamic cavitation: Effect of geometrical parameters and different oxidizing additives

increases the oxidation potential of $\cdot\text{OH}$ radicals [5-6, 14]. Additionally, the enhancement in the extent of decolorization greatly depends on the fact that whether the dye molecule is present in molecular or ionic state. Under acidic condition, RB13 exists in its molecular state and hence RB13 locate itself at the cavity/water interface due to its hydrophobic nature where the concentration of $\cdot\text{OH}$ radicals is maximum giving higher decolorization rate. On other side, RB13 becomes hydrophilic in nature under basic condition thereby remaining in the bulk solution. Since $\cdot\text{OH}$ radicals are very reactive and therefore unlikely to diffuse in the bulk solution, and therefore decolorization rate is less under basic condition [10, 28]. Some similar observations have reported in the literature where acidic conditions favor destruction of organic pollutants using cavitation [9-10, 29-31]. Cai et al. [30] have studied the decolorization of Orange-G using orifice based HC at different pH values from 2.0 to 7.0 and maximum decolorization of 98.8% was obtained at pH value of 2.0 after 120 min of treatment. Saharan et al. [10] have also studied the effect of solution pH on the decolorization rate of Acid Red 88 dye using hydrodynamic cavitation at different pH ranging from 2 to 11 and reported that decolorization rate increases with a decrease in solution pH. A much lower decolorization rate was observed at pH 10.0 and almost 92% decolorization was achieved at pH 2.0.

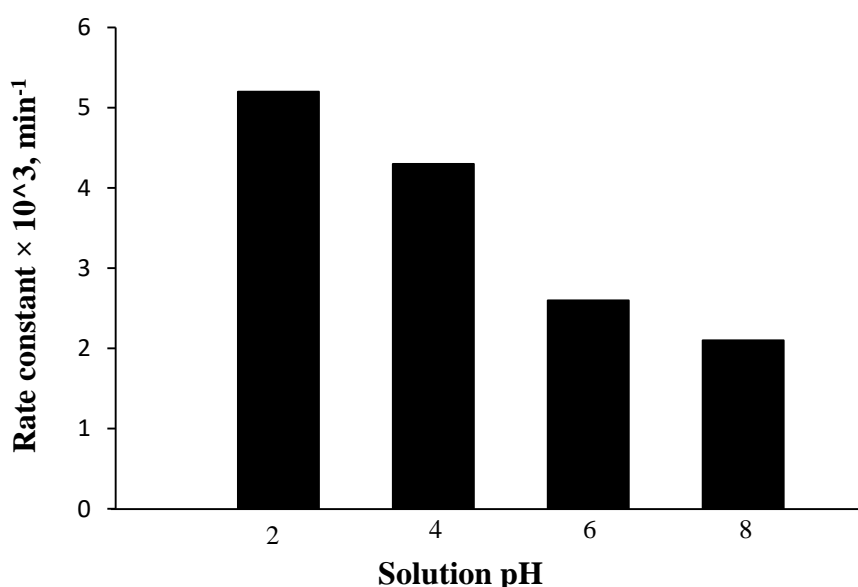


Figure 3.3: Effect of solution pH on decolorization rate of RB13. (Experimental conditions: inlet pressure, 0.4 MPa; volume of solution, 6 L; concentration, 30 ppm; slit venturi)

Table 3.2: Effect of solution pH on extent of decolorization

Solution pH	First order rate constant, $k \times 10^3$ (min^{-1})	Extent of decolorization (%)
2	5.2	47.47
4	4.3	42.44
6	2.6	32.36
8	2.1	22.58

3.3.3 Effect of initial RB13 concentration

The effect of initial concentration of RB13 on the decolorization was investigated using slit venturi as a cavitating device. Experiments were performed with different initial concentrations as 30, 40, 50 and 60 ppm at an operating inlet pressure of 0.4 MPa and solution pH of 2.0. The extent of decolorization is inversely proportional to its initial concentration of dye. The observed results are shown in Figure 3.4 and Table 3.3. It was observed that % decolorization decreased from 47% to 19% with an increase in the initial concentration of RB13 from 30 to 60 ppm.

To correlate the obtained data, first order kinetics was expected and degradation rate constants were calculated. The degradation kinetics can be expressed by equation (3.2):

$$\ln\left(\frac{C_t}{C_0}\right) = -kt \quad (3.2)$$

It has been observed that the plot of $\ln(C_t/C_0)$ v/s time is a straight line passing through the origin (as shown in Figure 3.4) which confirms that the decolorization of RB13 using HC follows first order kinetics. Many other authors have also reported that degradation of organic pollutants using HC follows first order kinetic [2, 31]. It was observed that the decolorization rate constant decreased from 5.2×10^{-3} to $1.7 \times 10^{-3} \text{ min}^{-1}$ for an increase in the concentration from 30 to 60 ppm. The obtained lower decolorization rate at higher concentration can be attributed to the fact that the total quantity of pollutant molecules increases with an increase in the initial concentration whereas the total concentration of $\cdot\text{OH}$ radicals remains constant in the system. Similar results related to a reduction in the degradation rate with an increase in initial concentration have been reported in literature [4, 6, 11, 31]. Patil et al. [6] have investigated the effect of initial concentration of imidacloprid on the degradation rate using

Chapter 3: Degradation of reactive blue 13 using hydrodynamic cavitation: Effect of geometrical parameters and different oxidizing additives

HC and found a decrease in the degradation rate with an increase in initial concentration of the pollutant. Rajoriya et al. [11] have illustrated the degradation of Rhodamine 6G (Rh6G) using HC and reported that degradation kinetics of Rh6G using HC follows first order reaction kinetic. They have observed that degradation rate was decreased from $2.9 \times 10^{-3} \text{ min}^{-1}$ to $0.7 \times 10^{-3} \text{ min}^{-1}$ for an increase in the concentration from 10 ppm to 50 ppm. Patil and Gogate [5] have also observed similar effects for the degradation of methyl parathion using hydrodynamic cavitation.

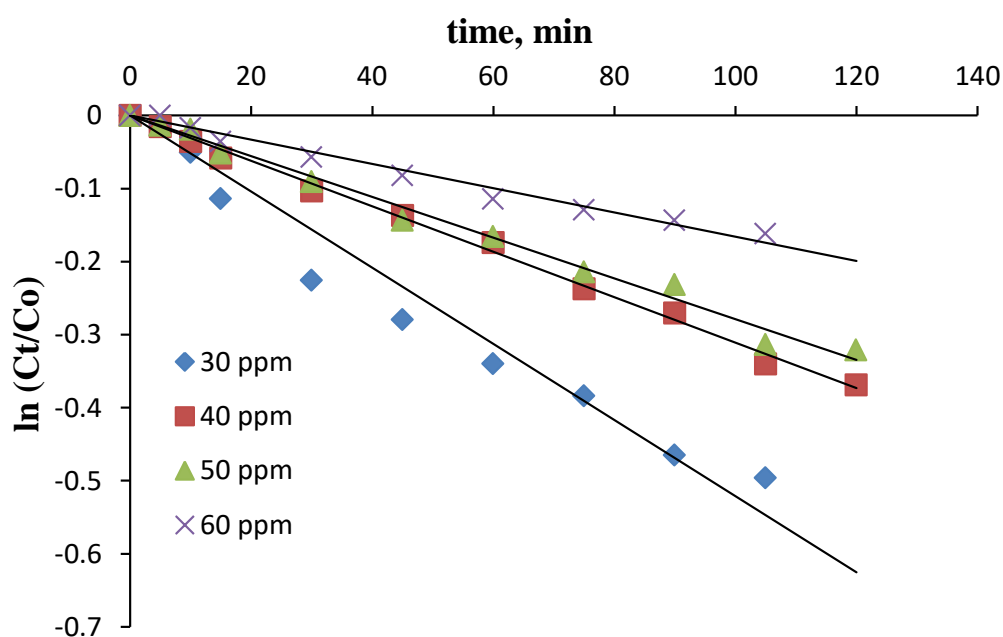


Figure 3.4: First order kinetic fitting into RB13 decolorization at different initial concentrations. (Experimental conditions: inlet pressure, 0.4 MPa; volume of solution, 6 L; solution pH, 2; slit venturi)

Table 3.3: Effect of initial concentration on extent of decolorization

Concentration (ppm)	First order rate constant, $k \times 10^3 \text{ (min}^{-1}\text{)}$	Extent of decolorization (%)
30	5.2	47.47
40	3.1	31.85
50	2.8	28.47
60	1.7	19.45

3.3.4 Optimization of different cavitating devices

The optimization of cavitating devices used in the present work is essential for getting the maximum decolorization efficiency of organic pollutants using HC. Two critical parameters such as operating inlet pressure and cavitation number affect the cavitation intensity at the downstream side of the cavitating device i.e. the number of cavities being generated and their final collapse pressure. Thus, it is necessary to optimize the operating inlet pressure and cavitation number for all the cavitating devices. The experiments were conducted at different inlet pressures to examine the efficiency of HC with different cavitating devices. The solution pH was kept constant at 2.0 for all the experiments. Figure 3.5 shows the effect of cavitation number on the decolorization rate of RB13. It was found that the decolorization rate increased with a decrease in cavitation number till an optimum value and then further decreased or remained constant for all the cavitating devices used. The decolorization rate of RB13 was higher in case of a slit venturi as compared to other cavitating devices. The maximum 47% decolorization with first order rate constant of $5.2 \times 10^{-3} \text{ min}^{-1}$ was achieved in slit venturi at an optimum inlet pressure of 0.4 MPa and cavitation number of 0.08. The decolorization rate of RB13 increases with a decrease in cavitation number. As the operating inlet pressure increases, the velocity at the throat of the cavitating devices also increases, and consequently, the cavitation number reduces (as per equation (3.1)), which shows the generation of higher number of cavities. The lower cavitation number creates more cavities resulting into a large amount of $\cdot\text{OH}$ radicals. Hence, more number of $\cdot\text{OH}$ radicals produced at a lower cavitation number increases the extent of degradation of the organic pollutants. Moreover, at lower cavitation number, the velocity will be higher at the throat of a cavitating device and hence the number of passes through cavitating device will also be higher for the same time of treatment. Pollutant molecules are exposed to the cavitating conditions for a longer time due to the higher number of passes resulting into higher decolorization rate of pollutant molecules. The number of passes can be determined using equation (3.3).

$$\text{Number of passes of liquid} = \left(\frac{\text{Volumetric flow rate}}{\text{Total volume of RB13 solution in the storage tank}} \right) \times \text{Treatment time} \quad (3.3)$$

But a very low cavitation number (higher inlet pressure) beyond an optimum value leads to the condition of choked cavitation [9, 28]. The optimum cavitation number strongly depends on the physico-chemical properties and geometrical parameters of the cavitating device. It can be seen from Figure 3.5 that the optimum cavitation number is different for different

Chapter 3: Degradation of reactive blue 13 using hydrodynamic cavitation: Effect of geometrical parameters and different oxidizing additives

devices, indicating that cavitation number is a strong function of geometrical parameters. The effect of these geometrical parameters on the cavitation yield is discussed in detail in next sections. The optimum inlet pressure and corresponding cavitation number for all the cavitating devices used in the present work are given in Table 3.4.

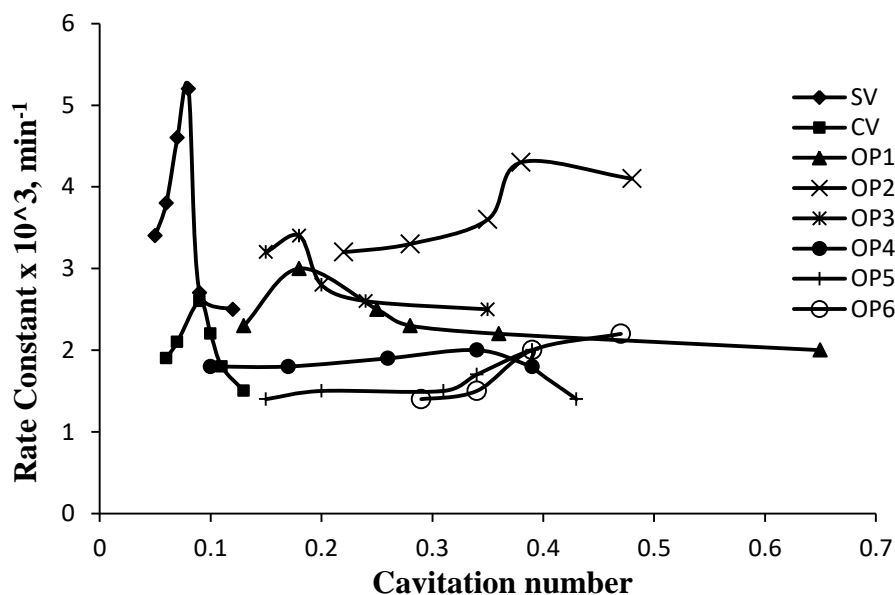


Figure 3.5: Effect of cavitation number on decolorization rate of RB13. (Experimental conditions: initial concentration, 30 ppm; pH of the solution, 2.0; volume of solution, 6 L)

Table 3.4: Effect of geometrical parameters (α , β) on decolorization rate of RB13

Cavitating devices/parameters	B	α , mm^{-1}	First order rate constant, $k \times 10^3 \text{ (min}^{-1}\text{)}$	Extent of decolorization (%)	Optimum inlet pressure, MPa	C_v
SV	0.011	2.64	5.2	47	0.4	0.08
CV	0.011	2.00	2.6	32	0.8	0.09
OP1	0.025	1.33	3.0	34	0.8	0.18
OP2	0.025	2.28	4.1	44	0.3	0.38
OP3	0.025	4.14	3.4	42	0.7	0.20
OP4	0.011	2.00	2.0	27	0.4	0.34
OP5	0.011	2.64	2.2	31	0.4	0.39
OP6	0.011	4.31	2.2	28	0.2	0.47

Experimental Conditions: volume of solution: 6 L, dye initial concentration: 30 ppm, solution pH: 2.0.

3.3.5 Effect of geometrical parameters

The geometrical parameters play an important role in determining the overall efficiency of decolorization process using HC. The parameters such as cavitation activity, number of cavitation events, the residence time of the cavities in a low-pressure zone, and pressure recovery rate in the downstream section significantly depend on the geometry of a cavitating device. The effect of different geometrical parameters of the cavitating device on decolorization efficiency of RB13 is presented in next sections:

3.3.5.1 Effect of α (throat perimeter/throat cross-sectional area)

A parameter α is defined as a ratio of throat perimeter to its cross-sectional area. In the present work, effect of α were investigated, and obtained results are shown in Table 3.4. It has been reported that higher throat perimeter for the same flow area increases the frequency of turbulence leading to more efficient cavity collapse and thus resulting into higher collapse pressure of a cavity [18, 32]. It has also been reported that cavitating devices having higher α value for a given flow area generates more cavities resulting into higher cavitation yield [23]. To observe the effect of α value on the decolorization efficiency of RB13, the shape of throat was changed from circular to rectangular with variable length and height of the throat as shown in Table 3.1 and 3.4. Three orifice plates having different α value were designed by varying the length and height of a rectangular throat as shown in Table 3.1 and 3.4 for each flow area.

The results obtained using OP1, OP2 and OP3 were compared to evaluate the effect of α (mm^{-1}) on the decolorization efficiency whereas the total flow area (throat cross-sectional area) of these cavitating devices was same (7.065 mm^2). In this study, the value of α lies in the range from 1.33 mm^{-1} for OP1 to 4.14 mm^{-1} for OP3. It can be observed from Table 3.4 that the decolorization rate of RB13 increases with an increase in the value of α up to an optimum value of 2.28 and slightly decreases thereafter. A maximum 44% decolorization with a first order rate constant of $4.1 \times 10^{-3} \text{ min}^{-1}$ was achieved using OP2. Similar observation can be made with results obtained using OP4, OP5, and OP6 as a cavitating device. Since, with an increase in the value of α for a given cross sectional area of throat, the intensity of turbulence and shear layer area increases, resulting into higher decolorization efficiency of the pollutant molecule. Also, for the same value of α (SV and OP5, CV and OP4), higher decolorization rate of RB13 was achieved in case of venturies than orifice plates

due to the smooth divergent and convergent section. Several studies have been reported in literature on optimizing α value in different applications [22-23, 33-35]. Sivakumar and Pandit [23] have investigated the degradation of Rhodamine B dye using multiple circular hole orifices and reported that degradation rate was increased from 2.67×10^{-5} to 5.33×10^{-5} sec^{-1} with an increase in α value from 0.8 to 4. They showed that higher value of α i.e. the plate having large number of holes (smaller diameter) was found to be more favorable as compared to the plate having small number of holes (larger diameter) due to higher throat perimeter.

In all, it can be concluded that the cavitation intensity of the cavitating devices depends on the value of α and its value should be kept higher for a given cross-sectional area.

3.3.5.2 Effect of β (throat area/pipe cross-sectional area)

The effect of another dimensionless geometrical parameter β known as a ratio of throat area to pipe cross-sectional area on decolorization rate of RB13 is shown in Table 3.4. In the present study, β value is varied from 0.011 to 0.025. It can be observed from Table 3.4 that the decolorization rate increases with an increase in the value of β . Orifice plates of different throat area (OP1 and OP4, OP2 and OP5, OP3 and OP6) were compared to observe the effect of β on the decolorization efficiency. Plates having larger value of β generate more cavities and thus gave higher decolorization rate. Higher decolorization rate of RB13 was achieved in case of OP1, OP2, and OP3 as compared to OP4, OP5, and OP6. Maximum 44% extent of decolorization with a first order rate constant of $4.1 \times 10^{-3} \text{ min}^{-1}$ was achieved with OP2 ($\beta = 0.025$) at an optimum inlet pressure of 0.3 MPa ($C_v = 0.38$) as compared to other plates (OP4, OP5, and OP6) having lesser β value (0.011). This is due to increasing flow area which enhances the number of cavitation events and thereby resulting into higher decolorization rate. Smaller ratio of throat area to pipe cross-sectional area produces more vaporous cavities which may result into choked cavitation and therefore is not useful for creating sonochemical effects. It has been reported that stable cavities are beneficial for application like wastewater treatment, whereas very low value of β is not required as it will only cause an increase in the operating cost. Similar observation was also made by Sivakumar and Pandit [23], they have reported that higher degradation of Rhodamine B obtained using orifice plate having β value of 0.022 at a cavitation number of 0.29, and the extent of degradation decreased with further increase in the value of β from 0.022 to 0.139. Since with a higher

throat area, velocity at the throat decreases which eventually decreases cavitation number resulting into lower degradation rate. For better degradation efficiency the cavitation number is reported to be in the range of 0.2-0.4 [28] and the area of throat should be set accordingly.

3.3.5.3 Effect of geometrical configurations (Comparison of venturies and orifice plates)

It has been reported that venturi has advantages over orifice plate due to their smooth convergent and divergent section which prevents early cavity collapse and enhances the cavity life. It can be seen from Table 3.4 that venturies gave higher decolorization than orifice plates. When circular venturi (CV) was compared with orifice plate (OP4) having a circular hole of similar α and β value, it was found that venturi gave higher decolorization than orifice plate. Similar observation were seen when slit venturi (SV) was compared with orifice plate (OP5) having a rectangular throat of same α and β value. Almost 47% decolorization was obtained using slit venturi as compared to only 31% obtained using orifice plate (OP5). It was observed that SV was found to be an optimum geometry among all the cavitating devices used in the present work. In case of venturies, pressure drop recovers smoothly due to the divergent angle and thus inhibits early collapse of the cavities resulting into higher growth of cavities before their violent collapse. An optimum divergent angle should be chosen for the desired cavitation intensity in a venturi because venturi having higher divergent angle will behave like an orifice plate thereby reducing the life of a cavity [15-16]. In case of orifice plates, the generated cavities in downstream section do not reach their maximum size due to the sudden pressure drop, resulting into a lower cavitation activity as compared to venturies. Hence, organic pollutant molecules will get longer exposure time under cavitating condition in case of venturies than orifice plates. It is observed that, for a given volumetric flow rate through HC reactor, the pressure head loss in the flow is lower in the case of venturies than orifice plates. In other words, for a given operating pressure, the volumetric flow rate is higher in the case of venturies than orifice plates, due to which venturies produce higher degradation efficiency than the orifice plates. These results clearly show that venturies are better than orifice plates of same flow area. Bashir et al. [16] and Kuldeep and Saharan [15] have studied different cavitating device and optimized various geometrical parameters for venturies and orifices. They have reported that venturies are better than orifice plate and higher throat perimeter is more beneficial since it

generates more cavities. Moreover by keeping a smooth divergence angle of 13° gives higher cavitation yield than higher angles.

3.3.6 HC combined with H_2O_2

The concentration of H_2O_2 in combination with HC plays an important role in determining the overall efficiency of decolorization process. Addition of H_2O_2 in HC system has positive effects on the decolorization process due to its high oxidation capacity (1.78 eV) and H_2O_2 can easily be dissociated into more reactive $\cdot OH$ radicals under cavitating conditions [5, 11, 14]. The experiments have been carried out at different molar ratios of dye to H_2O_2 concentration to observe its effect on the decolorization rate of RB13 at optimized inlet pressure of 0.4 MPa and solution pH 2.0 using a slit venturi as a cavitating device. The observed results are depicted in Figure 3.6 and Table 3.5. It was observed that the extent of decolorization of RB13 increased significantly with the addition of H_2O_2 till an optimum molar ratio of dye to H_2O_2 concentration (1:10), beyond which the extent of decolorization was constant. But, the decolorization rate was found to be higher at a molar ratio of dye to H_2O_2 concentration of 1:20, thus it has been selected as an optimum molar ratio at which about 91% decolorization with a first order rate constant of $46.6 \times 10^{-3} \text{ min}^{-1}$ was achieved. Beyond an optimal molar ratio of dye to H_2O_2 , the excess amount of H_2O_2 scavenges the $\cdot OH$ radicals produced in the system as shown in equation (3.7). The following reactions (equations (3.4)-(3.10)) can take place during the degradation of organic pollutants using a combination of HC and H_2O_2 process [11, 28, 36-38].



Chapter 3: Degradation of reactive blue 13 using hydrodynamic cavitation: Effect of geometrical parameters and different oxidizing additives



An experiment has also been carried out using H_2O_2 alone (in the absence of HC) at an optimum molar ratio of dye to H_2O_2 concentration (1:20) for 120 min of operation. A 30 ppm solution of RB13 was taken in a stirred tank, and solution pH was kept constant at 2.0. It was observed that almost 71% decolorization with a first order rate constant of $8.2 \times 10^{-3} \text{ min}^{-1}$ was achieved using H_2O_2 alone. TOC was also measured using HC and H_2O_2 individually, and almost 19% reduction in TOC was observed in the case of HC alone at the optimized conditions whereas no reduction in TOC was found with H_2O_2 alone for the same time of treatment (2 h). Hence, it can be said that H_2O_2 alone has an insignificant effect on the mineralization of RB13.

To quantify the effectiveness of combined process (HC+ H_2O_2), synergetic coefficient based on the decolorization rate was calculated for the combined process using the following equation (3.11):

$$\begin{aligned} \text{Synergetic coefficient} &= \frac{k_{(\text{HC}+\text{H}_2\text{O}_2)}}{k_{\text{HC}} + k_{\text{H}_2\text{O}_2}} \quad (3.11) \\ &= 46.6 \times 10^{-3} / (5.2 \times 10^{-3} + 8.2 \times 10^{-3}) \\ &= 3.47 \end{aligned}$$

Synergetic coefficient was found to be 3.47 indicating that the synergetic effect can be easily established for this combined process. Hence, it can be concluded that a combination of HC and H_2O_2 can be used at an optimal molar ratio to get higher decolorization as well as mineralization efficiency of the organic pollutants. Similar observations for enhanced decolorization rate can be seen in the literature for different organic pollutants [2, 8-11, 39]. Rajoriya et al. [11] have reported that the degradation rate of Rhodamine 6G (Rh6G) increased using hydrodynamic cavitation by the addition of H_2O_2 . They have observed that 32% decolorization was achieved using HC alone at a solution pH of 10.0 and operating inlet pressure of 5 bar. Whereas, % decolorization was enhanced to 54% in the presence of H_2O_2 at an optimum molar ratio of Rh6G to H_2O_2 (1:30) and beyond which a decrease in the extent of decolorization was observed due to the scavenging actions of unutilized H_2O_2 .

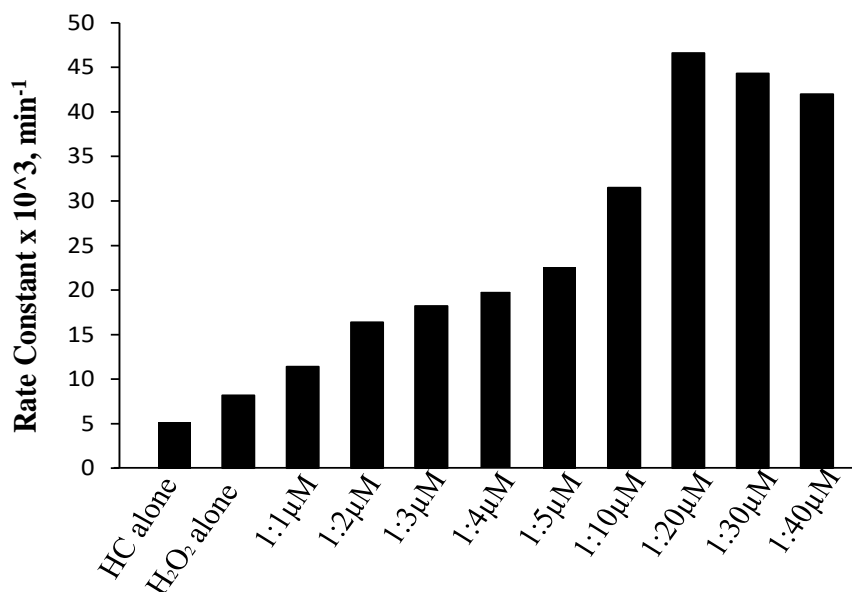


Figure 3.6: Effect of H₂O₂ addition on decolorization rate of RB13. (Experimental conditions: initial concentration, 30 ppm; solution pH, 2.0; volume of solution, 6 L; pressure, 0.4 MPa, slit venturi)

Table 3.5: Effect of H₂O₂ addition on extent of decolorization

Process	Molar ratio of RB13: H ₂ O ₂	First order rate constant, $k \times 10^3 (\text{min}^{-1})$	Extent of decolorization (%)
HC alone	–	5.2	47.47
H ₂ O ₂ alone	1:20	8.2	71.08
HC + H ₂ O ₂	1:1	11.4	71.46
	1:2	16.4	85.52
	1:3	18.2	85.61
	1:4	19.9	85.86
	1:5	22.6	86.12
	1:10	31.5	91.28
	1:20	46.6	91.49
	1:30	44.3	91.73
	1:40	42.0	90.20

Experimental conditions: initial concentration, 30 ppm; solution pH, 2.0; volume of solution, 6L; pressure, 4 bar

3.3.7 HC combined with oxygen

The addition of oxygen due to its oxidation potential (1.23 eV) can be used to intensify the generation of other oxidizing species in the presence of HC. Oxygen can react with water molecule under cavitating conditions to form two $\cdot\text{OH}$ radicals per molecule of oxygen as shown in equations ((3.12)-(3.13)) [40-42].



These additional formed $\cdot\text{OH}$ radicals can enhance the degradation efficiency. The oxygen molecule can also react with $\cdot\text{H}$ radicals (generated via dissociation of H_2O molecule) which produce $\cdot\text{OH}$ and $\text{HO}_2\cdot$ radical as shown in the following equations (3.15) and (3.16).



In order to study the effect of combination of HC with oxygen on the decolorization rate of RB13, experiments were carried out using slit venturi at an inlet pressure of 0.4 MPa and solution pH of 2.0. The oxygen flow rate was varied over the range of 1–4 L.min⁻¹. The obtained results are shown in Figure 3.7 and Table 3.6. It was observed that the extent of decolorization increased with an increase in the oxygen flow rate from 1 to 2 L.min⁻¹ and decreased with a further increase in the oxygen flow rate to 4 L.min⁻¹. Maximum decolorization of 65% with a first order rate constant of $8.6 \times 10^{-3} \text{ min}^{-1}$ was achieved at an optimum oxygen flow rate (2 L.min⁻¹). The lower decolorization at higher oxygen flow rate may be attributed to the fact that at higher O_2 flow rate, the entire downstream side of the cavitating device is choked due to the presence of excess amount of oxygen which causes the formation of cavity cloud and thus reducing the number of cavitation events due to incomplete cavity collapses. Also beyond an optimum oxygen flow rate, $\cdot\text{OH}$ radicals are scavenged by O_2 itself and thus resulting into lower decolorization of RB13 (equation (3.18)) [41-42]. In order to check the effect of air (78%-nitrogen, 21%-oxygen and 1%-other gases) on decolorization rate of RB13, an experiment was also carried out using HC combined with air (1.5 L.min⁻¹). The air was injected directly at the throat of the cavitating device. The

Chapter 3: Degradation of reactive blue 13 using hydrodynamic cavitation: Effect of geometrical parameters and different oxidizing additives

decolorization rate of RB13 was observed as $5.5 \times 10^{-3} \text{ min}^{-1}$ using HC in the presence of air at the same experimental condition and almost 53% decolorization was obtained (as shown in Table 3.6). This may be due to the presence of reactive gaseous species in the air which enhances the rate of generation of $\cdot\text{OH}$ radical thereby increases the rate of decolorization of dye molecule.

Synergetic effect for HC combined with oxygen has been calculated using the following equation (3.18).

$$\begin{aligned} \text{Synergetic coefficient} &= \frac{k_{(\text{HC}+\text{O}_2)}}{k_{\text{HC}} + k_{\text{O}_2}} && (3.18) \\ &= 8.6 \times 10^{-3} / (5.2 \times 10^{-3} + 1.4 \times 10^{-3}) \\ &= 1.30 \end{aligned}$$

The synergetic coefficient of the combined process (HC+Oxygen) is found to be 1.3. Synergetic effect observed has been credited to the fact that the combination of HC and oxygen generates higher concentration of hydroxyl radicals as compared to individual processes. The obtained synergetic coefficient in case of HC in combination with oxygen was lower than that obtained in the case of HC combined with ozone is mainly due to the fact that the extent of decolorization for process using ozone alone is 5 times higher than that of the process using oxygen alone

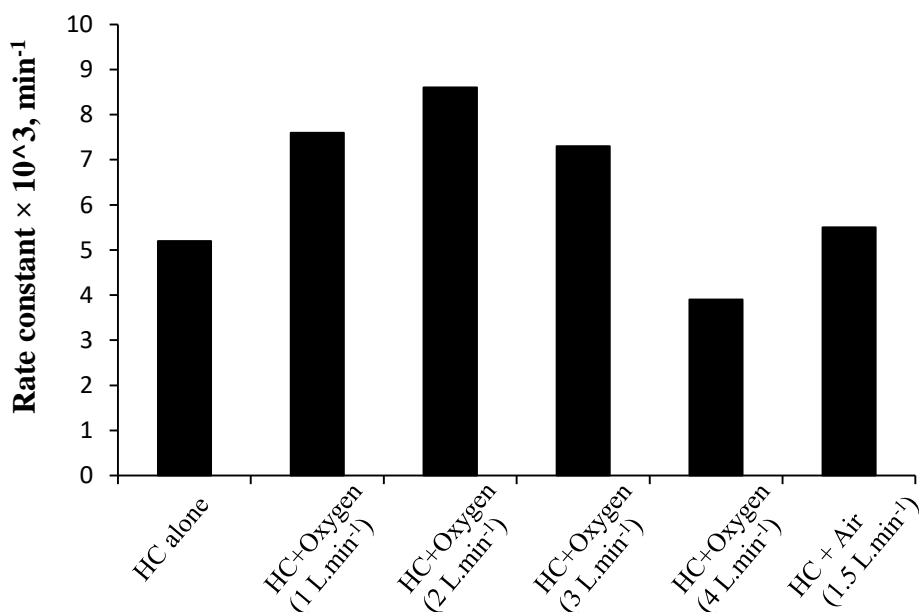


Figure 3.7: Effect of oxygen dosages on decolorization rate of RB13. (Experimental conditions: inlet pressure, 0.4 MPa; volume of solution, 6 L; solution pH, 2; slit venturi)

Table 3.6: Effect of oxygen dosages on extent of decolorization and first order rate constant

Process	Oxygen flow rate (L/min)	First order rate constant, $k \times 10^3$ (min^{-1})	Extent of decolorization (%)
HC alone	-	5.2	47.47
Oxygen alone	2	1.4	17.09
HC + Air (1.5 L/min)	-	5.5	52.77
HC + Oxygen	1	7.6	61.31
	2	8.6	65.48
	3	7.3	62.47
	4	3.9	39.44

3.3.8 Effect of addition of ferrous sulphate

The combination of HC and ferrous sulphate ($\text{FeSO}_4 \cdot 7\text{H}_2\text{O}$) may further enhance the generation of $\cdot\text{OH}$ radicals. It has been reported that approximately $71 \mu\text{M}$ of H_2O_2 is produced during HC [11]. It is well known that Fe^{2+} in the presence of H_2O_2 provides $\cdot\text{OH}$ radicals (as shown in equation (3.19)) and the subsequent Fe^{3+} ions react with hydrogen

Chapter 3: Degradation of reactive blue 13 using hydrodynamic cavitation: Effect of geometrical parameters and different oxidizing additives

peroxide, which gives the intermediate complex (Fe-OOH^{2+}) as shown in equations (3.19-3.21). Therefore, considering the fact that H_2O_2 molecules are produced during HC, an experiment was planned to initiate the Fenton oxidation by adding FeSO_4 during HC. The main reactions during the combined process of HC and FeSO_4 are as follows (equations (3.19-3.25)) [28, 38].



The effect of addition of ferrous sulphate was investigated at five different molar ratio of H_2O_2 : $\text{FeSO}_4 \cdot 7\text{H}_2\text{O}$ as 1:2, 1:3, 1:5, 1:7, and 1:10 considering that $71 \mu\text{M}$ of H_2O_2 is produced during HC. It should be noted that no additional H_2O_2 was added during the experiments and H_2O_2 produced during HC was only considered. The variations in %decolorization with loading of ferrous sulphate are given in Table 3.7. It can be seen that the extent of decolorization increased with an increase in the loading of ferrous sulphate till an optimum ratio of 1:3 and a further loading led to a decrease in the extent of decolorization. Almost 66% decolorization with first order rate constant of $8.6 \times 10^{-3} \text{ min}^{-1}$ was achieved at an optimum loading of ferrous sulphate (1:3). Higher decolorization rate obtained with the addition of ferrous sulphate can be attributed to the fact that higher quantum of $\cdot\text{OH}$ radicals were generated due to the initiation of Fenton mechanism.

Similar observations of improvement in the decolorization rate using HC combined with Fenton's reagent have been reported in literature. Joshi and Gogate [14] have illustrated the degradation of dichlorvos using a combination of HC and Fenton process and reported that

Chapter 3: Degradation of reactive blue 13 using hydrodynamic cavitation: Effect of geometrical parameters and different oxidizing additives

the maximum degradation of 91.5% was observed at an optimum ratio of 1:3 (H₂O₂ to ferrous sulphate). They reported that the combined process was 7 times better than using only HC for the degradation of dichlorvos. Jadhav et al. [43] have investigated the degradation of imidacloprid with hydrodynamic cavitation at different loadings of FeSO₄.7H₂O:H₂O₂ as 1:20 to 1:50 and reported that % degradation increased significantly from 6.15 to almost 97% in 15 min of treatment time with increasing the loading of Fenton's reagent (FeSO₄.7H₂O:H₂O₂ as 1:40).

Overall, it can be concluded that a combination of HC and FeSO₄.7H₂O (ferrous sulphate) can be effectively used to increase the degradation rate of organic pollutant.

Table 3.7: Effect of addition of ferrous sulphate on decolorization of RB13

Molar ratio of H ₂ O ₂ : FeSO ₄ .7H ₂ O	First order rate constant, $k \times 10^3$ (min ⁻¹)	Extent of decolorization (%) in 120 min
1:2	5.9	48.67±1.8
1:3	8.6	66.30±2.5
1:5	5.8	52.10±2.3
1:7	5.1	49.01±1.9
1:10	4.1	45.79±2.1
HC alone	5.2	47.47±2.3

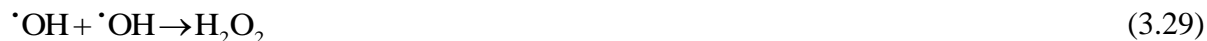
Experimental conditions: initial concentration, 30 ppm; pH of solution, 2.0; inlet pressure, 0.4 MPa.

3.3.9 HC combined with ozone

Ozone (O₃) with a high oxidation potential (2.08 eV) is capable of degrading the organic pollutants. The combination of HC and ozone can be used to achieve the maximum degradation efficiency due to improved mass transfer of ozone molecules under the effects of HC. Moreover, under the cavitation effect, O₃ gets easily decomposed and yields molecular O₂ and atomic oxygen O (³P) which reacts with water molecules to form [•]OH radicals. The following reactions (equations (3.26)-(3.31)) can occur during the process of HC coupled with ozone [8, 11, 38].



Chapter 3: Degradation of reactive blue 13 using hydrodynamic cavitation: Effect of geometrical parameters and different oxidizing additives



The experiments have been carried out at various loadings of ozone ($1\text{-}4 \text{ g.h}^{-1}$) to observe the effect of combination of HC with ozonation on the decolorization rate of RB13. All the experiments were conducted at the optimum conditions i.e. inlet pressure of 0.4 MPa and solution pH of 2.0. The ozone was injected at the throat of venturi to directly expose it to the cavitating condition. It was observed that almost 100% decolorization achieved using HC in combination with 1 g.h^{-1} ozone for an initial RB13 concentration of 30 ppm. Since the decolorization is very fast and therefore optimization of ozone dosages was done based on the complete mineralization (reduction in TOC) of RB13 as mineralization is a slow process. Also, initial TOC (total organic carbon) was found to be only 6 ppm when initial concentration of RB13 was taken as 30 ppm. Therefore, there may be chances of higher experimental error. In order to avoid the experimental error and to observe the distinguishable TOC reduction, a higher concentration of RB13 (150 ppm) was chosen to analyze TOC with respect to time. The values of rate constant for mineralization of RB13 are shown in Figure 3.8 and Table 3.8. It was observed that the extent of mineralization increased with an increase in the feed rate of ozone from 1 to 3 g.h^{-1} and remained constant afterward. A maximum reduction in TOC of 72% with a mineralization rate constant as $17.5 \times 10^{-3} \text{ min}^{-1}$ was achieved at ozone feed rate of 3 g.h^{-1} in 120 min of treatment. Based on these results, ozone feed rate of 3 g.h^{-1} was chosen as an optimum loading.

An experiment was carried out using only ozonation (at an optimum ozone feed rate of 3 g.h^{-1}) to determine the synergetic effect of combined process. The desired volume of RB13 solution (6 L) was filled in the storage tank, and ozone was directly injected into the solution. Then, samples were withdrawn at regular time of interval. Around 37% TOC reduction with a rate constant of $3.6 \times 10^{-3} \text{ min}^{-1}$ was observed in 120 min at the ozone feed rate of 3 g.h^{-1} .

Chapter 3: Degradation of reactive blue 13 using hydrodynamic cavitation: Effect of geometrical parameters and different oxidizing additives

To quantify the effectiveness of combined process (HC + Ozone), Synergetic coefficient based on the mineralization rate constant can be calculated for the combined process using following equation (3.32):

$$\begin{aligned} \text{Synergetic coefficient} &= \frac{k_{(HC+O_3)}}{k_{HC} + k_{O_3}} & (3.32) \\ &= 17.5 \times 10^{-3} / (1.4 \times 10^{-3} + 3.6 \times 10^{-3}) = 3.5 \end{aligned}$$

The calculated value of synergetic coefficient of combined process is 3.5, which indicates synergetic effect over an individual process. The trends of the obtained results in present study can be validated with similar literature reports [3, 8, 11]. Gogate and Patil [3] have investigated the effect of ozone in combination with HC at two different loadings of ozone (0.576 g.h⁻¹ and 1.95 g.h⁻¹) for the degradation of Triazophos. It was observed that almost 82% degradation achieved at the ozone feed rate of 1.95 g.h⁻¹ in combination with HC. Wu et al. [44] have investigated the degradation of succinic acid using HC in combination with H₂O₂ and O₃. They have reported that degradation rate of succinic acid increased from 1.81 to 3.95 μM.min⁻¹ with an increase in ozone flow rate from 50 to 200 mL.min⁻¹. They have concluded that an increase in the concentration of O₃ in bulk solution under the HC effect is the main cause for an increase in the degradation rate of succinic acid.

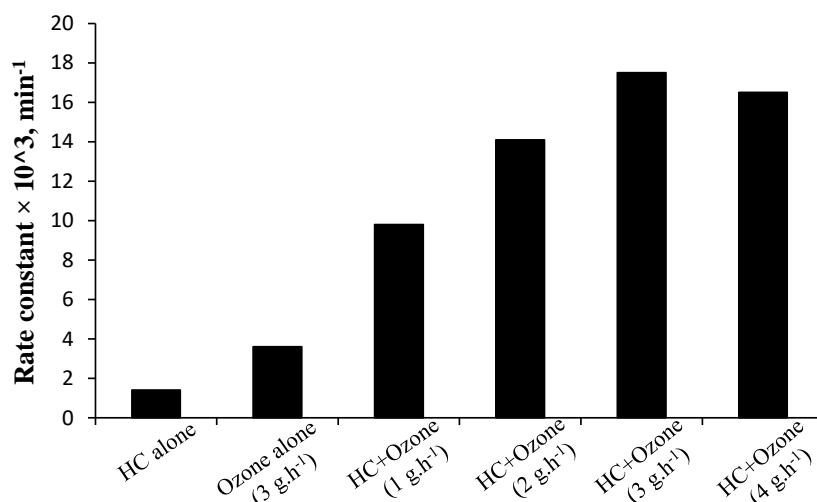


Figure 3.8: Effect of ozone addition on mineralization rate of RB13. (Experimental conditions: initial concentration, 150 ppm; volume of solution, 6 L; solution pH, 2; inlet pressure, 0.4 MPa)

Chapter 3: Degradation of reactive blue 13 using hydrodynamic cavitation: Effect of geometrical parameters and different oxidizing additives

Table 3.8: Effect of ozone addition on the decolorization and mineralization of RB13

Process	Flow rate of ozone (g/h)	Reduction in TOC (%) in 120min	Mineralization rate constant, $k \times 10^3(\text{min}^{-1})$	Decolorization (%)	Decolorization rate constant, $k \times 10^3(\text{min}^{-1})$
HC alone	–	19.06	1.4	7.39	0.5
Ozone alone	3	37.08	3.6	85.41	122.0
HC + Ozone	1	63.97	9.8	98.15	283.7
	2	70.69	14.1	99.10	296.2
	3	71.76	17.5	99.17	335.8
	4	71.38	16.5	99.24	375.1

Experimental conditions: initial concentration, 150 ppm; pH of solution, 2.0; inlet pressure, 4 bar.

3.3.10 Mineralization study

Mineralization study is mostly used as an effective process to quantify the organic strength of effluents. It is well known that complete decolorization of the dye pollutants does not mean that the dye is completely oxidized, but the mineralization of the dye in terms of TOC reduction indicates the complete oxidation of dye molecule into CO_2 and H_2O . Hence a reduction in TOC was estimated for different processes (HC alone, Ozone alone, HC + H_2O_2 , HC + Oxygen, and HC + Ozone). RB13 solution of 150 ppm (corresponding TOC as 29.5 ppm) was chosen to study the effect of various processes on mineralization. The rate constants of mineralization and reduction in TOC (%) using various processes at optimized conditions are given in Table 3.9. The observed results have indicated that HC + Ozone process is more efficient than any other processes. It was found that 19% reduction in TOC with a mineralization rate of $1.4 \times 10^{-3} \text{ min}^{-1}$ was achieved when the degradation was conducted using HC alone. About 25% reduction in TOC was found by adding hydrogen peroxide at an optimum molar ratio of RB13 to H_2O_2 (1:20) in combination with HC. This is due to the fact that the degradation by-products are more difficult to oxidize than their parent molecule. Almost 18% TOC was reduced using a combination of HC and oxygen (optimum feed rate of oxygen as $2 \text{ L}\cdot\text{min}^{-1}$) which indicates that primary by-products were not mineralized easily into CO_2 and H_2O using HC + O_2 . In the case of hybrid process of HC and ozone at an optimum feed rate of ozone ($3 \text{ g}\cdot\text{h}^{-1}$), TOC reduction was significantly increased

Chapter 3: Degradation of reactive blue 13 using hydrodynamic cavitation: Effect of geometrical parameters and different oxidizing additives

to 72% in 2 h of treatment which was higher than that obtained in HC and HC + H₂O₂, and HC + Oxygen. A high rate of TOC reduction ($17.5 \times 10^{-3} \text{ min}^{-1}$) was achieved using HC + Ozone. During experimentation using ozone alone, it is important to note that there was no change in TOC reduction in initial 60 min and after that 37% TOC was reduced in next 60 min at ozone feed rate of 3 g.h⁻¹. It was also found that the rate of TOC reduction (mineralization process) of dye is a relatively slower than decolorization rate. From the above results, it is clear that HC combined with ozonation contributed more to the decolorization as well as mineralization of the dye.

Table 3.9: Reduction in TOC, and mineralization rate constant using various processes

Process	Reduction in TOC (%) in 120min	Mineralization rate constant, $k \times 10^3 \text{ (min}^{-1}\text{)}$
HC alone	19.06	1.4
Ozone alone	37.08	3.6
HC + Ozone	71.76	17.5
HC + Oxygen	18.10	1.0
HC + H ₂ O ₂	24.65	2.3

Experimental Conditions: slit venturi; solution pH, 2.0; volume of solution, 6 L; inlet pressure of 0.4 MPa; initial concentration, 150 ppm.

3.4 Novelty of the work

- To the best of our knowledge, the treatment of RB13 dye using HC has not yet been reported.
- The present work reports the effect of different geometrical parameters such as α (ratio of throat perimeter to its cross-sectional area) and β (ratio of throat area to pipe cross-sectional area) of the single hole orifice plate having circular and rectangular throat which has been reported for first time.
- Effect of addition of ferrous sulphate and oxygen feed rate on the decolorization rate of RB13 using HC has also been investigated in this study, which is reported for first time.
- This study also presents the implementation of hybrid methods of HC in combination with ozone to achieve the maximum decolorization efficiency of RB13.

3.5 Summary of the chapter

This work shows that the efficiency of hydrodynamic cavitation is strongly influenced by the geometrical parameters such as α and β and operating parameters such as inlet pressure and cavitation number. The maximum extent of decolorization of RB13 was obtained using slit venturi at an optimum inlet pressure of 0.4 MPa ($C_v = 0.08$). It has been found that higher flow area is better for higher cavitation yield and for a given cross section area of throat it is always better to have higher throat perimeter for maximum degradation efficiency using HC. Amongst all the different cavitating devices used in the current work, slit venturi gave higher decolorization efficiency as compared to all the orifice plates. This is due to its smooth divergent section which enhances the cavity life resulting into increased overall cavitation yield. Furthermore it was observed that solution pH also affects the degradation efficiency of pollutants using HC and for RB13, pH 2.0 was found to be optimum. The degradation of organic pollutants can be improved significantly by adding different oxidizing agents during HC. It has been found that the decolorization and mineralization of RB13 increased when HC was combined with ozone, oxygen, H_2O_2 , and ferrous ion. The combined process of HC with ozone at an optimum feed rate of 3 g.h^{-1} provides complete decolorization of RB13 in 15 min with 72 % TOC reduction in 120 min. The combined HC and ozone was found to be best process for the decolorization and mineralization of RB13.

The next chapter presents different study on the photo-degradation of 4-Acetamidophenol (4-AMP), a bio-refractory pharmaceutical pollutant, commonly present in wastewater in combination with hydrodynamic and acoustic cavitation. A novel samarium and nitrogen doped TiO_2 photocatalysts were synthesized, characterized and its photocatalytic efficiency studied for the degradation of 4-AMP in combination with cavitation.

References

1. P. Braeutigam, M. Franke, R.J. Schneider, A. Lehmann, A. Stolle, B. Ondruschka, Degradation of carbamazepine in environmentally relevant concentrations in water by hydrodynamic-acoustic cavitation (HAC), *Water Res.* 46 (2012) 2469–2477.
2. S.R. Jadhav, V.K. Saharan, D.V. Pinjari, S. Sonawane, D. Saini, A. Pandit, Synergetic effect of combination of AOP's (hydrodynamic cavitation and H_2O_2) on the degradation of neonicotinoid class of insecticide, *J. Hazard. Mater.* 261 (2013) 139–147.

Chapter 3: Degradation of reactive blue 13 using hydrodynamic cavitation: Effect of geometrical parameters and different oxidizing additives

3. P.R. Gogate, P.N. Patil, Combined treatment technology based on synergism between hydrodynamic cavitation and advanced oxidation processes, *Ultrason. Sonochem.* 25 (2015) 60–69.
4. X. Wang, Y. Zhang, Degradation of alachlor in aqueous solution by using hydrodynamic cavitation, *J. Hazard. Mater.* 161 (2009) 202–207.
5. P.N. Patil, P.R. Gogate, Degradation of methyl parathion using hydrodynamic cavitation: Effect of operating parameters and intensification using additives, *Sep. Purif. Technol.* 95 (2012) 172–179.
6. P.N. Patil, S.D. Bote, P.R. Gogate, Degradation of imidacloprid using combined advanced oxidation processes based on hydrodynamic cavitation, *Ultrason. Sonochem.* 21 (2014) 1770–1777.
7. X. Wang, J. Jia, Y. Wang, Degradation of C.I. Reactive Red 2 through photocatalysis coupled with water jet cavitation, *J. Hazard. Mater.* 185 (2011) 315–321.
8. M.M. Gore, V.K. Saharan, D.V. Pinjari, P.V. Chavan, A.B. Pandit, Degradation of reactive orange 4 dye using hydrodynamic cavitation based hybrid techniques, *Ultrason. Sonochem.* 21 (2014) 1075–1082.
9. V.K. Saharan, M.P. Badve, A.B. Pandit, Degradation of Reactive Red 120 dye using hydrodynamic cavitation, *Chem. Eng. J.* 178 (2011) 100–107.
10. V.K. Saharan, A.B. Pandit, P.S. SatishKumar, S. Anandan, Hydrodynamic cavitation as an advanced oxidation technique for the degradation of Acid Red 88 dye, *Ind. Eng. Chem. Res.* 51 (2012) 1981–1989.
11. S. Rajoriya, S. Bargole, V.K. Saharan, Degradation of a cationic dye (Rhodamine 6G) using hydrodynamic cavitation coupled with other oxidative agents: Reaction mechanism and pathway, *Ultrason. Sonochem.* 34 (2017) 183–194.
12. A.A. Pradhan, P.R. Gogate, Removal of p-nitrophenol using hydrodynamic cavitation and Fenton chemistry at pilot scale operation, *Chem. Eng. J.* 156 (2010) 77–82.
13. M.V. Bagal, P.R. Gogate, Degradation of 2, 4-dinitrophenol using a combination of hydrodynamic cavitation, chemical and advanced oxidation processes, *Ultrason. Sonochem.* 20 (2013) 1226–1235.
14. R.K. Joshi, P.R. Gogate, Degradation of dichlorvos using hydrodynamic cavitation based treatment strategies, *Ultrason. Sonochem.* 19 (2012) 532–539.
15. Kuldeep, V. K. Saharan, Computational study of different venturi and orifice type hydrodynamic cavitating devices, *J. Hydrodynamics* 28 (2016) 293–305.

16. A. Bashir, A.G. Soni, A.V. Mahulkar, A.B. Pandit, The CFD driven optimization of a modified venturi for cavitation activity, *Can. J. Chem. Eng.* 89 (2011) 1366-1375.
17. J.S. Krishnan, P. Dwivedi, V.S. Moholkar, Numerical Investigation into the Chemistry Induced by Hydrodynamic Cavitation, *Ind. Eng. Chem. Res.* 45 (2006) 1493–1504.
18. V.S. Moholkar, A.B. Pandit, Bubble behavior in hydrodynamic cavitation: effect of turbulence, *AIChE J.* 43 (1997) 1641–1648.
19. J.B. Bhasarkar, S. Chakma, V.S. Moholkar, Mechanistic features of oxidative desulfurization using sono-Fenton–peracetic acid (ultrasound/ Fe^{2+} – CH_3COOH – H_2O_2) system, *Ind. Eng. Chem. Res.* 52 (2013) 9038–9047.
20. S. Chakma, V. S. Moholkar, Mechanistic analysis of hybrid sono-photo-ferrioxalate system for decolorization of azo dye, *J. Tai. Inst. Chem. Eng.* 60 (2016) 469–478.
21. V.K. Saharan, M.A. Rizwani, A.A. Malani, A.B. Pandit, Effect of geometry of hydrodynamically cavitating device on degradation of orange-G, *Ultrason. Sonochem.* 20 (2013) 345–353.
22. P. Senthilkumar, M. Sivakumar, A.B. Pandit, Experimental quantification of chemical effects of hydrodynamic cavitation, *Chem. Eng. Sci.* 55 (2000) 1633–1639.
23. M. Sivakumar, A.B. Pandit, Wastewater treatment: a novel energy efficient hydrodynamic cavitation technique, *Ultrason. Sonochem.* 9 (2002) 123–131.
24. N.P. Vichare, P.R. Gogate, A.B. Pandit, Optimization of hydrodynamic cavitation using a model reaction, *Chem. Eng. Tech.* 23 (2000) 683–690.
25. P. Senthilkumar, A.B. Pandit, Modeling hydrodynamic cavitation, *Chem. Eng. Technol.* 22 (1999) 1017-1027.
26. Y.T. Shah, A.B. Pandit, V.S. Moholkar, *Cavitation Reaction Engineering*, Springer Science & Business Media, 2012.
27. Y. Yan, R.B. Thorpe, Flow regime transitions due to cavitation in the flow through an orifice, *Int. J. Multiphase Flow* 16 (1990) 1023–1045.
28. S. Rajoriya, J. Carpenter, V. K. Saharan, A.B. Pandit, Hydrodynamic cavitation: an advanced oxidation process for the degradation of bio-refractory pollutants, *Rev. Chem. Eng.* 32 (2016) 379-411.
29. M.V. Bagal, P.R. Gogate, Sonochemical degradation of alachlor in the presence of process intensifying additives, *Sep. Purif. Technol.* 90 (2012) 92–100.

30. M. Cai, J. Su, Y. Zhu, X. Wei, M. Jin, H. Zhang, C. Don, Z. Wei, Decolorization of azo dyes Orange G using hydrodynamic cavitation coupled with heterogeneous Fenton process, *Ultrason. Sonochem.* 28 (2016) 302–310.
31. J. Wang, X. Wang, P. Guo, J. Yu, Degradation of reactive brilliant red K-2BP in aqueous solution using swirling jet-induced cavitation combined with H₂O₂, *Ultrason. Sonochem.* 18 (2011) 494–500.
32. V. S. Moholkar, A. B. Pandit, Modeling of hydrodynamic cavitation reactors: a unified approach, *Chem. Eng. Sci.* 56 (2001) 6295–6302.
33. Y. Huang, Y. Wu, W. Huang, F. Yang, X. Ren, Degradation of chitosan by hydrodynamic cavitation, *Polym. Degrad. Stab.* 98 (2013) 37–43.
34. B. Balasundaram, S.T.L. Harrison, Optimising orifice geometry for selective release of periplasmic products during cell disruption by hydrodynamic cavitation, *Biochem. Eng. J.* 54 (2011) 207–209.
35. D. Ghayal, A.B. Pandit, V.K. Rathod, Optimization of biodiesel production in a hydrodynamic cavitation reactor using used frying oil, *Ultrason. Sonochem.* 20 (2013) 322–328.
36. K.P. Mishra, P.R. Gogate, Intensification of degradation of Rhodamine B using hydrodynamic cavitation in the presence of additives, *Sep. Purif. Technol.* 75 (2010) 385–391.
37. S. Chakma, V.S. Moholkar, Physical mechanism of sono-Fenton process, *AIChE J.* 59 (2013) 4303–4313.
38. V.K. Saharan, D.V. Pinjari, P.R. Gogate, A.B. Pandit, Advanced Oxidation Technologies for Wastewater Treatment: An Overview, In *Industrial Wastewater Treatment, Recycling and Reuse*, V.V. Ranade and V.M. Bhandari, eds, Elsevier, Butterworth, Heinemann, UK, (2014) 141-191.
39. R.H. Jawale, P.R. Gogate, A.B. Pandit, Treatment of cyanide containing wastewater using cavitation based approach, *Ultrason. Sonochem.* 21 (2014) 1392–1399.
40. T. Sivasankar, V.S. Moholkar, Physical insights into the sonochemical degradation of recalcitrant organic pollutants with cavitation bubble dynamics, *Ultrason. Sonochem.* 16 (2009) 769–781.
41. T. Sivasankar, V.S. Moholkar, Physical features of sonochemical degradation of nitroaromatic pollutants, *Chemosphere* 72 (2008) 1795–1806.

Chapter 3: Degradation of reactive blue 13 using hydrodynamic cavitation: Effect of geometrical parameters and different oxidizing additives

42. T. Sivasankar, V.S. Moholkar, Mechanistic approach to intensification of sonochemical degradation of phenol, *Chem. Eng. J.* 149 (2009) 57–69.
43. S.R. Jadhav, V.K. Saharan, D.V. Pinjari, S. Sonawane, D. Saini, A. Pandit, Intensification of degradation of imidacloprid in aqueous solutions by combination of hydrodynamic cavitation with various advanced oxidation processes (AOPs), *J. Env. Chem. Eng.* 1 (2013) 850–857.
44. Z. Wu, G. Cravotto, B. Ondruschka, A. Stolle, W. Li, Decomposition of chloroform and succinic acid by ozonation in a suction-cavitation system: Effects of gas flow, *Sep. Purif. Technol.* 161 (2016) 25-31.

CHAPTER 4

Synthesis and characterization of Samarium and Nitrogen doped TiO₂ photocatalysts for photo-degradation of 4-Acetamidophenol in combination with hydrodynamic and acoustic cavitation

Chapter 4: Synthesis and characterization of Samarium and Nitrogen doped TiO₂ photocatalysts for photo-degradation of 4-Acetamidophenol in combination with hydrodynamic and acoustic cavitation

4.1 Introduction

Nowadays, the presence of pharmaceutical compounds in the aquatic environment causes a serious environmental problem. Due to their extensive production for use and the actual consumption in modern societies, they are detected in surface waters [1-2], sewage effluents [3-4], rivers [5], ground waters as well as drinking water [6-7]. 4-Acetamidophenol (4-AMP) is one such pharmaceutical compound found at concentration levels up to 65 $\mu\text{g L}^{-1}$ in wastewater from effluent treatment plants [8] and also in lower concentrations (ngL^{-1} - $\mu\text{g L}^{-1}$) in the surface water resources because of the direct disposal of treated and untreated sewage [9]. 4-AMP is more popularly known as paracetamol (*N*-Acetyl-4-aminophenol) which is generally used to reduce the fever and relieve pain especially in osteoarthritis patients. 4-AMP is generally safe at the advisable dosage, but when it is used in excess amounts, liver microsomes oxidize 4-AMP to a toxic metabolite that cause liver damage and even death [10]. Considering the negative impacts of pharmaceutical compounds on human health and environment, it is required to eliminate them from wastewater before discharge and also restrict the accumulation into natural sources. Due to their bio-recalcitrant nature and chemical stability, conventional treatment processes are inefficient to completely degrade 4-AMP. Hence, it is very important to develop an efficient technique to treat such drugs present in aquatic environments or in the effluents. In literature, various combinations or individual operations of advanced oxidation processes (AOPs) involving cavitation, Fenton and photocatalytic oxidation have been employed by many researchers for the effective treatment of organic pollutants [11-16] with varying results on extent of degradation and the optimum operating parameters. Photocatalytic oxidation process based on TiO₂ semiconductor is reported to be an effective process for the degradation of various organic pollutants in water due to the properties of TiO₂ such as good chemical stability, high efficiency, non-toxicity, and eco-friendly nature [17-20]. However, due to its high band gap energy (3.2 eV), ultraviolet irradiation is essential for triggering the photocatalytic activity of TiO₂ and typically TiO₂ absorbs only 3-5 % of solar irradiation, hence limiting its practical use to ultraviolet range only (i.e. for $\lambda \leq 387 \text{ nm}$) [21, 22]. In addition, the fast recombination rate of generated electron-hole (e^-h^+) pairs within the photocatalyst is the major drawback that decreases the photocatalytic efficiency of TiO₂ [21, 23]. To improve the photocatalytic efficiency of TiO₂, many authors have reported doping of TiO₂ with various metals and non-

Chapter 4: Synthesis and characterization of Samarium and Nitrogen doped TiO₂ photocatalysts for photo-degradation of 4-Acetamidophenol in combination with hydrodynamic and acoustic cavitation

metals (e.g. Pt, Ag, Au, N, C, S) [13, 24-27], transition metals (e.g. Fe, Co) [14, 28-31], and rare earth metals (e.g. Ce, Sm, La) [32, 33-36]. Among these doped materials, especially, doping of TiO₂ with samarium and nitrogen not only reduces the recombination rate of photo-generated electron-hole pairs but also cause an increase in their wavelength response to visible region. In addition, N-doped TiO₂ particle is better utilized for photocatalytic degradation due to its comparable atomic size, small ionization energy, stability and capability to reduce the energy band gap of TiO₂ [26]. Moreover, presence of Sm being a rare earth element retards the TiO₂ transformation from anatase phase to rutile phase, which is beneficial for higher photocatalytic activity [22, 35]. Therefore, rare earth doped TiO₂ has attracted researcher's great interest [34-36]. In the last few decades, several techniques such as hydrothermal process, precipitation, ultrasound assisted sol-gel, solvothermal, sol-hydrothermal approaches etc. had been reported to synthesize doped TiO₂ based photocatalyst [26, 33, 37-38]. The physical and chemical properties of doped TiO₂ depend on the method of synthesis. Compared to other methods, ultrasound assisted sol-gel method is relatively a novel and efficient method for the preparation of nano-crystalline materials due to the capability of producing products of uniform structure, crystallinity and shape [26, 33-34]. Sonochemical route provides uniform distribution of the reactants during the synthesis as well as increases the phase purity of the photocatalyst with more specific surface area compared to conventional methods for the preparation of TiO₂ samples [33]. During ultrasonication, the collapse of bubbles/cavities generates localized "hot spots" where temperatures can reach up to 5,000 K and pressures of about 1000 atm [26]. These extreme conditions can obviously accelerate the condensation and/or hydrolysis reaction during the synthesis [33].

In the case of only photocatalytic oxidation, the reduction in efficiency of photocatalysts with continuous use is mainly due to the blockage of UV active sites and adsorption of organic pollutants at the surface of photocatalyst, thus reducing the degradation rate. In the last decade, many studies have reported the use of ultrasound in combination with photocatalytic oxidation to enhance the photocatalytic activity [30, 32, 39]. Photocatalytic oxidation in the presence of cavitation gives higher photo-degradation efficiency of organic pollutants due to the enhanced generation of the reactive species such as hydroxyl radicals ($\cdot\text{OH}$) and superoxide radicals ($\text{O}_2^{\cdot-}$). It is also reported that due to cavity oscillation and subsequent

Chapter 4: Synthesis and characterization of Samarium and Nitrogen doped TiO₂ photocatalysts for photo-degradation of 4-Acetamidophenol in combination with hydrodynamic and acoustic cavitation

collapse, high pressure liquid jets and shock waves are created which causes continuous cleaning of the catalyst surface thereby increasing the catalytic activity. Though many studies on the combination of ultrasound and photocatalytic oxidation for the treatment of organic pollutants have been reported, the studies are limited to laboratory scale [32, 34]. Use of ultrasound in combination with photocatalysis on a large scale has limitations for the treatment of wastewater due to its low energy efficiency and higher maintenance cost. In recent years, a new alternative technology i.e. HC combined with photocatalysis is found to be superior as compared to US in combination with photocatalysis due to its low cost and higher energy efficiency and it is also feasible for large-scale operation especially in the area of wastewater treatment [40-41]. HC alone does not give high percentage degradation but in combination with photocatalytic oxidation, it can provide higher extent of degradation due to the synergistic effects [39]. HC coupled with photocatalysis can overcome the limitations of photocatalytic oxidation i.e. irreversible adsorption of pollutants and their degradation products on the photocatalyst surface, which blocks the active sites. HC combined with photocatalytic oxidation also causes continuous cleaning of the catalyst surface and thereby provides more active sites for UV irradiation. Few studies have been reported on the application of HC combined with photocatalysis for the degradation of organic pollutants from wastewater [31, 39]. Bethi et al. [31] investigated the degradation of crystal violet dye using hydrodynamic cavitation operated individually as well as in combination with photocatalytic oxidation. It was reported that almost 45% degradation of crystal violet dye is obtained using HC alone at pH of 6.5 and inlet pressure of 5 bar whereas using 0.8% (mole %) of Fe-doped TiO₂ photocatalyst in combination results in almost complete degradation (98%). Raut-Jadhav et al. [39] also reported beneficial results with combination of HC and Nb₂O₅ photocatalysis with 55.18% degradation of imidacloprid at 15 bar operating inlet pressure and 200 mg/L of catalyst. According to the literature analysis and to the best of our knowledge, no studies has been reported in literature on the degradation of 4-AMP using HC coupled with photocatalysis using pure and Sm/N doped TiO₂ photocatalysts. Also, the analysis of studies with different compounds revealed that the extent of degradation obtained and the optimum operating conditions are strongly dependent on the type of pollutant and the configuration of hydrodynamic cavitation. Hence, keeping in mind the requirement of the development of an energy efficient process suitable for large scale operation that can also give enhanced degradation, photocatalytic degradation of 4-AMP over Sm and N-doped TiO₂

Chapter 4: Synthesis and characterization of Samarium and Nitrogen doped TiO₂ photocatalysts for photo-degradation of 4-Acetamidophenol in combination with hydrodynamic and acoustic cavitation

in the presence of hydrodynamic and acoustic cavitation was investigated for the first time in the present work. Another specific objective of this study was also to compare the photocatalytic activity of pure and doped (Sm and N) TiO₂ photocatalysts synthesized using ultrasound assisted sol-gel and conventional processes. The characterization of pure and doped TiO₂ photocatalysts was also performed and also the effects of various process parameters on the extent of degradation using different combination approaches were evaluated. With an objective of intensifying the degradation, experiments were also performed for the combination approach of photocatalytic oxidation with hydrodynamic and acoustic cavitation at optimal operating conditions. The degradation by-products formed during HC+photocatalytic process were also identified through mass-spectroscopy to understand the degradation mechanism and evaluate whether any toxic intermediates are formed.

4.2 Materials and methods

4.2.1 Materials

4-Acetamidophenol (98%) was procured from M/s Fisher Scientific Pvt. Ltd. Mumbai, India. All 4-AMP solutions and standards were prepared using double distilled water. Titanium butoxide (Ti(C₄H₉O)₄, 97%) from Sigma-Aldrich was used as the titanium precursor. Glacial acetic acid, urea, and 1-butanol (99.0% pure) were obtained from M/s Merck Ltd., Mumbai, India. Samarium (III) acetate hydrate (99.9%) was also obtained from Sigma Aldrich, Mumbai, India. Solution pH was adjusted using aqueous solutions of NaOH and H₂SO₄ as required. All the chemicals used were of analytical grade and used as received from the suppliers for the experiments without any further purification.

4.2.2 Synthesis of pure TiO₂ and doped TiO₂ photocatalysts

4.2.2.1 Conventional sol-gel process (CSP)

Pure and doped TiO₂ photocatalysts were synthesized using the conventional approach in the presence of stirring and without ultrasound [26, 33-34]. Samarium (III) acetate hydrate and urea were selected for the synthesis of Sm-doped TiO₂ and N-doped TiO₂ respectively. A typical synthesis process involved various stages. In the first stage, 5 mL of titanium butoxide (precursor) was dissolved dropwise into 30 mL of 1-butanol under magnetic stirring. 5 mL of

Chapter 4: Synthesis and characterization of Samarium and Nitrogen doped TiO₂ photocatalysts for photo-degradation of 4-Acetamidophenol in combination with hydrodynamic and acoustic cavitation

glacial acetic acid solution was subsequently added and the mixture was kept for 24 h at ambient conditions. In the second stage, calculated amount of Samarium (III) acetate hydrate according to molar ratios (Sm:TiO₂) of 1.0, 1.5, and 2.0 were dissolved in 20 mL of water and added to the solution obtained in the first stage. In third stage, gel was obtained under normal stirring for 4 h after the addition of 30 mL of double distilled water. Finally, obtained product was dried in an oven at 110°C for 24 h and calcined in a muffle furnace at 450°C for 2 h. Similar process was adopted for the synthesis of N-doped TiO₂ photocatalyst with different molar ratios (N:TiO₂) as 0.5, 0.75, 1.0, and 1.5. Urea was used as a precursor for doping N on TiO₂ and the quantity of urea was taken considering the atomic ratio of N to urea as 2:1. In addition, pure TiO₂ photocatalyst was also prepared according to the above procedure without the addition of samarium/nitrogen precursor.

4.2.2.2 Ultrasound assisted sol-gel process (USP)

In the USP synthesis, 5 mL of titanium butoxide was mixed into 30 mL of 1-butanol and 5 mL of glacial acetic acid was added. Subsequently, mixture was sonicated using an ultrasonic horn (VCX 750, Sonics, USA) with rated power of 750 W and frequency of 20 kHz operated for 10 min with a 5s on and 5s off cycle and 40% amplitude. After 24 h, desired amounts of Samarium (III) acetate hydrate as required for maintaining the molar ratios (Sm:TiO₂) of 1.0, 1.5, and 2.0 was dissolved in 20 mL of water and then mixed with the above solution which was further sonicated for 10 min keeping same duty cycle. The remaining process was same as described for the conventional sol-gel process. For synthesizing N-doped TiO₂, the same procedure was followed except for different precursor with different molar ratios (N:TiO₂) of 0.5, 0.75, 1.0, and 1.5. Pure TiO₂ was also prepared according to the above procedure without adding Sm and N precursor. The schematic of the ultrasound assisted sol-gel synthesis approach has been shown in Figure 4.1.

Chapter 4: Synthesis and characterization of Samarium and Nitrogen doped TiO₂ photocatalysts for photo-degradation of 4-Acetamidophenol in combination with hydrodynamic and acoustic cavitation

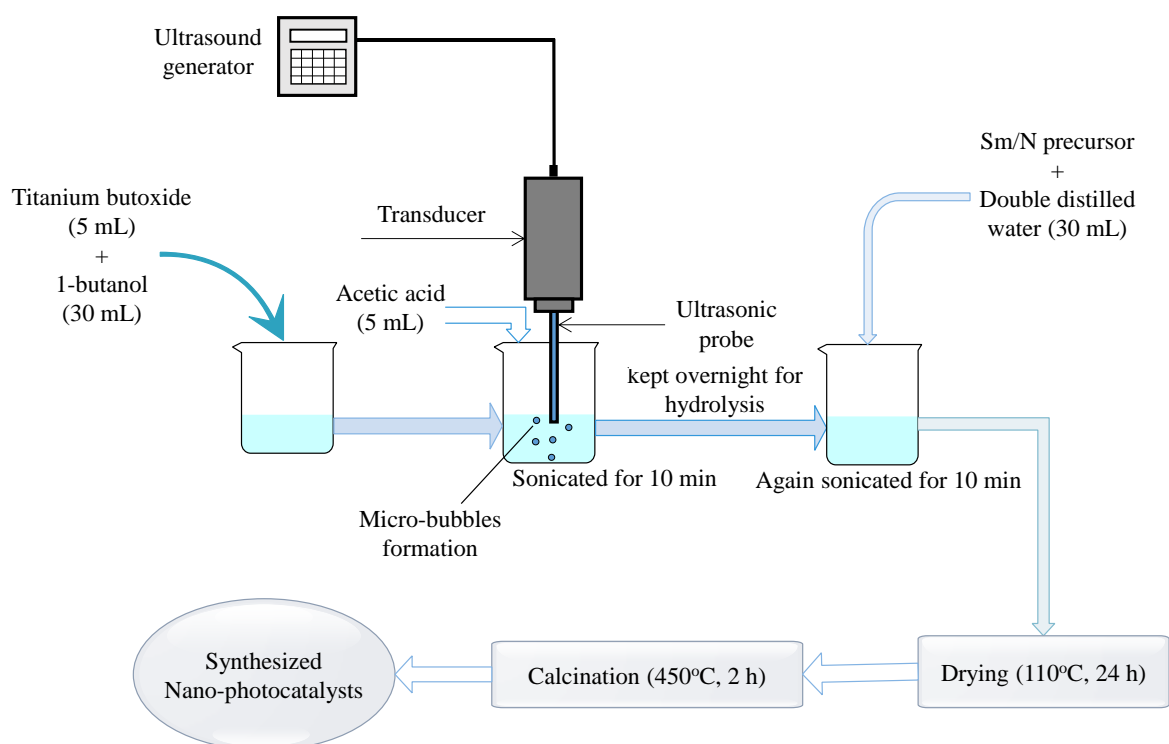


Figure 4.1: Schematic representation of the ultrasound assisted sol-gel synthesis process

4.2.3 Characterization Techniques

The prepared photocatalysts were analyzed using different characterization techniques. Phase and average crystallite size of the prepared samples were determined by powder XRD with a PANalytical X'Pert diffractometer using Cu K α radiations at 45 kV and 40 mA. For all the samples, XRD measurements were taken in the 2θ range of 10-70° with a step size of 0.02 and a scan step time of 0.7 per sec. FTIR (Perkin Elmer) was performed in the wavenumber range of 400-4000 cm⁻¹. In order to study the surface morphology, FESEM (Nova Nano SEM 450) was used. The FESEM was also equipped with an EDX spectroscopy (X-flash 6TI30 Bruker) used for the elemental analysis of the prepared photocatalyst. The photoluminescence (PL) spectra was obtained at room temperature using a Micro Raman Spectrometer (STR500, AIRIX Corporation) with a 374 nm emitting diode laser as an excitation source. The ultraviolet-visible diffusion reflectance spectra (UV-vis DRS) of photocatalysts was recorded using a UV-Vis NIR Spectrophotometer (Perkin Elmer Lambda 750) in the wavelength range of 300-550 nm. X-ray photoelectron spectroscopy (XPS) was performed using an Omicron ESCA (Electron Spectroscopy for Chemical Analysis) with a

Chapter 4: Synthesis and characterization of Samarium and Nitrogen doped TiO₂ photocatalysts for photo-degradation of 4-Acetamidophenol in combination with hydrodynamic and acoustic cavitation

monochromatic Al $K\alpha$ source and a charge neutralizer. All the binding energies in XPS were calibrated with respect to the C 1s peak at 284.6 eV of the surface adventitious carbon.

4.2.4 Degradation of 4-AMP

4.2.4.1 Photocatalytic oxidation:

The photocatalytic experiments were performed in a batch mode (Figure 4.2a). The photocatalytic activity of the pure and doped TiO₂ was evaluated through degradation of 4-AMP in an aqueous solution under UV and visible light. A 400 mL 4-AMP solution (50 ppm) was used for all the experiments. The magnetic stirrer (power input- 500 W) was used to keep the solution uniformly mixed. The solution was stirred in dark for 30 min in order to confirm adsorption/desorption equilibrium prior to irradiation. Nearly 9% of 4-AMP was adsorbed on the surface of TiO₂ (2.0 g/L dosage) and adsorption equilibrium was achieved in 30 min and thereafter 4-AMP concentration remained constant. After attainment of equilibrium, the photocatalytic reaction was started by switching on the light at time, $t = 0$ min. The solution was irradiated using UV lamp (nominal power: 300 W) and also incandescent lamp ($\lambda > 420$ nm, 300 W). The radiated power of the UV lamp was 3.0 W for the wavelength range of 280-315 nm and 13.6 W for the wavelength range of 315-400 nm and the lamp was set to an irradiation intensity of 2.47 W/cm². The distance between the lamp and the solution surface was 10 cm. The reaction temperature during photocatalysis was maintained at room temperature using cooling water circulation. During the photocatalytic degradation, samples (3 mL) were collected at regular intervals, and then filtered using a nylon filter paper with a pore size of 0.45 μ m to remove the suspended solids from the samples before analysis. The photocatalytic degradation of 4-AMP was calculated according to the following equation (4.1):

$$\text{Extent of Degradation of 4-AMP (\%)} = \frac{C_0 - C}{C} \times 100 \quad (4.1)$$

To optimize the catalyst loading, experiments were conducted by varying catalyst loading over the range of 0.5 to 3 g/L with 50 ppm of 4-AMP solutions at natural pH. Experiments were performed at three different pH as 2.0 (acidic medium), 6.8 (natural pH), and 10 (basic medium) in order to optimize the solution pH. The effect of initial concentration of 4-AMP on the degradation rate was studied over the range of 50-200 ppm.

Chapter 4: Synthesis and characterization of Samarium and Nitrogen doped TiO₂ photocatalysts for photo-degradation of 4-Acetamidophenol in combination with hydrodynamic and acoustic cavitation

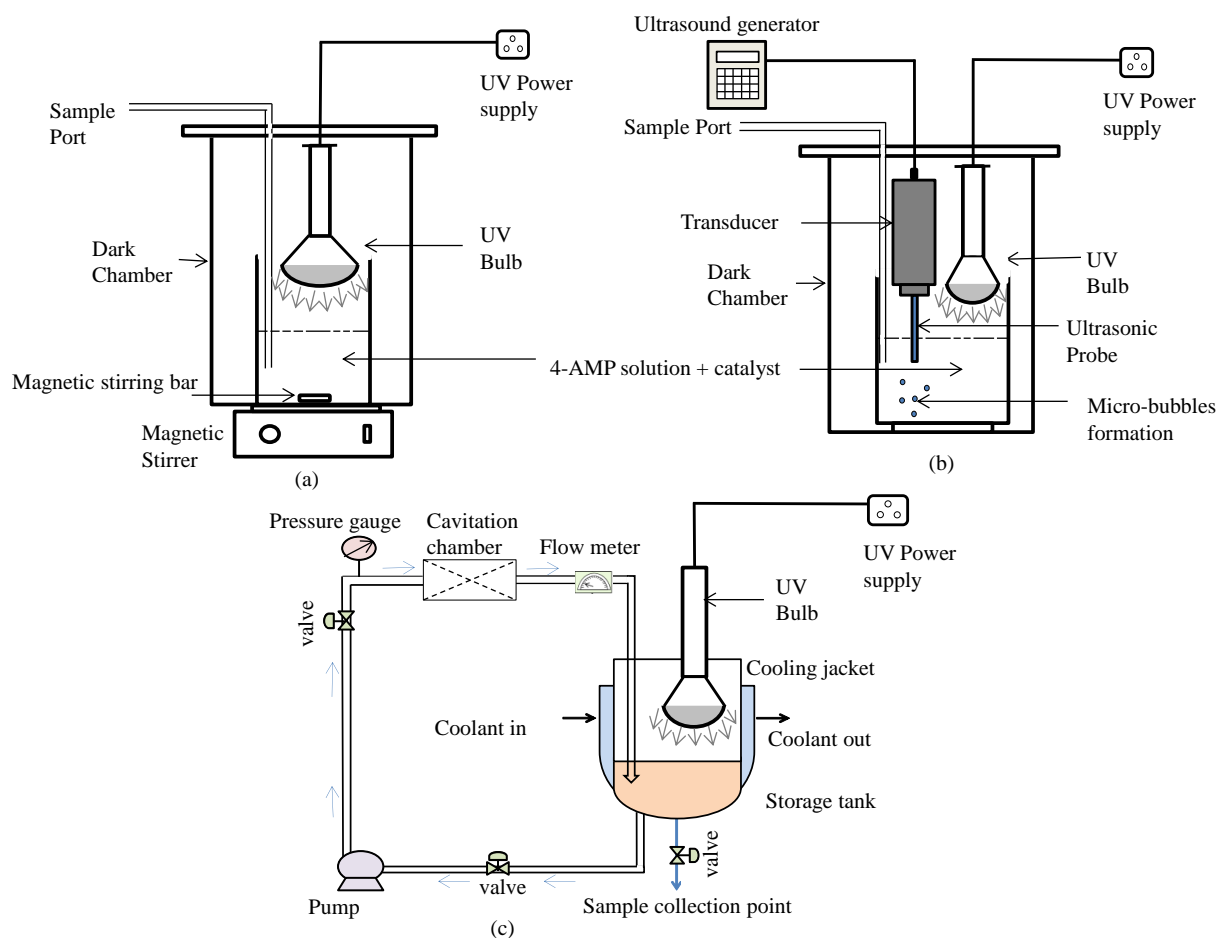


Figure 4.2: Schematic representation of experimental set-ups: (a) photocatalytic reactor, (b) photocatalytic reactor combined with US, and (c) HC reactor coupled with photocatalysis

4.2.4.2 Combination of ultrasound (US) and photocatalysis:

The combination of US and photocatalysis was investigated using ultrasonic horn operated at a frequency of 20 kHz and input power of 750 W. A schematic representation of experimental set-up used for this study is shown in Figure 4.2b. The height of the ultrasonic horn was adjusted using a metal stand and in all the experiments, tip of the horn was kept 25 mm below the free surface of solution. Pure and doped photocatalysts (optimum loading as 2 g/L) were added into 400 ml of 50 ppm 4-AMP solution. Sonolysis (US), sono-photolytic (US+UV), and sono-photocatalytic (US+UV+Catalyst) experiments were conducted at the optimized conditions of pH, initial concentration and catalyst loading as applicable in the same experimental setup. Throughout the degradation studies, 4-AMP solution was sonicated

Chapter 4: Synthesis and characterization of Samarium and Nitrogen doped TiO₂ photocatalysts for photo-degradation of 4-Acetamidophenol in combination with hydrodynamic and acoustic cavitation

in the absence or presence of catalysts and light source depending on the type of the treatment approach. All the experiments were performed for a total time of 180 min.

4.2.4.3 Combination of HC and photocatalysis:

The details of HC reactor set-up used in the present work has been explained in chapter 2 (Section 2.2.2; Figure 2.1) including the geometric details of cavitating device (slit venturi) and the optimum conditions of operating inlet pressure and cavitation number. The HC reactor setup fitted with the slit venturi was provided with a high pressure piston pump of rated power 1.1 kW which delivered fluid flow rate in the range of 0-20 L/min with output pressure in the range of 0-20 bar. As reported in our previous chapter 2, higher decolorization rate of Rhodamine 6G was achieved using slit venturi as compared to circular venturi and an optimum inlet pressure of 5 bar ($C_v = 0.07$). Hence, all the experiments with HC were performed at an optimum inlet pressure of 5 bar. The UV lamp was placed above the water surface in the holding tank of HC reactor for the hybrid HC+photocatalytic experiments. All the photocatalytic experiments in combination with the HC were conducted using 3 L solutions of 4-AMP having an initial concentration of 50 ppm and optimum pH (6.8).

4.2.5 Analytical Methods

Concentration of 4-AMP solutions was analyzed quantitatively using the high performance liquid chromatography (HPLC, LC-20AD XR, Shimadzu) equipped with a C-18 column having dimensions of 150 × 4.6 mm and PDA detector at detection wavelength as 254 nm using a mixture of acetonitrile and de-ionized water (50:50) as the mobile phase (flow rate of 0.8 mL/min). The 20 µL sample volume was injected and retention time for 4-AMP was found to be 2.45 min. The pH of solution during the degradation studies was measured using a pH meter (Hanna Instruments, USA). All experiments were repeated at least two times to check the reproducibility and the experimental errors were found to be within ±2% of the reported average values. The degradation byproducts of 4-AMP were analyzed using the liquid chromatography-mass spectroscopy (make: Xevo G2-SQ-Tof, Waters, USA) using C18 column (4.6 mm x 150 mm) and mobile phase as mixture of acetonitrile and de-ionized water (50:50 proportion and flow rate of 0.8 mL/min used for 10 min).

Chapter 4: Synthesis and characterization of Samarium and Nitrogen doped TiO₂ photocatalysts for photo-degradation of 4-Acetamidophenol in combination with hydrodynamic and acoustic cavitation

To correlate the obtained data using kinetic models, an integral approach was used for data fitting. It was observed that first order kinetics fitted well and the rate constants of 4-AMP degradation were calculated using the kinetic plots based on following equation (4.2):

$$\ln\left(\frac{C_o}{C}\right) = kt \quad (4.2)$$

4.3. Results and discussion

4.3.1 Characterization of photocatalysts

4.3.1.1 XRD patterns

XRD patterns of ultrasonically and conventionally prepared un-doped and Sm/N-doped photocatalysts (Sm/TiO₂ : 1.5; N/TiO₂ : 1) are shown in Figure 4.3. In the case of catalysts obtained using USP, all the prepared samples showed similar XRD patterns with major diffraction peaks at $2\theta = 25.3^\circ, 37.7^\circ, 48.1^\circ, 53.8^\circ, 55.1^\circ, 62.6^\circ,$ and 68.6° corresponding to (101), (004), (200), (105), (211), (204), and (116) confirming the presence of anatase phase (JCPDS card no. 21-1272). As shown in Figure 4.3. (a), the rutile phase was also observed for the un-doped and doped TiO₂ with the minor peak of the (210) diffraction at the angle of $\theta = 44.2^\circ$ (JCPDS card no. 21-1276), however, the anatase phase has the predominant presence. The peaks for pure TiO₂ and TiO₂ doped with Sm and N appeared same, but in the case of doped TiO₂ samples, reduction in peak intensity was observed, which may be attributed to the fact that doping affects the crystal growth but not the crystal structure of TiO₂ [13]. No additional peaks of Sm and N were detected in the XRD spectrum, which is therefore indicative of their successful doping into the TiO₂ lattice structure [13]. It was reported that anatase phase of synthesized TiO₂ has higher photocatalytic activity as compared to other crystalline phases (rutile and brookite) [22]. In the case of catalysts obtained using CSP, a major peak corresponding to (101) reflections of the anatase phase of pure and doped TiO₂ was observed at the angle of 25.3° , whereas the minor peaks were observed at 37.8° (004), 47.9° (200), 53.9° (105), and 62.6° (204) (JCPDS card no.21-1272). The lower peak intensity observed for doped TiO₂ photocatalyst as compared to pure sample indicate the uniform dispersion of dopant materials on the TiO₂ surface. As depicted in Figure 4.3, comparison of pure and doped TiO₂ synthesized by USP with that prepared

Chapter 4: Synthesis and characterization of Samarium and Nitrogen doped TiO₂ photocatalysts for photo-degradation of 4-Acetamidophenol in combination with hydrodynamic and acoustic cavitation

by CSP revealed that the crystallinity and peak intensities are higher and sharper for the samples prepared using USP as compared to the CSP. Higher peak intensity exhibited that the anatase phase of TiO₂ was more crystalline in nature. The crystallite sizes of the synthesized photocatalysts were also calculated using Scherrer's formula according to equation (4.3) [34] based on broad peak at 25.3° (101) and the values are presented in Table 4.1.

$$D = \frac{k\lambda}{\beta \cos\theta} \quad (4.3)$$

It can be seen from Table 4.1 that photocatalysts (pure and doped TiO₂) prepared using USP have smaller size than those prepared using CSP, which can be attributed to the effect of micro-jets formed under cavitation during ultrasonication in terms of avoiding the interaction between crystals thereby resulting in smaller and uniform crystallite size of the photocatalysts [33]. It was also observed that doped TiO₂ photocatalysts had smaller crystallite sizes as compared to pure TiO₂ prepared from both the processes. Smaller crystallite size is mainly due to de-agglomeration of the particles. This indicates that doping materials into TiO₂ lattice inhibited the growth of crystal size thereby resulting in smaller crystallite size of TiO₂ [34]. Considering the better characteristics for the catalysts obtained using USP, further characterization studies were performed only for the photocatalysts obtained using USP.

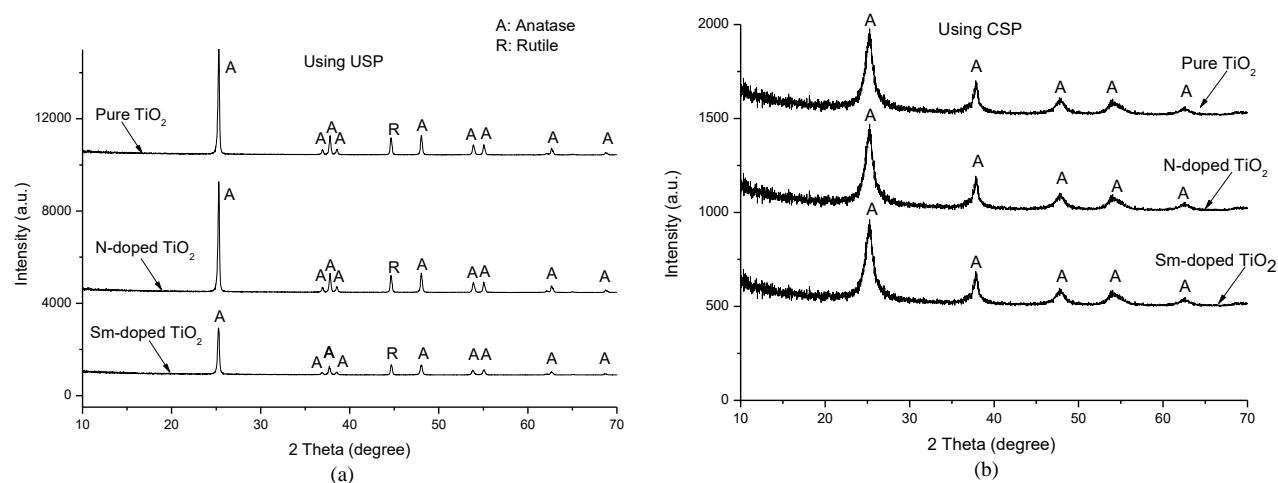


Figure 4.3: XRD patterns of pure TiO₂, N-doped TiO₂ and Sm-doped TiO₂ synthesized using (a) ultrasound assisted sol-gel (b) conventional sol gel process

Chapter 4: Synthesis and characterization of Samarium and Nitrogen doped TiO₂ photocatalysts for photo-degradation of 4-Acetamidophenol in combination with hydrodynamic and acoustic cavitation

Table 4.1: The crystallite sizes of photocatalysts synthesized using USP and CSP

Type of photocatalysts	USP		CSP	
	Crystal size, nm	Crystal phase	Crystal size, nm	Crystal phase
Pure TiO ₂	90	Anatase	115	Anatase
Sm-doped TiO ₂	50	Anatase	68	Anatase
N-doped TiO ₂	40	Anatase	58	Anatase

4.3.1.2 FT-IR spectroscopy analysis

FTIR analysis was performed to investigate the surface chemical bonding state of the prepared photocatalysts and establish the key functional groups. Figure 4.4 shows the FT-IR spectrum of the synthesized pure and doped TiO₂ samples obtained using USP. It can be seen from Figure 4.4 that all spectra exhibited six absorption peaks in the regions 462-509, 616-631, 877-955, 1424-1429, 1739-1775, and 3573-3574 cm⁻¹. Previous studies have reported that absorption peaks in the regions of 3420–3450 cm⁻¹ [43], 3570 cm⁻¹ [33] due to the O-H stretching and over the range of 1630–1640 cm⁻¹ [44], 1703 cm⁻¹ [33] due to the O-H bending vibration modes of the adsorbed water molecules on the TiO₂ surface are observed. In the present work, the absorption peaks were in the region of 3573-3574 cm⁻¹ and in the region 1739-1775 cm⁻¹, which can be assigned to the O-H stretching and bending vibration modes of H₂O respectively on the surface of TiO₂ photocatalyst. It has been reported that the absorption peak at 1396 cm⁻¹ is associated to the stretching vibration of -C-H corresponding to the R-H group present in the residual titanium precursor [45]. In this study, peak observed at about 1424-1429 cm⁻¹ can be assigned to the -C-H stretching vibration. The absorption peaks in the region 877-955 cm⁻¹ (main peak of 955 cm⁻¹) can be assigned to the TiO₂ [46]. The peaks in the region of 616-631 cm⁻¹ obtained in the present work can be attributed to Ti-O stretching vibration. Finally, the absorption peaks over the range of 462-509 cm⁻¹ are assigned to the stretching vibration of Ti-O-Ti in anatase phase. In all, there was no additional peak found with doped materials on the surface of TiO₂, which indicated the proper dispersion of dopant materials. Shirsath et al. [33] analyzed the FTIR spectra of pure TiO₂ and cerium and iron doped TiO₂ synthesized by sonochemical method and reported that

Chapter 4: Synthesis and characterization of Samarium and Nitrogen doped TiO₂ photocatalysts for photo-degradation of 4-Acetamidophenol in combination with hydrodynamic and acoustic cavitation

no extra peak for doped materials was observed in the FTIR spectra attributed to the efficient dispersion of doping materials.

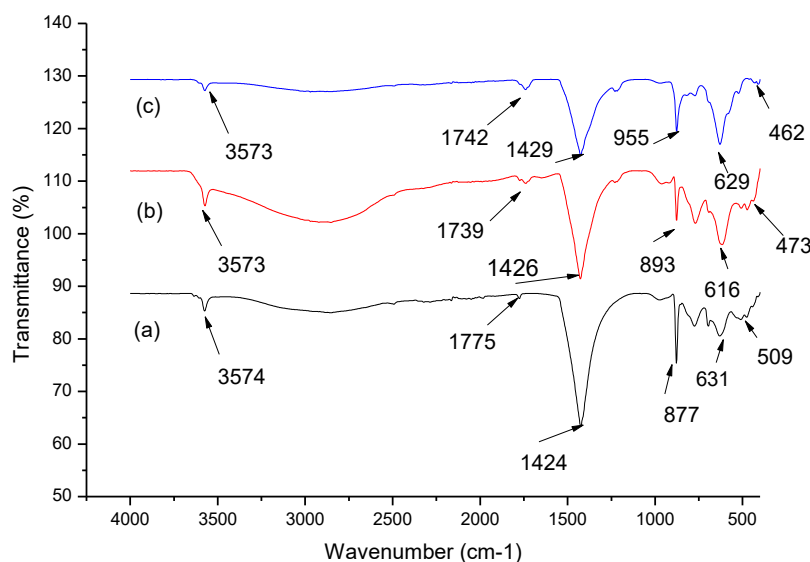


Figure 4.4: FTIR spectra of synthesized photocatalysts: (a) Pure TiO₂, (b) N-TiO₂, and (c) Sm-TiO₂

4.3.1.3 FESEM with EDX analysis

The morphology of synthesized pure and doped TiO₂ photocatalysts obtained using the USP was analyzed using FESEM and the obtained results for the SEM images have been depicted in Figure 4.5. In the case of pure TiO₂ the photocatalyst nanoparticles seemed to have a spherical shape with porous aggregated structure as observed in Figure 4.5 (a). The SEM image of TiO₂ doped with nitrogen as observed in Figure 4.5 (b), indicates a nonporous compact interlinked structure with uniform sized particles. It can be seen from Figure 4.5 (c), that slightly agglomerated spherical particles with uniform size (narrow distribution) were observed after the doping of samarium on the surface of TiO₂. Hence, it can be established that Sm and N-doping into TiO₂ did not have significant effect on the morphology but it affected the particle size of photocatalysts which was also confirmed using XRD analysis. Thus, the obtained reduction in crystallite size of photocatalysts due to doping elements as observed from SEM analysis also matched the predictions of XRD results. In order to quantify the elemental composition of TiO₂ doped with Sm/N, EDX analysis was also performed. The results exhibited that the formation of Sm/N doped TiO₂ was pure and there

Chapter 4: Synthesis and characterization of Samarium and Nitrogen doped TiO₂ photocatalysts for photo-degradation of 4-Acetamidophenol in combination with hydrodynamic and acoustic cavitation

was no additional impurity introduced during doping process (Figure 4.5). The elemental analysis for doped elements i.e. N and Sm in TiO₂ indicated that the concentrations by weight are 8.51 % and 51.41% respectively and the corresponding molar ratios are N/TiO₂:1 and Sm/TiO₂:1.5 respectively (Sm being having much higher atomic weight as compared to N gives higher weight percentage).

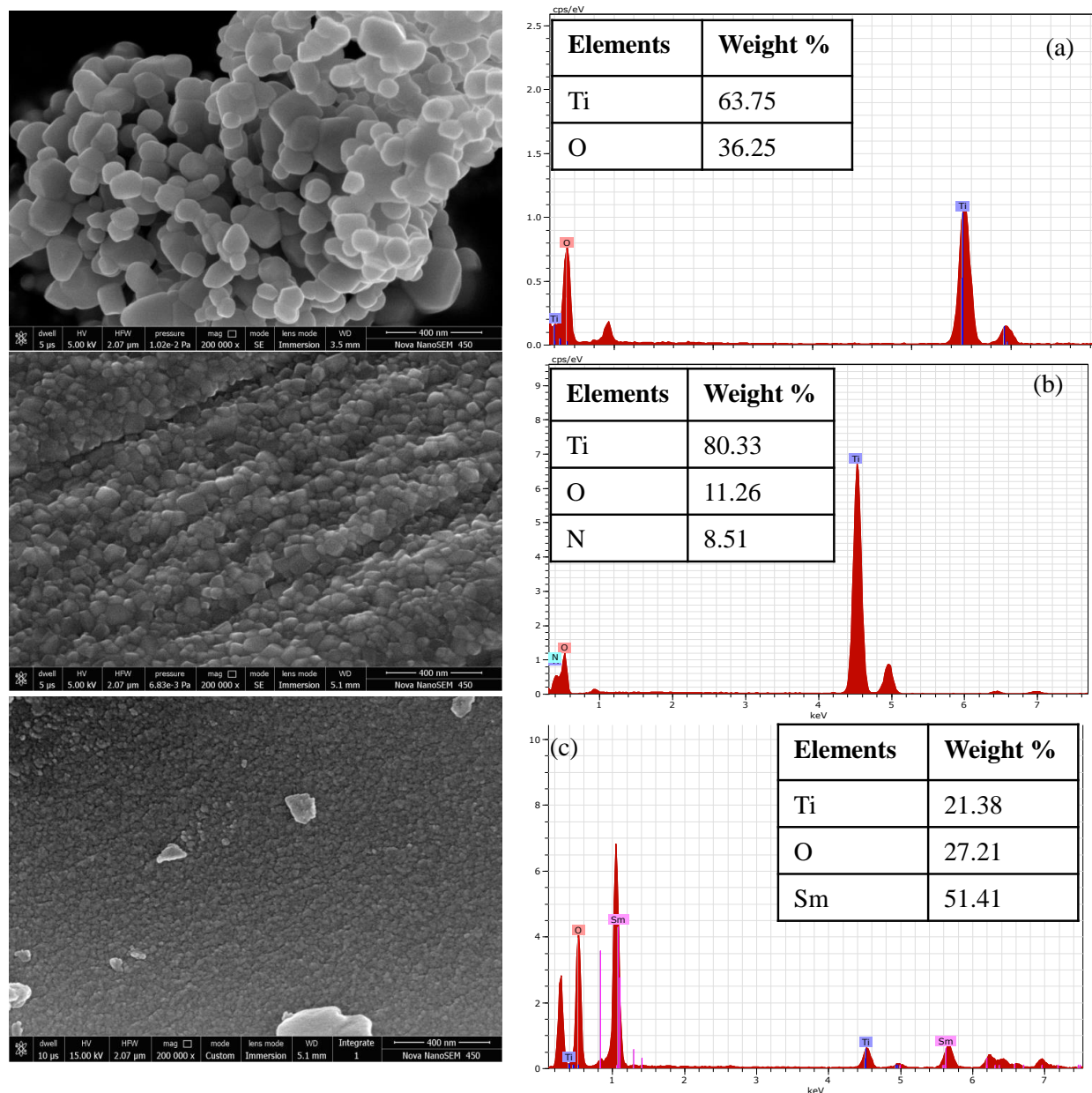


Figure 4.5: FESEM images with EDX of synthesized photocatalysts: (a) pure TiO₂, (b) N-TiO₂, and (c) Sm-TiO₂

4.3.1.4 Photoluminescence (PL) analysis

Photocatalytic activity of the photocatalyst is mainly affected due to the transfer behavior of the photo-generated electron (e^-) - hole (h^+) pairs and their rate of recombination [35] which is determined by PL analysis. It is well known that the higher PL intensity indicates a faster recombination rate of electron-hole pairs, whereas lower PL intensity indicates reduced electron-hole pair recombination rate [47]. Figure 4.6 shows the PL spectra of the pure and doped TiO₂. The PL spectra of the pure and doped photocatalysts indicated that the peak wavelengths were the same, but the PL intensities of the doped TiO₂ catalysts (Figure 4.6 (b) and (c)) were lower than that of pure TiO₂ (Figure 4.6 (a)); with N-TiO₂ having the least PL intensity. The lower value of PL intensity of doped TiO₂ indicates that the recombination of charge carriers is effectively suppressed by doping materials (N and Sm). The doping material on the lattice of TiO₂ reduces the electron-hole recombination rate, and thereby enhances the photocatalytic activity.

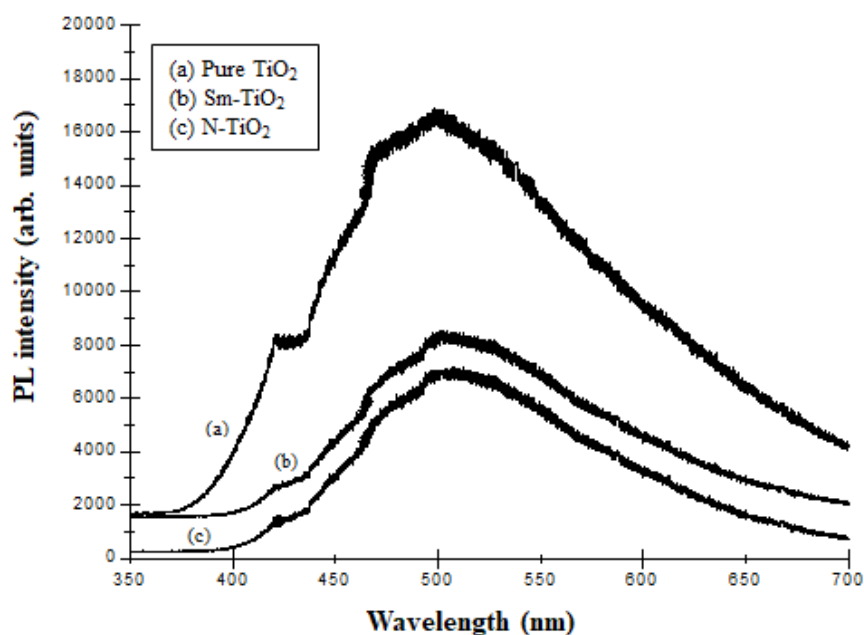


Figure 4.6: PL spectra of (a) pure TiO₂ (b) Sm-TiO₂, and (c) N-TiO₂

4.3.1.5 Diffuse reflectance spectra (DRS) analysis

Optical absorption properties of pure and doped TiO₂ photocatalysts were studied using UV-vis NIR spectrometer in diffuse reflectance mode. Figure 4.7a depicts the UV-vis diffuse

Chapter 4: Synthesis and characterization of Samarium and Nitrogen doped TiO₂ photocatalysts for photo-degradation of 4-Acetamidophenol in combination with hydrodynamic and acoustic cavitation

reflectance spectra of the pure and doped photocatalysts. It can be seen from Figure 4.7a that after doping with Samarium and nitrogen, the response of TiO₂ photocatalysts showed red shifts (toward higher wavelengths). The red shift of the absorption edge resulted in a reduction of the band gap energy and the recombination rate of electron hole pairs. The experimental data of diffuse reflectance were analyzed using the Kubelka-Munk equation (4.4) to estimate the Kubelka-Munk function $F(R)$, [48-50] as follows:

$$F(R) = \left(\frac{(1-R)^2}{2R} \times hv \right)^{0.5} \quad (4.4)$$

Where, $F(R)$ is the absorption coefficient, R is the measured absolute reflectance of the photocatalyst and hv is the photon energy. Figure 4.7 b presents the Kubelka-Munk plots for the pure and doped photocatalysts. Kubelka–Munk plots of $[F(R)*hv]^{0.5}$ vs (hv) was used to determine the band gap energy (E_g), which is the value of the intercept of the extrapolated linear part of the plot at $[F(R)*hv]^{0.5} = 0$ (x axis). The band gap energies of pure TiO₂, Sm-TiO₂ and N-TiO₂ photocatalysts were found to be 3.19, 3.10 and 2.98 eV respectively. As the introduction of samarium and nitrogen onto the TiO₂ surface have reduced the band gap energy of the TiO₂ photocatalyst, these doped TiO₂ catalysts may provide better photocatalytic efficiency in the presence of low intensity light as well as visible light region than pure TiO₂.

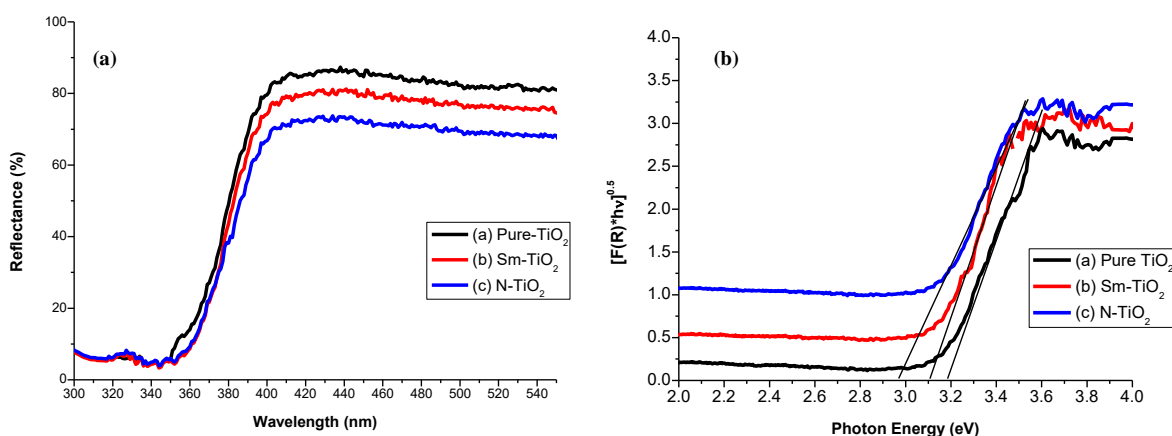


Figure 4.7 (a): UV-Vis diffuse reflectance spectra **(b):** Kubelka-Munk plots and band gap energy estimation of (a) pure TiO₂ (b) Sm-TiO₂, and (c) N-TiO₂

Chapter 4: Synthesis and characterization of Samarium and Nitrogen doped TiO₂ photocatalysts for photo-degradation of 4-Acetamidophenol in combination with hydrodynamic and acoustic cavitation

4.3.1.6 X-ray photoelectron spectroscopy (XPS) analysis

The electronic states and the binding energies of each element present in the photocatalyst samples were determined by XPS. The XPS survey spectra of pure and doped TiO₂ are shown in Figure 4.8. The binding energies were calibrated by taking the carbon C 1s peak (284.6 eV) as the reference. The spectra confirmed the presence of all the elements (Sm, N, Ti, O) used in the preparation of the pure and doped TiO₂ photocatalysts. High resolution XPS spectra of Ti 2p, O 1s, N 1s, and Sm 3d are also shown in Figure 4.9 (a-d). Previous studies have reported that the binding energies of Ti 2p were found at 458.9 and 464.5 eV for spin orbit constituents, Ti 2p_{3/2} and Ti 2p_{1/2} respectively [51-53]. In the present work, Figure 4.9a presents the XPS spectra of Ti 2p in which two prominent peaks were observed at 458.2 and 464.0 eV binding energies for Ti 2p_{3/2} and Ti 2p_{1/2} respectively. The XPS of O 1s is shown in Figure 4.9 (b) and two prominent peaks were observed. The peak at 529.5 eV is the characteristic peak of Ti–O bond. An additional peak for O 1s was observed at about 531.2 eV which may be attributed to the presence of the hydroxyl O atoms [52]. Previous studies suggested that the N 1s peak of the N-doped TiO₂ was commonly observed between 395 and 402 eV [53-57]. The peak at 399 eV is attributed to nitrogen replaces the oxygen in the crystal lattice of TiO₂ [53]. In this study, the presence of a peak at the binding energy of 399 eV confirmed the successful doping of nitrogen into the TiO₂ lattice structure. As observed in Figure 4.9 (c), the N 1s peak of the prepared TiO₂ at 399 eV may be attributed to the interstitial N species with the possibility of N-O-Ti or Ti-N-O bond formation [58-59]. Figure 4.9 (d) depicts the XPS spectrum of Sm 3d. The peak at 1083.43 eV corresponds to the bond of Sm-O-Ti. It has been reported in literature that the binding energy for Sm 3d is 1083.2 eV in Sm₂O₃ [60]. The XPS results confirmed the presence of Sm in the form of Sm₂O₃ in the doped photocatalyst. XPS study indicated the successful incorporation of samarium and nitrogen as dopants into TiO₂ at binding energies of 1083.43 and 399 eV respectively.

Chapter 4: Synthesis and characterization of Samarium and Nitrogen doped TiO₂ photocatalysts for photo-degradation of 4-Acetamidophenol in combination with hydrodynamic and acoustic cavitation

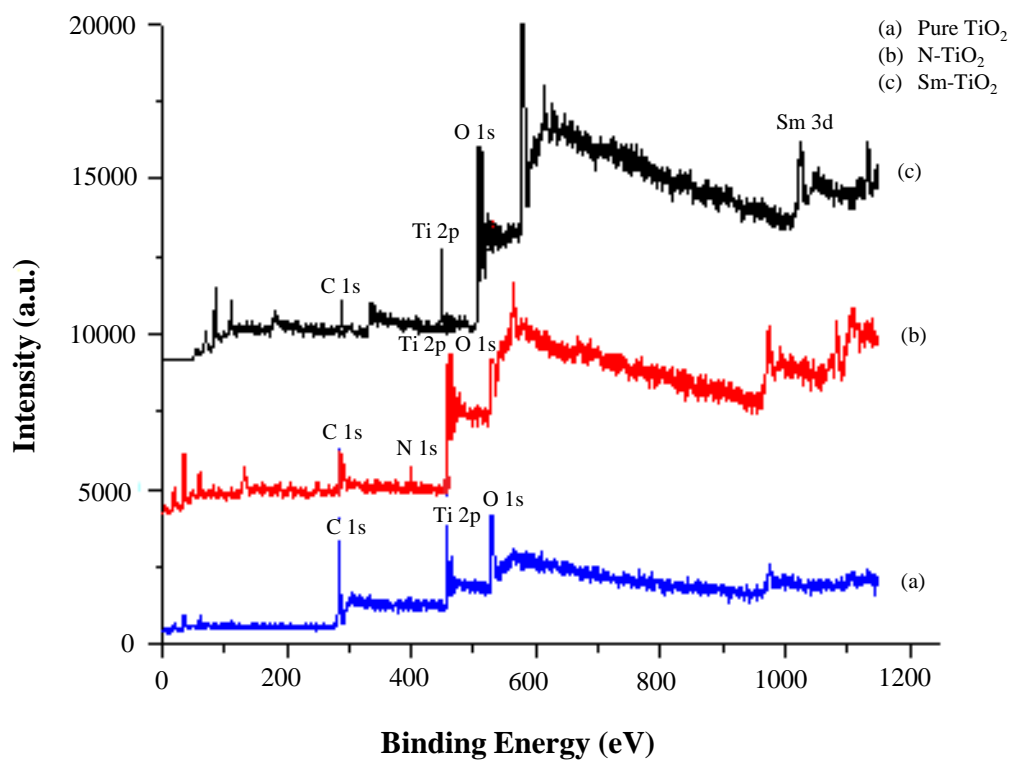


Figure 4.8: Survey XPS spectrum of (a) pure TiO₂ (b) N-TiO₂, and (c) Sm-TiO₂

Chapter 4: Synthesis and characterization of Samarium and Nitrogen doped TiO₂ photocatalysts for photo-degradation of 4-Acetamidophenol in combination with hydrodynamic and acoustic cavitation

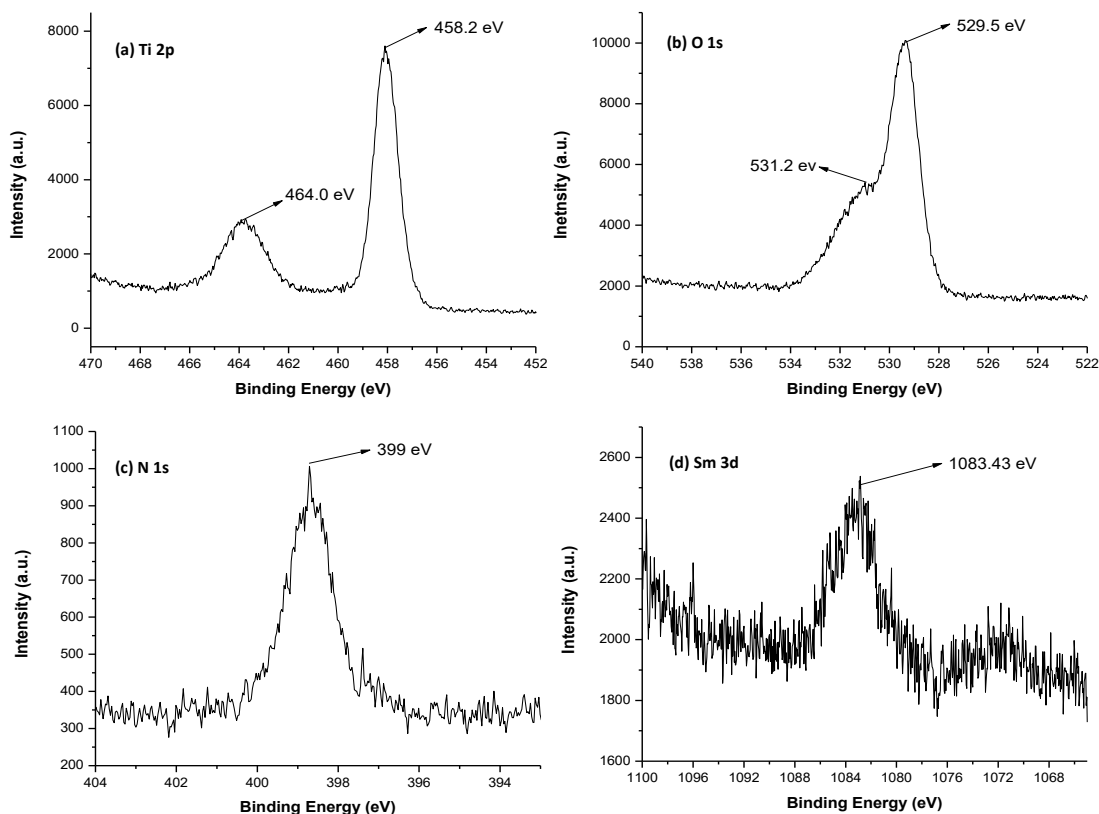


Figure 4.9: High resolution XPS spectrum of (a) Ti 2p (b) O 1s (c) N 1s (d) Sm 3d core levels.

4.3.2 Degradation of 4-AMP using photocatalytic oxidation

4.3.2.1 Effect of pure TiO₂ loading on the extent of degradation

To optimize the loading of TiO₂ photocatalyst, amount of pure TiO₂ (without any doping) was varied over the range of 0.5 to 3.0 g/L for photocatalytic oxidation of 4 AMP solution with an initial concentration of 50 ppm at natural pH of 6.8. The obtained results are shown in Figure 4.10 and it can be seen from the figure that photocatalytic degradation of 4-AMP increased with an increase in the loading of pure TiO₂ from 0.5 g/L to an optimum value of 2 g/L and then decreased with a further increase in the catalyst loading. The maximum degradation of 49.7% with a first order rate constant of $4.4 \times 10^{-3} \text{ min}^{-1}$ was achieved at an optimum TiO₂ loading of 2 g/L. The reduction in the degradation rate of 4-AMP beyond an optimum value can be attributed to an increase in the turbidity of solution which decreases the penetration of UV light into the 4-AMP solution. Also, particle-particle interactions

Chapter 4: Synthesis and characterization of Samarium and Nitrogen doped TiO₂ photocatalysts for photo-degradation of 4-Acetamidophenol in combination with hydrodynamic and acoustic cavitation

increase photocatalyst agglomeration at higher solid loading of the photocatalyst which reduces surface area of photocatalyst thereby reducing the photo-degradation rate [61]. Hence, 2.0 g/L of catalyst was further used to perform all the experiments in the present study. It was also observed that the extent of degradation obtained using catalyst obtained by USP was much higher than that obtained using conventional process of synthesis. Only 17 % degradation was achieved using conventionally prepared TiO₂ at the optimum loading of 2 g/L, that was found to be lower than the extent of degradation obtained using the catalyst synthesized using USP. The higher effectiveness for the catalyst obtained using USP may be attributed to the smaller particle size and higher surface area of photocatalysts obtained using USP than that obtained using CSP.

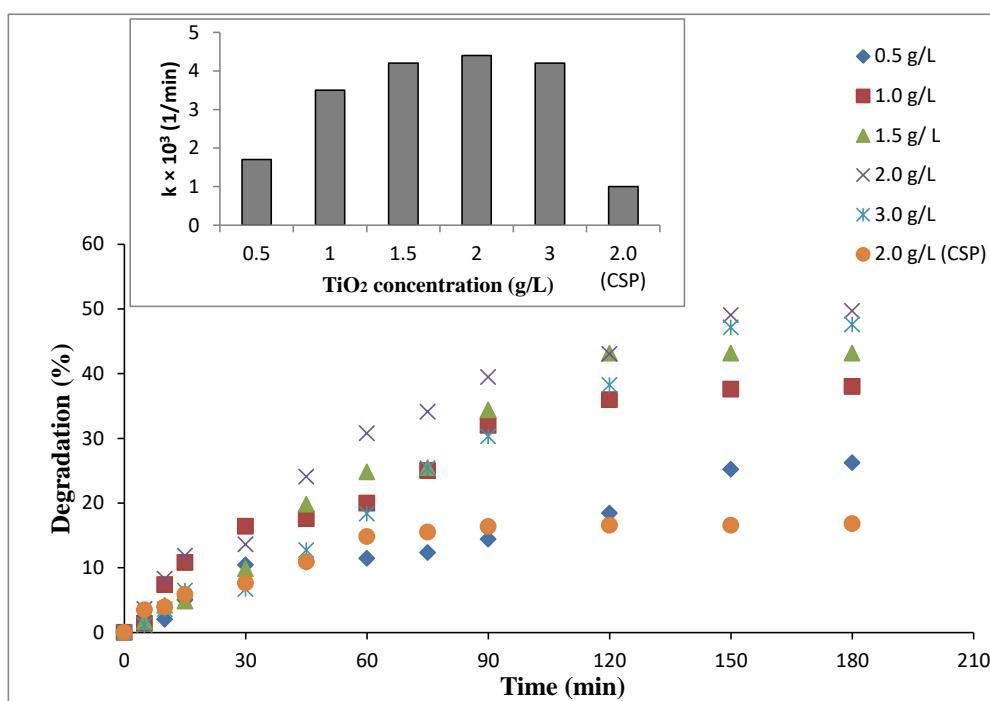


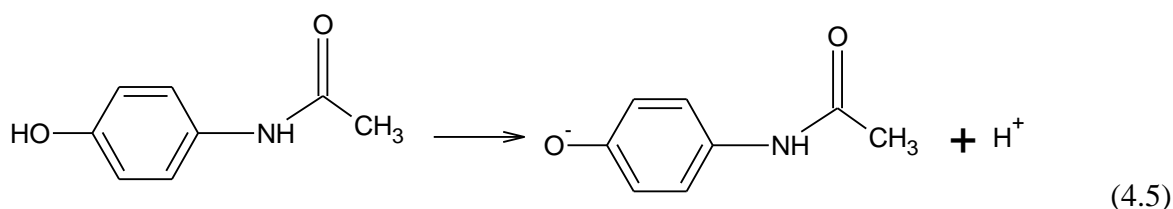
Figure 4.10: Effect of catalyst loading on degradation rate of 4-AMP (Conditions: solution volume: 400 mL, initial concentration: 50 ppm, natural pH: 6.8, treatment time: 180 min)

4.3.2.2 Effect of Solution pH on the extent of degradation

Solution pH plays an important role in deciding the efficacy of the photocatalytic degradation, since it affects the surface charge of the TiO₂ photocatalyst, charge and state of the organic molecules, adsorption on the catalyst surface and also the generation of reactive

Chapter 4: Synthesis and characterization of Samarium and Nitrogen doped TiO₂ photocatalysts for photo-degradation of 4-Acetamidophenol in combination with hydrodynamic and acoustic cavitation

oxygen species [62]. The zeta potential of the doped and undoped TiO₂ photocatalyst was measured at different pH using Zeta Sizer (NanoZS, Malvern UK) and is shown in Figure 4.11. It has been observed that the zeta potential of Pure TiO₂ photocatalyst is -1.4 mV at pH 2.0 which is close to the point of zero charge (pH_{ZPC}) and the negative charge density (zeta potential value) increases as the solution pH increases. The pH_{ZPC} values of Sm-TiO₂, and N-TiO₂ photocatalyst are obtained at 8.3 pH and 4.5 pH respectively. Moreover, the pKa value of 4-AMP is 9.5 and above the pKa value the compound becomes anionic according to equation (4.5) and remained in the molecular state (nonionic) at the solution pH below its pKa value [63].



Experiments were performed at three different pH conditions such as acidic (2.0), natural (6.8), and basic (10.0) to examine the effect of solution pH on degradation rate of 4-AMP, at an initial concentration of 50 ppm and optimum catalyst loading of 2 g/L. The natural pH of the solution was found to be 6.8 when 2 g/L of TiO₂ was added into the 50 ppm 4-AMP solution. The effect of solution pH on the 4-AMP degradation is depicted in Figure 4.12. It was observed that the maximum degradation of 49.7% was achieved at the natural pH of 6.8, and the degradation rates were lower under both acidic and basic conditions. At very high pH (pH = 10), as the hydroxyl group of 4-AMP changed into phenolic anions (pH > pKa), 4-AMP becomes negatively charged. Therefore, the strong repulsion between the negatively charged 4-AMP molecules and negatively charged TiO₂ surface (pH > pH_{PZC}) does not allow the 4-AMP molecules to remain in the vicinity or interact with the catalyst surface where the concentration of hydroxyl radicals is maximum [64]. This causes a reduction in the degradation rate as only few of the generated radicals at the catalyst surface diffuse in the bulk for possible reaction and the rest recombined into H₂O₂. At natural pH, the surface charge of the TiO₂ photocatalyst is negative whereas, 4-AMP is primarily in its non-ionic form and hence due to its hydrophobicity it will remain in the vicinity of the catalyst surface and interaction between the 4-AMP and hydroxyl radicals is maximum [62]. Therefore, the maximum degradation rate was observed at pH of 6.8. On the other hand, excess amount of

Chapter 4: Synthesis and characterization of Samarium and Nitrogen doped TiO₂ photocatalysts for photo-degradation of 4-Acetamidophenol in combination with hydrodynamic and acoustic cavitation

H⁺ ions at very low solution pH (acidic) also caused a decrease in the degradation rate due to the scavenging of the $\cdot\text{OH}$ radicals. Therefore, the natural pH of solution (6.8) was used for all the further experiments. Similar results have also been reported in the literature that strongly acidic or basic conditions inhibit the oxidation of 4-AMP [63].

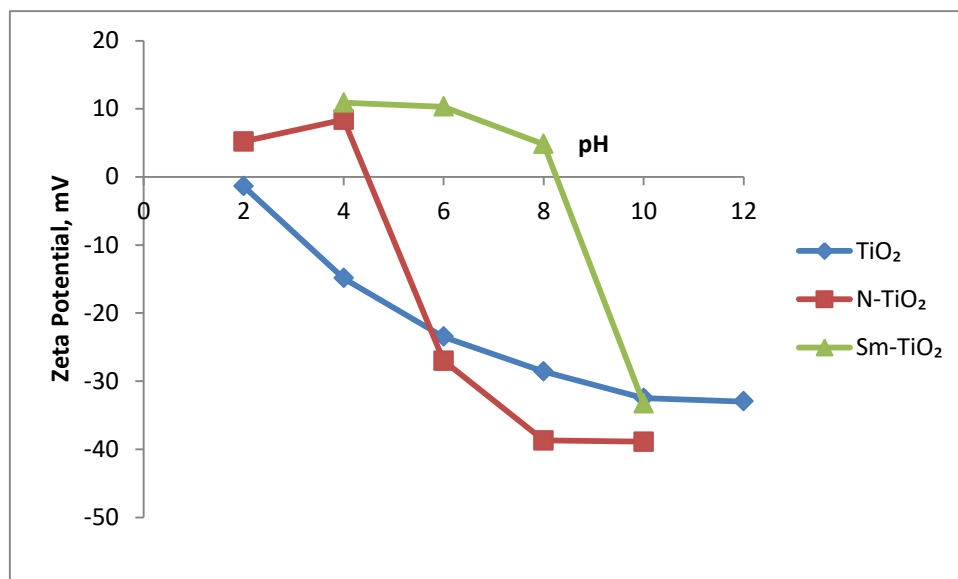


Figure 4.11: Zeta potential of TiO₂, N-TiO₂ and Sm-TiO₂ at different pH

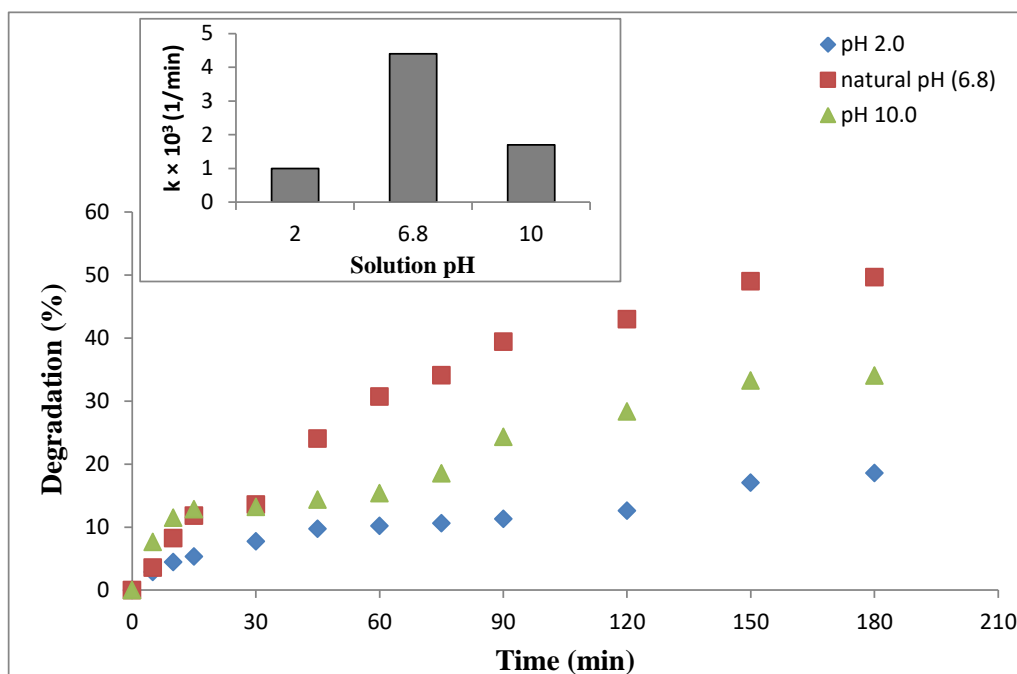


Figure 4.12: Effect of solution pH on degradation rate of 4-AMP (Conditions: solution volume: 400 mL, initial concentration: 50 ppm, TiO₂ loading: 2 g/L, treatment time: 180 min)

Chapter 4: Synthesis and characterization of Samarium and Nitrogen doped TiO₂ photocatalysts for photo-degradation of 4-Acetamidophenol in combination with hydrodynamic and acoustic cavitation

4.3.2.3 Effect of 4-AMP initial concentration

To investigate the effect of 4-AMP initial concentration on the degradation rate, photocatalytic degradation experiments were also performed using varying initial concentrations as 50, 100, and 200 ppm at the optimized pH of 6.8 and catalyst loading of 2 g/L. The obtained results are depicted in Figure 4.13. It was observed that extent of degradation decreased from 49.7% with a rate constant of $4.4 \times 10^{-3} \text{ min}^{-1}$ to 17.3% with a rate constant of $1.1 \times 10^{-3} \text{ min}^{-1}$ for an increase in the initial concentration of 4-AMP from 50 to 200 ppm. The obtained lower degradation rate at higher initial concentration may be attributed to the following reasons: (a) greater quantity of pollutant molecules adsorbed on the surface of TiO₂ at higher concentrations hindered the diffusion of hydroxyl ions to the TiO₂ surface which led to a decrease in the formation of reactive species (b) the amount of catalyst used and light intensity remained constant even at higher 4-AMP concentrations but the generated reactive species for the propagation reactions with 4-AMP on the catalyst surface are constant which led to the lower degradation rate (c) a high concentration of 4-AMP absorbed greater number of photons which decreased the availability of the photons to activate the photocatalyst leading to lower generation of oxidizing species. The observed results indicate that the irradiation of UV light on the surface of photocatalyst is the rate limiting step. Considering the higher rate constants and extents of degradation at lower concentration, initial concentration of 50 ppm was used in all the remaining experiments.

Chapter 4: Synthesis and characterization of Samarium and Nitrogen doped TiO₂ photocatalysts for photo-degradation of 4-Acetamidophenol in combination with hydrodynamic and acoustic cavitation

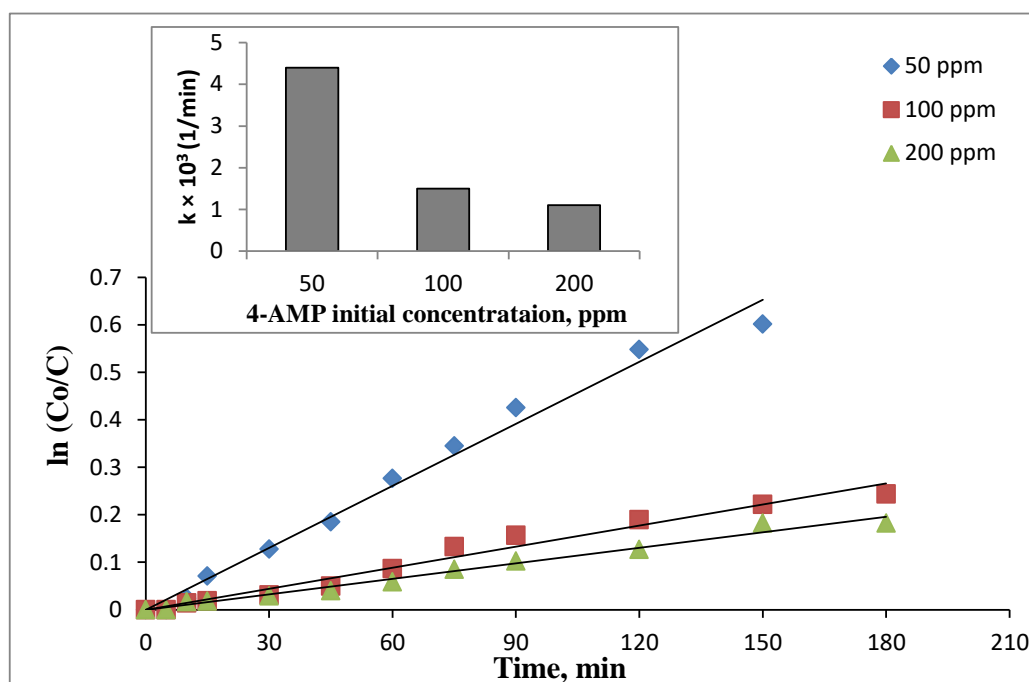


Figure 4.13: First order kinetic fitting for 4-AMP degradation at different initial concentrations (Conditions: solution volume: 400 mL, TiO₂ loading: 2 g/L, solution pH: 6.8 treatment time: 180 min)

4.3.2.4 Effect of dopants

The photocatalytic degradation of 4-AMP under UV light irradiation was also performed using doped photocatalysts in order to explore the photocatalytic activity of both Sm and N doped TiO₂ and establish the possible superiority as compared to pure TiO₂. In the present work, photocatalysts were synthesized in various molar ratios of Sm to TiO₂ (1, 1.5, and 2) and N to TiO₂ (0.5, 0.75, 1.0, and 1.5). The extent of degradation and rate constants obtained using different types of doped TiO₂ photocatalysts are depicted in Figure 4.14. It was observed that both the doped (Sm and N) TiO₂ photocatalyst exhibited a higher photocatalytic efficiency in degradation of 4-AMP as compared to pure TiO₂ photocatalyst. From Figure 4.14 (a), it can be also observed that extent of degradation and pseudo-first order rate constant increased with an increase in the molar ratio of N to TiO₂ from 0.5 to an optimum value of 1.0. Photocatalytic degradation of 4-AMP (50 ppm solution concentration) was enhanced from 49.7% using pure TiO₂ to almost 63 % degradation with a first order rate constant of $6.5 \times 10^{-3} \text{ min}^{-1}$ using N-doped TiO₂ at optimum N/TiO₂ ratio as 1, which is attributed to the reduced band gap energy from 3.19 to 2.98 eV, as well as larger number of photons are absorbed by N-doped TiO₂ compared to the pure TiO₂. Also, nitrogen doping

Chapter 4: Synthesis and characterization of Samarium and Nitrogen doped TiO₂ photocatalysts for photo-degradation of 4-Acetamidophenol in combination with hydrodynamic and acoustic cavitation

enhanced the degradation rate as it restricted the recombination rate of electron hole pairs as observed in the study of PL spectra of the doped photocatalysts in section 4.3.1.4.

The results presented in Figure 4.14 (b) also confirmed similar results for Sm doping with increased photo-degradation of 4-AMP with an increase in molar ratio of Sm to TiO₂ from 1 to optimum of 1.5 and then decreasing marginally for a further increase in Sm proportion. A maximum of 60 % degradation was achieved at the optimum 1.5 molar ratio (Sm/TiO₂), which can be attributed to following reasons [34-35]: (a) inhibition of electrons and holes recombination and (b) reduced band gap energy of the doped photocatalysts as compared to the pure TiO₂ as evidenced by UV-DRS spectra. Overall, the order of photocatalytic efficiency for the photocatalysts was N/TiO₂ (1 molar ratio) > Sm/TiO₂ (1.5 molar ratio) > pure TiO₂. Higher photocatalytic efficiency obtained in N-doped TiO₂ as compared to Sm-doped TiO₂ even with the low molar ratio (N/TiO₂:1) can be attributed to the reduced band gap energy (2.98 eV) of N-doped TiO₂ as compared to the Sm-doped TiO₂ (3.10 eV) and pure TiO₂ (3.19 eV).

Chapter 4: Synthesis and characterization of Samarium and Nitrogen doped TiO₂ photocatalysts for photo-degradation of 4-Acetamidophenol in combination with hydrodynamic and acoustic cavitation

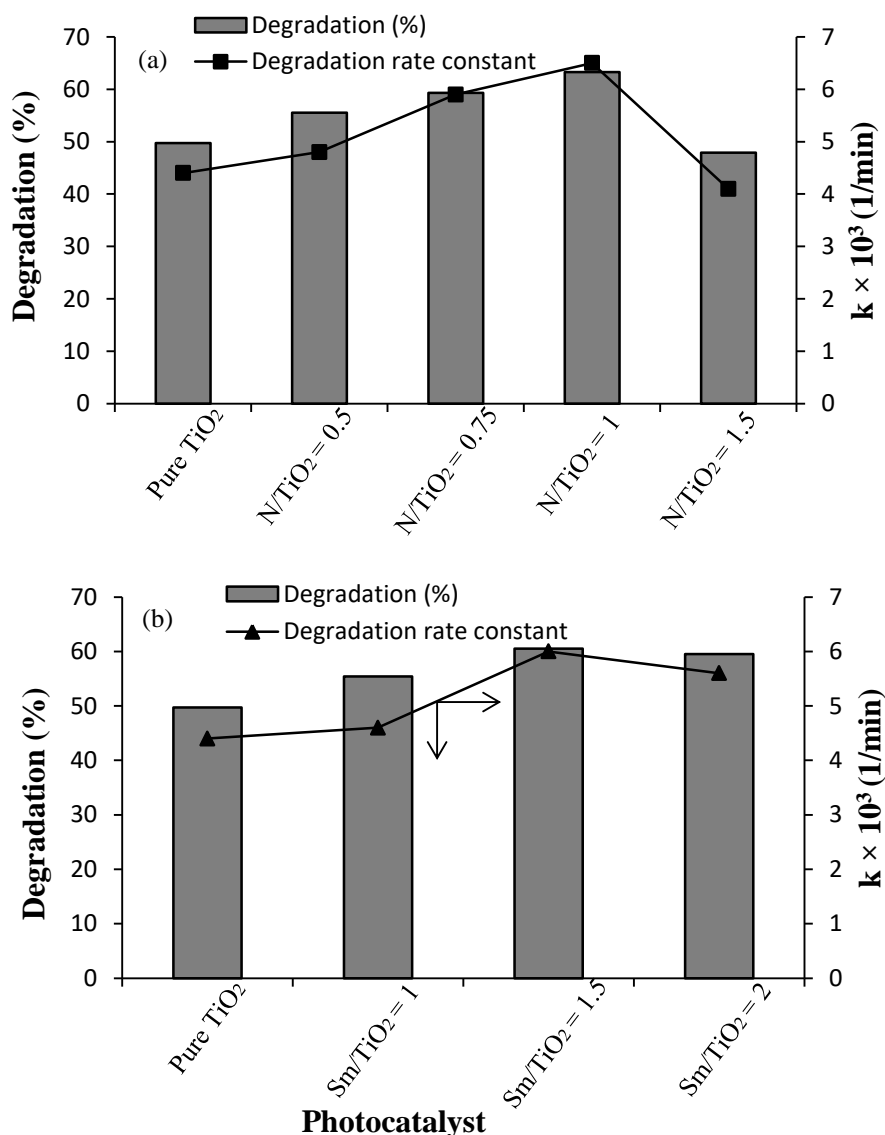


Figure 4.14: Photocatalytic degradation of 4-AMP over different (a) N-doped TiO₂ and (b) Sm-doped TiO₂ (Conditions: solution volume: 400 mL, initial concentration: 50 ppm, catalyst loading: 2 g/L, solution pH: 6.8 treatment time: 180 min)

4.3.2.5 Comparison of photocatalytic activity for UV and visible light irradiations

Comparison of photocatalytic activity of undoped TiO₂, Sm-doped TiO₂ (Sm/TiO₂ = 1.5 as the optimum molar ratio) and N-doped TiO₂ (N/TiO₂ = 1 as the optimum molar ratio) catalysts was made under both UV and visible light irradiations. From the presented data in Table 4.2, it can be seen that extent of degradation and rate constant of 4-AMP were found to be higher under UV light irradiation as compared to visible light. As presented in Table 4.2, almost 50 %, 60 %, and 63 % of 4-AMP was degraded using pure TiO₂, Sm-doped TiO₂, and

Chapter 4: Synthesis and characterization of Samarium and Nitrogen doped TiO₂ photocatalysts for photo-degradation of 4-Acetamidophenol in combination with hydrodynamic and acoustic cavitation

N-doped TiO₂ respectively, in 180 min of treatment under UV light irradiation whereas photocatalyst exhibited lower photo-degradation efficiencies under visible light irradiation (extent of degradation as 20.5% for pure TiO₂, 21.6% for Sm-doped TiO₂ and 28.3% for N-doped TiO₂). The activity of photocatalyst is greatly dependent on the light intensity, which determines the photon energy emitted by the surface of photocatalyst for a given wavelength. Considering the fact that energy of photons under visible region is lower, the amount of light absorption by photocatalyst surface will also be significantly reduced leading to lower photo-degradation efficiency in the presence of visible light irradiation [65] as compared to the UV irradiations.

In both the cases of light irradiations, photocatalytic performance for the 4-AMP degradation was found to be higher for doped photocatalysts as compared to pure TiO₂. It was also observed that N-doped TiO₂ photocatalyst gave higher photocatalytic efficiency (by almost 30%) under visible light as compared to pure TiO₂ and Sm-doped TiO₂. It proved that N-doped TiO₂ photocatalyst can be activated under visible light effectively due to the reduced band gap energy.

Table 4.2: Photocatalytic activity of different photocatalyst prepared using USP under UV and visible light irradiation

Type of photocatalyst	UV light irradiation		Visible light irradiation	
	Degradation (%)	$k \times 10^3, \text{min}^{-1}$	Degradation (%)	$k \times 10^3, \text{min}^{-1}$
Pure TiO ₂	49.7	4.4	20.5	1.5
Sm/TiO ₂ (1.5 molar ratio)	60.5	6.0	21.6	1.7
N/TiO ₂ (1.0 molar ratio)	63.3	6.5	28.3	2.1

(Conditions: solution volume: 400 mL, catalyst dosage: 2 g/L, solution pH: 6.8 treatment time: 180 min)

4.3.2.6 Degradation of 4-AMP using ultrasound coupled with photolytic and photocatalysis

Degradation of 4-AMP was studied using different combination approaches as well. Initially, the combination with ultrasound (US) viz. sono-photolytic (US+UV), and sono-

Chapter 4: Synthesis and characterization of Samarium and Nitrogen doped TiO₂ photocatalysts for photo-degradation of 4-Acetamidophenol in combination with hydrodynamic and acoustic cavitation

photocatalytic (US+UV+Catalyst) approaches was investigated and observed results are shown in Figure 4.15. It was found that US coupled with UV irradiations enhanced the degradation rate as compared to ultrasound alone. The obtained degradation rate constants using photocatalytic and sono-photocatalytic processes were found to be higher as compared to only sonication and sono-photolytic process. Almost 5.3 folds higher degradation rate of 4-AMP was obtained using photocatalytic oxidation than the combination of US with UV in the absence of catalyst confirming the major role played by the catalyst. Further it was observed that photocatalytic oxidation in the presence of US (US+UV+N-doped TiO₂) resulted in maximum degradation rate of 4-AMP under optimized process conditions with the actual extent of degradation being 87 % ($k = 10.8 \times 10^{-3} \text{ min}^{-1}$) in 180 min of operation time whereas only 63 % degradation ($k = 6.5 \times 10^{-3} \text{ min}^{-1}$) was achieved using only photocatalytic oxidation in the absence of sonication. The higher degradation obtained with the combination is attributed to the turbulence created by ultrasound induced cavitation that enhances mass transfer of pollutants between surface of the photocatalysts and liquid phase [32]. US also improved the photocatalytic efficiency by continuous cleaning and polishing of photocatalyst surfaces, separating agglomerated solid particles, and producing large quantum of hydroxyl radicals [66]. In addition to this, the gas pockets trapped in the agglomerates of the photocatalyst provide nuclei for transient cavitation events (producing additional $\cdot\text{OH}$ radicals) that further augment the rate of degradation. Synergetic coefficient of combined process was calculated on the basis of degradation rate constants for individual and combined processes using following equation (4.6):

$$\begin{aligned} \text{Synergetic coefficient} &= \frac{k_{(\text{US+UV+N-TiO}_2)}}{k_{\text{US}} + k_{(\text{UV+N-TiO}_2)}} & (4.6) \\ &= 10.8 \times 10^{-3} / (0.7 \times 10^{-3} + 6.5 \times 10^{-3}) \\ &= 1.5 \end{aligned}$$

Synergetic coefficient of 1.5 showed that the two processes worked in synergy giving much higher extent of degradation and the rate constants. It was observed that the first order rate constant increased significantly from $6.5 \times 10^{-3} \text{ min}^{-1}$ in the case of only photocatalytic degradation to $10.8 \times 10^{-3} \text{ min}^{-1}$ for the combination of US+UV+N-TiO₂.

Chapter 4: Synthesis and characterization of Samarium and Nitrogen doped TiO₂ photocatalysts for photo-degradation of 4-Acetamidophenol in combination with hydrodynamic and acoustic cavitation

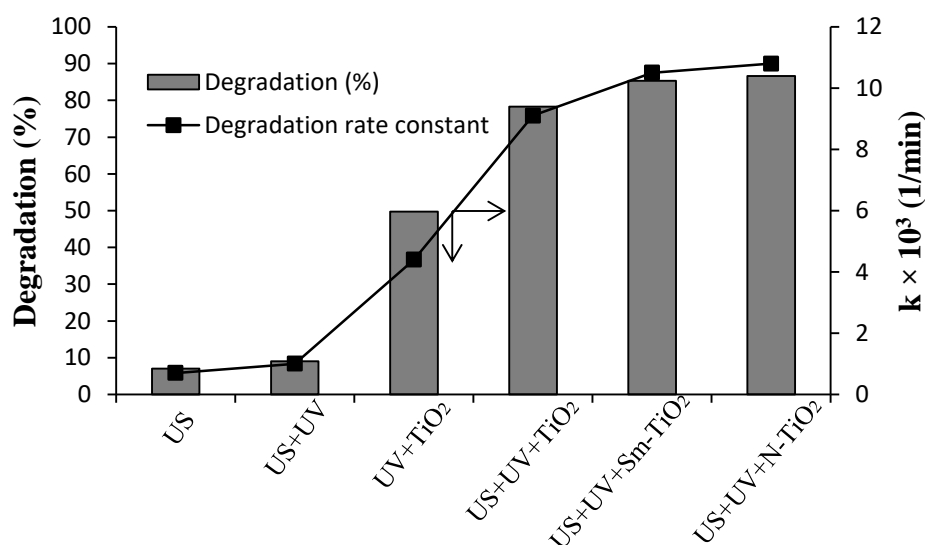


Figure 4.15: Effect of combination of AC and photocatalytic process on degradation rate of 4-AMP (Conditions: solution volume: 400 mL, initial concentration: 50 ppm, catalyst loading: 2 g/L, solution pH: 6.8 treatment time: 180 min)

4.3.2.7 Degradation of 4-AMP using hydrodynamic cavitation coupled with photolytic and photocatalysis

Combination of photocatalysis with hydrodynamic cavitation using slit venturi as the cavitating device was also investigated. All the experiments related to HC in the presence of photocatalyst were performed at an optimum operating inlet pressure of 5 bar, natural pH of 6.8, and 50 ppm solution of 4-AMP. The obtained results are shown in Figure 4.16. It can be seen that almost 8 % degradation with a rate constant of $0.7 \times 10^{-3} \text{ min}^{-1}$ was achieved using HC alone whereas nearly 15 % degradation with a rate constant of $1.1 \times 10^{-3} \text{ min}^{-1}$ was obtained using HC in the presence of UV irradiations (without catalyst). The extent of degradation obtained using combined HC with UV is almost 2 times higher than that obtained using HC alone, which may be due to the enhanced formation of $\cdot\text{OH}$ radicals than from the individual process such as HC alone. It was also observed that the first order rate constant of $4.4 \times 10^{-3} \text{ min}^{-1}$ observed for photocatalytic oxidation was further enhanced to $9.7 \times 10^{-3} \text{ min}^{-1}$ (almost 80 % degradation in 180 min) using a combination of HC/UV/pure TiO₂. The enhanced degradation rate using HC/UV/pure TiO₂ process may be attributed to the fact that the surrounding surface of photocatalyst is continuously cleaned and refreshed due to the generation of turbulence and micro-cavities in the presence of HC and it keeps the

Chapter 4: Synthesis and characterization of Samarium and Nitrogen doped TiO₂ photocatalysts for photo-degradation of 4-Acetamidophenol in combination with hydrodynamic and acoustic cavitation

photocatalytic activity for longer irradiation times therefore enhancing the photo-degradation rate [67]. The de-agglomeration of TiO₂ photocatalysts under the cavitating conditions enhance the overall surface area thereby leading to larger active sites to generate higher quantum of reactive species like [•]OH radicals [68]. From Figure 4.16, the photocatalytic activity of N-doped TiO₂ was also observed to be higher as compared to pure and Sm-doped TiO₂ with almost 91% of 4-AMP was degraded using HC/UV/N-dopedTiO₂ after 180 min of treatment time. The doped Nitrogen atoms enhanced the UV light absorption which inhibited the recombination rate of electron and hole pairs and enhanced the yield of generated reactive species thus further improving the photocatalytic activity as discussed before. The hybrid method (HC in combination with UV and the catalyst) exhibited a synergetic effect over an individual method and the calculated value of the synergetic coefficient was 1.82 which also indicated that higher amount of [•]OH radicals were generated using hybrid process than a single process operated individually. It was also observed that the synergetic effect was higher in the case of HC combined with photocatalysis (almost 1.2 times) as compared to US in combination with the photocatalytic oxidation. The operation of HC combined with photocatalytic oxidation has also offered the significant advantage of a larger scale of operation i.e. processing a larger volume (15 times higher) than ultrasonication in combination with photocatalysis. Thus, it can be said that HC offers more promise as compared to ultrasound with higher effectiveness for degradation and also feasibility for large scale operations.

Chapter 4: Synthesis and characterization of Samarium and Nitrogen doped TiO₂ photocatalysts for photo-degradation of 4-Acetamidophenol in combination with hydrodynamic and acoustic cavitation

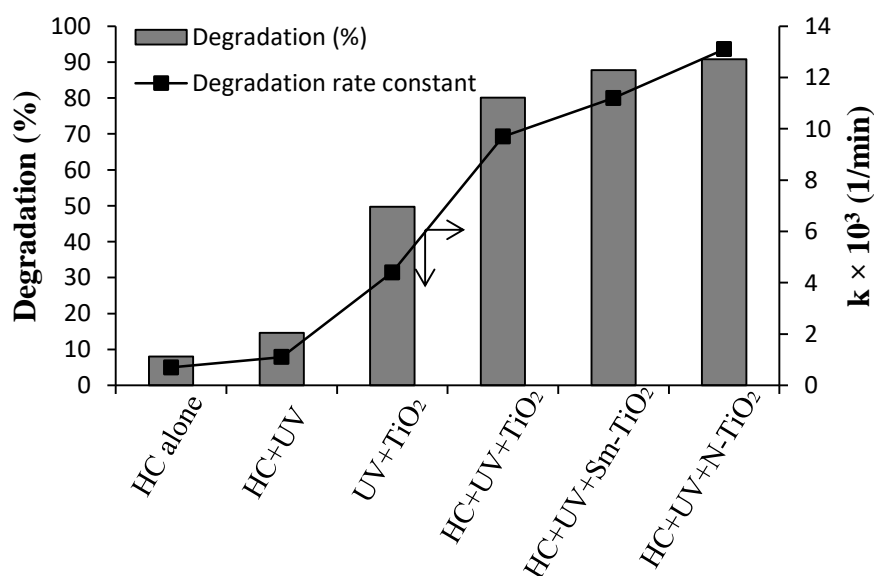


Figure 4.16: Effect of combination of HC and photocatalytic process on degradation rate of 4-AMP (Conditions: solution volume: 3 L, initial concentration: 50 ppm, catalyst loading: 2 g/L, solution pH: 6.8 treatment time: 180 min)

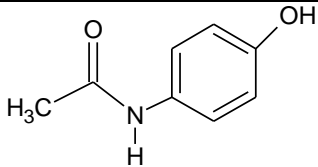
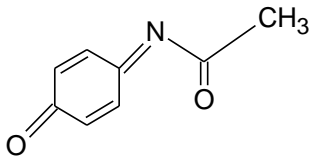

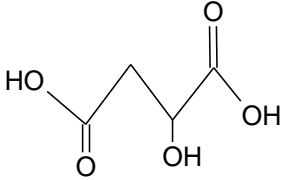
4.3.2.8 Analysis of by-products formed during HC+photocatalytic oxidation process

In order to identify the by-products formed during the photo-degradation, LC-MS analysis was applied for the treated sample analysis. The samples collected during photocatalytic oxidation in the presence of HC (where maximum degradation of 91% was achieved) were analyzed using LC-MS. Eight degradation by-products of 4-AMP were detected in the samples and their possible molecular structures are given in Table 4.3. The analysis revealed that major peak of parent compound (4-AMP) with $m/z = 151$ reduced significantly with an increase in the treatment time. The possible detected compounds were N-acetyl-p-benzoquinone imine ($m/z = 149$), muconic acid ($m/z = 142$), malic acid ($m/z = 134$), hydroxyhydroquinone ($m/z = 126$), succinic acid ($m/z = 118$), hydroquinone ($m/z = 110$), malonic acid ($m/z = 104$), and oxalic acid ($m/z = 90$). There are mainly two possible mechanisms for the photo-catalytic degradation of 4-AMP in the presence of HC viz. attack of $\cdot\text{OH}$ radicals toward the breakage of electron rich aromatic compound and secondly the N-hydroxylation reaction process. At the start of degradation, N-acetyl-p-benzoquinone imine ($m/z = 149$) is one of the major intermediates formed through N-hydroxylation process which is further degraded into smaller compounds. The oxidative attack by hydroxyl radicals on $-\text{N}=\text{H}$ bond

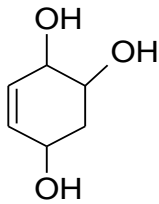
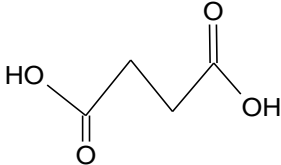
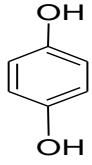
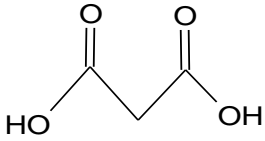
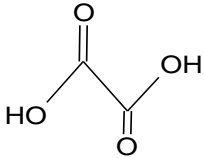
Chapter 4: Synthesis and characterization of Samarium and Nitrogen doped TiO₂ photocatalysts for photo-degradation of 4-Acetamidophenol in combination with hydrodynamic and acoustic cavitation

which connects the amine group to the aromatic ring may lead to the formation of other smaller compounds consisting dicarboxylic acids. The breakage of $-N=H$ bond and substituted alcohol group in the parent molecule may result into biodegradable acids of cyclic chain such as muconic and malic acids. Muconic acid ($m/z = 142$) was further degraded into possible intermediates as malic acid, hydroxy-hydroquinone, and succinic acid. This reaction involves initial attack by the $\cdot H$ and $\cdot OH$ radicals generated under cavitating conditions. The obtained degradation by-product i.e. hydroquinone ($m/z = 110$) can also be further oxidized into malonic acid ($m/z = 104$) and oxalic acid ($m/z = 90$). Similar degradation by-products were also reported by other researchers in their studies using different processes [63, 69-70] based on hydroxyl radicals.

Table 4.3: Identified degradation intermediates formed during photocatalytic degradation of 4-AMP in the presence of HC

S.N.	Name of compound	Molecular weight (m/z)	Probable molecular structure
I.	4-Acetamidophenol (parent molecule)	151	
II.	N-acetyl-p-benzoquinone imine	149	
III.	Muconic acid	142	
IV.	Malic acid	134	

Chapter 4: Synthesis and characterization of Samarium and Nitrogen doped TiO₂ photocatalysts for photo-degradation of 4-Acetamidophenol in combination with hydrodynamic and acoustic cavitation

V.	Hydroxy-hydroquinone	126	
VI.	Succinic acid	118	
VII.	Hydroquinone	110	
VIII.	Malonic acid	104	
IX.	Oxalic acid	90	

4.4 Energy efficiency evaluation

Energy consumption analysis plays an important role in choosing the feasible pollutant degradation process. Hence, the evaluation of energy required to treat the organic pollutants is necessary so that an efficient technique could be established for possible application on an industrial scale for the treatment. The comparison criteria used in this work for analysis was based on the energy efficiency (EE) which is defined as the amount of pollutant degraded per unit energy delivered (mg/J). In all cases, the treatment time was taken as 180 min for energy efficiency evaluation. The main energy consuming units in the photocatalytic process are the UV lamp and magnetic stirrer, whereas for the sonophotocatalytic process the additional power consumption is by the ultrasonic horn along with that for the photocatalytic process. The energy consumption for the HC+photocatalytic process is due to the pump and UV lamp. The energy efficiency obtained for the different processes at the optimized conditions is

Chapter 4: Synthesis and characterization of Samarium and Nitrogen doped TiO₂ photocatalysts for photo-degradation of 4-Acetamidophenol in combination with hydrodynamic and acoustic cavitation

summarized in Table 4.4 and sample calculations for energy efficiency are provided in appendix. It was observed that the energy efficiency for the photocatalysis (UV+N-TiO₂) was higher as compared to sonolysis (US), sonophotolysis (US+UV) and sonophotocatalytic (US+UV+N-TiO₂). It was observed that the energy delivered per unit volume in the case of photocatalytic degradation process was lower than sonolysis and sonophotocatalytic process. The EE in the case of only US and US+UV were similar but the energy requirement for the sonophotolysis process was higher than sonolysis. With the use of photocatalytic oxidation alone, the extent of degradation was found to be almost 63% and the EE has been observed as 1.46×10^{-6} mg/J. The required energy for all the experiments related to the hydrodynamic cavitation was lower than all the experiments related to the ultrasonication and photocatalytic oxidation alone. Table 4.4 indicates that energy required per unit volume was found to be lower in the case of HC+UV+N-TiO₂ among all the hybrid processes applied in the present study. This hybrid method exhibited better efficiency with higher degradation (almost 91%) and higher EE of 9.0×10^{-6} mg/J. In the case of HC+UV+N-TiO₂, the EE was enhanced 6.2 and 8.5 folds than HC+UV and HC alone respectively. Overall, HC coupled with photocatalysis was found to be more energy efficient as compared to others. Hence, it can be concluded that HC in combination with photocatalytic oxidation has a potential to give efficient 4-AMP degradation and can be hence used as an efficient treatment technology to reduce the organic load (especially POP, persistent organic pollutants) from wastewater.

Table 4.4: Energy Efficiency Evaluation of different processes under optimized conditions

Type of process	$k \times 10^3$ (min ⁻¹)	% Degradation in 180 min	(Energy delivered/volume $\times 10^{-6}$) (J/L)	(Energy efficiency $\times 10^6$) (mg/J)
Only US	0.7	7.0	20.2	0.17
US+UV	1.0	9.4	28.3	0.17
UV+N-TiO ₂	4.4	63.3	21.6	1.46
*US+UV+N-TiO ₂	10.8	86.6	41.8	1.03
Only HC	0.7	8.3	3.96	1.05
HC+UV	1.1	14.6	5.04	1.45
*HC+UV+N-TiO ₂	13.1	90.8	5.04	9.00

* Sample calculations for energy efficiency are shown in Appendix

Chapter 4: Synthesis and characterization of Samarium and Nitrogen doped TiO₂ photocatalysts for photo-degradation of 4-Acetamidophenol in combination with hydrodynamic and acoustic cavitation

4.5 Novelty of the work

- In the present work, Sm and N doped TiO₂ photocatalysts have been synthesized using CSP and USP and photocatalytic activity of both the catalysts has been evaluated for the degradation of 4-AMP using different combinations of UV irradiation, HC and US for the first time.
- Comparison of the photocatalytic activity of pure and doped (Sm and N) TiO₂ photocatalysts under UV and visible light were also made.
- The degradation by-products formed during HC+photocatalytic process were also identified through LC-MS.
- The present work also reports the energy consumption analysis based on the amount of pollutant degraded per unit energy supplied for all the approaches applied.

4.6 Summary of the chapter

In the current work, pure and doped TiO₂ photocatalysts were successfully synthesized using conventional and ultrasound assisted sol-gel processes. The particle size of pure and doped photocatalysts prepared by USP was found to be smaller than that obtained using CSP. It was also established that 4-AMP can be degraded using photocatalytic oxidation and the effect of degradation can be enhanced by optimizing the process parameters i.e. catalyst loading (2 g/L), 4-AMP initial concentration (50 ppm), and natural pH of the solution (6.8). Photocatalytic degradation of 4-AMP followed first-order degradation kinetics and almost 63% of 4-AMP was degraded using only photocatalytic oxidation at the optimized conditions. It was found that photocatalytic degradation efficiency of 4-AMP was significantly enhanced using doped TiO₂. The molar ratios of Sm/TiO₂ of 1.5 and N/TiO₂ of 1.0 were found to be the optimum dopant molar concentration to achieve the maximum photocatalytic activity. Doping of TiO₂ with Sm and N resulted into improved photocatalytic efficiencies due to the enhanced separation efficiency of photo-generated electron-hole (e⁻ - h⁺) pair. The photocatalytic oxidation in the presence of US and HC was also studied in order to improve the photocatalytic efficiency at the optimized conditions. In the case of US combined with photocatalytic oxidation, degradation of 4-AMP significantly enhanced to almost 87% whereas almost 91% degradation was achieved in 180 min using HC+UV+N/TiO₂. Using LC-MS analysis, eight degradation by-products of 4-AMP during

Chapter 4: Synthesis and characterization of Samarium and Nitrogen doped TiO₂ photocatalysts for photo-degradation of 4-Acetamidophenol in combination with hydrodynamic and acoustic cavitation

the combined process of HC and photocatalytic oxidation were determined, with three aromatic compounds and five aliphatic acids. Photocatalytic oxidation combined with HC was also demonstrated to be more energy efficient process. Overall the current work has established that a novel combination of HC (slit venturi used as a cavitating device), UV and photocatalysts can be effectively applied for the treatment of wastewater containing persistent organic pollutants at large scale operation.

Once the efficiency of HC and its hybrid methods have been established for different organic pollutants, the next challenge was the application of the same for the treatment of real industrial effluent. Since, textile is an important industry in Rajasthan catered by more than 600 textile industries situated in the towns of Bhilwara, Balotra and Jaipur, textile dyeing industry (TDI) effluent was collected and studied for the applicability of HC based hybrid methods for its treatment which is presented in the next chapter.

Chapter 4: Synthesis and characterization of Samarium and Nitrogen doped TiO₂ photocatalysts for photo-degradation of 4-Acetamidophenol in combination with hydrodynamic and acoustic cavitation

Appendix

Energy efficiency Calculation for US+UV+N-TiO₂ process:

Total Energy supplied = power supplied for (ultrasonic horn + UV lamp + magnetic stirrer) in 180 min.

$$\begin{aligned} &= (750+300+500) \text{ (J/s)} \times (180 \times 60) \text{ (sec)} \\ &= 16.74 \times 10^6 \text{ J} \end{aligned}$$

Volume of the treated sample = 0.4 L

Energy delivered per unit volume = $16.74 \times 10^6 / 0.4 = 41.85 \times 10^6$ J/L

Mass of 4-AMP degraded (mg) = (Initial conc.) x (% degradation) x (volume of treated sample)

$$\begin{aligned} &= 50 \text{ (mg/L)} \times 0.866 \times 0.4 \text{ (L)} \\ &= 17.32 \text{ mg} \end{aligned}$$

Energy Efficiency = mass of 4-AMP degraded / total power supplied

$$\begin{aligned} &= 17.32 / 16.74 \times 10^6 \\ &= 1.03 \times 10^{-6} \text{ mg/J} \end{aligned}$$

Energy efficiency Calculation for HC+UV+N-TiO₂ process:

Total Energy supplied = power supplied for (HC set up pump + UV lamp) in 180 min.

$$\begin{aligned} &= (1100+300) \text{ (J/s)} \times (180 \times 60) \text{ (sec)} \\ &= 15.12 \times 10^6 \text{ J} \end{aligned}$$

Volume of the treated sample = 3.0 L

Energy delivered per unit volume = $15.12 \times 10^6 / 3.0 = 5.04 \times 10^6$ J/L

Mass of 4-AMP degraded (mg) = (Initial conc.) x (% degradation) x (volume of treated sample)

$$\begin{aligned} &= 50 \text{ (mg/L)} \times 0.908 \times 3.0 \text{ (L)} \\ &= 136.2 \text{ mg} \end{aligned}$$

Energy Efficiency = mass of 4-AMP degraded / total power supplied

$$\begin{aligned} &= 136.2 / 15.12 \times 10^6 \\ &= 9 \times 10^{-6} \text{ mg/J} \end{aligned}$$

Chapter 4: Synthesis and characterization of Samarium and Nitrogen doped TiO₂ photocatalysts for photo-degradation of 4-Acetamidophenol in combination with hydrodynamic and acoustic cavitation

References

- [1] S.D. Kim, J. Cho, I.S. Kim, B.J. Vanderford, S.A. Snyder, Occurrence and removal of pharmaceuticals and endocrine disruptors in South Korean surface, drinking, and waste waters, *Water Res.* 41 (2007) 1013-1021.
- [2] A.Y.C. Lin, Y.T. Tsai, Occurrence of pharmaceuticals in Taiwan's surface waters: impact of waste streams from hospitals and pharmaceutical production facilities, *Sci. Total Environ.* 407 (2009) 3793-802.
- [3] M. Carballa, F. Omil, J.M. Lema, M. Llompart, C. Garcia-Jares, I. Rodriguez, M. Gomez, T. Ternes, Behaviour of pharmaceuticals, cosmetics and hormones in a sewage treatment plant, *Water Res.* 38 (2004) 2918-2926.
- [4] L. Lishman, S.A. Smyth, K. Sarafin, S. Kleywegt, J. Toito, T. Peart, P. Seto, Occurrence and reductions of pharmaceuticals and personal care products and estrogens by municipal wastewater treatment plants in Ontario, Canada. *Sci. Total Environ.* 367 (2006) 544-558.
- [5] Y. Yoon, J. Ryu, J. Oh, B.G. Choi, S.A. Snyder, Occurrence of endocrine disrupting compounds, pharmaceuticals, and personal care products in the Han River (Seoul, South Korea), *Sci. Total Environ.* 408 (2010) 636-643.
- [6] P.E. Stackelberg, E.T. Furlong, M.T. Meyer, S.D. Zaugg, A.K. Henderson, D.B. Reissman, Persistence of pharmaceutical compounds and other organic wastewater contaminants in a conventional drinking-water treatment plant, *Sci. Total Environ.* 329 (2004) 99-113.
- [7] M.J. Benotti, R.A. Trenholm, B.J. Vanderford, J.C. Holady, B.D. Stanford, S.A. Snyder, Pharmaceuticals and endocrine disrupting compounds in US drinking water, *Environ. Sci. Technol.* 43 (2008) 597-603.
- [8] E. Villaroel, J. Silva-Agredo, C. Petrier, G. Taborda, R.A. Torres-Palma, Ultrasonic degradation of acetaminophen in water: Effect of sonochemical parameters and water matrix, *Ultrason. Sonochem.* 21(2014) 1763-1769.
- [9] E. Moctezuma, E. Leyva, C.A. Aguilar, R. A. Luna, C. Montalvo, Photocatalytic degradation of paracetamol: Intermediates and total reaction mechanism, *Journal of Hazardous Materials* 243 (2012) 130-138.

Chapter 4: Synthesis and characterization of Samarium and Nitrogen doped TiO₂ photocatalysts for photo-degradation of 4-Acetamidophenol in combination with hydrodynamic and acoustic cavitation

- [10] C.C. Su, A.C. Crisanto, P.D. Maria Lourdes, M.C. Lu, Effect of UV light on acetaminophen degradation in the electro-Fenton process. *Sep. Purif. Technol.* 120 (2013) 43-51.
- [11] A.A. Pradhan, P.R. Gogate, Removal of p-nitrophenol using hydrodynamic cavitation and Fenton chemistry at pilot scale operation, *Chem. Eng. J.* 156 (2010) 77–82.
- [12] M. Tamimi, S. Qourzal, N. Barka, A. Assabbane, Y. Ait-ichou, Methomyl degradation in aqueous solutions by fenton's reagent and the photo-fenton system, *Sep. Purif. Technol.* 61 (2008) 103–108.
- [13] P.S.S. Kumar, S. Radhakrishnan, A. Sambandam, J. Madhavan, P. Maruthamuthu, M. Ashokkumar, Photocatalytic degradation of Acid Red 88 using Au–TiO₂ nanoparticles in aqueous solutions, *Water res.* 42 (2008) 4878-4884.
- [14] P. Sathishkumar, A. Sambandam, P. Maruthamuthu, T. Swaminathan, M. Zhou, M. Ashokkumar, Synthesis of Fe³⁺ doped TiO₂ photocatalysts for the visible assisted degradation of an azo dye, *Colloids Surf., A: Physicochemical and Eng. Aspects* 375 (2011) 231-236.
- [15] S. Rajoriya, S. Bargole, V. K. Saharan, Degradation of reactive blue 13 using hydrodynamic cavitation: Effect of geometrical parameters and different oxidizing additives, *Ultrason. Sonochem.* 37 (2017) 192-202.
- [16] D. Panda, S. Manickam, Recent advancements in the sonophotocatalysis (SPC) and doped-sonophotocatalysis (DSPC) for the treatment of recalcitrant hazardous organic water pollutants, *Ultrason. Sonochem.* 36 (2017) 481-496.
- [17] A. Fujishima, T.N. Rao, D.A. Tryk, Titanium dioxide photocatalysis, *J. Photochem. Photobiol. C: Photochem. Rev.* 1(2000) 1-21.
- [18] H. Fan, G. Li, F. Yang, L. Yang, S. Zhang, Photodegradation of cellulose under UV light catalysed by TiO₂, *J. Chem. Technol. Biotechnol.* 86 (2011) 1107-1112.
- [19] M.R. Hoffmann, S.T. Martin, W. Choi, D.W. Bahnemann, Environmental applications of semiconductor photocatalysis, *Chem. Rev.* 95 (1995) 69-96.
- [20] E. M. Samsudin, S. B. A. Hamid, J. C. Juan, W. J. Basirun, G. Centi, Enhancement of the intrinsic photocatalytic activity of TiO₂ in the degradation of 1,3,5-triazine herbicides by doping with N,F, *Chem. Eng. J.* 280 (2015) 330-343.

Chapter 4: Synthesis and characterization of Samarium and Nitrogen doped TiO₂ photocatalysts for photo-degradation of 4-Acetamidophenol in combination with hydrodynamic and acoustic cavitation

- [21] D. Chakraborty, S.S. Gupta, Photo-catalytic decolourisation of toxic dye with N-doped titania: A case study with Acid Blue 25, *J. Environ. Sci.* 25 (2013) 1034-1043.
- [22] M. Pelaez, N.T. Nolan, S.C. Pillai, M.K. Seery, P. Falaras, A.G. Kontos, P.S. Dunlop, J.W. Hamilton, J.A. Byrne, K. O'shea, M.H. Entezari, D.D. Dionysiou, A review on the visible light active titanium dioxide photocatalysts for environmental applications, *Appl. Catal., B Environ.* 125 (2012) 331-349.
- [23] V. Likodimos, Photonic crystal-assisted visible light activated TiO₂ photocatalysis, *Appl. Catal., B Environ.* 230 (2018) 269-303.
- [24] V. Iliev, D. Tomova, L. Bilyarska, A. Eliyas, L. Petrov, Photocatalytic properties of TiO₂ modified with platinum and silver nanoparticles in the degradation of oxalic acid in aqueous solution, *Appl. Catal., B Environ.* 63 (2006) 266-271.
- [25] S. Anandan, P. Sathish Kumar, N. Pugazhentiran, J. Madhavan, P. Maruthamuthu, Effect of loaded silver nanoparticles on TiO₂ for photocatalytic degradation of Acid Red 88, *Sol. Energy Mater. Sol. Cells* 92 (2008) 929-937.
- [26] X.K. Wang, C. Wang, W.L. Guo, J.G. Wang, A novel single-step synthesis of N-doped TiO₂ via a sonochemical method, *Mater. Res. Bull.* 46 (2011) 2041-2044.
- [27] K.M. Reddy, B. Baruwati, M. Jayalakshmi, M.M. Rao, S.V. Manorama, S-, N-and C-doped titanium dioxide nanoparticles: synthesis, characterization and redox charge transfer study, *J. Solid State Chem.* 178 (2005) 3352-3358.
- [28] V.K. Saharan, A.B. Pandit, P.S.S. Kumar, S. Anandan, Hydrodynamic cavitation as an advanced oxidation technique for the degradation of acid red 88 dye, *Ind. Eng. Chem. Res.* 51 (2011) 1981-1989.
- [29] W. Choi, A. Termin, M.R. Hoffmann, The role of metal ion dopants in quantum-sized TiO₂: correlation between photoreactivity and charge carrier recombination dynamics, *J. Phys. Chem.* 98 (1994) 13669-13679.
- [30] J. Madhavan, P.S.S. Kumar, A. Sambandam, F. Grieser, M. Ashokkumar, Sonophotocatalytic degradation of monocrotophos using TiO₂ and Fe³⁺, *J. Hazard. Mater.* 177 (2010) 944-949.
- [31] B. Bethi, S.H. Sonawane, G.S. Rohit, C.R. Holkar, D.V. Pinjari, B.A. Bhanvase, A. B. Pandit, Investigation of TiO₂ photocatalyst performance for decolorization in the presence of hydrodynamic cavitation as hybrid AOP, *Ultrason. Sonochem.* 28 (2016) 150-160.

Chapter 4: Synthesis and characterization of Samarium and Nitrogen doped TiO₂ photocatalysts for photo-degradation of 4-Acetamidophenol in combination with hydrodynamic and acoustic cavitation

- [32] P. Sathishkumar, R.V. Mangalaraja, O. Rozas, H.D. Mansilla, M.A. Gracia-Pinilla, M.F. Meléndrez, A. Sambandam, Sonophotocatalytic degradation of Acid Blue 113 in the presence of rare earth nanoclusters loaded TiO₂ nanophotocatalysts, *Sep. Purif. Technol.* 133 (2014) 407-414.
- [33] S.R. Shirsath, D.V. Pinjari, P. R. Gogate, S. H. Sonawane, A. B. Pandit, Ultrasound assisted synthesis of doped TiO₂ nano-particles: characterization and comparison of effectiveness for photocatalytic oxidation of dyestuff effluent, *Ultrason. Sonochem.* 20 (2013) 277-286.
- [34] H. Eskandarloo, A. Badieli, M.A. Behnajady, G.M. Ziarani, Ultrasonic-assisted sol-gel synthesis of samarium, cerium co-doped TiO₂ nanoparticles with enhanced sonocatalytic efficiency, *Ultrason. Sonochem.* 26 (2015) 281-292.
- [35] Q. Xiao, Z. Si, J. Zhang, C. Xiao, Z. Yu, G. Qiu, Effects of samarium dopant on photocatalytic activity of TiO₂ nanocrystallite for methylene blue degradation, *J. Mater. Sci.* 42 (2007) 9194-9199.
- [36] X. Yan, J. He, D.G. Evans, X. Duan, Y. Zhu, Preparation, characterization and photocatalytic activity of Si-doped and rare earth-doped TiO₂ from mesoporous precursors, *Appl. Catal., B: Environ.* 55 (2005) 243-252.
- [37] C.Y. Teh, T.Y. Wu, J.C. Juan, An application of ultrasound technology in synthesis of titania-based photocatalyst for degrading pollutant, *Chem. Eng. J.* 317 (2017) 586-612.
- [38] X. Chen, S.S. Mao, Titanium dioxide nanomaterials: synthesis, properties, modifications, and applications, *Chem. Rev.* 107 (2007) 2891-2959.
- [39] S.R. Jadhav, V.K. Saharan, D.V. Pinjari, S. Sonawane, D. Saini, A. Pandit, Intensification of degradation of imidacloprid in aqueous solutions by combination of hydrodynamic cavitation with various advanced oxidation processes (AOPs), *J. Environ. Chem. Eng.* 1 (2013) 850–857.
- [40] S. Rajoriya, J. Carpenter, V.K. Saharan, A.B. Pandit, Hydrodynamic cavitation: an advanced oxidation process for the degradation of bio-refractory pollutants, *Rev. Chem. Eng.* 32 (2016) 379–411.
- [41] M. Sivakumar, A. B. Pandit, Wastewater treatment: a novel energy efficient hydrodynamic cavitation technique, *Ultrason. Sonochem.* 9 (2002) 123–131.

Chapter 4: Synthesis and characterization of Samarium and Nitrogen doped TiO₂ photocatalysts for photo-degradation of 4-Acetamidophenol in combination with hydrodynamic and acoustic cavitation

- [42] S. Rajoriya, S. Bargole, V.K. Saharan, Degradation of a cationic dye (Rhodamine 6G) using hydrodynamic cavitation coupled with other oxidative agents: Reaction mechanism and pathway, *Ultrason. Sonochem.* 34 (2017) 183-194.
- [43] Y. Li, C. Xie, S. Peng, G. Lu, S. Li, Eosin Y-sensitized nitrogen-doped TiO₂ for efficient visible light photocatalytic hydrogen evolution, *J. Mol. Catal. A: Chem.* 282 (2008) 117–123.
- [44] U.G. Akpan, B.H. Hameed, Enhancement of the photocatalytic activity of TiO₂ by doping it with calcium ions, *J. Colloid Interface Sci.* 357 (2011) 168-178.
- [45] M.A. Mohamed, W.N.W. Salleh, J. Jaafar, A. F. Ismail, N.A.M. Nor, Photodegradation of phenol by N-Doped TiO₂ anatase/rutile nanorods assembled microsphere under UV and visible light irradiation, *Mater. Chem. Phys.* 162 (2015) 113-123.
- [46] A.M.T. Silva, C.G. Silva, G. Dražić, J.L. Faria, Ce-doped TiO₂ for photocatalytic degradation of chlorophenol, *Catal. Today* 144, (2009) 13-18.
- [47] R. Velmurugan, B. Krishnakumar, B. Subash, M. Swaminathan, Preparation and characterization of carbon nanoparticles loaded TiO₂ and its catalytic activity driven by natural sunlight, *Sol. Energy Mater. Sol. Cells* 108 (2013) 205-212.
- [48] F. Spadavecchia, G. Cappelletti, S. Ardizzone, C.L. Bianchi, S. Cappelli, C. Oliva, P. Scardi, M. Leoni, P. Fermo, Solar photoactivity of nano-N-TiO₂ from tertiary amine: role of defects and paramagnetic species, *Appl. Catal., B: Environ.* 96 (2010) 314-322.
- [49] R. Lo'pez, R. Go'mez, Band-gap energy estimation from diffuse reflectance measurements on sol–gel and commercial TiO₂: a comparative study, *J. Sol-Gel Sci. Technol.* 61 (2012) 1–7.
- [50] Y. Wu, M. Xing, J. Zhang, Gel-hydrothermal synthesis of carbon and boron co-doped TiO₂ and evaluating its photocatalytic activity, *J. Hazard, Mater.* 192 (2011) 368–373.
- [51] V. Dinkar, S. Shridhar, E. Madhukar, E. Anil, H. Nitin, Sm-Doped TiO₂ Nanoparticles With High Photocatalytic Activity For ARS Dye Under Visible Light Synthesized By Ultrasonic Assisted Sol-Gel Method, *Oriental J. of Chemistry* 32 (2016) 933-940.

Chapter 4: Synthesis and characterization of Samarium and Nitrogen doped TiO₂ photocatalysts for photo-degradation of 4-Acetamidophenol in combination with hydrodynamic and acoustic cavitation

- [52] Y. Ma, J. Zhang, B. Tian, F. Chen, L. Wang, Synthesis and characterization of thermally stable Sm, N co-doped TiO₂ with highly visible light activity, *J. Hazard. Mat.* 182 (2010) 386-393.
- [53] M. Xing, J. Zhang, F. Chen, New approaches to prepare nitrogen-doped TiO₂ photocatalysts and study on their photocatalytic activities in visible light. *Appl. Catal. B Environ.* 89 (2009) 563-569.
- [54] Y.C. Zhang, M. Yang, G. Zhang, D.D. Dionysiou, HNO₃-involved one-step low temperature solvothermal synthesis of N-doped TiO₂ nanocrystals for efficient photocatalytic reduction of Cr (VI) in water, *Appl. Catal. B Environ.* 142-143 (2013) 249-258.
- [55] J. Ananpattarachai, P. Kajitvichyanukul, S. Seraphin, Visible light absorption ability and photocatalytic oxidation activity of various interstitial N-doped TiO₂ prepared from different nitrogen dopants, *J. Hazard. Mater.* 168 (2009) 253-261.
- [56] Z. Wang, W. Cai, X. Hong, X. Zhao, F. Xu, C. Cai, Photocatalytic degradation of phenol in aqueous nitrogen-doped TiO₂ suspensions with various light sources, *Appl. Catal. B Environ.* 57 (2005) 223-231.
- [57] D. H. Wang, L. Jia, X. L. Wu, L. Q. Lu, A.W. Xu, One-step hydrothermal synthesis of N-doped TiO₂/C nanocomposites with high visible light photocatalytic activity, *Nanoscale* 4 (2012) 576-584.
- [58] L. Wan, J.F. Li, J.Y. Feng, W. Sun, Z.Q. Mao, Improved optical response and photocatalysis for N-doped titanium oxide (TiO₂) films prepared by oxidation of TiN, *Appl. Surf. Sci.* 253 (2007) 4764-4767.
- [59] M. Zhang, J. Wu, D. Lu, J. Yang, Enhanced visible light photocatalytic activity for TiO₂ nanotube array films by co doping with tungsten and nitrogen, *Int. J. Photoenergy* 2013 (2013) 1-8.
- [60] J. Tang, X. Chen, Y. Liu, W. Gong, Z. Peng, T. Cai, L. Luo, Q. Deng, Samarium-doped mesoporous TiO₂ nanoparticles with improved photocatalytic performance for elimination of gaseous organic pollutants, *Solid State Sciences*, 15 (2013) 129-136.
- [61] S.K. Kansal, A.H. Ali, S. Kapoor, Photocatalytic decolorization of biebrich scarlet dye in aqueous phase using different nanophotocatalysts, *Desalination* 259 (2010) 147-155.

Chapter 4: Synthesis and characterization of Samarium and Nitrogen doped TiO₂ photocatalysts for photo-degradation of 4-Acetamidophenol in combination with hydrodynamic and acoustic cavitation

- [62] N. Jallouli, K. Elghnji, H. Trabelsi, M. Ksibi, Photocatalytic degradation of paracetamol on TiO₂ nanoparticles and TiO₂/cellulosic fiber under UV and sunlight irradiation, *Arab. J.Chem.* 10 (2017) S3640–S3645.
- [63] L. Yang, E.Y. Liya, M.B. Ray, Degradation of paracetamol in aqueous solutions by TiO₂ photocatalysis, *Water res.* 42 (2008) 3480-3488.
- [64] X. Zhang, F. Wu, X.W. Wu, P. Chen, N. Deng, Photodegradation of acetaminophen in TiO₂ suspended solution, *J. Hazard. Mater.* 157 (2008) 300–307.
- [65] E.B. Simsek, Solvothermal synthesized boron doped TiO₂ catalysts: Photocatalytic degradation of endocrine disrupting compounds and pharmaceuticals under visible light irradiation, *Appl. Catal., B: Environ.* 200 (2017) 309-322.
- [66] J. Madhavan, P.S.S. Kumar, S. Anandan, M. Zhou, F. Grieser, M. Ashokkumar, Ultrasound assisted photocatalytic degradation of diclofenac in an aqueous environment. *Chemosphere*, 80 (2010) 747-752.
- [67] M.V. Bagal, P.R. Gogate, Degradation of diclofenac sodium using combined processes based on hydrodynamic cavitation and heterogeneous photocatalysis, *Ultrason. Sonochem.* 21 (2014) 1035-1043.
- [68] Y.C. Chen, P. Smirniotis, Enhancement of photocatalytic degradation of phenol and chlorophenols by ultrasound, *Ind. Eng. Chem. Res.* 41(2002) 5958-5965.
- [69] A.G. Trovo, R.F.P. Nogueira, A. Agueera, A.R. Fernandez-Alba, S. Malato, Paracetamol degradation intermediates and toxicity during photo-Fenton treatment using different iron species, *Water res.* 46 (2012) 5374-5380.
- [70] M. Torun, Ö. Gültekin, D. Şolpan, O. Güven, Mineralization of paracetamol in aqueous solution with advanced oxidation processes, *Environ. Techn.* 36 (2015) 970-982.

CHAPTER 5

Treatment of textile dyeing industry effluent using hydrodynamic cavitation
in combination with advanced oxidation reagents

5.1 Introduction

In recent years, effluents from the textile processing industry have become a cause of serious environmental concern. The use of synthetic chemical dyes by the textile industries in the various textile processing operations such as dyeing, printing, bleaching and finishing operations has resulted in the release of large amounts of dye-containing industrial wastewater. Textile is an important industry in Rajasthan catered by textile industries situated in towns of Bhilwara, Balotra, Barmer and Sanganer (Jaipur) and account for nearly 20 % of the investment made in the state. Rajasthan contributes over 7.5 % of India's production of cotton and blended yarn (235,000 tonnes in 2002-03) and over 5 % of fabrics (60 million sq. meters) and has a leading position in spinning of polyester viscose yarn & synthetic suiting and processing. Bhilwara well known as “Textile City” with around 22 textile processing houses and 8 dye houses has emerged a leading centre for processing of synthetic fabric and its share in the polyester/viscose fabrics is around 50 % in India. Moreover, Balotra is famous for its dyeing and printing of cotton and polyester fabrics and is an important business centre with more than 600 textile industries and it imparts appreciable amount on the economy of India. These textile processing industries which came into existence in nineteen seventies have been growing at such a rapid pace and the wastewaters discharged by them have become a serious environmental threat. According to Mewar Chamber of Commerce and Industry (MCCI) data, the 500 textile units require approx. 25 million litres of water per day and currently only about 30% to 45% of the effluent is recycled and some units are permitted to discharge only up to 30%. In order to handle the huge quantity of wastewater generated by these textile industries several measures taken up by Government agencies as well as by the associations/trusts of these industrialists, include setting up common effluent treatment plants described as ad-hoc solutions only, as they treat the wastewater only to some extent and only a part of it is recovered for reuse. The industry's poor effluent management system has poisoned the area's groundwater causing high TDS, hardness, alkalinity etc. and nearby rivers affecting agriculture. There is an increasing incidence in health problems related to environmental issues that originate from inadequate decontamination of these wastewaters.

There are about 2324 textile industries in India [1]. More than ten thousands dyes are being used commercially and approximately 7×10^5 tons of synthetic dyes are produced per annum worldwide [2-3]. Textile wastewaters are found to have large quantity of suspended particles, varied pH, dark colored, with high chemical oxygen demand (COD) and high total organic

Chapter 5: Treatment of textile dyeing industry effluent using hydrodynamic cavitation in combination with advanced oxidation reagents

carbon (TOC) [4-6]. The presence of highly suspended solid particles with their strong color provides high turbidity in the textile effluents. Even very low concentration of these dyes (less than 1 ppm for some dyes) induce color in water that is highly observable and undesirable and adversely affects the water bodies such as rivers, lakes etc. [7-8]. Most of the dyes are toxic and bio-recalcitrant in nature and therefore conventional biological processes are found to be inefficient for treatment of textile effluents [3]. The untreated textile wastewaters due to the presence of carcinogenic compounds are therefore very hazardous and toxic to human beings and animals also.

Considering the fact that the aquatic environment is damaged by the wastewaters discharged from textile dyeing industries, it is required to develop an eco-friendly and energy efficient technique to treat the textile effluent before its discharge into the aquatic environment. Several conventional strategies comprised of various combinations of physical, chemical, and biological oxidation processes were developed for treatment of textile effluents in last one decade [6, 9-13]. However, these processes produce large amount of secondary pollutants which ultimately increase the load on overall treatment facility [5, 13]. In recent years, cavitation as an advanced oxidation process (AOP) has been receiving greater attention for the treatment of wastewater [14-17]. In the last two decades, ultrasonication has been studied for wastewater treatment [18-20], however it has not found any application so far on an industrial scale due to the higher maintenance costs involved and lower energy efficiency [15].

An alternative cavitation technology i.e. HC has been found to be more energy efficient as compared to acoustic cavitation for the degradation of organic pollutants and which can also be operated in a continuous mode [14,17, 21-24]. The degradation efficiency of HC can be improved by combining with other advanced oxidation processes/oxidizing agents such as H_2O_2 , Fenton's reagent, ozone and photocatalytic oxidation [15-16, 22, 25-27]. Mishra and Gogate [25] investigated the degradation of Rhodamine B dye using HC in the presence of intensifying additives. They found that almost 59.3% degradation and 30% TOC reduction were achieved using HC alone at an optimized inlet pressure of 4.84 atm and solution pH of 2.5. The degradation efficiency was further increased to 99.9% along with 55% reduction in TOC when HC was combined with hydrogen peroxide (200 mg/L). Gogate and Bhosale [26] studied the combined approach for the degradation of Orange Acid II dye and reported that combination of HC with oxidizing agents such as sodium persulfate, H_2O_2 and NaOCl was

Chapter 5: Treatment of textile dyeing industry effluent using hydrodynamic cavitation in combination with advanced oxidation reagents

found to be better as compared to use of the individual oxidants. Almost complete degradation of Orange Acid II was obtained in 60 min using HC in combination with sodium persulfate (535.72 mg/L) oxidant.

Although many studies report on the degradation of synthetically prepared dye wastewater using HC coupled with various oxidative additives mostly at low concentration ranges (i.e. 50-100ppm), however no study has been reported so far for real textile dyeing industry (TDI) effluent. It is necessary to study the efficacy of HC and its hybrid processes for treating real TDI effluents before applying on an industrial scale. This study focuses on investigating the performance of HC system for treating the TDI effluent. Effects of process parameters (operating inlet pressure and dilution) on the TOC, COD and color reduction were investigated. In order to enhance the efficiency of HC, the effect of advanced oxidative reagents such as oxygen, ozone, and Fenton in combination with HC were also studied.

5.2 Material and methods

5.2.1 Textile dyeing industry (TDI) effluent

TDI effluent was taken from the collection tank after dyeing, printing, and finishing processes in a textile dyeing industry (details not given due to confidentiality issues), located at Sanganer industrial zone, Jaipur, India. The characteristic of the TDI effluent is presented in Table 5.1. It is important to note that the samples were collected on different days for experiments and sample characteristics were found to be different and therefore a range has been specified instead of a fixed value for these parameters (Table 5.1). Dyes (reactive, direct, and acid dyes), detergents, chlorinated compounds and dissolved salts are the likely pollutants that make up the TOC and COD of the TDI effluent. The TDI effluent was initially filtered using a screen filter to remove large suspended particles and further used for all the experiments.

Table 5.1: Characteristics of TDI effluent

Parameter	Range	Unit
pH	6.8-7.0	–
Color	olive green	–
Total suspended solids (TSS)	2634-3167	mg/L
Total dissolved solids (TDS)	2935-4386	mg/L
Total solids (TS)	5569-7553	mg/L
Chemical oxygen demand (COD)	2560-4640	mg/L
Total organic carbon (TOC)	556-1184	mg/L

5.2.2 Chemicals

Hydrogen Peroxide (30%, w/v) of AR grade and ferrous sulphate heptahydrate ($\text{FeSO}_4 \cdot 7\text{H}_2\text{O}$) were obtained from Lobachemie (India). The chemicals used in the COD analysis i.e. silver sulfate, potassium dichromate, ferrous ammonium sulfate heptahydrate, mercuric sulfate, concentrated sulfuric acid and ferroin indicator were of analytical grade and purchased from Lobachemie. Ortho-phosphoric acid and sodium peroxodisulfate for TOC study were obtained from Merck, India. Tap water was used for the dilution study. All chemicals as received from suppliers were used for the experiments without any further purification.

5.2.3 Experimental set-up and procedure

HC reactor set-up used in the present work was similar to that used for the degradation of Rh6G (Chapter 2; Figure 2.1). HC reactor was provided with a slit venturi as the cavitating device. The details of the reactor set-up and slit venturi have been reported in our previous Chapter 2 (Section 2.2.2). In this study, all experiments were carried out for treating constant effluent volume of 6 L. Total treatment time was 120 min for all the experiments and samples were drawn at regular time intervals for analysis. Initially, the effect of operating inlet pressure on COD, TOC and color reduction of TDI effluent was investigated by varying the pressure between 3-10 bar. At the optimized inlet pressure, the dilution study was conducted at different dilution proportions. In order to enhance the efficiency of HC, effect of advanced oxidative reagents such as oxygen, ozone, and Fenton's reagent in combination with HC were also investigated. Pure O_2 was generated using an oxygen

Chapter 5: Treatment of textile dyeing industry effluent using hydrodynamic cavitation in combination with advanced oxidation reagents

concentrator (Eltech Engineers, India) and oxygen feed rate was varied from 1 to 4 L/min. Ozone was generated by an ozone generator (high voltage corona discharge ozonator, maximum ozone rate: 10 g/h, Eltech Engineers, India). Experiments using HC combined with ozone were performed at different feed rates of ozone varying from 1 to 5 g/h. The oxygen feed rate to the ozonator and the outlet volumetric flow rate of ozone oxygen gas mixture was 5 L/min. The weight percentage of ozone in the outlet ozone gas mixture was found to be in the range of 0.23 to 1.2 wt% for the ozone flow rates between 1 and 5 g/h and the rest accounted for oxygen. The gases (Air, oxygen, and ozone) were injected directly at the throat of slit venturi through a nozzle thereby exposing gases directly to the cavitation effect. For all the experiments related to HC in combination with gases, silicon antifoaming agent was used to settle down the foams during the treatment. Four different ratios of ferrous sulphate to H₂O₂ (1:1, 1:2, 1:5, and 1:10) were used to examine the combined effect of HC and Fenton's reagent on TOC, COD and color reduction of effluent. Fenton's reagents were added in to the solution from the top of HC reactor.

5.2.4 Analytical procedure

Total organic carbon (TOC) content of TDI effluent was measured using TOC analyzer (make: GE InnovOx). The COD of the effluent was estimated by standard open reflux titrimetric method [28]. Color was measured by UV/Vis-Spectrophotometer (Shimadzu-1800) at 964 nm. Total dissolved solids (TDS) were measured using ion meter (Model: ORION VERSA STAR 91). Total solids (TS) were determined by drying the effluent sample at 104°C in an oven (Make: DAIHAN Scientific Co. Ltd.). All experiments were studied in triplicate and the experimental errors were found to be within ±3% of the reported average values.

5.3 Results and discussion

5.3.1 Effect of operating inlet pressure

The inlet pressure and cavitation number are the two major parameters that affect the cavitation conditions inside the cavitating device and influencing the efficiency of HC system [15-17]. In order to investigate the effect of inlet pressure on the treatment of TDI effluent, experiments were performed by varying inlet pressure from 3 to 10 bar. The obtained results are shown in Figure 5.1 and Table 5.2. Table 5.3 presents the cavitation number, velocity, and flow rate through cavitating device. It was observed that TOC and

Chapter 5: Treatment of textile dyeing industry effluent using hydrodynamic cavitation in combination with advanced oxidation reagents

COD reduction increased with an increase in the inlet pressure from 3 bar to an optimum value of 5 bar ($C_v = 0.07$), beyond which TOC and COD reduction decreased. An increase in TOC and COD reduction rate with an increase in inlet pressure or decrease in cavitation number may be attributed to the fact that more cavities are formed at higher inlet pressure leading to the generation of more $\cdot\text{OH}$ radicals. However at inlet pressure i.e. beyond an optimum pressure, choked cavitation (condition of cavity cloud formation) takes place which reduces the cavitation intensity due to coalescence of cavities [15, 17]. Maximum percentage reduction in TOC, COD and color was found to be almost 17%, 12% and 25% respectively at an optimum inlet pressure of 5 bar in 120 min. The percentage TOC and COD reduction was only 9.3% and 3.5% respectively at 10 bar operating pressure. Pseudo-first order kinetics was fitted in to the TOC data to find the mineralization rate constants. It was observed that the mineralization rate constant enhanced from $1.7 \times 10^{-3} \text{ min}^{-1}$ to $2.0 \times 10^{-3} \text{ min}^{-1}$ with an increase in pressure from 3 to 5 bar and decreased thereafter. This study clearly indicated that there was no significant reduction in TOC, COD, and color beyond an optimum pressure. Therefore, inlet pressure in HC system was kept at 5 bar for all the remaining sets of experiments. Similar trends were reported in the literature for the degradation of synthetic dyes wastewater by other authors [25-26, 29]. Patil et al. [29] reported an optimum pressure of 4 bar using slit venturi in HC for the degradation of imidacloprid whereas Gogate and Bhosale [26] reported an optimum pressure of 5 bar using 2 mm circular hole orifice plate in HC for the degradation of orange acid II dye.

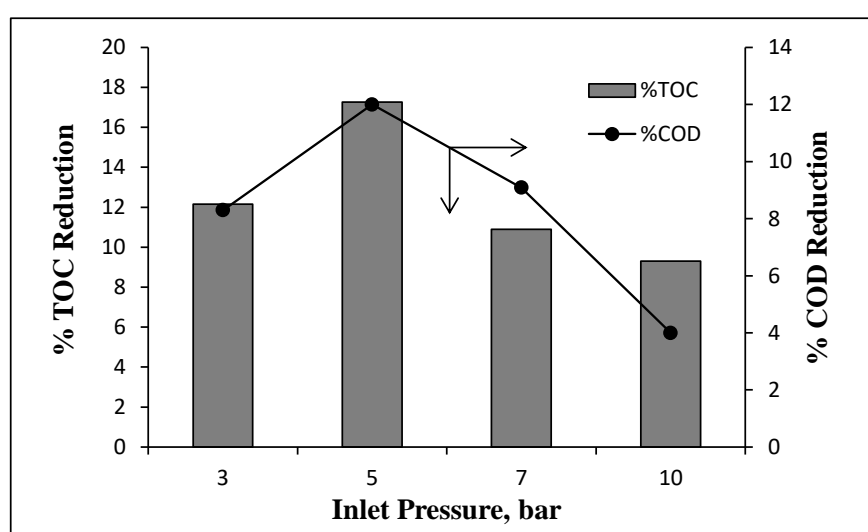


Figure 5.1: Effect of inlet pressure on TOC and COD reduction of TDI effluent using HC alone (Conditions: solution volume, 6 L; pH, 6.8; treatment time, 120 min)

Chapter 5: Treatment of textile dyeing industry effluent using hydrodynamic cavitation in combination with advanced oxidation reagents

Table 5.2: Effect of inlet pressure on TOC and COD reduction of TDI effluent

Inlet pressure (bar)	TOC, mg/L			COD, mg/L		
	Initial	Final	% TOC reduction	Initial	Final	% COD reduction
3	790	694	12.15	3840	3520	8.3
5	880	729	17.15	4000	3520	12.0
7	685	610	10.9	3520	3200	9.09
10	610	553	9.3	4480	4300	4.0

Table 5.3: Hydrodynamic characteristics and cavitation number of the experimental setup

Pressure (bar)	Flow rate through cavitating device (LPH)	Velocity (m/s)	Cavitation number (C_v)
3	518	45.86	0.092
5	592	52.55	0.070
7	631	55.74	0.062
10	695	61.48	0.051

5.3.2 Effect of dilution on TOC and COD reduction

The effect of dilution of TDI effluent on TOC and COD reduction was investigated using HC at an optimum inlet pressure of 5 bar. TDI effluent samples were diluted using tap water in various proportions such as 25%, 50%, and 75% dilution (% V/V). The observed values for TOC and COD reduction are shown in Table 5.4. The total amount of COD and TOC removed (mg/L) decreased with an increase in the dilution from 0 to 75%. It can be seen from Table 5.4 that maximum quantum of TOC and COD reduction was found to be 151 mg/L and 480 mg/L respectively for samples with no dilution. Whereas, only 61 mg/L of TOC and 160 mg/L of COD was reduced for the 75% diluted effluent. Since the rate of degradation is proportional to the TOC and COD values, the COD and TOC removal rate decreased with increase in dilution ratios. Therefore, it can be concluded that dilution of TDI effluent is not an economical option for the treatment of TDI effluent using HC. Moreover, large amount of water is required for dilution. Based on the above results, experiments were further performed with no dilution at an optimum inlet pressure of 5 bar. It had been reported that the rate of degradation of pollutant under the effect of HC

Chapter 5: Treatment of textile dyeing industry effluent using hydrodynamic cavitation in combination with advanced oxidation reagents

followed first order kinetics and therefore higher initial concentration of the pollutant gave higher degradation rate [16, 23, 29-30]. Raut-Jadhav et al. [22] investigated the effect of dilution on the treatment of pesticide industrial wastewater using HC. They concluded that dilution had no significant effect on the degradation of wastewater using HC.

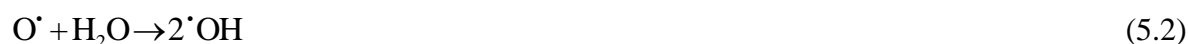
Table 5.4: Effect of dilution on TOC and COD reduction of TDI effluent

% dilution	Initial TOC, mg/L	Total quantum of TOC reduced, mg/L	% TOC reduction	Initial COD, mg/L	Total quantum of COD reduced, mg/L	% COD reduction
0 % dilution	880	151	17.2	4000	480	12.0
25 % dilution	610	113	18.5	2400	320	13.3
50 % dilution	521	102	19.6	1480	240	16.2
75 % dilution	245	61	24.9	690	160	23.3

(Conditions: solution volume, 6 L; pH, 6.8; pressure, 5 bar; treatment time, 120 min)

5.3.3 Treatment of TDI effluent using HC coupled with oxygen

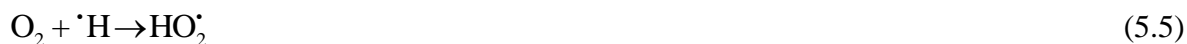
The addition of oxygen (oxidation potential of 1.23 eV) in the presence of HC was used to intensify the mineralization/decolorization of TDI effluent. Oxygen can react with H₂O molecule under cavitating conditions to form two hydroxyl ([•]OH) radicals per molecule of oxygen as shown in equations ((5.1)-(5.2)) [31-33].



These extra [•]OH radicals can intensify the efficiency of HC system. In addition to the above two reactions, oxygen molecule can also react with [•]H radicals (generated via dissociation of H₂O molecule) to give [•]OH and HO₂[•] radicals as shown in the following equations (5.4) and (5.5).



Chapter 5: Treatment of textile dyeing industry effluent using hydrodynamic cavitation in combination with advanced oxidation reagents



In order to study the combined effect of HC and oxygen on the TOC, COD and color reduction of TDI effluent, experiments were performed at an optimum inlet pressure of 5 bar. Oxygen flow rate was varied in the range of 1 to 4 L/min. The obtained results are given in Figure 5.2 and Table 5.5. It was observed that the extent of TOC, COD and color reduction increased with an increase in the oxygen flow rate from 1 to 2 L/min and decreased with a further increase in the oxygen flow rate to 4 L/min. HC combined with oxygen was found to be more effective as compared to the individual processes. The rate constant of $2.0 \times 10^{-3} \text{ min}^{-1}$ (17.27% TOC reduction) obtained using only HC was significantly enhanced to $6.3 \times 10^{-3} \text{ min}^{-1}$ (48.05% TOC reduction) using HC in combination with 2 L/min of oxygen. COD and color reduction at this condition was found to be 33.3 % and 62.11% respectively. Also, total quantum of TOC reduction was enhanced from 151 mg/L obtained using HC alone to 568 mg/L obtained using HC combined with oxygen (2 L/min). Lower extent of TOC, COD, and color reduction at higher loading of oxygen may be attributed to the fact that flooding of the downstream section of the venturi with gas bubbles at high gas flow rate dampens the cavitation activity and thereby reduced the degradation efficiency. In addition to this, beyond an optimum oxygen flow rate, $\cdot\text{OH}$ radicals are scavenged by O_2 itself (equation 5.6) and thus result in lower efficiency of HC system [32-33]. In order to examine the effect of air on the TOC, COD and color reduction of TDI effluent, one experiment was also conducted using HC in the presence of air (1.5 L/min). The atmospheric air was sucked in to the throat of slit venturi where pressure was lower than the atmospheric pressure. It can be seen from Figure 5.2 that TOC, COD, and color were almost reduced by 23.8%, 17.39%, and 28.18% respectively which were slightly higher than that obtained using HC alone. It can be seen that pure oxygen is more beneficial than atmospheric air when used in combination with HC for the treatment of TDI effluent.

Chapter 5: Treatment of textile dyeing industry effluent using hydrodynamic cavitation in combination with advanced oxidation reagents

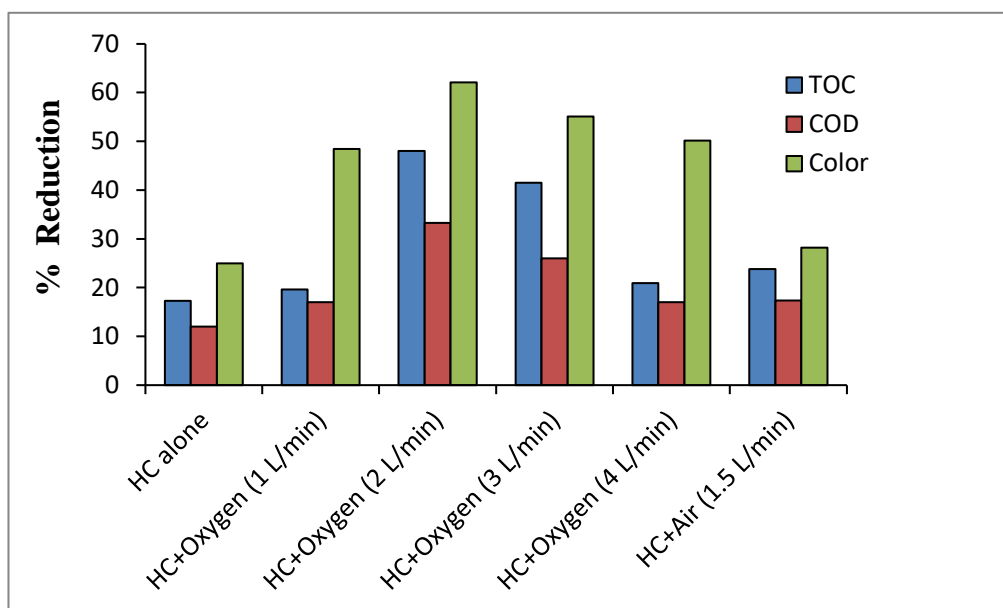


Figure 5.2: Effect of addition of oxygen on the TOC, COD and color reduction of TDI effluent (Conditions: solution volume, 6 L; pH, 6.8; pressure, 5 bar; treatment time, 120 min)

Table 5.5: Effect of addition of oxygen on the TOC, COD and color reduction of TDI effluent

Process	Oxygen flow rate (L/min)	TOC, mg/L			COD, mg/L			% Color reduction
		Initial	Final	%TOC reduction	Initial	Final	%COD reduction	
HC alone	-	880	729	17.15	4000	3520	12.0	25.0
HC + Air (1.5 L/min)	-	768	585	23.82	3680	3040	17.39	28.18
HC + Oxygen	1	1146	921	19.63	3840	3180	17.1	48.46
	2	1182	614	48.05	3840	2560	33.3	62.11
	3	1069	625	41.53	3600	2662	26.0	55.07
	4	907	717	20.94	2720	2240	17.6	50.16

5.3.4 Treatment of TDI effluent using HC coupled with ozone

In order to investigate the combined effect of HC and O₃, experiments were conducted at an optimum inlet pressure of 5 bar and solution pH of 6.8. Ozone feed rates were varied from 1 to 5 g/h to achieve the optimum feed rate of ozone. Ozone was injected at the throat of venturi in order to directly expose it to the cavitation effects. The obtained results are given

Chapter 5: Treatment of textile dyeing industry effluent using hydrodynamic cavitation in combination with advanced oxidation reagents

in Figure 5.3 and Table 5.6. It was observed that the extent of TOC and COD reduction increased with an increase in ozone feed rate up to 3 g/h and then decreased. It should be noted here that color of TDI effluent was reduced to almost 88% at 3 g/h ozone feed rate and remained constant thereafter. This may be attributed to higher mass transfer rate of ozone and higher number of $\cdot\text{OH}$ radicals generated in the presence of HC [17]. The combined treatment (HC+O₃) resulted in almost 48% TOC reduction with a rate constant of $6.4 \times 10^{-3} \text{ min}^{-1}$ and 22.72% COD reduction at 3 g/h ozone feed rate in 120 min whereas HC alone gave only 17% TOC reduction with a rate constant of $2.0 \times 10^{-3} \text{ min}^{-1}$ and 12% COD reduction under the optimized conditions. The mineralization rate constants obtained using HC combined with ozone were found to be almost 3.2 times higher than that obtained using HC alone. The effectiveness of combined HC and ozone for ozone injection directly into a tank was also studied. Almost 41% TOC and 12% COD reduction was achieved for the case of ozone injected in the solution tank which was lower than that obtained by injecting ozone at the throat of venturi. Higher reduction in TOC and COD in the case of ozone injection at the throat of slit venturi may be due to three reasons: 1) Ozone molecules were directly exposed to the cavitating conditions and thereby increased generation of $\cdot\text{OH}$ radicals, 2) Turbulence created in the downstream of a cavitating device improved the dispersion of ozone molecules into the solution, and 3) Higher contact time between the ozone and pollutant molecules in the process line between the cavitating device and storage tank increased its reactivity. The degradation reaction mechanism of the combined process of HC and ozone has been explained in Chapter 2 (Section 2.3.6).

The study of ozone alone as an oxidation agent without cavitation was also carried out at the optimized feed rate of O₃ (3 g/h) to compute the synergetic coefficient of the hybrid process. During the experimentation using ozone alone, the ozone gas was directly introduced into the storage tank which was filled with the desired volume (6 L) of TDI effluent. The main pipe line consisting of slit venturi was closed and solution was circulated through the bypass line in the reactor setup. The samples were taken at a regular time interval and analyzed for COD and TOC. It can be seen from Figure 5.3 that 20.14% TOC reduction with a first order rate constant of $2.5 \times 10^{-3} \text{ min}^{-1}$ was obtained using 3 g/h ozone feed rate. Almost 75% color and 15% COD was reduced at the same ozone feed rate. Mineralization rate constant ($6.4 \times 10^{-3} \text{ min}^{-1}$) for the HC coupled with ozone was found to be higher than that obtained for the case

Chapter 5: Treatment of textile dyeing industry effluent using hydrodynamic cavitation in combination with advanced oxidation reagents

of ozone alone ($2.5 \times 10^{-3} \text{ min}^{-1}$) and only HC alone ($2.0 \times 10^{-3} \text{ min}^{-1}$). Synergetic coefficient of coupling HC with ozone can be calculated using following equation (5.7).

$$\begin{aligned} \text{Synergetic coefficient} &= \frac{k_{(HC+O_3)}}{k_{HC} + k_{O_3}} \quad (5.7) \\ &= 6.4 \times 10^{-3} / (2.0 \times 10^{-3} + 2.5 \times 10^{-3}) \\ &= 1.42 \end{aligned}$$

The synergetic coefficient for this hybrid process was found to be 1.42 indicating the synergetic effect of the combined process. Raut-Jadhav et al. [22] investigated the treatment of the pesticide industry effluent using HC in combination with H_2O_2 and ozone with a circular venturi as the cavitating device. They reported 36.26% COD reduction with a rate constant of $3.45 \times 10^{-3} \text{ min}^{-1}$ and 26.20% TOC reduction with a rate constant of $2.48 \times 10^{-3} \text{ min}^{-1}$ using HC+ O_3 (3 g/h) whereas 15% COD and 6.58% TOC reduction using HC alone.

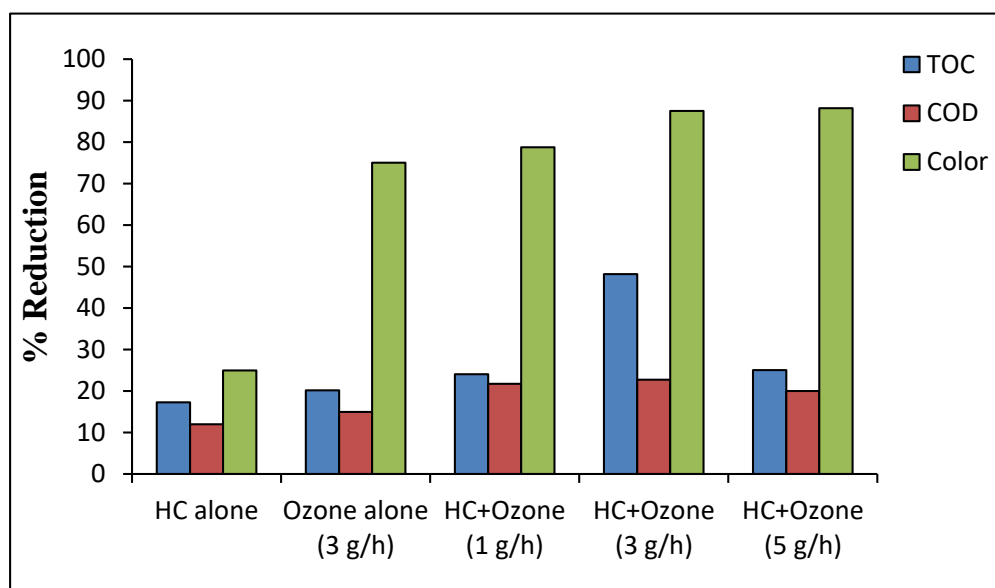


Figure 5.3: Effect of addition of ozone on the TOC, COD and color reduction of TDI effluent (Conditions: solution volume, 6 L; pH, 6.8; pressure, 5 bar; treatment time, 120 min)

Chapter 5: Treatment of textile dyeing industry effluent using hydrodynamic cavitation in combination with advanced oxidation reagents

Table 5.6: Effect of ozone addition on the TOC, COD and color reduction of TDI effluent

Process	flow rate of ozone (g/h)	TOC, mg/L			COD, mg/L			% Color reduction
		Initial	Final	%TOC reduction	Initial	Final	%COD reduction	
HC alone	-	880	729	17.15	4000	3520	12.0	25.0
Ozone alone	3	713	569	20.19	2880	2435	15.45	75.0
HC + Ozone	1	774	588	24.03	3680	2880	21.73	78.77
	3	863	447	48.2	3520	2720	22.72	87.54
	5	775	581	25.03	3200	2560	20.0	88.22

5.3.5 Treatment of TDI effluent using HC coupled with Fenton's reagent

It has been reported that Fenton's reagent in combination with HC was found to be a more effective process for treating the wastewater containing bio-refractory pollutants [16, 19]. Initially the effect of H₂O₂ (dose: 5 ml/L) in combination with HC on the treatment of TDI effluent was investigated and found that it was incapable of decolorizing and mineralizing the TDI effluent because of the large complex dye molecules. This may be due to the scavenging effect of H₂O₂ which may be overcome by adding Fenton's reagent for degradation.

In this study using HC+Fenton's reagent, 5 mL of H₂O₂ per liter of effluent solution was used. The calculated amount of FeSO₄.7H₂O was added according to different ratios of FeSO₄.7H₂O:H₂O₂ (1:1, 1:2, 1:5, and 1:10). The obtained results are depicted in Table 5.7. It was observed that the extent of mineralization increased with an increase in the ratio of Fe²⁺:H₂O₂. Maximum 48% TOC reduction was obtained in just 15 min at an optimum ratio (Fe²⁺:H₂O₂) of 1:5. It has been observed that the extent of mineralization (TOC reduction) increased from 28.5% to 48.4% with an increase in the ratio of Fe²⁺:H₂O₂ from 1:1 to 1:5 and then decreased. At the optimized loading of Fenton's reagent, almost complete decolorization (97.7%) was achieved in 60 min whereas almost 38% COD was removed in 120 min. Figure 5.4 shows the difference in the color of TDI effluent after the treatment using HC combined with Fenton process. The reactions during the process of HC coupled with Fenton's reagent have been explained in earlier chapter 3 (Section 3.3.8). An experiment was also carried out using Fenton reagent alone at an optimum ratio of FeSO₄.7H₂O:H₂O₂ (1:5) to distinguish the synergetic effect of the combined process. It was observed that 10.9% TOC reduction with

Chapter 5: Treatment of textile dyeing industry effluent using hydrodynamic cavitation in combination with advanced oxidation reagents

mineralization rate constant of $8.3 \times 10^{-3} \text{ min}^{-1}$ was achieved using Fenton alone. Synergetic coefficient was found to be 2.48 indicating that the synergetic effect can be easily established for this combined process. Chakinala et al. [24] investigated the treatment of industrial effluent using HC coupled with heterogeneous Fenton oxidation. In their study, they used zero-valent iron as a catalyst. They found that about 60% and 40% TOC reduction was obtained using HC in the presence of iron pieces and copper windings on iron pieces respectively in 150 min. A similar observation was also made by Raut-Jadhav et al. [34]. They reported that the degradation rate of imidacloprid increased significantly with an increase in the ratio of $\text{Fe}^{2+}:\text{H}_2\text{O}_2$. Almost 6% degradation of imidacloprid was obtained using HC alone whereas almost complete degradation (97.77%) was achieved by applying the combination of HC and Fenton process ($\text{Fe}^{2+}:\text{H}_2\text{O}_2$ as 1:40).

Table 5.7: Effect of addition of Fenton's reagent on the TOC, COD and color reduction of TDI effluent

Process	Ratios of $\text{FeSO}_4 \cdot 7\text{H}_2\text{O}:\text{H}_2\text{O}_2$	% TOC reduction in 15 min	% COD reduction in 120 min	% Color reduction in 60 min
Fenton	1:5	10.9	9.5	59.9
HC+Fenton	1:1	28.5	22.7	90.1
	1:2	39.4	26.1	92.6
	1:5	48.4	38.1	97.7
	1:10	35.2	31.2	91.7

(Conditions: solution volume, 6 L; pH, 6.8; pressure, 5 bar)



Figure 5.4: Physical appearance of TDI effluent (a) before and (b) after 60 min treatment using HC combined with Fenton's reagent

5.3.6 Characteristics of treated TDI effluent obtained from different processes

The characteristics of treated TDI effluent from all processes at their optimized conditions were also evaluated in the present work. The obtained results are given in Table 5.8. All hybrid methods used in the current study provided greater reduction efficiencies in terms of TOC, COD and color reduction than with HC alone. It was observed that the combined process of HC and Fenton's reagent gave highest TOC and COD reduction as compared to others. Almost complete decolorization (97.7%) was obtained in 60 min using this combined process. It can be seen from Table 5.8 that the maximum removal in TS and TDS was found to be as 64.4% and 51.1% using HC+Fenton which is almost 6.1 and 6.7 times higher than that obtained using HC alone. The reduction in TS using HC+Fenton is due to two mechanisms i.e. 1) Reduction in TDS due to the oxidation of organic pollutants by the $\cdot\text{OH}$ radicals, 2) Reduction in TSS due to precipitation by the FeSO_4 coagulant. However, the combined process of HC and Fenton may not be economical on an industrial level due to the additional loading of reagents (ferrous sulphate and hydrogen peroxide). In addition to this, separation of unreacted ferrous ions and H_2O_2 would affect the overall economics of a wastewater treatment. However, the hybrid processes of HC in combination with gaseous additives i.e. oxygen, air and ozone do not require any extra chemicals and these processes may be cheaper as compared to HC+Fenton for the treatment of real industrial effluent at an industrial scale. The maximum permissible limits for COD and TDS are reported as 250

Chapter 5: Treatment of textile dyeing industry effluent using hydrodynamic cavitation in combination with advanced oxidation reagents

mg/L and 2100 mg/L respectively as per Rajasthan pollution control board regulations. The TDS of the treated TDI effluent was found to be well below the permissible limit. However, the COD of the treated TDI effluent is significantly higher than the permissible limit and therefore will require further treatment using conventional biological treatment process.

Table 5.8: Comparison of the characteristics of TDI effluent for all processes at the optimized conditions

Parameters		Process			
		HC alone	HC+O ₂	HC+O ₃	HC+Fenton
%TOC reduction		17.2	48.1	48.2	48.4
Rate constant for TOC reduction, k x 10 ³ , min ⁻¹		2.0	6.3	6.4	41.8
%COD reduction		12.0	33.3	22.7	38.1
Rate constant for COD reduction, k x 10 ³ , min ⁻¹		2.5	2.9	3.1	4.3
%Color reduction		24.8	62.1	88.1	97.7
TDS, mg/L	Initial	2935	2089	1973	3291
	Final	2689	1757	1526	1612
% TDS reduction		8.4	15.9	22.6	51.1
TS, mg/L	Initial	5569	3556	3926	4277
	Final	5032	2941	2867	1523
% TS reduction		9.6	17.3	26.9	64.4

5.4 Novelty of the work

- Treatment of real textile dyeing industry (TDI) effluent using hydrodynamic cavitation based hybrid methods has been reported for the first time which highlights the potential of hydrodynamic cavitation for the treatment of such effluents on an industrial scale.

5.5 Summary of the chapter

The present work reports the effective use of HC in combination with advanced oxidative reagents such as air, oxygen, ozone and Fenton's reagent to reduce TOC, COD and color of

Chapter 5: Treatment of textile dyeing industry effluent using hydrodynamic cavitation in combination with advanced oxidation reagents

the TDI effluent. The efficiency of HC reactor is affected by process parameters such as inlet pressure and dilution. Maximum reduction in TOC, COD, and color were 17.27%, 12%, and 25% respectively using HC alone at 5 bar operating inlet pressure. The dilution study did not show any significant impact on the actual quantum of pollutant degraded. All combined treatment approaches i.e. HC+O₂, HC+O₃, and HC+Fenton exhibited higher TOC, COD, and color reduction as compared to that obtained using HC alone. Among all the hybrid approaches used in the present study, HC in combination with Fenton's reagent gave highest percentage reduction in TOC, COD, and color. Almost complete decolorization (97.7%) was achieved using this combined strategy (HC+Fenton) along with 48% and 38% reduction in TOC and COD respectively. Overall, it is understood that HC based hybrid processes may be a better option for the treatment of TDI effluent.

References

1. Advance methods for treatment of textile industry effluents, Resource Recycling Series, Central Pollution Control Board, India, 2007.
2. H. Zollinger, Synthesis, Properties of Organic Dyes and Pigments, In: Color Chemistry, VCH Publishers, New York, 1987, pp. 92-102.
3. T. Robinson, G. McMullan, R. Marchant, P. Nigam, Remediation of dyes in textile effluent: a critical review on current treatment technologies with a proposed alternative, *Bioresour. Technol.* 77(3) (2001) 247-255.
4. M. Kobya, O.T. Can, M. Bayramoglu, Treatment of textile wastewaters by electrocoagulation using iron and aluminum electrodes, *J. Hazard. Mater.* 100 (2003) 163-178.
5. S.H. Lin, M.L. Chen, Treatment of textile wastewater by electrochemical methods for reuse, *Water Res.* 31 (1997) 868–876.
6. S.H. Lin, C.F. Peng, Treatment of textile wastewater by electrochemical method, *Water Res.* 28 (1994) 277–282.
7. P. Nigam, G. Armour, I.M. Banat, D. Singh, R. Marchant, Physical removal of textile dyes and solid state fermentation of dyeadsorbed agricultural residues, *Bioresour. Technol.* 72 (2000) 219–226.
8. S. Wijetunga, X.F. Li, C. Jian, Effect of organic load on decolourization of textile wastewater containing acid dyes in upflow anaerobic sludge blanket reactor, *J. Hazard. Mater.* 177 (2010) 792-798.

9. Y.M. Slokar, A.M.L. Marechal, Methods of decoloration of textile wastewaters, *Dye Pigments*. 37 (1998) 335–356
10. O'Neill, Cliona, F.R. Hawkes, S.R.R. Esteves, D.L. Hawkes, S.J. Wilcox, Anaerobic and aerobic treatment of a simulated textile effluent, *J. Chem. Technol. Biotechnol.* 74 (1999) 993-999.
11. V.K. Gupta, I. Ali, T.A. Saleh, A. Nayak, S. Agarwal, Chemical treatment technologies for waste-water recycling-an overview, *Rsc Adv.* 2, (2012) 6380-6388.
12. S.F. Kang, C.H. Liao, M.C. Chen, Pre-oxidation and coagulation of textile wastewater by the Fenton process, *Chemosphere*, 46 (2002) 923-928.
13. A.G. Vlyssides, M. Loizidou, P.K. Karlis, A.A. Zorpas, D. Papaioannou, Electrochemical oxidation of a textile dye wastewater using a Pt/Ti electrode, *J. Hazard. Mater.* B70 (1999) 41–52
14. V.K. Saharan, M.P. Badve, A.B. Pandit, Degradation of Reactive Red 120 dye using hydrodynamic cavitation, *Chem. Eng. J.* 178 (2011) 100–107
15. S. Rajoriya, S. Bargole, V.K. Saharan, Degradation of a cationic dye (Rhodamine 6G) using hydrodynamic cavitation coupled with other oxidative agents: reaction mechanism and pathway, *Ultrason. Sonochem.* 34 (2017) 183–194.
16. S. Rajoriya, S. Bargole, V.K. Saharan, Degradation of reactive blue 13 using hydrodynamic cavitation: Effect of geometrical parameters and different oxidizing additives, *Ultrason. Sonochem.* 37 (2017) 192-202.
17. S. Rajoriya, J. Carpenter, V.K. Saharan, A.B. Pandit, Hydrodynamic cavitation: an advanced oxidation process for the degradation of bio-refractory pollutants, *Rev. Chem. Eng.* 32 (2016) 379–411.
18. P.R. Gogate, M. Sivakumar, A.B. Pandit, Destruction of Rhodamine B using novel sonochemical reactor with capacity of 7.5 l, *Sep. Purif. Technol.* 34 (2004) 13-24.
19. N. Golash, P.R. Gogate, Degradation of dichlorvos containing wastewaters using sonochemical reactors, *Ultrason. Sonochem.* 19 (2012) 1051-1060.
20. M. Sivakumar, A.B. Pandit, Ultrasound enhanced degradation of Rhodamine B: optimization with power density, *Ultrason. Sonochem.* 8 (2001) 233-240.

Chapter 5: Treatment of textile dyeing industry effluent using hydrodynamic cavitation in combination with advanced oxidation reagents

21. K.V. Padoley, V.K. Saharan, S.N. Mudliar, R.A. Pandey, A.B. Pandit, Cavitationally induced biodegradability enhancement of a distillery wastewater, *J. Hazard. Mater.* 219 (2012) 69-74.
22. S. Raut-Jadhav, M.P. Badve, D.V. Pinjari, D.R. Saini, S.H. Sonawane, A.B. Pandit, Treatment of the pesticide industry effluent using hydrodynamic cavitation and its combination with process intensifying additives (H_2O_2 and ozone), *Chem. Eng. J.* 295 (2016) 326-335.
23. A.G. Chakinala, P.R. Gogate, A.E. Burgess, D.H. Bremner, Treatment of industrial wastewater effluents using hydrodynamic cavitation and the advanced Fenton process, *Ultrason. Sonochem.* 15 (2008) 49-54.
24. A.G. Chakinala, P.R. Gogate, A.E. Burgess, D.H. Bremner, Industrial wastewater treatment using hydrodynamic cavitation and heterogeneous advanced Fenton processing, *Chem. Eng. J.* 152 (2009) 498-502.
25. K.P. Mishra, P.R. Gogate, Intensification of degradation of Rhodamine B using hydrodynamic cavitation in the presence of additives, *Sep. Purif. Technol.* 75 (2010) 385–391.
26. P.R. Gogate, G.S. Bhosale, Comparison of effectiveness of acoustic and hydrodynamic cavitation in combined treatment schemes for degradation of dye wastewaters, *Chem. Eng. Process.* 71 (2013) 59–69.
27. B. Bethi, S.H. Sonawane, G.S. Rohit, C.R. Holkar, D.V. Pinjari, B.A. Bhanvase, A.B. Pandit, Investigation of TiO_2 photocatalyst performance for decolorization in the presence of hydrodynamic cavitation as hybrid AOP, *Ultrason. Sonochem.* 28 (2016) 150–160.
28. APHA, AWWA, WPCF, Standard Methods for the Examination of Water and Wastewater, 20th ed., American Public Health Association, Washington DC, 1998.
29. P.N. Patil, S.D. Bote, P.R. Gogate, Degradation of imidacloprid using combined advanced oxidation processes based on hydrodynamic cavitation, *Ultrason. Sonochem.* 21 (2014) 1770–1777.
30. X. Wang, Y. Zhang, Degradation of alachlor in aqueous solution by using hydrodynamic cavitation, *J. Hazard. Mater.* 161 (2009) 202–207.

31. T. Sivasankar, V.S. Moholkar, Physical insights into the sonochemical degradation of recalcitrant organic pollutants with cavitation bubble dynamics, *Ultrason. Sonochem.* 16 (2009) 769–781.
32. T. Sivasankar, V.S. Moholkar, Physical features of sonochemical degradation of nitroaromatic pollutants, *Chemosphere* 72 (2008) 1795–1806.
33. T. Sivasankar, V.S. Moholkar, Mechanistic approach to intensification of sonochemical degradation of phenol, *Chem. Eng. J.* 149 (2009) 57–69.
34. S. Raut-Jadhav, V.K. Saharan, D. Pinjari, S. Sonawane, D. Saini D, A. Pandit, Intensification of degradation of imidacloprid in aqueous solutions by combination of hydrodynamic cavitation with various advanced oxidation processes (AOPs). *J. Env. Chem. Eng.* 1 (2013) 850–857.

CHAPTER 6

Conclusions and Recommendations for Future Work

6.1 Conclusions

This research work establishes that hydrodynamic cavitation can be used for the efficient degradation of bio-refractory pollutants and hybrid HC techniques have the potential to be used as an effective treatment technology on an industrial scale. Process intensification has been achieved by combining HC with conventional oxidation processes as well as advanced oxidation processes. However, process parameters such as solution pH, initial concentration of pollutants, dosages of different oxidizing agents, inlet pressure, cavitation number etc. and the geometrical parameters of the cavitating devices which are specific to the chosen hybrid technique needs to be optimized in order to obtain the maximum degradation efficiency of organic pollutants. Following important conclusions can be drawn based on the present experimental work with respect to the different pollutant degradation/hybrid technique studied:

- The decolorization rate of Rh6G was influenced by the initial concentration of dye, solution pH, inlet pressure, and cavitation number using HC. The degradation mechanism was validated through the formation of H_2O_2 concentration in the HC system that confirmed that the $\cdot\text{OH}$ radicals were formed during cavitation. Hybrid treatment schemes such as HC in combination with H_2O_2 and ozone gave better degradation efficiency as compared to individual oxidation process under optimized conditions. A possible degradation pathway and reaction mechanism of Rh6G was proposed. Overall, the obtained results revealed that the combination of HC (slit venturi as a cavitating device) with ozone was a better technique to completely mineralize Rh6G.
- The efficiency of hydrodynamic cavitation is strongly influenced by the geometrical parameters such as α and β and operating parameters such as inlet pressure and cavitation number. Different orifice and venturi cavitating devices with circular and rectangular slits were studied to maximize the cavitation yield. It has been found that higher flow area is better for higher cavitation yield and for a given cross section area of throat it is always better to have higher throat perimeter for maximum degradation efficiency using HC. Amongst all the different cavitating devices, venturi having rectangular throat gave higher decolorization efficiency as compared to orifice plates and circular venturi. The combined HC and ozone was found to be best process for the decolorization and mineralization of RB13.

- Sm and N doped TiO₂ photocatalysts were synthesized using conventional and ultrasound assisted sol-gel processes. Doping of TiO₂ with Sm and N resulted in improved photocatalytic efficiencies due to the enhanced separation efficiency of photo-generated electron-hole ($e^- - h^+$) pair. Photocatalytic oxidation combined with HC was also demonstrated to be more energy efficient process for the degradation of 4-Acetamidophenol (4-AMP). Using LC-MS analysis, eight degradation by-products of 4-AMP during the combined process of HC and photocatalytic oxidation were determined, with three aromatic compounds and five aliphatic acids. This work has established that a novel combination of HC, UV and photocatalysts can be effectively applied for the treatment of wastewater containing persistent organic pollutants.
- The potential of HC based hybrid methods for the treatment of textile dyeing industry (TDI) effluent was explored for its industrial application. The TDI effluent characteristics were in the range of COD: 2560-4640 mg/L, TOC: 556-1184 mg/L, TS: 5569-7553 mg/L, TDS: 2395-4386 mg/L and pH: 6.8-7.0. It was observed that HC combined with advanced oxidation reagents such as Fenton's reagent, oxygen and ozone had the potential to treat the TDI effluent. Among the various hybrid approaches, HC in combination with Fenton's reagent gave the highest percentage reduction in TOC, COD, and color. Overall, this treatment technique was able to mineralize the complex molecules which are hard to degrade by conventional approaches and therefore HC based hybrid techniques can be used as a pretreatment tool prior to the conventional process in order to enhance the efficiency of overall treatment facility.

6.2 Recommendations for Future Work

In view of the potential of the HC technique for treating the bio-refractory pollutants present in wastewater and its application on an industrial scale, some of the recommendations for future work are in the following:

- Current studies are focused on using orifice and venturi based HC reactor for wastewater treatment. More studies need to be conducted to maximize the cavitation events occurring inside the cavitating device by designing the orifice plates with multiple holes (approximately 100 holes with perimeter to throat area ratio greater than 10) in order to increase the HC efficiency.
- New simulators may be developed to represent HC reactors where one can see the effect of various geometrical and operating parameters and physico-chemical properties of the

wastewater under consideration on the degradation efficiency, which will be helpful for engineers in designing HC reactors.

- New design configurations for continuous operations on a large scale may be developed for these batch hybrid techniques such as HC+Fenton, HC+Ozone and HC+Photocatalyst so that they can be effectively utilized on an industrial scale. More studies will also be required using hybrid flow cells or semi batch reactors while operating advanced oxidation processes using a sequential or simultaneous approach for the process operation.
- Few studies report that HC is efficient when used as a pretreatment technology prior to the conventional biological treatment processes. It would be worthwhile to study the different type of hybrid HC reactors as a pretreatment tool to the biological treatment process at a pilot plant scale for the different types of industrial wastewater. This would help in understanding the effect of HC pretreatment on the efficiency of biological treatment process and data thus generated would be helpful in designing HC reactor for the existing common effluent treatment plant.
- The combination of HC with AC with simultaneous approach can also be tried to create intensive cavitation effects which might be promising for the treatment of wastewater in the future.

Sunil Rajoriya, Jitendra Carpenter, Virendra Kumar Saharan* and Aniruddha B. Pandit

Hydrodynamic cavitation: an advanced oxidation process for the degradation of bio-refractory pollutants

DOI 10.1515/revce-2015-0075

Received December 14, 2015; accepted February 11, 2016; previously published online March 25, 2016

Abstract: In recent years, water pollution has become a major problem for the environment and human health due to the industrial effluents discharged into the water bodies. Day by day, new molecules such as pesticides, dyes, and pharmaceutical drugs are being detected in the water bodies, which are bio-refractory to microorganisms. In the last two decades, scientists have tried different advanced oxidation processes (AOPs) such as Fenton, photocatalytic, hydrodynamic, acoustic cavitation processes, etc. to mineralize such complex molecules. Among these processes, hydrodynamic cavitation (HC) has emerged as a new energy-efficient technology for the treatment of various bio-refractory pollutants present in aqueous effluent. In this review, various geometrical and operating parameters of HC process have been discussed emphasizing the effect and importance of these parameters in the designing of HC reactor. The advantages of combining HC with other oxidants and AOPs such as H_2O_2 , ozone, Fenton process, and photocatalytic process have been discussed with some recommendation for large-scale operation. It has been observed that the geometry of the HC device and other operating parameters such as operating pressure and cavitation number are the key design parameters that ultimately decide the efficacy and potentiality of HC in degrading bio-refractory pollutants on an industrial scale.

Keywords: cavitation number; cavitation yield; hybrid methods; hydrodynamic cavitation; industrial wastewater treatment.

1 Introduction

The treatment of wastewater containing bio-refractory pollutants (which have the tendency to resist the conventional biological treatment) from various industries has been a major environmental problem. Water is being polluted by industrial and commercial actions, agricultural practices, and day-to-day human activities. Human health is affected by water pollution typically due to the contamination of drinking water from waste streams. Several industries such as pesticides, dyes, textiles, and many other industries are continuously polluting water as they contain large quantities of organic pollutants. These organic molecules are bio-refractory or very toxic to microorganisms. Hence, conventional biological methods are not capable of completely degrading such complex compounds due to high toxicity and carcinogenicity (Saharan et al. 2011, 2013). In the past years, many researchers have developed various methods for the degradation of organic pollutants such as carbon bed adsorption, biological methods, oxidation using chlorination and ozonation, electrochemical methods, membrane processes, and many other advanced oxidation processes (AOPs) (Mrowetz et al. 2003, Gogate and Pandit 2005, Martin et al. 2008, Rajoriya and Kaur 2014, Secondes et al. 2014, Dai et al. 2015). Most of the AOPs such as Fenton process, photocatalytic, hydrodynamic, and acoustic cavitation (AC) have been established in research laboratories effectively, but several challenges are faced by many industries to scale them up. In general, AOPs are a set of processes that involve the generation of highly reactive and non-selective hydroxyl radicals ($\cdot OH$), which have high oxidation potential (2.80 eV) and are capable of oxidizing toxic organic/inorganic compounds and non-biodegradable pollutants (Behnajady et al. 2008a, Mendez-Arriaga et al. 2009, Wang and Zhang 2009, Bagal and Gogate 2012). Among all the AOPs, hydrodynamic cavitation (HC) process is found to improve the treatment ability to a greater extent and gives better energy efficiency for the removal/degradation of bio-refractory pollutants on an industrial

*Corresponding author: Virendra Kumar Saharan, Department of Chemical Engineering, MNIT, Jaipur-302017, India, e-mail: vksaharan.chem@mnit.ac.in

Sunil Rajoriya and Jitendra Carpenter: Department of Chemical Engineering, MNIT, Jaipur-302017, India

Aniruddha B. Pandit: Chemical Engineering Department, Institute of Chemical Technology, Matunga, Mumbai-400019, India

Jitendra Carpenter, Mandar Badve, Sunil Rajoriya, Suja George, Virendra Kumar Saharan* and Aniruddha B. Pandit

Hydrodynamic cavitation: an emerging technology for the intensification of various chemical and physical processes in a chemical process industry

DOI 10.1515/revce-2016-0032

Received July 13, 2016; accepted September 12, 2016; previously published online December 20, 2016

Abstract: Hydrodynamic cavitation (HC) has been explored by many researchers over the years after the first publication on hydrolysis of fatty oils using HC was published by Pandit and Joshi [Pandit AB, Joshi JB. Hydrolysis of fatty oils: effect of cavitation. Chem Eng Sci 1993; 48: 3440–3442]. Before this publication, most of the studies related to cavitation in hydraulic system were concentrated to avoid the generation of cavities/cavitating conditions. The fundamental concept was to harness the energy released by cavities in a positive way for various chemical and mechanical processes. In HC, cavitation is generated by a combination of flow constriction and pressure-velocity conditions, which are monitored in such a way that cavitating conditions will be reached in a flowing system and thus generate hot spots. It allows the entire process to operate at otherwise ambient conditions of temperature and pressure while generating the cavitating conditions locally. In this review paper, we have explained in detail various cavitating devices and the effect of geometrical and operating parameters that affect the cavitation conditions. The optimization of different cavitating devices is discussed, and some strategies have been suggested for designing these devices for different applications. Also, various applications of HC such as wastewater treatment, preparation of nanoemulsions, biodiesel synthesis, water disinfection, and nanoparticle synthesis were discussed in detail.

Keywords: biodiesel synthesis; hydrodynamic cavitation; microbial cell disruption; nanomaterials; wastewater treatment.

*Corresponding author: Virendra Kumar Saharan, Department of Chemical Engineering, Malaviya National Institute of Technology, Jaipur 302017, India, e-mail: vksaharan.chem@mnit.ac.in

Jitendra Carpenter, Sunil Rajoriya and Suja George: Department of Chemical Engineering, Malaviya National Institute of Technology, Jaipur 302017, India

Mandar Badve and Aniruddha B. Pandit: Department of Chemical Engineering, Institute of Chemical Technology, Mumbai 400019, India

1 Introduction

In the last decade, cavitation technique has been extensively studied, and it has been successfully applied for the various physical, chemical, and biological processes. This novel technique not only produces the desirable transformation but also reduces the total processing cost and is found to be more energy efficient than many other conventional techniques. Cavitation offers immense potential for the intensification of various physical and chemical processes in an energy efficient manner (Gogate and Kabadi 2009).

Cavitation is defined as a phenomenon of formation, growth, and collapse of microbubbles or cavities, occurring in a few milli- to microseconds at multiple locations in the reactor and thus releases large magnitude of energy in a short span of time (Mahulkar and Pandit 2010). Cavitation is initiated with the formation of vapor cavities (bubbles or voids) when liquid enters into the low-pressure region, and subsequently these cavities attain a maximum size under the conditions of isothermal expansion. In the successive compression cycle, an immediate adiabatic collapse occurs, resulting in the formation of supercritical state of high local temperature and pressure, known as hot spot. The chemical and physical transformations required for the process occur because of these intense temperature and pressure conditions that are generated in these hot spots. The mechanical or physical effects of cavitation, such as the microjet streaming and high-intensity local turbulence, are mainly responsible for the intensification of physical processes such as synthesis of nanoemulsion, nanoparticle formation, microbial disruption, and disinfection. By contrast, its chemical effects, such as the generation of highly reactive free radicals in the aqueous environment, are mainly responsible for the intensification of chemical processes such as synthesis of chemicals, degradation of the water pollutants, etc.

Cavitation can be generated in a liquid medium either through flow variation in a flowing liquid known as hydrodynamic cavitation (HC) or by passing ultrasonic waves through the liquid known as acoustic



Degradation of a cationic dye (Rhodamine 6G) using hydrodynamic cavitation coupled with other oxidative agents: Reaction mechanism and pathway



Sunil Rajoriya, Swapnil Bargole, Virendra Kumar Saharan*

Chemical Engineering Department, Malaviya National Institute of Technology, Jaipur 302017, India

ARTICLE INFO

Article history:

Received 1 April 2016

Received in revised form 15 May 2016

Accepted 18 May 2016

Available online 20 May 2016

Keywords:

Rhodamine 6G

Hydrodynamic cavitation

Circular and slit venturi

Intensification

Ozonation

Hydrogen peroxide

ABSTRACT

In the present study, decolorization and mineralization of a cationic dye, Rhodamine 6G (Rh6G), has been carried out using hydrodynamic cavitation (HC). Two cavitating devices such as slit and circular venturi were used to generate cavitation in HC reactor. The process parameters such as initial dye concentration, solution pH, operating inlet pressure, and cavitation number were investigated in detail to evaluate their effects on the decolorization efficiency of Rh6G. Decolorization of Rh6G was marginally higher in the case of slit venturi as compared to circular venturi. The kinetic study showed that decolorization and mineralization of the dye fitted first-order kinetics. The loadings of H₂O₂ and ozone have been optimized to intensify the decolorization and mineralization efficiency of Rh6G using HC. Nearly 54% decolorization of Rh6G was obtained using a combination of HC and H₂O₂ at a dye to H₂O₂ molar ratio of 1:30. The combination of HC with ozone resulted in 100% decolorization in almost 5–10 min of processing time depending upon the initial dye concentration. To quantify the extent of mineralization, total organic carbon (TOC) analysis was also performed using various processes and almost 84% TOC removal was obtained using HC coupled with 3 g/h of ozone. The degradation by-products formed during the complete degradation process were qualitatively identified by liquid chromatography-mass spectrometry (LC-MS) and a detailed degradation pathway has been proposed.

© 2016 Elsevier B.V. All rights reserved.

1. Introduction

In recent years, the discharge of wastewater coming from various textile industries is becoming a major environmental problem due to loading of the enormous quantity of different toxic dyes. It is estimated that nearly 18–20% of the total production of dyes is discharged into the environment during dyeing process [1–4]. Among most of the toxic dyes, Rhodamine 6G dye is mostly used as a colorant in the textile industries. It is a non-volatile compound, highly water soluble, and dark reddish purple in color. It has some other applications in the biochemistry research laboratories where this dye is used as a diagnostic tool to detect the antigen in a liquid sample. Rh6G is also utilized for fluorescence microscopy and fluorescence correlation spectroscopy in the area of biotechnology [5]. Water containing Rhodamine dyes causes irritation of the skin, eyes and respiratory system of human beings. It has also medically verified that drinking water contaminated with Rhodamine dyes is highly carcinogenic and poisonous to living organisms [6–7].

Hence, these toxic pollutants must be treated before releasing them into the environment. These pollutants contain larger complex molecules (i.e. aromatic compounds) which cannot be treated efficiently by biological methods and other conventional methods such as adsorption, coagulation by chemical agents and membrane filtration. These methods are very costly and cannot mineralize these pollutants and rather separate them physically from the wastewater which causes secondary load on the environment. But over the past years, advanced oxidation processes (AOPs) such as Fenton, Photo-Fenton, photocatalytic process, and cavitation have been employed successfully by many authors [8–15] for the treatment of such pollutant molecules. In last decade, cavitation has also emerged as an effective oxidative process to degrade the organic pollutants present in wastewater. The phenomena of cavitation may be described in three sections as (1) nucleation: formation of cavities within the liquid; (2) growth of bubbles/cavities under the fluctuating surrounding pressure field; (3) subsequent collapse of cavities: violent implosion of vapor/gas filled cavities. In recent years, most of the researchers have focused on the use of acoustic cavitation in the area of wastewater treatment. However, it was observed that utilization of acoustic cavitation

* Corresponding author.

E-mail address: virusuict@gmail.com (V.K. Saharan).



Degradation of reactive blue 13 using hydrodynamic cavitation: Effect of geometrical parameters and different oxidizing additives



Sunil Rajoriya, Swapnil Bargole, Virendra Kumar Saharan*

Chemical Engineering Department, Malaviya National Institute of Technology, Jaipur 302017, India

ARTICLE INFO

Article history:

Received 20 July 2016

Received in revised form 29 December 2016

Accepted 5 January 2017

Available online 7 January 2017

Keywords:

Reactive Blue 13

Hydrodynamic cavitation

Venturi and orifice geometry

Decolorization

Gaseous additives

ABSTRACT

Decolorization of reactive blue 13 (RB13), a sulphonated azo dye, was investigated using hydrodynamic cavitation (HC). The aim of research article is to check the influence of geometrical parameters (total flow area, the ratio of throat perimeter to its cross-sectional area, throat shape and size, etc.) and configuration of the cavitating devices on decolorization of RB13 in aqueous solution. For this purpose, eight cavitating devices i.e. Circular and slit venturi, and six orifice plates having different flow area and perimeter were used in the present work. Initially, the effects of various operating parameters such as solution pH, initial dye concentration, operating inlet pressure and cavitation number on the decolorization of RB13 have been investigated, and the optimum operating conditions were found. Kinetic analysis revealed that the decolorization and mineralization of RB13 using HC followed first order reaction kinetics. Almost 47% decolorization of RB13 was achieved using only HC with slit venturi as a cavitating device at an optimum inlet pressure of 0.4 MPa and pH of the solution as 2.0. It has been found that in case of orifice plates, higher decolorization rate of $4 \times 10^{-3} \text{ min}^{-1}$ was achieved using orifice plate 2 (OP2) which is having higher flow area and perimeter ($\alpha = 2.28$). The effect of process intensifying agents (hydrogen peroxide and ferrous sulphate) and different gaseous additives (oxygen and ozone) on the extent of decolorization of RB13 were also examined. Almost 66% decolorization of RB13 was achieved using HC combined with 2 L min^{-1} of oxygen and in combination with ferrous sulphate (1:3). Nearly 91% decolorization was achieved using HC combined with H_2O_2 at an optimum molar ratio (dye: H_2O_2) of 1:20 while almost complete decolorization was observed in 15 min using a combination of HC and ozone at 3 g h^{-1} ozone feed rate. Maximum 72% TOC was removed using HC coupled with 3 g h^{-1} ozone feed rate.

© 2017 Elsevier B.V. All rights reserved.

1. Introduction

In recent years, industrial wastewater containing reactive azo dyes is becoming a major source of water pollution. These dyes are used in paper, fabric, printing, and mainly textile industries because of their easiness for application on fibers and a variety of bright colors available. The rate of fixation of reactive dyes on the fibers is very low, therefore 40% of dyestuff is discharged into the environment [1]. All the reactive azo dyes contain one or more azo bonds ($-\text{N}=\text{N}-$), and color appears in dyes due to the presence of azo bond and associated chromophores. Wastewaters containing reactive dyes are toxic, mutagenic, and carcinogenic to mankind as well as animals. Conventional treatment processes such as adsorption, coagulation, membrane separation, and biological process are not capable in decolorization and complete mineralization of dye wastewater. Also, these processes provide a poor

performance in breaking larger complex molecules and take longer time for completion of treatment. On the other side, these processes can only transfer organic load from one phase to other phases rather than eliminating the organic load from discharge waste. Hence, alternative treatment techniques are required for the effective treatment of reactive azo dyes [1,2]. In recent years, a new advanced oxidation technique, hydrodynamic cavitation (HC) has been successfully implemented by many researchers for the degradation of various organic pollutants present in water such as pharmaceuticals [3,4], insecticides [5–9], dyes [10–14], and other polymer and phenolic compounds [15–17]. HC process does not produce any secondary load during the treatment process due to the high oxidative capability. It has also been reported that HC technique is energy efficient and cost-effective in degrading organic pollutants, and feasible to scale up on an industrial level [13,18–20]. In HC, cavitation can be produced by pressure variation in a flowing liquid through cavitating devices such as venturi or orifice plates etc. When, liquid passes through the geometries, the kinetic energy/velocity of the fluid increases at an expense of

* Corresponding author.

E-mail address: vksaharan.chem@mnit.ac.in (V.K. Saharan).



Treatment of textile dyeing industry effluent using hydrodynamic cavitation in combination with advanced oxidation reagents

Sunil Rajoriya, Swapnil Bargole, Suja George, Virendra Kumar Saharan*

Department of Chemical Engineering, MNIT, Jaipur, 302017, India



HIGHLIGHTS

- Textile dyeing industry effluent was treated using hydrodynamic cavitation based hybrid methods.
- Optimum operating conditions for all processes were addressed.
- Use of Fenton's reagent in combination with HC led to higher reduction in TOC, COD and color.

ARTICLE INFO

Article history:

Received 31 August 2017

Received in revised form

19 November 2017

Accepted 2 December 2017

Available online 5 December 2017

Keywords:

Textile dyeing industry effluent

Hydrodynamic cavitation

Slit venturi

Color reduction

COD and TOC reduction

ABSTRACT

Treatment of textile dyeing industry (TDI) effluent was investigated using hydrodynamic cavitation (HC) and in combination with advanced oxidation reagents such as air, oxygen, ozone and Fenton's reagent. Slit venturi was used as the cavitating device in HC reactor. The effects of process parameters such as inlet pressure, cavitation number, effluent concentration, ozone and oxygen flow rate, loading of H₂O₂ and Fenton's reagent on the extent of reduction of TOC, COD and color were studied. Efficiency of the hybrid treatment processes were evaluated on the basis of their synergetic coefficient. It was observed that almost 17% TOC, 12% COD, and 25% color removal was obtained using HC alone at inlet pressure of 5 bar and pH of 6.8. The rate of reduction of TOC and COD decreased with dilution of the samples. HC in combination with Fenton's reagent (FeSO₄·7H₂O:H₂O₂ as 1:5) was most effective with reduction of 48% TOC and 38% COD in 15 min and 120 min respectively with almost complete decolorization (98%) of the TDI effluent. Whereas HC in combination with oxygen (2 L/min) and ozone (3 g/h) produced reduction of 48% TOC, 33% COD, 62% decolorization and 48% TOC, 23% COD, 88%, decolorization of TDI effluent respectively.

© 2017 Elsevier B.V. All rights reserved.

1. Introduction

In recent years, effluents from the textile processing industry have become a cause of serious environmental concern. The use of synthetic chemical dyes by the textile industries in the various textile processing operations such as dyeing, printing, bleaching and finishing operations has resulted in the release of large amounts of dye-containing industrial wastewater. There are about 2324 textile industries in India [1]. More than ten thousands dyes are being used commercially and approximately 7×10^5 tons of synthetic dyes are produced per annum worldwide [2,3]. Textile wastewaters are found to have large quantity of suspended particles, varied pH, dark colored, with high chemical oxygen demand (COD) and high total organic carbon (TOC) [4–6]. The presence of highly suspended solid particles with their strong color provides high turbidity in the tex-

tile effluents. Even very low concentration of these dyes (less than 1 ppm for some dyes) induce color in water that is highly observable and undesirable and adversely affects the water bodies such as rivers, lakes etc. [7,8]. Most of the dyes are toxic and bio-recalcitrant in nature and therefore conventional biological processes are found to be inefficient for treatment of textile effluents [3]. The untreated textile wastewaters due to the presence of carcinogenic compounds are therefore very hazardous and toxic to human beings and animals also. Considering the fact that the aquatic environment is damaged by the wastewaters discharged from textile dyeing industries, it is required to develop an eco-friendly and energy efficient technique to treat the textile effluent before its discharge into the aquatic environment. Several conventional strategies comprised of various combinations of physical, chemical, and biological oxidation processes were developed for treatment of textile effluents in last one decade [6,9–13]. However, these processes produce large amount of secondary pollutants which ultimately increase the load on overall treatment facility [5,13]. In recent years, cavitation as an advanced oxidation process (AOP) has been receiving

* Corresponding author.

E-mail address: uksaharan.chem@mnit.ac.in (V.K. Saharan).



An advanced pretreatment strategy involving hydrodynamic and acoustic cavitation along with alum coagulation for the mineralization and biodegradability enhancement of tannery waste effluent

Shivendu Saxena, Sunil Rajoriya, Virendra Kumar Saharan*, Suja George*

Department of Chemical Engineering, MNIT, Jaipur 302017, India

ARTICLE INFO

Keywords:

Tannery waste effluent
Biodegradability index
Coagulation
Hydrodynamic cavitation
Ultrasonication

ABSTRACT

In the present study, coagulation followed by cavitation was studied as a pretreatment tool for tannery waste effluent (TWE) with the aim of reducing its COD, TOC, TSS etc. and enhancing its biodegradability to make it suitable for anaerobic digestion. Initially, coagulation was applied to TWE using alum as a coagulant. The residual pH of treated effluent was found to be around pH of 4.5 where maximum COD and TSS reduction was achieved. In order to enhance the efficiency of pretreatment process, coagulated tannery waste effluent (CTWE) was further subjected to hydrodynamic cavitation (HC) and ultrasonication (US). In case of HC, effect of process parameters such as inlet pressure and dilution on the treatment of CTWE was initially investigated. Lower operating pressure (5 bar) was more favorable for the treatment of CTWE using HC in order to enhance the biodegradability index (BI) from 0.14 to 0.57 in 120 min. The CTWE samples when subjected to 50% dilution, HC pretreatment exhibited higher percentage and quantum reduction in TOC and COD. On the other hand, pretreatment of TWE using coagulation followed by US demonstrated that BI of effluent was enhanced from 0.10 to 0.41 in 150 min. Energy efficiency evaluation for all processes at their optimized conditions was done based on the actual amount of COD reduced per unit energy delivered to the system. Coagulation followed by HC for the pretreatment of TWE was found to be six times more energy efficient as compared to coagulation followed by US.

1. Introduction

Leather is generally manufactured from skins/hides of animals such as cow, goat, sheep, and buffalo [1]. Tanning is that process in which the transformation of animal skins/hides takes place to form leather which is used for making various products such as bags, shoes, and jackets etc. Tanning process involves three steps such as: (a) acquisition and pre-treatment of raw animal skins/hides, (b) treatment of the skin/hides with a tanning agent, and (c) drying and shining the skins/hides to make leather suitable for product manufacturers. Leather industries produce highly polluting wastewater as they consume approximately 300 kg of chemicals (lime, salt, chromium, tannin acids etc.) and 34–56 m³ of water per ton of raw hide [2,3] when processed according to the conventional methods. These wastewaters due to their highly fluctuating pH conditions, high organic and dissolved solids content induce direct and indirect stress on the aquatic environment especially by depressing the dissolved oxygen content in the water, which is very important for the aquatic life. Various toxic pollutants such as propylene glycol and oxides, acrylate esters, chromium, cadmium sulfate,

tannins, organic and inorganic acids etc., are generally present in tannery wastewaters at very high concentrations. Tannery waste effluents (TWE) are characterized by their high chemical oxygen demand (COD), biochemical oxygen demand (BOD), total organic carbon (TOC), variation in pH, solid contents, conductivity, and turbidity [4–7]. Leather industries contribute to the economy of the developing countries such as Turkey, China, India, Pakistan Brazil and Ethiopia [8–11] as they produce around 18 billion square feet of leather annually worldwide with an estimated value of almost \$40 billion [12]. The treatment of tannery effluent due to the higher concentration of organic load with low biodegradability is a serious environmental challenge today. In the last decade, various chemical treatment processes such as coagulation-flocculation, adsorption, ion exchange, and electrochemical techniques have been studied for their applicability to treat the tannery effluents [13–16]. In addition, studies of coagulation in combination with nano-filtration as well as adsorption techniques using activated carbon and cationic/anionic polymers showed higher removal efficiencies in terms of COD and TSS for the pretreatment of tannery effluents [5,17,18]. However, these combined methods are incapable to break the larger

* Corresponding authors.

E-mail addresses: vksaharan.chem@mnit.ac.in (V.K. Saharan), sgeorge.chem@mnit.ac.in (S. George).

<https://doi.org/10.1016/j.ultsonch.2018.02.035>

Received 26 October 2017; Received in revised form 19 February 2018; Accepted 21 February 2018

Available online 22 February 2018

1350-4177/ © 2018 Elsevier B.V. All rights reserved.